

TEST AND EVALUATION
OF
VEHICLE ARRESTING, ENERGY ABSORBING, AND IMPACT ATTENUATION SYSTEMS

F I N A L R E P O R T

ON

CONTRACT NO. CPR-11-5851

For

U. S. Department of Transportation
Federal Highway Administration

By

Texas Transportation Institute
Texas A&M Research Foundation
College Station, Texas

November 30, 1971

FOREWORD

The information contained herein was developed on Research and Development Contract No. CPR-11-5851 sponsored by the Protective Systems Group, Structures and Applied Mechanics Division, Office of Research and Development, Federal Highway Administration, U. S. Department of Transportation. This work was a part of the 4S research program entitled "Structural Systems in Support of Highway Safety."

The basic objective of this project was to conduct full-scale vehicle crash tests and evaluate various vehicle arresting, energy absorbing, and impact attenuation systems. In addition, research work was done to establish the feasibility of using steel drums, lightweight cellular concrete, corrugated metal pipe, and concrete pipe as an energy absorbing material for vehicle impact attenuation systems.

As of the writing of this report, several of the vehicle impact attenuation systems developed or tested and evaluated on this project have been successfully implemented on our nation's highways.

The opinions, findings, and conclusions expressed in this report are those of the research staff of the Texas Transportation Institute and not necessarily those of the Federal Highway Administration.

ACKNOWLEDGMENTS

Since this report is intended to summarize the research effort and experience gained over a four and one-half year period, it is impossible to acknowledge all of the persons, companies, and agencies for their cooperation and support in advancing the field of vehicle impact attenuation.

The researchers gratefully acknowledge the assistance and support of C. F. Scheffey (Director, Office of Research, FHWA), F. J. Tamanini (Chief, Structures and Applied Mechanics Division, FHWA), and John Viner (Leader, Protective Systems Group, FHWA) who established the 4S program, guided and worked closely with the Institute's staff in accomplishing this work.

In addition, a debt of gratitude is due many other engineers from industry, state highway departments, other research agencies, and universities who developed or participated in the development of various impact attenuation systems as follows:

L. Montanaro, Van Zelm Associates, Inc., Providence, Rhode Island
(Dragnet System)

John Nixon and Paul Tutt, Texas Highway Department
(Modular Crash Cushion - Steel Drums)

K. J. Boedecker, Jr., U. S. Steel Corporation
(Modular Crash Cushion - Steel Drums)

Ronald J. Hansen, University of Denver, Denver, Colorado
(Modular Crash Cushion - Steel Drums)

Grant W. Walker, Energy Absorption Systems, Sacramento, California
(Hi-Dro Cushion)

Charles Y. Warner, Brigham Young University, Provo, Utah
(Hi-Dro Cushion)

Bernard Mazelsky, Aerospace Research Assoc., West Covina, California
(Tor-Shok and Roto-Shok Energy Absorption System)

N. W. Magyar, Martin Marietta Corporation, Baltimore, Maryland
(Dual Entrapment Guardrail or Median Barrier)

William E. Woolam and Louis R. Garza, Southwest Research Institute,
San Antonio, Texas
(Energy Absorbing Bridge Rail - Fragmenting Tube)

Wayne Henneberger and Robert L. Reed, Texas Highway Department
(Texas T1 Bridge Rail - Guardrail System)

Malcom D. Graham and William C. Burnett, New York State Dept.
of Transportation, Albany, New York
(New York Box Beam Bridge Rail - Guardrail System)

Robert M. Riddell, North American Rockwell Corporation,
Ashtabula, Ohio
(Fiberglas Median Barrier)

J. D. Michie and M. E. Bronstad, Southwest Research Institute,
San Antonio, Texas
(Concrete Pipe Impact Systems)

The cooperative exchange of information with John L. Beaton and
Eric F. Nordlin of the California Division of Highways who were engaged
in similar work during this period is also acknowledged.

Sincere thanks and our personal appreciation are extended to all
these men as we struggled together in these early "pioneer" days in
the development of vehicle impact attenuation systems to make our
nation's highways safer.

ADMINISTRATIVE STAFF

Mr. Fred J. Benson, Dean of College of Engineering
Texas A&M University

Mr. C. J. Keese, Director
Texas Transportation Institute

Dr. C. V. Wootan, Associate Director
Texas Transportation Institute

Dr. T. J. Hirsch, Research Engineer
Head, Structural Research Division
Texas Transportation Institute

Dr. D. L. Ivey, Research Engineer
Head, Highway Safety Research Center
Texas Transportation Institute

Mrs. Judy Davis, Comptroller
Texas A&M Research Foundation

Mr. Walter Winkelmann, Administrative Assistant
Highway Safety Research Center

PROJECT STAFF

Dr. T. J. Hirsch, Research Engineer, Principal Investigator

Dr. D. L. Ivey, Research Engineer, Co-Principal Investigator

Mr. Gordon G. Hayes, Physics Research Associate, Research Evaluation and Reporting

Mr. James Bradley, Photographic Instrumentation Specialist, Photographic Research Instrumentation

Mr. George A. Shute, Electronics Instrumentation Specialist, Electronic Research Instrumentation and Vehicle Dynamics Research

Mr. Eugene Buth, Assistant Research Engineer, Engineering and Construction

Mr. Don Cangelose, Test Track Supervisor, Vehicle Dynamics Research

Mr. A. J. Stocker, Assistant Research Engineer, Safety and Crash Tests

Mr. Richard Zimmer, Electronics Instrumentation Specialist

Mrs. Mary Ann Pittman, Research Associate

Mrs. Loretta Mosley, Technician

Mrs. Selma Clack, Draftsman

Mr. Monroe C. White, Engineering Research Associate

Mr. I. J. Taylor, Research Instrumentation Specialist

Mr. Harry L. Smith, Engineering Research Associate

Dr. J. E. Martinez, Assistant Research Engineer

Mr. J. J. Jumper, Research Assistant

Mr. Yuce Baskurt, Research Assistant

Dr. Robert M. Olson, Research Engineer

TABLE OF CONTENTS

	Page
FORWARD	ii
ACKNOWLEDGMENTS	iii
ADMINISTRATIVE STAFF	v
PROJECT STAFF	vi
CHAPTER I INTRODUCTION	I.1
Vehicle Impact Attenuation By Breakaway Structures . .	2
Vehicle Impact Attenuation By Crash Cushions And Longitudinal Barriers	3
References	5
CHAPTER II SCOPE OF PROGRAM	II.1
Summary Of Systems Tested And Evaluated	1
Evaluation Criteria Or Procedure	3
References	9
CHAPTER III HUMAN TOLERANCE CRITERIA: A LITERATURE SURVEY	III.1
Introduction	1
Voluntary Tolerance Limits	1
Research Using Cadavers	6
Anthropometric Dummies	6
Animal Studies	7
Clinical Observations	8
Dynamic Overshoot Or Undershoot	9
Secondary Collision	9
Severity Index	10
Discussion	11
References	12
CHAPTER IV TEST SUMMARIES	IV.1
Computation Of Average Decelerations	1
Data Tables	4
Part 1. Vehicle Impact Attenuation Barriers (Crash Cushions Without Redirection Capabilities)	IV.1.1
A. Rigid (Or Immovable) Wall	1.2
B. Dragnet Vehicle Arresting System	1.5
C. Timber Post Energy Absorbing Barrier	1.17
D. Concrete Pipe Impact System	1.21
E. Polyurethane Foam Impact Attenuation Barrier.	1.26

	Page
Part 2. Vehicle Impact Attenuation Barriers (Crash Cushions With Redirection Capabilities) . . .	IV.2.1
A. Modular Crash Cushion (Steel Drums)	2.2
B. The HI-DRO Cushion Vehicle Impact Attenuator.	2.33
C. Tor-Shok Energy Absorbing Protective Barrier.	2.45
D. Lightweight Cellular Concrete Vehicle Crash Cushion	2.49
E. Corrugated Metal Pipe Crash Cushion	2.66
Part 3. Longitudinal Redirection Barriers	IV.3.1
A. One-Way Entrapment Guardrail And Median Barrier	3.2
B. Energy Absorbing Bridge Rail (Fragmenting Tube)	3.11
C. Texas T1 Bridge Rail-Guardrail System	3.19
D. New York Box Beam Bridge Rail-Guardrail System	3.27
E. Roto-Shok Energy-Absorbing Barrier	3.34
F. Fiberglas Median Barrier	3.39
References	3.43
CHAPTER V SUMMARY AND CONCLUSIONS	V.1
Introduction	1
Energy Absorbing Barriers	1
Momentum Transfer or Inertia Barriers	4
Vehicle Impact Attenuation--Geometric And Design Details	7
Summary Of Desired Vehicle Impact Attenuation Barrier Characteristics	14
I. Vehicle Impact Attenuation Barriers (Crash Cushions Without Redirection Capability)	17
II. Vehicle Impact Attenuation Barriers (Crash Cushions With Redirection Capabilities)	18
Longitudinal Barriers (Guardrails, Bridge Rails, And Median Barriers)	19
Summary Of Desired Longitudinal Barrier Characteristics	19
III. Longitudinal Barriers (Guardrails, Bridge Rails, And Median Barriers)	19
Evaluation Of A Crash Cushion Or Longitudinal Barrier	20
References	24

	Page
APPENDIX A: TEST TRACE AND VEHICLE CONTROL	A.1
Introduction	1
Testing Facilities	3
Vehicle Guidance	4
Speed Control	7
APPENDIX B: PHOTOGRAPHIC INSTRUMENTATION	B.1
APPENDIX C: PHOTOGRAPHIC DATA ANALYSIS	C.1
Position Measurements	1
Angular Calibration of Films	3
Time Relationships	8
Information From Time-Coordinate Data	9
Other Speed And Orientation Measurements	11
An Additional Time-Position Technique	15
Conclusions	16
APPENDIX D: ELECTRONIC INSTRUMENTATION	D.1
Carrier System	1
Telemetry	1
Transducers	5
APPENDIX E: ELECTRONIC DATA ANALYSIS	E.1
Choosing A Filter Frequency	1
Analysis Of Filtered Accelerometer Traces	11
References	13
APPENDIX F: TECHNICAL MEMORANDA	
1....Barrel Protective Barrier	
1S...The Modular Crash Cushion	
2....Tor-Shok Energy Absorbing Protective Barrier	
2S...Tor-Shok and Roto-Shok Energy Absorbing Protective Barriers	
3....One-Way Guardrail Installation	
4....Dragnet Vehicle Arresting System	
5....Timber Post Energy Absorbing Protective Barrier	
6....Polyurethane Foam Impact Attenuation Barrier	
7....The Effect of Vehicle Collision with Aluminum Roadside Sign Structures Mounted on Frangible Bases	
8....Energy-Absorbing Bridge Rail (Fragmenting Tube)	

- 9....Feasibility of Lightweight Cellular Concrete Vehicle Crash Cushions
- 9S...Evaluation of Crash Cushions Constructed of Lightweight Cellular Concrete
- 10...Texas T1 Bridge Rail Systems
- 11...Performance of the "HiDro Cushion" Vehicle Impact Attenuator
- 12...New York Box-Beam Bridge Rail-Guardrail
- 13...Impact Response of Fifty-Foot Luminaire Support Structures
- 14...Fiberglas Median Barrier
- 15...A Hybrid Barrier For Use At Bridge Piers In Medians (Modular Crash Cushion Plus Concrete Median Barrier)
- 16...Feasibility of Concrete Pipe Crash Cushions
- 17...The Modular Crash Cushion: Design Data From Static Crush Tests of Steel Drums and of Corrugated Steel Pipes
- 18...A Feasibility Study Of Using Corrugated Steel Pipes In Modular Crash Cushions
- 19...Feasibility Study of Vehicle Crash Cushions Constructed of Readily Available Materials
- 20...Feasibility of Snagging A Vehicle With Hook And Cable System

CHAPTER I

INTRODUCTION

In 1969 the United States of America had a population of approximately 200,000,000 people and 100,000,000 motor vehicles (1 vehicle for every 2 people). Present estimates by the National Safety Council indicate there were approximately 25,000,000 accidents involving motor vehicles (1 accident for every 4 vehicles). The deaths attributed to motor vehicles were approximately 61,000;^{1*} injuries were approximately 4,000,000; and property damage was approximately \$12,000,000,000.

On high-speed freeways, expressways, and interstate highway facilities, an analysis of the accident statistics indicates that 60% of the deaths and injuries due to motor vehicle accidents are the result of single vehicle accidents leaving the roadway, overturning, or colliding with fixed objects adjacent to or near the travelway.² Approximately 7% of these fatalities and injuries resulted from collisions with highway sign supports placed along our roadways; approximately 5% of these fatalities and injuries resulted from collisions with lightpoles; approximately 20% resulted from collisions with guardrails, bridge rails, and median barriers; and the remaining 28% overturned or struck other fixed objects such as bridge piers, concrete walls and abutments, trees, utility poles, etc. It is not known how many of the guardrail collision fatalities and injuries involved guardrails which were used to protect such rigid obstacles as bridge piers, sign posts, lightpoles, etc.

*Superscript numerals refer to corresponding numbers in the References at the end of this section.

In the early 1960's, researchers and highway engineers realized that protecting many of the rigid obstacles along our roadway with guardrails did not necessarily reduce the hazards of the roadway facility but merely substituted, in many cases, another more serious hazard than the one guarded.

VEHICLE IMPACT ATTENUATION BY BREAKAWAY STRUCTURES

In 1963 the Texas Transportation Institute (TTI) and the Texas Highway Department in cooperation with the Federal Highway Administration (FHWA) developed the first successful breakaway highway signs to replace the rigidly-mounted roadside signs which were widely used by the highway departments of this nation.^{3,4} The breakaway roadside signs were designed to support the sign background and message and to withstand the design wind loads, but included a breakaway base and hinge mechanism which allowed the sign post to yield under a vehicle collision and allowed the colliding vehicle to travel safely along its path with only a small change in speed (approximately 1 to 2 mph speed change). The first breakaway roadside signs were installed in Texas in 1965, and at the present time some 80,000 breakaway signs have been installed along the 69,000 miles of state-maintained highways in Texas. These signs were so successful that the Federal Highway Administration has made the breakaway design mandatory for all signs on Federal-aid highway construction throughout the nation.

This "breakaway" principle has now been applied to highway illumination supports (lightpoles).⁵ Such breakaway lightpoles are now being installed along our nation's highways with gratifying results.

Research currently under way at TTI has shown that it is feasible to apply the breakaway principle to large overhead sign bridge structures.⁶ The "breakaway" sign bridge has been successfully tested with vehicle impact speed in excess of 70 mph. This project is sponsored by 21 different state highway agencies in cooperation with FHWA.

VEHICLE IMPACT ATTENUATION BY CRASH CUSHIONS AND LONGITUDINAL BARRIERS

Since many rigid obstacles along our roadway cannot be removed or made breakaway, highway engineers began seriously considering the feasibility of vehicle impact attenuation devices in 1965. In July 1967 the Texas Transportation Institute published a research report entitled "A Feasibility Study of Impact Attenuation or Protective Devices for Fixed Highway Obstacles."⁷ This research was sponsored by fourteen state highway departments and the Federal Highway Administration, Project HPR-2(104), Contract No. CPR-11-3550. In December 1966 the Federal Highway Administration, Office of Research and Development, Structures and Applied Mechanics Division initiated a research program on "Structural Systems in Support of Highway Safety" (4S Program).⁸

Under the 4S Program several vehicle impact attenuation, entrapment, and redirection longitudinal barriers have been developed. In March 1967 the Federal Highway Administration entered into a contract with the Texas Transportation Institute (TTI) to conduct "Tests and Evaluations of Prototypes and Models of Vehicle Arresting, Energy Absorbing, and Impact Attenuation Systems." Summaries of the significant tests are presented in this report.

Several of the devices tested under this project were developed by TTI, however, most of them were developed by other contractors under the FHWA 4S Program.

CHAPTER I REFERENCES

1. Key Issues in Highway Loss Reduction, Proceedings Insurance Institute for Highway Safety, 1970 Symposium, page 173.
2. Hirsch, T. J., "The Highway: Options for Loss Reduction", Paper No. 700199, Society of Automotive Engineers, Jan. 1970.
3. Rowan, Neilon J., et. al., "Impact Behavior of Sign Supports - II," Research Report 68-2 on Texas Highway Department, HPR Project 2-5-63-68, Texas Transportation Institute, Texas A&M University, Sept. 1965.
4. "Break-Away Roadside Sign Support Structures," Vol. 1 of Final Report on FHWA Contract CPR-11-3550, Texas Transportation Institute, Texas A&M University, July 1967.
5. Edwards, Thomas C., et. al., "Development of Design Criteria for Safer Luminaire Supports," NCHRP Report 77, 1969.
6. "Safety Provisions for Support Structures on Overhead Sign Bridges," Final Report on FHWA Contract No. FH-11-7032, Texas Transportation Institute, Texas A&M University, Sept. 1970.
7. "A Feasibility Study of Impact Attenuation or Protective Devices for Fixed Highway Obstacles," Vol. 3 of Final Report on FHWA Contract CPR-11-3550, Texas Transportation Institute, Texas A&M University, Jan. 1967.
8. Tamanini, F. J., "Designing Fail-Safe Structures for Highway Safety," Public Roads, Vol. 36, No. 6, February 1971.

CHAPTER II

SCOPE OF PROGRAM

SUMMARY OF SYSTEMS TESTED AND EVALUATED

The barriers tested and evaluated in this program may be categorized into three (3) basic types as follows:

1. Vehicle Impact Attenuation Barriers (or Crash Cushions) which must be capable of decelerating a selected vehicle impacting head-on in such a manner that occupants restrained by seat belts can survive, preferably uninjured.
2. Vehicle Impact Attenuation Barriers (or Crash Cushions) with additional capability of redirecting selected vehicles which impact it along its length (or side) in such a manner that passengers restrained by seat belts can survive, preferably uninjured.
3. Longitudinal Barriers (Guardrails, Bridge Rails, and Median Barriers) which must be capable of redirecting a selected vehicle that impacts it along its length in such a manner that occupants restrained by seat belts can survive, preferably uninjured.

It should be pointed out that many of the barrier designs tested in this program were in the early stages of development. In many cases the tests were conducted to evaluate the feasibility of the basic energy-absorbing principle. Consequently, in some cases, the barrier design details have been modified considerably since these early (or pioneer) designs were tested and evaluated under this program.

A summary of the barrier systems tested and evaluated is as follows:

1. Vehicle Impact Attenuation Barriers (Crash Cushions) without redirection capability -
 - a. Dragnet Vehicle Arresting System - developed by Van Zelm Associates, Inc., 1475 Elmwood Avenue, Providence, Rhode Island.
 - b. Timber Post Energy Absorbing Barrier - developed by Texas Transportation Institute and Federal Highway Administration.
 - c. Concrete Pipe Impact Attenuation System - developed by Federal Highway Administration, Southwest Research Institute, and Texas Transportation Institute.
 - d. Polyurethane Foam Impact Attenuation Barrier - developed by Texas Transportation Institute and Federal Highway Administration.
2. Vehicle Impact Attenuation Barriers (Crash Cushions) with redirection capability -
 - a. Modular Crash Cushion (Steel Drums) - developed by Texas Transportation Institute, Texas Highway Department, and Federal Highway Administration.
 - b. Hi-Dro Cushion Crash Moderation System (Water-filled Cylinders or Cells) - developed by Energy Absorption Systems, Inc., 221 N. LaSalle Street, Chicago, Illinois.
 - c. Tor-Shok Energy Absorbing Protective Barrier - developed by Aerospace Research Associates, Inc., 2017 West Garvey Avenue, West Covina, California.
 - d. Lightweight Cellular Concrete Crash Cushion - developed by Texas Transportation Institute and Federal Highway Administration, based on a feasibility study conducted by Cornell Aeronautical Laboratory, Inc.⁴

- e. Corrugated Metal Pipe Crash Cushion - developed by Texas Transportation Institute and Federal Highway Administration.
3. Longitudinal Redirection Barriers (Guardrails, Bridge Rails, and Median Barriers) -
 - a. One Way (Entrapment) Guardrail or Median Barrier - developed by Martin Marietta Corporation, Baltimore, Maryland.
 - b. Energy Absorbing Bridge Rail (Fragmenting Tube) - developed by Southwest Research Institute and Federal Highway Administration.
 - c. Texas T1 Bridge Rail-Guardrail System - developed by the Texas Highway Department.
 - d. New York Box Beam Bridge Rail-Guardrail System - developed by Department of Transportation of the State of New York.
 - e. Roto-Shok Energy Absorbing Barrier - developed by Aerospace Research Associates, Inc., 2017 West Garvey Avenue, West Covina, California.
 - f. Fiberglas Median Barrier (Flower Pot Concept) - developed by North American Rockwell Corporation, Ashtabula, Ohio.

EVALUATION CRITERIA OR PROCEDURE

At the beginning of this program, very limited data were available to establish service, design, or performance criteria for the impact attenuation barriers to be tested and evaluated. The objectives of the FHWA 4S Program were to reduce the number of highway fatalities and to minimize injuries from single vehicles leaving the road, overturning, or striking some fixed object near the roadway.

Objective criteria concerning the probability of a human occupant surviving a collision with an impact attenuation system are extremely elusive. A mere listing of some of the variables which have a significant influence on a vehicle occupant's survivability will illustrate this.

Vehicle characteristics - weight, speed, impact angle, crushing and fendering characteristics, safety equipment, etc.

Occupant characteristics - weight, size, sex, physical condition, position in vehicle, restraint systems used (if any), etc.

At the beginning of this project (and even now) very limited data were available concerning human tolerance to impact accelerations (or decelerations). In 1961 Cornell Aeronautical Laboratory suggested tolerable limits of deceleration where the duration did not exceed 200 milliseconds and the rate of onset did not exceed 500 g's per second.^{1*} These are shown in Table II.1.

TABLE II.1. TENTATIVE TOLERABLE DECELERATION LIMITS SUGGESTED BY CORNELL AERONAUTICAL LABORATORY¹

Occupant Restraint	Maximum Deceleration (g's)		
	Lateral	Longitudinal	Total
Unrestrained	3	5	6
Lap Belt	5	10	12
Lap Belt and Shoulder Harness	15	25	25

*Superscript numerals refer to corresponding numbers in the References at the end of this section.

Based on this and other data discussed in Chapter III, "Human Tolerance Criteria: A Literature Survey," the Federal Highway Administration suggested the following criteria be used for testing and evaluating vehicle impact attenuation devices.²

Vehicle Weight Range	- 2,000 to 4,500 lb
Vehicle Speed	- 60 mph
Impact Angle	- up to 25° as measured from the direction of the roadway
Average Permissible Vehicle Deceleration	- 12 g's max. while preventing actual impact or penetration of the protected hazard
Max. Occupant Deceleration Onset Rate	- 500 g's per second

These criteria were intended to apply to a variety of impact conditions and hopefully will provide a survivable environment for lap belted or lap and shoulder belted occupants. If the vehicle occupants are unrestrained, reasonable and practical criteria are extremely difficult to establish because of the extremely complex nature of possible secondary collisions within the vehicle interior. The 12 g average deceleration limit of the suggested criteria corresponds to a minimum 10 ft stopping distance for a 60 mph impact.

For impact attenuation barriers to be effective and acceptable for use on our nation's highways, a careful analysis (which occurred during the project) indicated that it would be desirable for such barriers to have the following characteristic:

I. Vehicle Impact Attenuation Barriers (Crash Cushions) -

- A. A crash cushion should smoothly stop a selected vehicle impacting it head-on. The vehicle should not vault over the barrier and should not become unstable and roll over. It would be desirable for such crash cushions to have the capability of stopping a vehicle impacting anywhere along its length and at any angle up to the maximum design conditions of impact speed, vehicle weight, and impact angle.
- B. A crash cushion should minimize vehicle decelerations in such a manner that occupants restrained by seat belts can survive, preferably uninjured.
- C. A crash cushion should remain essentially intact during and following a vehicle collision. A vehicle impact should not dislodge any hazardous elements into the travelway.
- D. A crash cushion should be compatible with the roadway and fixed object it is guarding. It should not protrude into the travelway or shoulders provided for emergency or evasive maneuvers by a vehicle.
- E. A crash cushion should be susceptible of quick repair. All elements of a barrier should be so designed that when repairs are necessary they can be done quickly and with a minimum of special equipment.
- F. A crash cushion should be mechanically reliable and dependable. It should be durable and stand up under extreme environmental exposure -- heat and cold, wet and dry, and corrosive elements (salts, etc.) expected under service conditions.
- G. The foregoing requirements should be met by giving emphasis first to safety, second to economics, and third to aesthetics.

II. Vehicle Impact Attenuation Barriers (Crash Cushions) with Redirection Capabilities -

- A. A crash cushion with redirection capabilities should satisfy all the service requirements of a simple crash cushion of item I when a selected vehicle impacts it head-on.
- B. A crash cushion with redirection capabilities should restrain and smoothly redirect a selected vehicle which impacts it along its length or side. The impacting vehicle should not penetrate or vault over the barrier. The vehicle should not snag or pocket under side angle impacts.
- C. A crash cushion with redirection capabilities should be compatible with adjoining or abutting longitudinal barriers (guardrails, bridge rails, or median barriers) in order to prevent collisions with the ends of the adjoining or abutting barriers. A smooth redirection should be obtained at the transition point between the two barriers.

III. Longitudinal Barriers (Guardrails, Bridge Rails, and Median Barriers) -

- A. A longitudinal barrier should laterally restrain a selected vehicle. The impacting vehicle should not penetrate or vault the barrier.
- B. A longitudinal barrier should minimize vehicle decelerations.
- C. A longitudinal barrier should smoothly redirect a colliding vehicle. Vehicle progression should be smooth following impact; it should not snag or pocket or roll over.
- D. A longitudinal barrier should remain intact following a collision. Vehicle impact should not dislodge any hazardous element into the travelway.

- E. A longitudinal barrier which serves vehicles and pedestrians should provide protection for both vehicle occupants and pedestrians. Sidewalks must be placed outboard of the vehicle-barrier railing.
- F. A longitudinal barrier should have a compatible transition between it and other adjoining or abutting barriers in order to prevent collisions with the ends of the adjoining barrier.
- G. A longitudinal barrier should have compatible beginning and end treatments. The end treatment should develop the required anchorage strength so the barrier can redirect colliding vehicles near the end. The end treatment should minimize the hazard of vehicles colliding with the ends.
- H. A longitudinal barrier should define the limits of the travelway yet provide adequate visibility. The driver's sight distance should not be obstructed on horizontal curves.
- I. A longitudinal barrier should be susceptible to quick repair.
- J. The foregoing requirements must be met by giving emphasis first to safety, second to economics, and third to aesthetics.

The foregoing criteria are subjective, yet a general overall evaluation of the effectiveness of a given system can be made using them. Highspeed movie film and other photographic documentation of a vehicle crash test are extremely useful for this purpose. Olson, Post, and McFarland were the first to propose criteria of this type for bridge rail systems.³

CHAPTER II REFERENCES

1. "Highway Barrier Analysis and Test Program," Summary Report for Period July 1960 - July 1961, Cornell Aeronautical Laboratory Report No. VJ-1472-V-3, July 1961.
2. Tamanini, F. J. and Viner, John G., "Structural Systems in Support of Highway Safety," paper presented at the American Society of Civil Engineer's National Meeting on Transportation Engineering, Washington, D. C., July 21-25, 1969.
3. Olson, Robert M., Post, Edward R., and McFarland, William F., "Tentative Service Requirements for Bridge Rail Systems," NCHRP Report 86, Highway Research Board, 1970.
4. Shoemaker, Norris E., "Research And Design of An Impact Absorbing Barrier For Fixed Highway Objects," Final Report on Contract No. FH-11-6657. Prepared by the Cornell Aeronautical Laboratory, Inc., Buffalo, New York, for the U.S. Department of Transportation, June 1968.

CHAPTER III

HUMAN TOLERANCE CRITERIA: A LITERATURE SURVEY

INTRODUCTION

The determination of a tolerable deceleration level is an elusive goal that defies a precise definition. The main reason for this is the long list of factors controlling deceleration. Foremost on the list are the magnitude of peak deceleration and the duration of this peak. Also shown to have a decisive effect on human tolerance is the rate of onset of deceleration. The type of body restraint system used, or the absence of one, also determines tolerable deceleration levels. Other factors influencing deceleration are: direction of the deceleration forces, environmental conditions, and the physical condition of the persons involved.

Research has been in progress for a number of years to answer some questions on tolerable deceleration levels. The following is a review of the state-of-the-art on human impact tolerance.

VOLUNTARY TOLERANCE LIMITS

Siegfried Ruff^{1*} was one of the first to use human subjects in conducting dynamic tests for the establishment of tolerance limits to longitudinal deceleration. His main reason for conducting the tests was to develop a proper restraint system for the German Air Force. A pendulum-like swing was devised which could produce decelerations of up to 100 g's, depending upon the height from which the swing was dropped. In many of the tests, Ruff himself was the subject in the seat of the swing. Based on data from the swing tests and data from actual crashes, it was concluded that men wearing the standard restraint of the German Air Force could easily tolerate a deceleration of 20 g's.

*Superscript numerals refer to corresponding numbers in the References at the end of this section.

The testing of air force restraint systems was also one of the primary reasons for live human experimentation conducted by Stapp. It was Stapp² who believed that "the primary instrument for measuring the effects of mechanical force on man is man," and he believed this to the ultimate for he was the test subject in many of the experiments.

In a series of tests in 1949, three men were subjected to decelerations from back to chest in a backward-facing, seated position.³ The subjects were seated in a sled which was propelled along a rail track. A sequence of brake units was activated to control the deceleration. The subjects were properly restrained with the military lap and shoulder strap combination. Accelerometers recorded head, chest, and sled decelerations. The subjects were examined prior to and after the test runs to note physical reactions. These men withstood sled decelerations of up to 30 g's for 0.11 sec at a rate of onset of 1000 g's per sec with no permanent injuries.

Another series of 51 tests was conducted with live humans seated facing forward. The most severe effects experienced were in a run in which the subject sustained 38.6 g's at a rate of onset of 1370 g's per sec. In another run, also at 38.6 g's but a rate of onset of 330 g's per sec, no ill effects resulted. The maximum applied peak of 45.4 g's, with a time duration of 0.044 sec at a rate of onset of 493 g's per sec was sustained with only delayed effects, such as general fatigue.

It appears from the above that one of the definite limiting factors on voluntary tolerance to linear deceleration is the rate of onset. Voluntary tolerance limits were reached when two subjects experienced a peak deceleration above 38 g's and a rate of onset greater than 1300 g's per

sec concurrently. It should be noted here that the changes in speed experienced were much higher than those experienced in automobile crashes.

A series of tests was run later to determine human response to decelerations in the range of automotive vehicle collision speeds.² The procedure was basically the same as in previous tests. Results of these tests are as follows:

1. *Healthy, adult male volunteer subjects exposed to impact deceleration in the seated forward facing position can withstand velocity changes corresponding to automobile crashes up to 30 peak g at rates of onset below 1,500 g per second while restrained by a 3 inch dacron or nylon seat belt bearing against the pelvic girdle, with minor, reversible injurious effects.*²

2. *Impact decelerations exceeding 1,000 g per second at higher than 25 g become progressively more difficult to withstand, even in the backward facing position, or with pelvic and shoulder girdle restraints, eliciting transient musculoskeletal or visceral pain, visual and cardiac changes and breathing difficulties, depending on body orientation and resultant force vectors.*²

Eiband in 1959 provided a graphical summary of the work done up to that time in the area of tolerance to impact decelerations.⁴ (See Figure III.1.) The various levels of injury are defined as follows: area of no injury; area of moderate injury, which includes slight injury of extremities and brief unconsciousness; and the area of severe injury, which includes fatal or near fatal injuries. The limit of voluntary human exposure was reached in a run reported by Stapp which was mentioned previously. The subject sustained a maximum uniform deceleration of 45 g's for 0.044 sec and received no weakening effects. The upper limit of the area of moderate injury was measured when a hog subject was exposed to 160 g's for about 0.004 sec. The 200 g deceleration above the area of severe injury was experienced by a human in a fall from a building. This value is an estimate, but the individual did survive the fall.

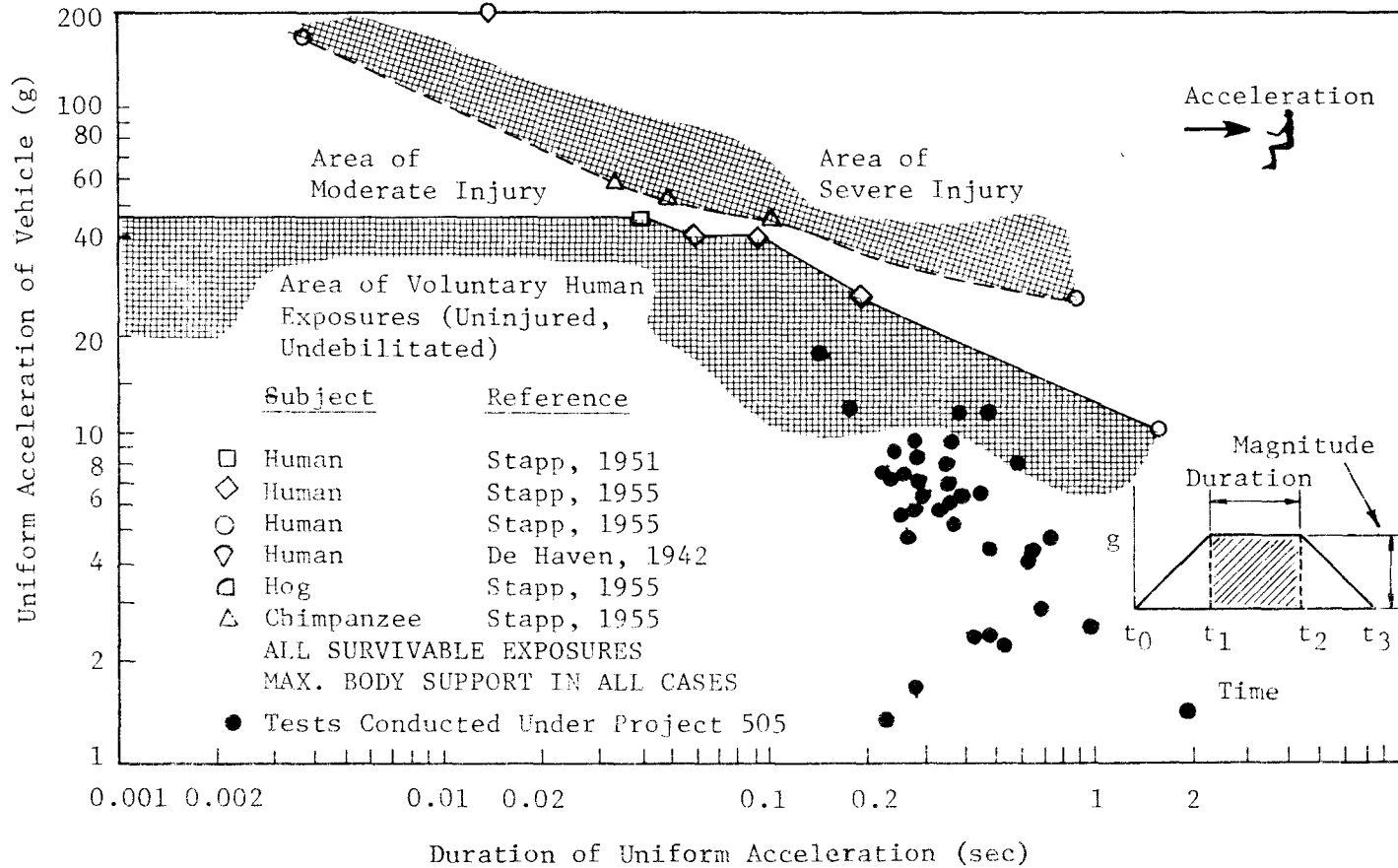


FIGURE III.1. MAXIMUM HUMAN TOLERANCE LIMITS TO LONGITUDINAL ACCELERATION (STERNUMWARD G)

It is interesting at this point to note where the average decelerations from tests conducted under this project would be plotted on the graph. Since Tables IV.1.-3. in the next chapter include a summary of average longitudinal decelerations for each test conducted, this can easily be done. All of the points fall well within the area of voluntary human exposure (no injury).

Reports on lateral or sideways deceleration are not as numerous as those on longitudinal deceleration because not as much work has been done in this area. In tests conducted at the Wright Air Development Center, five volunteer subjects were exposed to lateral decelerations in the WADC centrifuge.⁵ Exposures ceased because of "severe vascular engorgement" after a maximum of 7 g's was reached.

Human tolerance to lateral impact was also measured in a series of tests using 37 male volunteers restrained by the seat belt only.⁶ The deceleration device used was the Bopper, a seat-sled system with controlled deceleration by a mechanical brake. At first, the subjects were exposed to a maximum of 4 g's, and then the peak sled deceleration was increased by 2 g increments for each series until a voluntary upper limit was reached. No irreversible injuries were received when the men were exposed to an average maximum deceleration of 9.02 g's for about 0.1 sec. About half of the subjects reported receiving some physical discomfort after being subjected to an average maximum of 6.25 g's or more.

Another series of experiments was conducted later in which male volunteers restrained by seat belt and shoulder harness were subjected to lateral impacts.⁷ The same setup that was used in the previous tests was

again applied to these experiments. The tests were stopped after two men were exposed to maximum sled decelerations of 11.44 g's and 11.74 g's, due to the possibility of cardiovascular problems. Results of the runs are summarized below:

1. *"No permanent physiological changes have been reported for healthy young male volunteers while exposed to impacts of 11.59 g's average and durations of approximately 0.1 seconds."*⁷

(This 11.59 g's average is an average of all the maximum g's for a particular series.)

2. *"Exposure of volunteers to decelerations greater than approximately 12 g's laterally and time durations of approximately 0.1 seconds should be investigated with biological specimens other than man to investigate possible cardiovascular responses to impact."*⁷

RESEARCH USING CADAVERS

Human cadavers have been used in deceleration tests when volunteer subjects were not available or particularly when forces that cause bone damage needed to be measured. Most of the forehead impact data available has been obtained largely from experiments with cadavers.⁸ The advantage of using cadavers is obvious, since their structure and mass are identical to that of the live human. Significant research has been conducted at Wayne State University and is reported by Patrick, et al,⁹ Daniel and Patrick,¹⁰ and Mertz and Patrick,¹¹ among others.

ANTHROPOMETRIC DUMMIES

Research has been in progress for many years in California, where anthropometric dummies have been used as subjects in simulated vehicle impacts.¹² Severy and Mathewson¹³ believe that for decelerations above 5 g's, dummy movement corresponds reasonably well with that of the human.

Several 25-30 mph fixed-barrier collision tests were conducted with dummies in the vehicles. Peak decelerations of 14 g's to 19 g's were recorded, with rates of onset of 500 to 800 g's/sec. Photographic analysis indicated that humans restrained by lap belt and shoulder harness would have survived. Occupants with any less support would not have survived.

Chandler and Christian¹⁴ used several types of dummies to test human restraint systems, but found that significant variations occurred in dummy response to almost identical tests. Research is continuing in the hope of fabricating an anthropometric dummy which will simulate the complexity of the human body.

ANIMAL STUDIES

There are times when it is not feasible to use live humans, cadavers, or dummies in deceleration testing. For instance, when it is necessary to determine how an injury is produced, animals will usually be used. One of the major problems involved in using animals is that of interpreting the data from animal impact tests and applying it to g-forces on humans.¹⁵

Kornhauser¹⁶ has experimented with mice by dropping them in a carriage from a predetermined height. Wickstrom, et al,¹⁷ found that Belgian hares could withstand peak decelerations of 153 g's. The hare's flexible neck and light weight made such high decelerations tolerable. Guinea pigs have been used in tests to study various head support systems and have been exposed to impacts of 600 g's at initial velocities of up to 80 ft./sec.¹⁸ Among others who have reported on animal research are: Higgins and Schmall¹⁹, Snyder, et al²⁰; Ommaya, et al²¹; and Gurdjian, et al²².

CLINICAL OBSERVATIONS

Olson, Post and McFarland²³ have used crash test data reported by Michalski²⁴ to show a statistical relationship between deceleration environment and occupant injuries. After reviewing several hundred accidents in Oregon, Michalski surmised that the proportion of damaged vehicles in which injuries occurred was directly related to the square of the severity of damage to a vehicle as rated on a 7-point Vehicle Damage Rating Scale. This rating scale consists of pages of photographs of damaged vehicles, with each page containing pictures of a particular type of impact, front-end concentrated damage, front-end distributed damage, etc. The severity of damage, illustrated by the photographs, is indicated by an arbitrary scale from 1 to 7, with 7 being the most severe damage.

Using the results of Michalski's work and incorporating data from crash tests conducted by California, New York and at TTI, Olson, et al,²³ extended the previous work to include average vehicle decelerations. They postulate that the severity of damage to a vehicle provides an indication of vehicle decelerations and incidence of injury to unrestrained occupants. Research engineers at TTI were given photographs of damaged vehicles from crash tests at the above sites and were asked to rate them using the Damage Rating Scale. To keep their judgment as unbiased as possible, the engineers had no knowledge of the average deceleration levels.

Information obtained resulted in the following equations²³ which generally described the scattered data:

$$\text{For frontal impacts -- } G_{\text{long}} = 0.280 R^2 = 13.7 P$$

where G = average vehicle deceleration

R = Vehicle Damage Rating

P = Proportion of vehicles in which injuries occurred.

For angle impacts -- $G_{lat} = 0.204 R^2 = 10.0 P$

This means that approximately 80% of accidents in which the vehicle is subjected to 12 g's longitudinally would result in injury to unrestrained occupants. At the 6-g level, the probability of injury would be reduced to about 50%.

DYNAMIC OVERSHOOT OR UNDERSHOOT

Some research has been conducted on "dynamic overshoot" or "undershoot" but there seems to be varying opinions on how significant this phenomenon is. Everyone knows that the deceleration experienced by an individual seated in a car will be different from that of the vehicle, since no human can be rigidly attached to the vehicle.

Haley²⁵ reports on a 200-pound dummy restrained by an elastic nylon harness in which the deceleration of the dummy was twice that of the seat of the sled. Grime²⁶ disputes this by citing tests with restrained dummies in Britain. The decelerations of the dummy were nearer 1.0 to 1.5 times the deceleration of the seat, depending on dummy type, belt type, and arrangement of the belt on dummy. He believes this factor is even less with humans. Some researchers believe the factor can even be less than one (dynamic undershoot).

SECONDARY COLLISION

In more recent years, emphasis has shifted from whole-body tolerance limits to tolerance limits of individual parts of the body. Most researchers are becoming concerned about the "secondary collision" -- the occupant impacting the interior of the vehicle.

A great number of experiments have been conducted on forehead impacts. Patrick²⁷ used cadavers and animals to develop a g-time curve for forehead

impacts to a hard, flat surface. The upper limit of the curve is about 230 g's for a time duration of less than 0.005 sec. With increasing time, the g-limit is significantly reduced. The criteria for the limits of the curve was mild concussion with no after effects. Among others who have reported on head impact studies are Daniel and Patrick¹⁰; Patrick, et al⁸; Ewing, et al^{28, 29}; Lombard, et al¹⁸; and Mertz and Patrick¹¹.

Patrick, et al,^{9,30} have extended the previous work to include chest and knee impacts, also.

SEVERITY INDEX

Gadd³¹ approaches the problem of human tolerance to deceleration in a rather unique manner. He uses an exponential weighing factor to develop a theoretical solution. Using data from research conducted at Wayne State University and NASA (most data was for brief durations of impact), he concludes that one number defines the tolerance limit for a particular impact, and that number is obtained from the following equation:²⁶

$$I = \int a^n dt$$

Where a = acceleration, force or pressure

n = weighing factor greater than 1

t = time, seconds

I = severity index.

When acceleration is being measured in g's, a weighing factor constant of 2.5 is used for forehead impacts, and a severity index value of 1000 is used for the minimum threshold of serious internal head injury. These values are based on data published by Eiband and Patrick of Wayne State University. What this means is: If, after integrating the g-time

curve, the severity index is greater than 1000, it is concluded that the impact would have produced serious injury.

It should be noted that there are certain limitations of the index. One of these is the time duration, i.e., the length of time over which the severity index is valid. Also, this index applies only to the initial forehead contact with a vehicle interior.

Similar equations are being formulated for facial and chest impacts.

DISCUSSION

After reviewing the literature, the Federal Highway Administration under their 4S program (Structural Systems in Support of Highway Safety), has established an average permissible longitudinal deceleration of 12 g's,^{33,34} It should be emphasized that this deceleration level is for speeds less than 60 mph, with a maximum onset rate of 500 g's/sec, and for properly restrained passengers (lap belt).

It seems evident that it is not feasible to try to eliminate all possibility of occupant injury when designing deceleration devices such as those tested in this program, but the experience to date shows that these devices can keep the deceleration levels experienced by the occupants within tolerable limits.

CHAPTER III REFERENCES

1. Ruff, Siegfried, "Brief Acceleration: Less Than One Second," GERMAN AVIATION MEDICINE WWII, Vol. I, U.S. Gov't Printing Office, 1950.
2. Stapp, John P., "Voluntary Human Tolerance Levels," IMPACT INJURY AND CRASH PROTECTION, C. C. Thomas, Publishers, Springfield, Illinois, 1970.
3. Stapp, John P. WADC Air Force Technical Report 5915, Part 1, June 1949, "Human Exposure to Linear Deceleration, Part 1". "Preliminary Survey of Aft-Facing Seated Position, Part 2. The Forward Facing Position and Development of a Crash Harness," December 1951.
4. Eiband, A.M., "Human Tolerance to Rapidly Applied Accelerations: A Summary of the Literature," National Aeronautics and Space Administration Memo 5-19-59E, 1959.
5. Headley, R. M., "Human Tolerance and Limitations to Acceleration," AGARDograph No. 48.
6. Zaborowski, Albert B., "Human Tolerance to Lateral Impact with Lap Belt Only," PROCEEDINGS OF THE EIGHTH STAPP CAR CRASH CONFERENCE.
7. Zaborowski, Albert B., "Lateral Impact Studies: Lap Belt Shoulder Harness Investigations," PROCEEDINGS OF THE NINTH STAPP CAR CRASH CONFERENCE. University of Minnesota Press, 1966.
8. Patrick, Lawrence M., Lissner, Herbert R., and Gurdjian, E. S., "Survival by Design--Head Protection," PROCEEDINGS OF THE SEVENTH STAPP CAR CRASH CONFERENCE. C. C. Thomas, Publishers, 1965.
9. Patrick, L. M., Mertz, H. J., Jr., and Kroell, C. K., "Cadaver Knee, Chest, and Head Impact Loads," PROCEEDINGS OF THE ELEVENTH STAPP CAR CRASH CONFERENCE. New York: SAE, Inc., 1967.
10. Daniel, Roger P. and Patrick, L. M., "Instrument Panel Impact Study," PROCEEDINGS OF THE NINTH STAPP CAR CRASH CONFERENCE.
11. Mertz, H. J., Jr. and Patrick, L. M., "Investigation of the Kinematics and Kinetics of Whiplash," PROCEEDINGS OF THE ELEVENTH STAPP CAR CRASH CONFERENCE. New York: SAE, Inc., 1967.
12. Nahum, Alan M., Severy, Derwyn M., and Siegel, Arnold W., "Automobile Accidents Correlated with Collision Experiments: Head-on Collisions," PROCEEDINGS OF THE NINTH STAPP CAR CRASH CONFERENCE.
13. Severy, D. M. and Mathewson. J. H., "Technical Findings From Automobile Impact Studies," SAE TRANSACTIONS, Vol. 65, 1957.

14. Chandler, Richard F., and Christian, Robert A., "Comparative Evaluation of Dummy Performance Under G_x Impact," PROCEEDINGS OF THE THIRTEENTH STAPP CAR CRASH CONFERENCE. ^x
15. Patrick, Lawrence M. and Sato, Takashi B., "Methods of Establishing Human Tolerance Levels," IMPACT INJURY AND CRASH PROTECTION, C. C. Thomas, Publishers, Springfield, Illinois, 1970.
16. Kornhauser, M., STRUCTURAL EFFECTS OF IMPACT, Spartan Books, Baltimore, Cleaver-Hume Press, London.
17. Wickstrom, Jack, Martinez, John L., Johnston, David and Tappen, Neil C., "Acceleration-Deceleration Injuries of the Cervical Spine in Animals," PROCEEDINGS OF THE SEVENTH STAPP CAR CRASH CONFERENCE.
18. Lombard, C. F., Robbins, W. A., and Potter, G. L., "Some Factors Contributing to Head and Neck Injuries During Whole Body Impact Using Guinea Pig Subjects in +G Orientations," PROCEEDINGS OF THE TWELFTH STAPP CAR CRASH CONFERENCE. New York: SAE, Inc., 1968.
19. Higgins, Lawrence and Schmall, Robert A., "A Device for the Investigation of Head Injury Effected by Non-Deforming Head Accelerations," PROCEEDINGS OF THE ELEVENTH STAPP CAR CRASH CONFERENCE.
20. Snyder, Richard G., Young, Joseph W., and Snow, Clyde C., "Experimental Impact Protection with Advanced Automotive Restraint Systems: Preliminary Primate Tests with Air Bag and Inertial Reel/Inverted-Y Yoke Torso Harness," PROCEEDINGS OF THE ELEVENTH STAPP CAR CRASH CONFERENCE. New York: SAE, Inc., 1967.
21. Ommaya, A. K., Yarnell, P., Hirsch, A. E. and Harris, E. H., "Scaling of Experimental Data on Cerebral Concussion in Sub-Human Primates to Concussion Threshold for Man," PROCEEDINGS OF THE ELEVENTH STAPP CAR CRASH CONFERENCE. New York: SAE, Inc., 1967.
22. Gurdjian, E. S., Lissner, H. R. and Patrick, L. M., "Concussion - Mechanism and Pathology," PROCEEDINGS OF THE SEVENTH STAPP CAR CRASH CONFERENCE. C. C. Thomas, Publishers, Springfield, Illinois, 1965.
23. Olson, Robert M., Post, Edward R., and McFarland, William F., "Tentative Service Requirements for Bridge Rail Systems," Final Report on Project Number 12-8, NCHRP Report 86, February 1969.
24. Michalski, Charles S., "Model Vehicle Damage Scale: A Performance Test," TRAFFIC SAFETY, Vol. 12, No. 2, June 1968.
25. Haley, Joseph L. Jr., "Fundamentals of Kinetics and Kinematics as Applied to Injury Reduction," IMPACT INJURY AND CRASH PROTECTION, C. C. Thomas, Springfield, Illinois, 1970.

26. Grime, Geoffrey, "Discussion of 'Fundamentals of Kinetics and Kinematics as Applied to Injury Reduction,' by Joseph L. Halev, Jr.," IMPACT INJURY AND CRASH PROTECTION, C. C. Thomas, Publishers, Springfield, Illinois, 1970.
27. Patrick, L. M., "Human Tolerance to Impact -- Basis for Safety Design," SAE TRANSACTIONS, Vol. 74, 1966.
28. Ewing, Channing L., Thomas, Daniel J., Beeler, George W., Jr., Patrick, Lawrence M., and Gillis, David B., "Dynamic Response of the Head and Neck of the Living Human to $-G_x$ Impact Acceleration," PROCEEDINGS OF THE TWELFTH STAPP CAR CRASH CONFERENCE.
29. Ewing, C. L., Thomas, D. J., Patrick, L. M., Beeler, G. W. Jr., and Smith, M. J., "Living Human Dynamic Response to $-G_x$ Impact Acceleration -- 11-Accelerations Measured on the Head and Neck," PROCEEDINGS OF THE THIRTEENTH STAPP CAR CRASH CONFERENCE.
30. Patrick, L. M., Mertz, H. J., Jr., and Kroell, C. K., "Impact Dynamics of Unrestrained, Lap Belted, and Lap and Diagonal Chest Belted Vehicle Occupants," PROCEEDINGS OF THE TENTH STAPP CAR CRASH CONFERENCE.
31. Gadd, C. W., "Use of a Weighted-Impulse Criterion for Estimating Injury Hazard," SAE Paper 660793, 1966.
32. Tamanini, F. J. and Viner, John G., "Energy Absorbing Roadside Crash Barriers," CIVIL ENGINEERING, 1970.
33. Tamanini, F. J., "Designing 'Fail-Safe' Structures for Highway Safety," Presented at the National Structural Engineering Meeting, American Society of Civil Engineers, Portland, Oregon, 1970.

CHAPTER IV
TEST SUMMARIES

This chapter includes the following: a discussion of the methods used to compute average decelerations, three summary tables containing a brief summary of data obtained from the full-scale vehicle crash tests, and a brief description of each barrier tested with a discussion of crash test results.

COMPUTATION OF AVERAGE DECELERATIONS

Several methods were used to compute the average decelerations in Tables IV.1.-3. These methods are discussed below.

Accelerometer Analysis

For each test, average longitudinal (along vehicle longitudinal axis) and transverse (perpendicular to vehicle longitudinal axis) decelerations from accelerometer traces were calculated by determining the area under the trace in g-sec and dividing this by the time over which the area was taken, i.e.,

$$G_{\text{avg}} = \frac{\int_0^t a \, dt}{t} \quad (\text{a})$$

This method is explained in more detail in Appendix E.

High-Speed Film Analysis

Longitudinal Deceleration. Average longitudinal deceleration from high-speed film was computed as follows:

$$\text{Long. } G_{\text{avg}} = \frac{(V_i^2 - V_f^2)}{2gS_{\text{long}}} \quad (\text{parallel to vehicle path}) \quad (\text{b})$$

$$\text{or} = \frac{(V_i - V_f)}{\Delta t g} \quad (\text{parallel to vehicle path}) \quad (c)$$

$$\text{or} = \frac{(V_i \cos \theta)^2 - V_p^2}{2gS_{\text{long}}} \quad (\text{angle impacts only; perpendicular to vehicle path}). \quad (d)$$

Transverse Deceleration. Average transverse deceleration (perpendicular to barrier) was computed as follows:

$$\text{Trans. } G_{\text{avg}} = \frac{(V_i \sin \theta)^2}{2gS_{\text{lat}}} \quad (e)$$

$$\text{or} = \frac{(V_i \sin \theta)^2}{2g [AL \sin \theta - B (1 - \cos \theta) + D]} \quad (f)$$

The symbols used in the above equations are defined below:

V_i = initial speed, fps;

V_f = final speed or speed at loss of contact for angle impacts, fps;

V_p = speed when vehicle is parallel to barrier, fps;

g = 32.2 ft/sec²;

S_{long} = distance vehicle travels from impact until forward motion stops for head-on tests or distance in contact for angle tests in Equation (b); distance vehicle travels from impact to parallelism in Equation (d), ft;

S_{lat} = distance the vehicle's c.g. travels perpendicular to the barrier from impact to maximum lateral displacement, ft;

Δt = time from impact until forward motion stops for head-on tests or time in contact for angle tests, sec;

θ = initial angle of impact, deg;

AL = distance from vehicle's front end to c.g., ft;

B = one-half vehicle width, ft; and

D = lateral displacement of barrier, ft.

The summary tables and test discussions are divided into the following three categories:

		Chapter IV	
		Page No.	
		Data	Test
		Table	Descrip.
		-----	-----
Part 1.	Vehicle Impact Attenuation Barriers (Crash Cushions Without Redirection Capabilities)		
A.	Rigid (Or Immovable) Wall	4	1.2
B.	Dragnet Vehicle Arresting System	4	1.5
C.	Timber Post Energy Absorbing Barrier	5	1.17
D.	Concrete Pipe Impact System	5	1.21
E.	Polyurethane Foam Impact Attenuation Barrier	5	1.26
Part 2.	Vehicle Impact Attenuation Barriers (Crash Cushions With Redirection Capabilities)		
A.	Modular Crash Cushion (Steel Drums)	6	2.2
B.	The HI-DRO Cushion Vehicle Impact Attenuator	7	2.33
C.	Tor-Shok Energy Absorbing Protective Barrier	7	2.45
D.	Lightweight Cellular Concrete Vehicle Crash Cushion	8	2.49
E.	Corrugated Metal Pipe Crash Cushion	8	2.66
Part 3.	Longitudinal Redirection Barriers		
A.	One-Way Entrapment Guardrail And Median Barrier	10	3.2
B.	Energy Absorbing Bridge Rail (Fragmenting Tube)	10	3.11
C.	Texas T1 Bridge Rail-Guardrail System	11	3.19
D.	New York Box Beam Bridge Rail-Guardrail System	11	3.27
E.	Roto-Shok Energy-Absorbing Barrier	11	3.34
F.	Fiberglas Median Barrier	11	3.39

TABLE IV.1. SUMMARY OF CRASH TEST DATA - VEHICLE IMPACT ATTENUATION BARRIERS
WITHOUT REDIRECTION CAPABILITIES

Test No.	Vehicle				Avg. Decelerations*		Impact Duration msec.	Stopping Distance ft.	Remarks
	Weight lb.	Impact Speed mph	Final Speed mph	Angle of Attack deg.	Long. g	Trans. g			
505-IW	3270	53.3	0	head-on	25.0 ^b	-	99	3.8	Test run for comparison.
					"D R A G N E T"				
505-4A	1460	42	0	head-on	5.8 ^b	-	245	10.2	25,000 lb. metal tape
505-4B	4300	60	0	head-on	6.1 ^b	-	390	19.4	25,000 lb. metal tape
505-4C	1620	48	0	30°	5.5 ^b	-	282	13.8	25,000 lb. metal tape
505-4D	4520	54	0	30°	4.1 ^b	-	476	23.5	25,000 lb. metal tape
505-4E	3760	56	0	head-on	4.0 ^b	-	667	26.3	12,500 lb. metal tape
505-4F	3880	62	17	30°	4.1 ^{b**}	-	490 ^{**}	29.5 ^{**}	Metal tape expended. Vehicle not stopped. 12,500 lb. metal tape
505-3B	3600	57.3	48.8	5°	6.2 ^b	-	61	(4.9) contact	Cable broke--vehicle did not stop (25,000 lb. metal bender)

*Superscript letters refer to equations for computing decelerations discussed at the beginning of this chapter.

**Value given is for interval from impact until tape was expended.

TABLE IV.1. SUMMARY OF CRASH TEST DATA - VEHICLE IMPACT ATTENUATION BARRIERS
WITHOUT REDIRECTION CAPABILITIES (CONTINUED)

Test No.	Vehicle				Avg. Decelerations		Impact Duration msec.	Stopping Distance ft.	Remarks
	Weight lb.	Impact Speed mph	Final Speed mph	Angle of Attack deg.	Long. g	Trans. g			
505-5A	3880	54.5	0 (12.8)	head-on	"T I M B E R P O S T" 3.6 ^b (5.4) ^c		1313 (352)	27.3 (11.7) contact	Vehicle launched and was airborne. Vehicle slowed to 12.8 mph in 352 msec. and 11.7 ft. of penetration.
505-CPA	3950	40.5	21.6	head-on	"C O N C R E T E P I P E" 9.2 ^b		104	(4.3) contact	Vehicle impacted first row of pipe and was launched and was airborne.
505-6A	2060	48.1	0	head-on	"P O L Y U R E T H A N E F O A M B A R R I E R" 19.4 ^b		119	4.0	

TABLE IV.2. SUMMARY OF CRASH TEST DATA - VEHICLE IMPACT ATTENUATION BARRIERS WITH REDIRECTIONAL CAPABILITIES

Test No.	Vehicle				Avg. Decelerations*		Impact Duration msec.	Stopping Distance ft.	Remarks
	Weight lb.	Impact Speed mph	Final Speed mph	Angle of Attack deg.	Long. g	Trans. g			
									"MODULAR CRASH CUSHION (STEEL DRUMS)"
505-1A	3500	22	0	head-on	3.9 ^c	-	265	6.3	
505-1B	3380	63	8	head-on	14.2 ^c	-	177	(8.5) contact	Vehicle launched and was airborne.
505-1C	3520	59	0	head-on	14.2 ^c	-	188	7.1	
505-1D	4480	67	0	head-on	16.7 ^c	-	182	10.4	
505-1E	3200	60.2	0	head-on	9.1 ^b	-	346	13.3	
505 B-A	3000	56.9	0	20°	6.8 ^b	1.1 ^a	290	16.0	Vehicle did not re-direct as intended.
505 B-B	3080	59.3	26.7	20°	7.4 ^b	3.2 ^a	210	(12.6) contact	Vehicle redirected.
505 B-C	4180	46.6	0	head-on	6.2 ^b	-	365	11.7	
505 B-D	4350	56.8	19.0	20°	4.0 ^b	0.6 ^a	624	(24.2) contact	Vehicle redirected.
505 B-E	1500	58.2	0	head-on	9.1 ^b	-	280	12.4	

*Superscript letters refer to equations for computing decelerations discussed at the beginning of this chapter.

TABLE IV.2. SUMMARY OF CRASH TEST DATA - VEHICLE IMPACT ATTENUATION BARRIERS WITH REDIRECTIONAL CAPABILITIES (CONTINUED)

Test No.	Vehicle				Avg. Decelerations		Impact Duration msec.	Stopping Distance ft.	Remarks
	Weight lb.	Impact Speed mph	Final Speed mph	Angle of Attack deg.	Long. g	Trans. g			
505 M-A	4150	56.7	31.1	20°	2.6 ^b	3.9 ^e	513	(29.2) contact	Vehicle redirected.
505 M-B	3990	62.3	51.7	10°	1.3 ^b	3.0 ^e	414	(31.9) contact	Vehicle redirected.
505 M-C	1790	55.8	0	head-on	9.2 ^b	-	257	11.3	
"H I - D R O C U S H I O N"									
505 R-A	1820	42	0	head-on	4.5 ^b	-	740	13.2	
505 R-B	4650	64	0	head-on	7.9 ^b	-	340	17.3	
505 R-C	4410	54	0	20°	5.8 ^b	1.1 ^a	340	16.7	Vehicle did not redirect; anchor cable broke.
505 R-D	1680	59	0	head-on	7.1 ^b	-	580	16.3	
505 R-E	3710	59	25	20°	4.9 ^b	2.0 ^a	340	(19.4) contact	Vehicle redirected.
"T O R - S H O K B A R R I E R"									
505-2A	4600	34.1	0	head-on	6.6 ^b	-	218	5.9	
505-2B	2520	53.5	0	head-on	12.3 ^c	-	198	7.2	

TABLE IV.2. SUMMARY OF CRASH TEST DATA - VEHICLE IMPACT ATTENUATION BARRIERS
WITH REDIRECTIONAL CAPABILITIES (CONTINUED)

Test No.	Vehicle				Avg. Decelerations		Impact Duration msec.	Stopping Distance ft.	Remarks
	Weight lb.	Impact Speed mph	Final Speed mph	Angle of Attack deg.	Long. g	Trans. g			
505-2C	4940	59.4	0	head-on	9.9 ^c	-	273	12.9	
505-2D	5000	49.9	0	30°	8.1 ^c	-	280	14.0	Vehicle did not redirect as intended.
505-2E	3600	53.0	0	25°	8.5 ^b	-	212	10.9	Vehicle did not redirect as intended.
"L I G H T W E I G H T C E L L U L A R C O N C R E T E C R A S H C U S H I O N"									
505 V-A	3650	41.1	0	head-on	6.3 ^b	-	304	9.0	
505 V-B	3200	58.8	0	head-on	10.3 ^b	-	462	11.2	
505 V-C	4560	63.6	0	head-on	6.3 ^b	-	465	21.4	
505 V-D	3790	57.2	49.6	10°	1.3 ^b	2.4 ^a	(286)	(20.4) contact	Vehicle redirected.
505 V-E	3820	59.7	29.3	20°	5.6 ^b	3.3 ^a	(235)	(16.1) contact	Vehicle redirected.
505 V-F	2210	61.2	0	head-on	10.2 ^b	-	364	12.2	
"C O R R U G A T E D M E T A L P I P E C R A S H C U S H I O N"									
505 CSP-1	3750	58.4	0 (39.0)	head-on	4.0 ^b (10.2) ^b	- -	1528 (89)	28.7 (6.2)	Vehicle ramped and became airborne at 89 msec or 6.2 ft. penetration.

TABLE IV.2. SUMMARY OF CRASH TEST DATA - VEHICLE IMPACT ATTENUATION BARRIERS
WITH REDIRECTIONAL CAPABILITIES (CONTINUED)

Test No.	Vehicle				Avg. Decelerations		Impact Duration msec.	Stopping Distance ft.	Remarks
	Weight lb.	Impact Speed mph	Final Speed mph	Angle of Attack deg.	Long. g	Trans. g			
505 CSP-2	3810	59.8	44.9	20°	2.2 ^b	3.4 ^a	(344) contact	(23.8) contact	Vehicle redirected.
505 CSP-3	3880	62.3	0 (42.6)	head-on	4.8 ^b (9.3) ^b	- -	1167 (93)	27.2 (7.4)	Vehicle ramped and became airborne at 93 msec or 7.4 ft. penetration.

TABLE IV.3. SUMMARY OF CRASH TEST DATA - LONGITUDINAL REDIRECTION BARRIERS

Test No.	Vehicle					Barrier		Impact Duration msec	Avg. Decelerations*		Remarks
	Weight	Impact Speed	Final Speed	Impact Angle	Depart. Angle	Lateral Displ. of Rail	Long. Distance in Contact		Long.	Trans.	
	lb	mph	mph	deg.	deg.	ft.	ft.		g	g	
"ONE WAY ENTRAPMENT GUARDRAIL OR MEDIAN BARRIER"											
505-7A	1600	47	30	30	--	1.5	35+	854+	2.1 ^{**c}	2.0 ^{**c}	Vehicle vaulted rail and rolled over.
505-8A	4300	61	41	30	--	2.5	40+	705+	2.2 ^{**c}	1.8 ^{**c}	
505-9A	4180	64	45	20	--	2.0	40+	-	2.1 ^{**c}	2.2 ^{**c}	
505-10A	4400	59	51	10	--	1+	90+	1182+	0.7 ^{**c}	1.7 ^{**c}	
"ENERGY ABSORBING BRIDGE RAIL (FRAGMENTING TUBE)"											
505 FTA	3200	58.3	41.0	25	1±	0.6	21	290	2.1 ^b	5.3 ^f	
505 FTB	4720	54.8	34.0	25	10±	1.2	31	541	2.0 ^b	3.7 ^f	
505 FTC	1560	46.1	33.5	25	1±	0	17	336	2.0 ^b	4.7 ^f	
505 FTD	3270	61.8	26.0	25	5±	2+	32	568	3.3 ^b	4.3 ^f	

*Superscript letters refer to equations for computing decelerations discussed at the beginning of this chapter.
 **Average deceleration is calculated from Equation "c", $V_i - V_f / g\Delta t$, using speeds relative to vehicle's path at initial impact; where V_i is speed going into rail and V_f is speed at loss of contact with the rail. There are at least two longitudinal and two transverse averages calculated for each test, one for every rail impact. For each test, the larger value is reported here.

TABLE IV.3. SUMMARY OF CRASH TEST DATA - LONGITUDINAL REDIRECTION BARRIERS (CONTINUED)

Test No.	Vehicle					Barrier		Impact Duration msec	Avg. Decelerations*		Remarks
	Weight lb	Impact Speed mph	Final Speed mph	Impact Angle deg.	Depart. Angle deg.	Lateral Displ. of Rail ft.	Long. Distance in Contact ft.		Long. g	Trans. g	
"TEXAS T-1 BRIDGE RAIL - GUARDRAIL SYSTEM"											
505 T1A	1860	44.5	26.7	25	35±	0.1	13.1	408	2.2 ^d	4.7 ^e	T-1 Bridge Rail
505 T1B	3920	56.4	26.7	25	0	0.1	13.0	265	4.7 ^d	5.4 ^e	T-1 Bridge Rail
505 T1C	3670	58.0	39.8	25	45±	1.8	15.0	482	2.2 ^d	3.9 ^e	Guardrail Transition
505 T1D	3620	61.4	54.3	25	15±	0.1	14.5	257	0.2 ^d	6.8 ^e	Mod. T-1 Bridge Rail
"NEW YORK BOX BEAM BRIDGE RAIL - GUARDRAIL SYSTEM"											
505 NYA	3800	55.4	--	25	0	0.2	21.3	---	1.3 ^d	4.8 ^e	Vehicle Pocketed and Spun Out
505 NYB	3670	57.9	36.2	25	15±	1.2	20.0	541	2.1 ^d	5.1 ^e	
"ROTO-SHOK BARRIER"											
505-2F	4290	46.0	34.6	25	0	4.0	27.3 ^{**}	500	1.1 ^b	3.2 ^a	
"FIBERGLAS MEDIUM BARRIER"											
505 FGA	4150	54.0	0	25	0	5.3	38.0	946	2.6 ^b	2.2 ^e	Vehicle Snagged and Stopped

*Superscript letters refer to equations for computing decelerations discussed at the beginning of this chapter.

**Distance vehicle moved in contact with barrier.

C H A P T E R I V --- Part 1

Vehicle Impact Attenuation Barriers

(Crash Cushions Without Redirection Capabilities)

Part 1. A. --- RIGID (OR IMMOVABLE) WALLBARRIER AND TEST DESCRIPTION

Test 505-IW involved a 1963 Plymouth sedan impacting a rigid wall head-on at 53.3 mph (see Figures IV.1.A.1 and .2.) The 2 ft by 5 ft by 10 ft concrete wall which was used exceeded all SAE J 850 requirements. The 3270 lb vehicle was stopped in 3.8 ft, all of which was attributed to dynamic vehicle deformation. As expected, the peak longitudinal deceleration was high (35.0 g's), as was the average longitudinal deceleration (25.0 g's).

The results from this test were compared to those of other head-on crash tests and aided in the evaluation of the barriers.

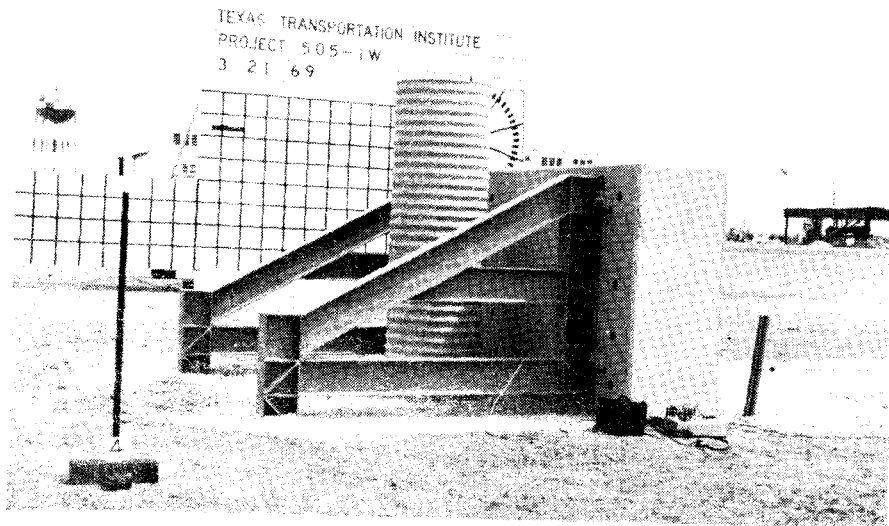


FIGURE IV.1.A.1. RIGID WALL AND VEHICLE, TEST 505-1W.

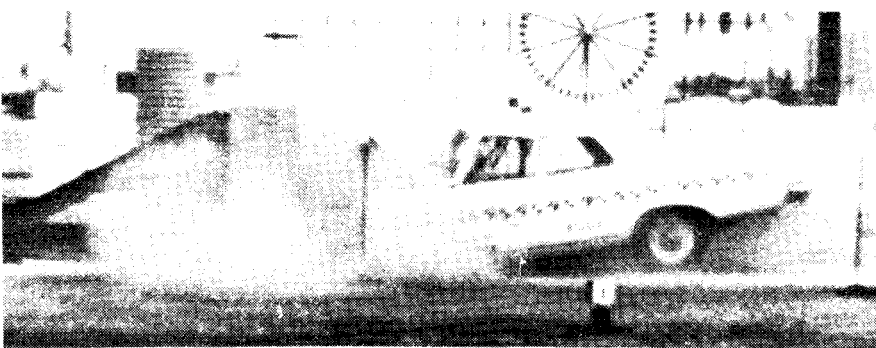
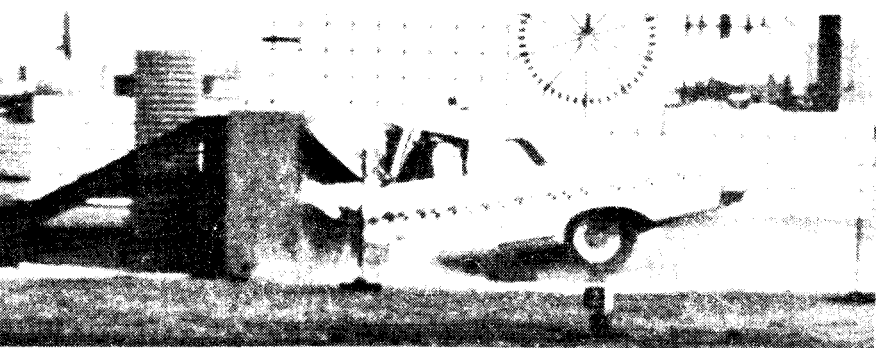
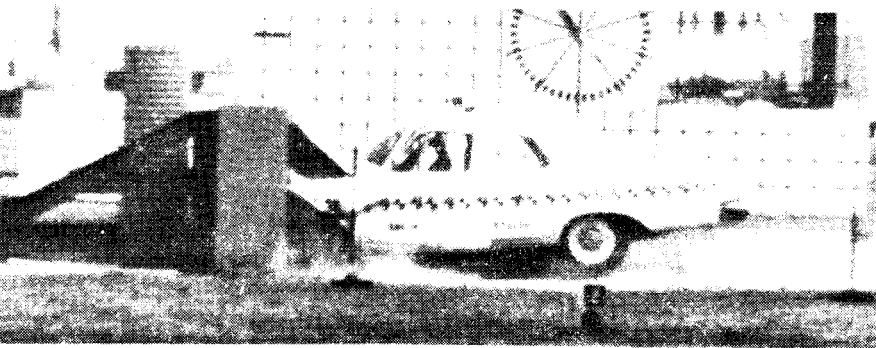
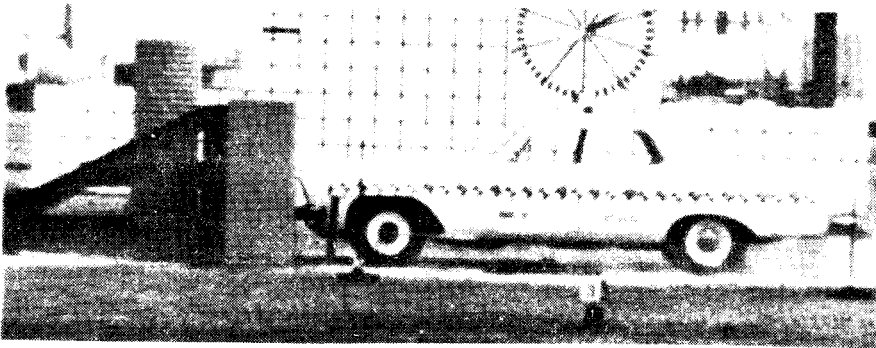


FIGURE IV.1.A.2. SEQUENTIAL PHOTOGRAPHS OF TEST 505-IW.

Part 1. B. --- "DRAGNET" VEHICLE ARRESTING SYSTEMDESCRIPTION OF ARRESTING SYSTEM

This system consists of a net made of steel cables attached at each end to Metal Bender energy absorbing devices as shown graphically in Figure IV.1.B.1. The Metal Benders, which are supported on rigid steel posts, are steel boxes containing a series of rollers around which the metal tape is bent back and forth as it is pulled through the case. Each end of the net is attached to one end of the metal tape extending from a Metal Bender. The Metal Benders are designed so that a specified force will be necessary to pull the metal tape through the case. This force is relatively independent of speed and environmental conditions and depends on the size of the tape used. By varying tape size, a number of different tape forces are available. Photographs of the arresting system used in these tests are shown in Figures IV.1.B.2. and IV.1.B.3.

TEST RESULTS

Test 505-4A involved a lightweight vehicle (1460 lb) directed head-on into the dragnet at a speed of 42 mph (see Figure IV.1.B.4.). The tape force for each Metal Bender was 25,000 lb. All components of the system performed as designed and the vehicle was stopped after penetrating 10.2 ft. The Metal Bender strap pullout accounted for 63% of the vehicle's initial kinetic energy of 87.1 kip-ft. The remaining energy was expended in stretching the net, crushing the vehicle, and increasing the vehicle's potential energy due to raising the center of gravity. The amount expended in increasing gravitational potential energy was only about one kip-ft.

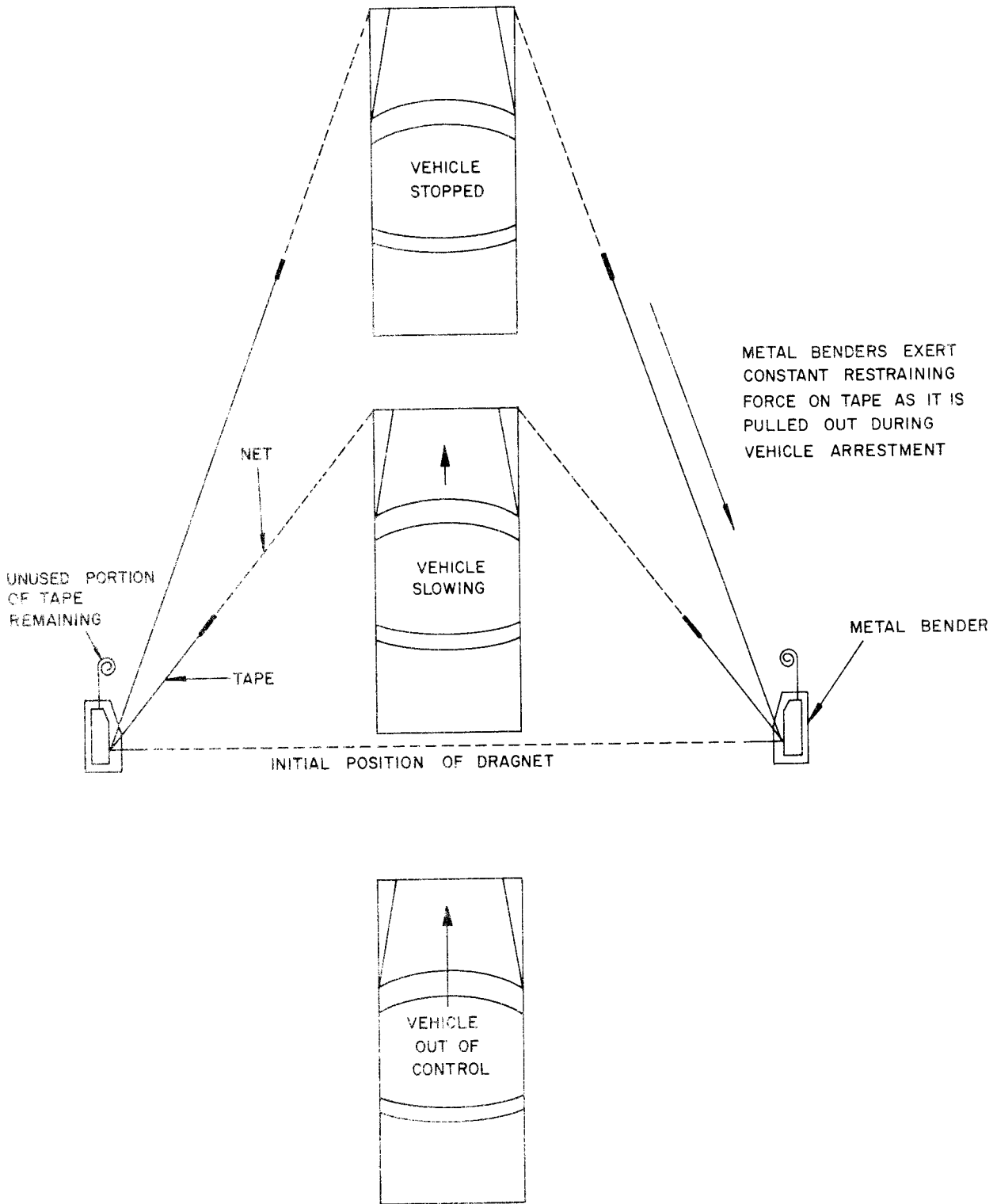


FIGURE IV.1.B.1. IDEALIZED FUNCTION OF DRAGNET ARRESTING SYSTEM

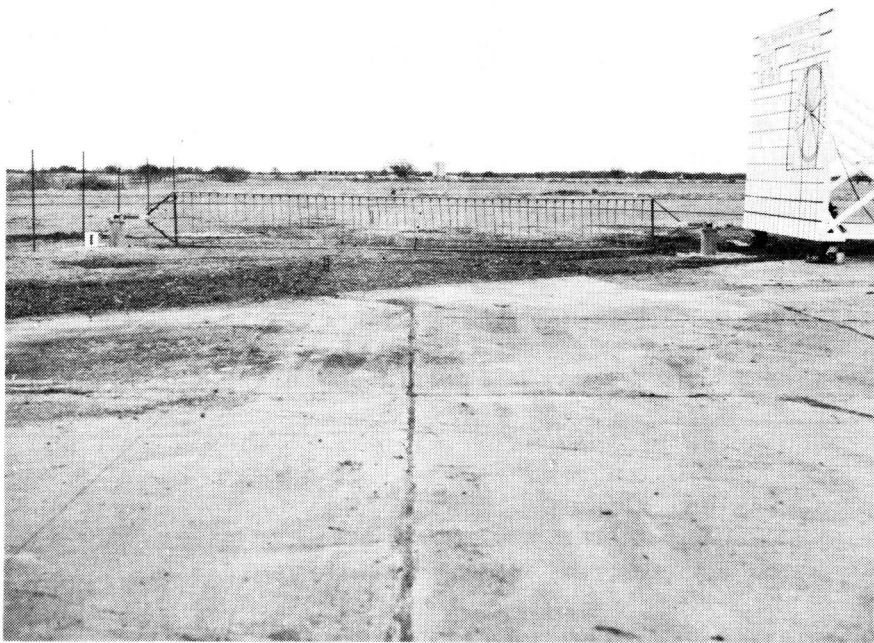
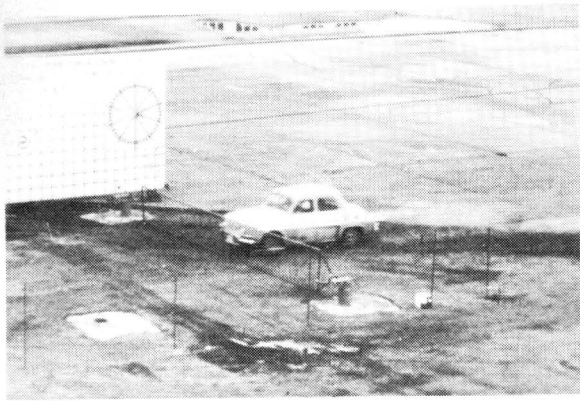


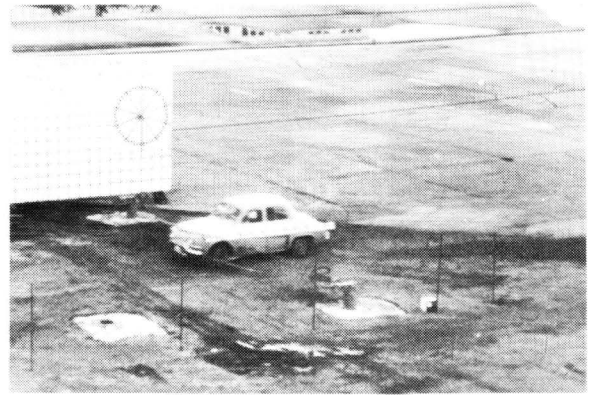
FIGURE IV.1.B.2. DRAGNET VEHICLE ARRESTING SYSTEM BEFORE TEST 505-4A



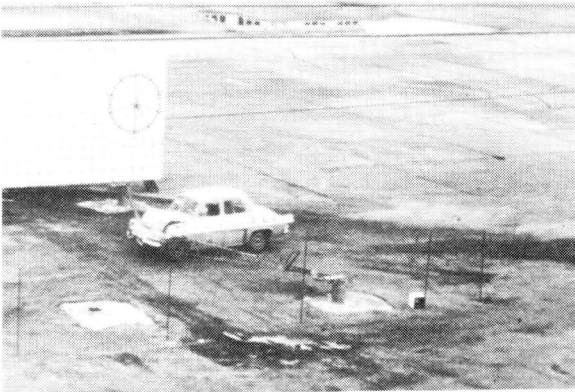
FIGURE IV.1.B.3. METAL BENDER WITH 25,000 LB. TAPE ATTACHED TO NET.



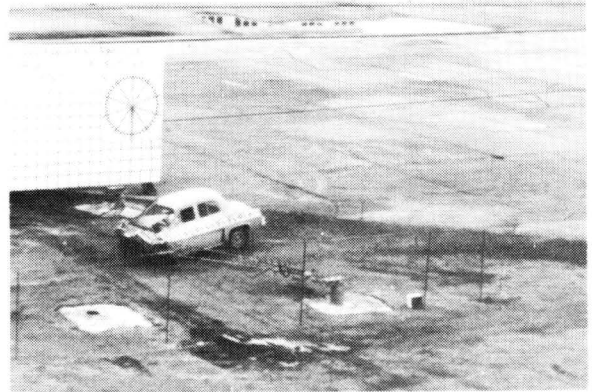
1



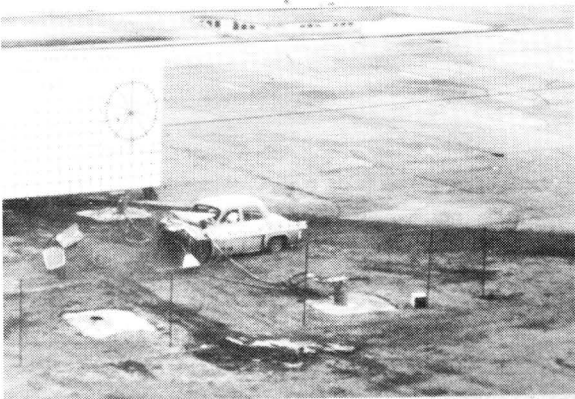
2



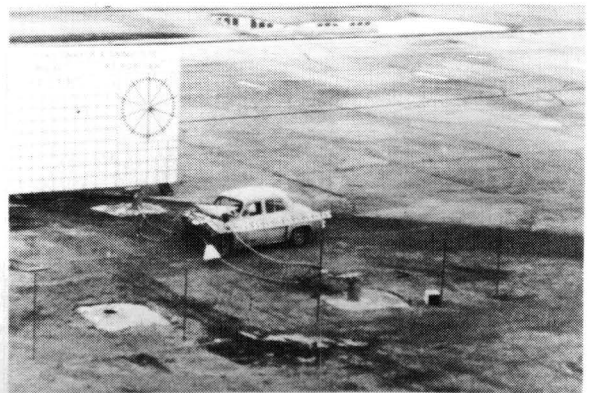
3



4



5



6

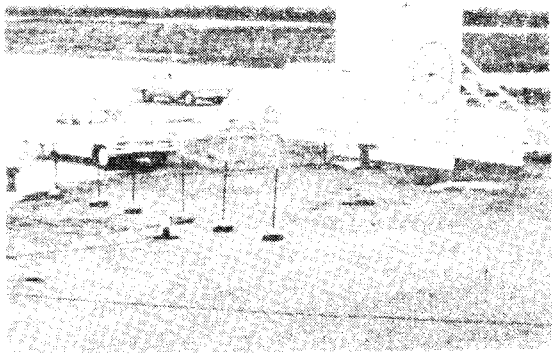
FIGURE IV.1.B.4. SEQUENTIAL PHOTOGRAPHS OF TEST 505-4A

The damage to the front of the vehicle was severe. The maximum longitudinal deceleration was 16 g's. The average deceleration was 5.8 g's over 0.245 seconds.

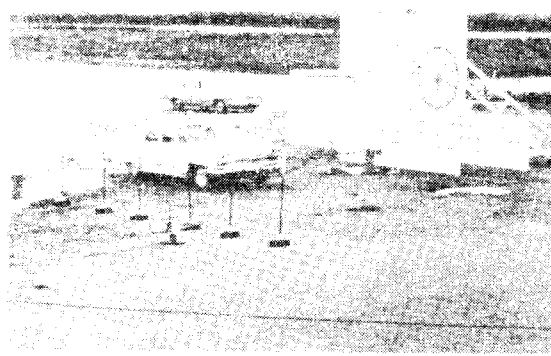
For Tests 4E and 4F in this series, the Metal Bender tape load was decreased to 12,500 lb and the net was raised about 4 in. off the ground to better entrap the front of the vehicles. Test 4E was conducted with a heavy vehicle (3760 lb) which was directed head-on into the dragnet at a speed of 56 mph (see Figure IV.1.B.5.). The vehicle was stopped in 26.3 ft and pulled out a total of 30.7 ft of tape, which is equivalent to 384 kip-ft, or 96% of the vehicle's kinetic energy. The vehicle had no significant rotational energy at maximum penetration, but had gained about 7 kip-ft of gravitational potential energy. The vehicle damage was minor, as would be expected since the maximum deceleration was only 7.0 g's, and the average deceleration was 4.0 g's.

CONCLUSIONS

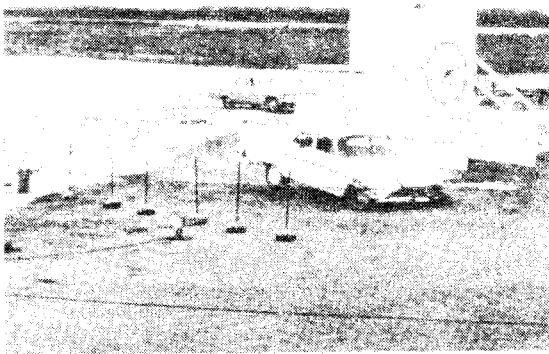
The Van Zelm dragnet vehicle arresting system performed basically as designed in all tests. The performance of the system was very good in four of the six tests. In Test 4D the dragnet was engaged too low on the front of the vehicle, which resulted in the vehicle's rear end vaulting the net after most of the longitudinal deceleration had occurred (see Figure IV.1.B.6.). In Test 4F the performance of the dragnet system was ideal until one of the tapes ran out (see Figure IV.1.B.7.). Had this tape been long enough to continue applying load until the vehicle was completely stopped, the performance probably would have been excellent. The energy absorbed by the Metal Benders ranged from 50% to 70% of the vehicle's



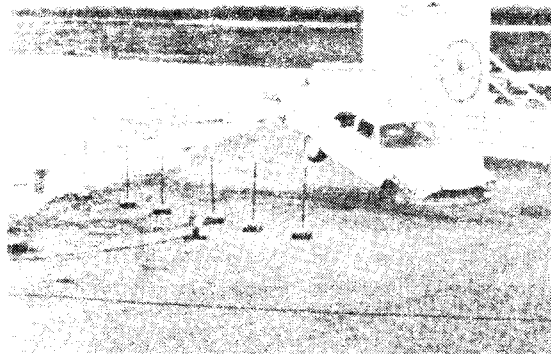
1



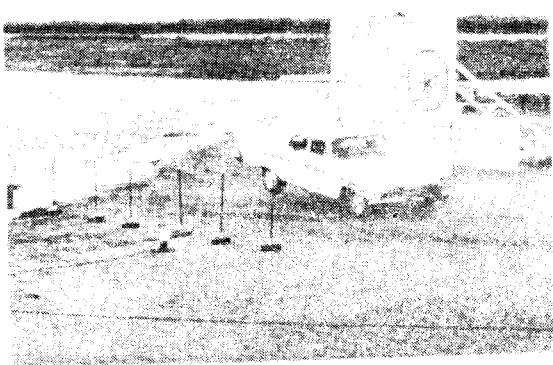
2



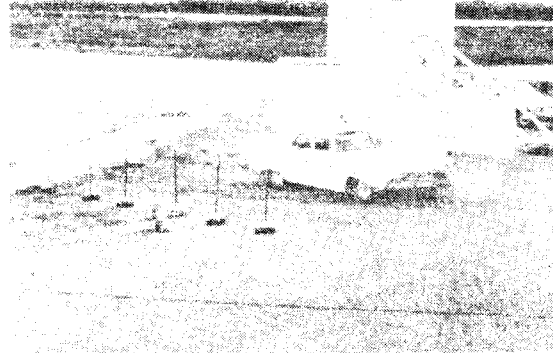
3



4



5

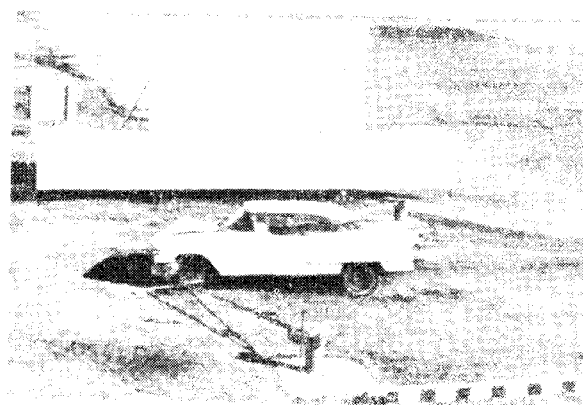


6

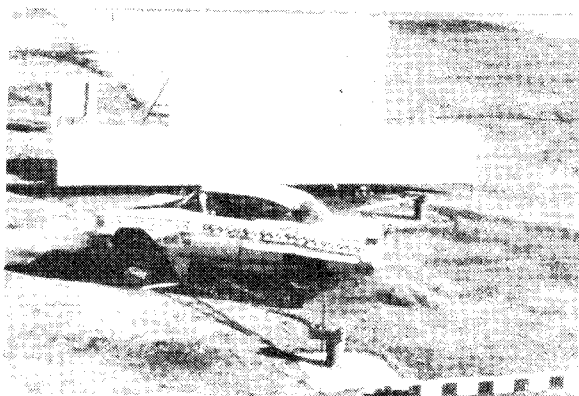
FIGURE IV.1.B.5. SEQUENTIAL PHOTOGRAPHS OF TEST 505-4E



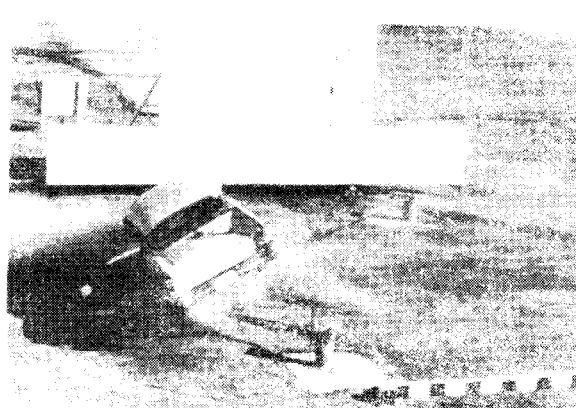
1



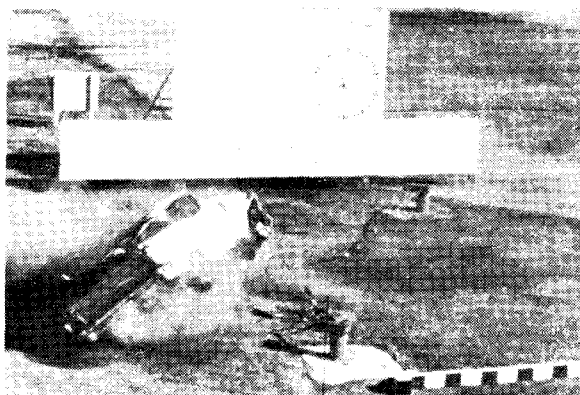
2



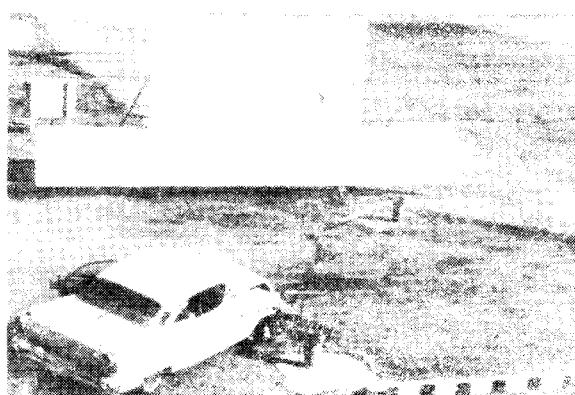
3



4

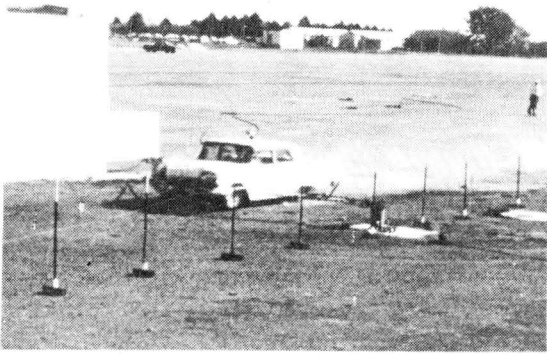


5

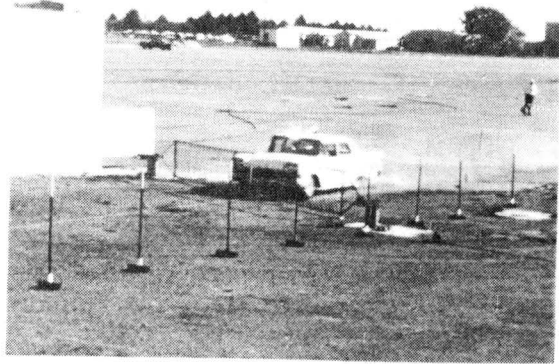


6

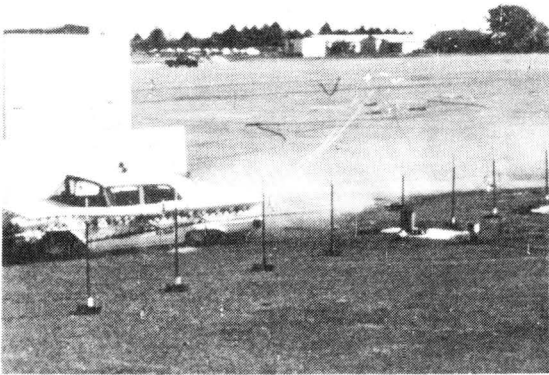
FIGURE IV.1.B.6. SEQUENTIAL PHOTOGRAPHS OF TEST 505-4D SHOWING BEHAVIOR OF NET DURING ARRESTMENT.



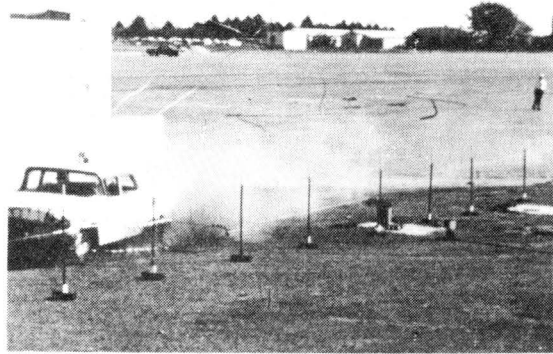
1



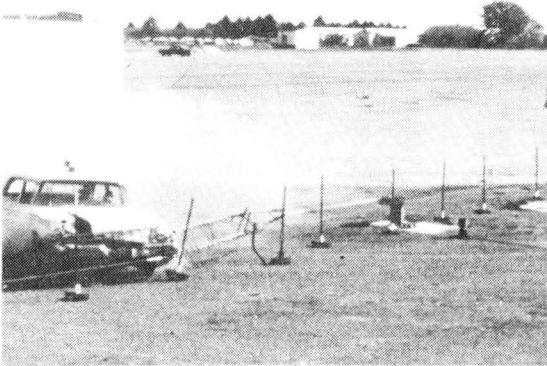
2



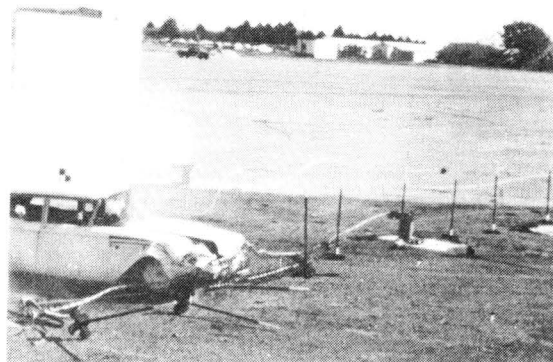
3



4



5



6

FIGURE IV.1.B.7. SEQUENTIAL PHOTOGRAPHS OF TEST 505-4F

initial kinetic energy for the first four tests which used the 25 kip tape loads. In the last two tests, the percent of energy absorbed by the Metal Benders ranged from 89% to 96%. Deceleration levels were reduced to a small fraction of those which would be expected in rigid barrier impacts. Increasing design tape load results in shortening the stopping distance, increasing the deceleration level, and increasing vehicle damage. For any given application of the dragnet system, the longer the allowable stopping distance, the more desirable are the deceleration characteristics of the system because a smaller tape load can be used.

The height of the net was shown to be an important factor in the performance of the system. The net should be positioned so that it completely entraps the front of the entering vehicle. If it is too low, a less desirable performance may be expected, as was found in Test 4D. Good performance was found when the lower main cable of the net was positioned 4 in. above the ground.

No permanent damage was sustained by the dragnet system during any of these tests. All major components were reusable except for the expendable metal tapes. The system can be applied to a variety of situations by varying the Metal Bender tape tension, the tape length, and the geometry of the installation. A variety of Metal Bender tape tensions are available.

This series of tests has shown that reasonably accurate predictions of vehicle stopping distance and deceleration levels can be obtained using the equations developed in Appendix B of Technical Memorandum 505-4 and given in Appendix F of this report. Detailed information concerning the other tests in this series, as well as recommendations for uses and modifications to the "Dragnet", are also available in Technical Memorandum 505-4.

A SECOND ARRESTING SYSTEM

Another arresting system employing Metal Benders and the use of a hook and cable system was tested to determine the feasibility of snagging a vehicle to bring it to a stop. A steel hook was welded to the frame of the vehicle. Each end of a 7/8 in. diameter steel cable 50 ft long was attached to a 25,000 lb capacity Metal Bender. The Metal Benders were anchored 12 ft apart and the cable was placed in a lazy W position and blocked up at the center 5 in. off the ground so the vehicle hook could engage it (see Figure IV.1.B.8.).

TEST RESULTS

The 3600 lb vehicle in test 505-3B engaged the cable at an angle of 5° while traveling at a speed of 57.3 mph. The cable broke 0.061 sec after the cable became taut and began exerting forces on the vehicle. During those 0.061 sec, the vehicle speed slowed to 48.8 mph over 4.9 ft of travel (see Figure IV.1.B.9.). This imposed an average longitudinal deceleration on the vehicle of 6.2 g's. Approximately 13.5 in. of tape was pulled out of each Metal Bender, accounting for approximately 56,000 ft-lbs of energy consumed. The cable apparently broke because of the sharp bend it made around the vehicle snagging hook.

Additional information about this test can be found in Technical Memorandum 505-20, given in Appendix F.

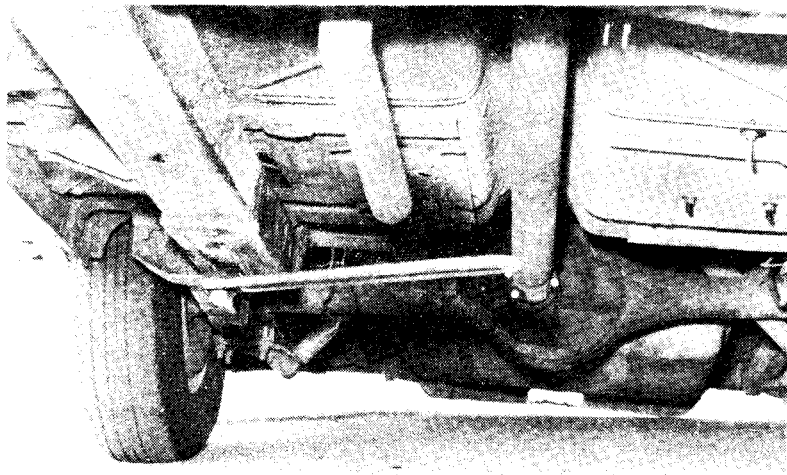
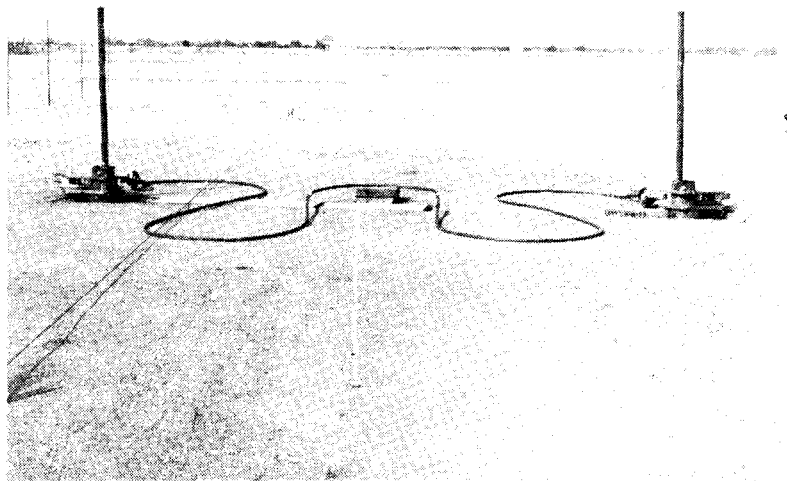


FIGURE IV.1.B.8. CABLE & METAL BENDER POSITION AND STEEL HOOK ATTACHED TO VEHICLE, BEFORE TEST 505-3B.

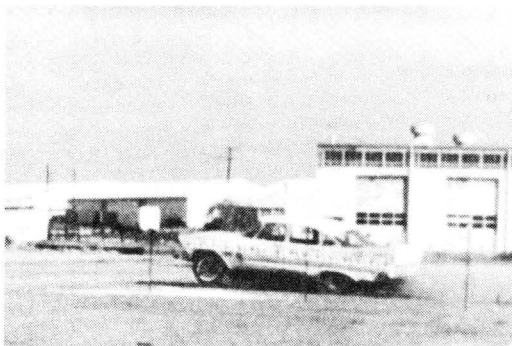
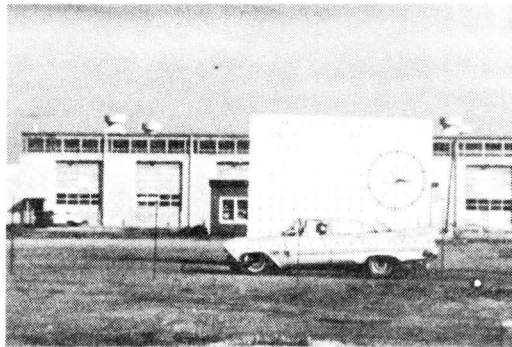
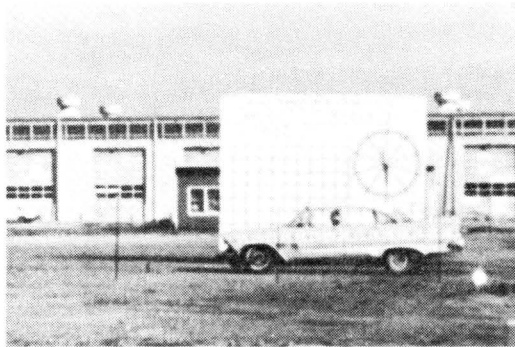
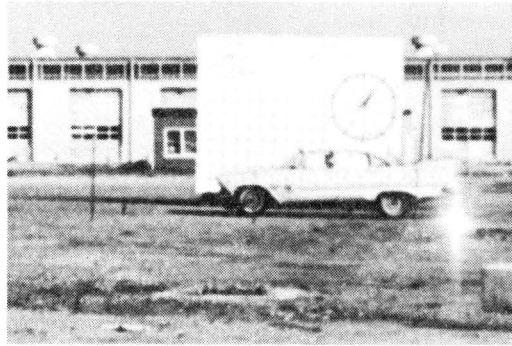
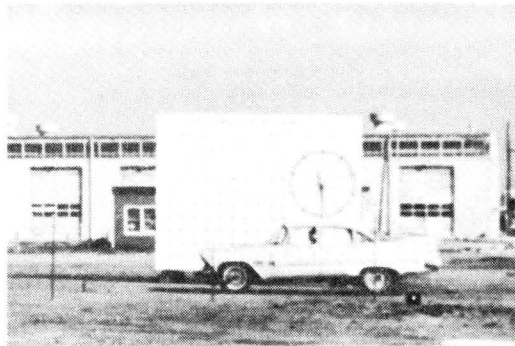
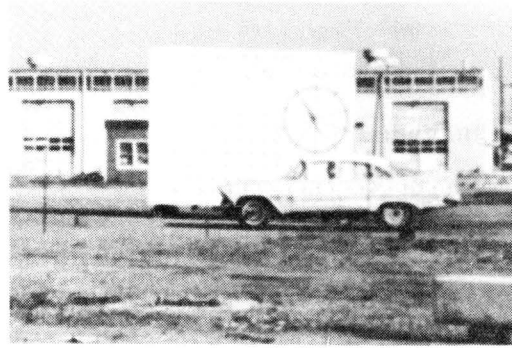
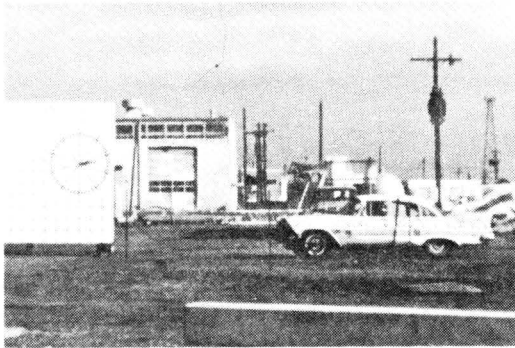


FIGURE IV.1.B.9. SEQUENTIAL PHOTOGRAPHS OF TEST 505-3B.

Part 1. C. --- TIMBER POST ENERGY ABSORBING BARRIERBARRIER DESCRIPTION

The purpose of the timber post energy absorbing protective barrier was to stop vehicles at low levels of deceleration. The system consisted of 49 creosoted timber posts, 6 in. in diameter by 6 ft long. The posts were embedded 3 ft in clayey soil. Behind the array of posts was a 2 ft diameter concrete post surrounded by a 3-ft thick shell of polyurethane foam. Figure IV.1.C.1. is a graphical representation of the system tested. At impact, the bending over of successive posts in the soil is intended to absorb the kinetic energy of the vehicle. The resistance provided by each timber post bending over in the soil exerts a stopping force on the vehicle. The cumulative effect of these forces provided by the posts was intended to decelerate the vehicle to the final condition of zero velocity.

TEST RESULTS

The 3880 lb vehicle struck the timber post barrier head-on at a speed of 54.5 mph. The barrier did not function as intended. The vehicle ramped on the posts and became airborne approximately 0.352 sec after initial contact. The change in speed at this time was 41.7 mph. The average longitudinal deceleration over the initial 0.352 sec interval was 5.4 g's; the peak longitudinal deceleration was 20 g's. The vehicle remained airborne for 0.96 sec, coming to rest on top of the posts. The vehicle damage was severe and damage to the timber post barrier was moderate.

Analysis of the high-speed films revealed that the front rows of posts were pushed over as intended, but that these "pushed-over" posts formed a ramp which resulted in the vehicle becoming airborne. The soil surrounding

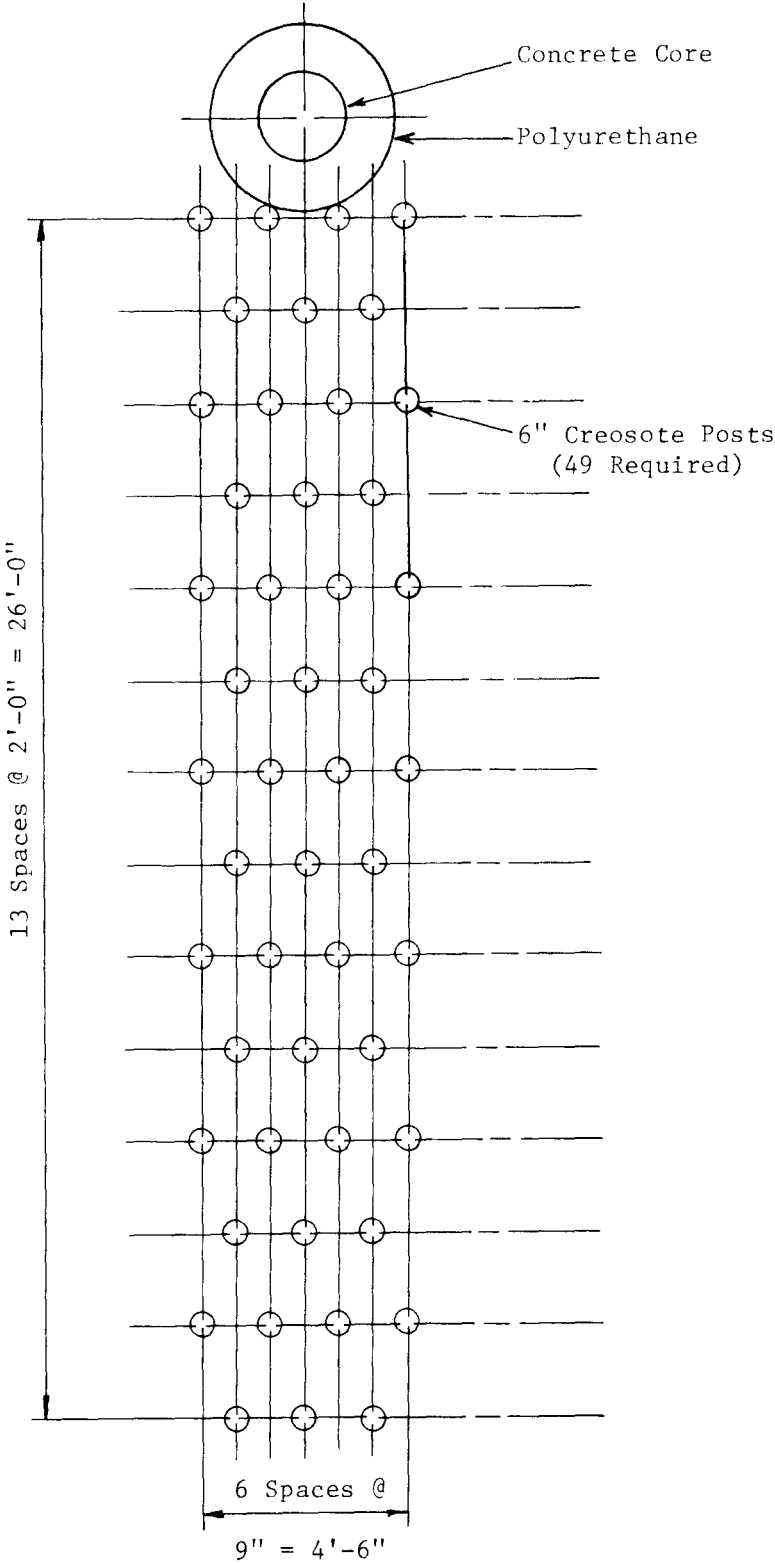


FIGURE IV.1.C.1. TIMBER POST ENERGY ABSORBING PROTECTIVE BARRIER

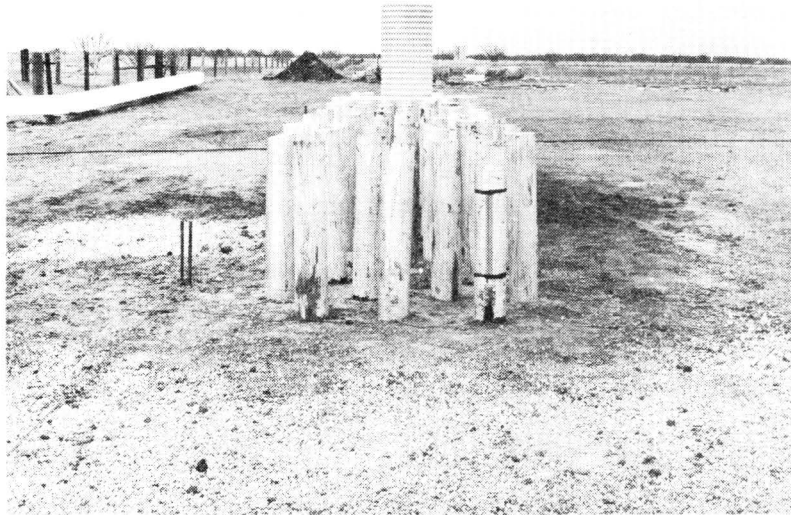


FIGURE IV.1.C.2. WOODEN POSTS BEFORE COLLISION



FIGURE IV.1.C.3. POSTS AND VEHICLE AFTER COLLISION
INITIAL VEHICLE SPEED 54.5 MPH
STOPPING DISTANCE 27.3 FT.,
AVERAGE VEHICLE DECELERATION 5.4 g's
(over first 0.352 sec following contact).

the timber posts and the depth of embedment has a great effect on the mode of energy transfer and also on the magnitude of the decelerations. The post spacing also appears to be a significant factor. Although the crash test did not yield the desirable behavior, modifications of this timber post barrier design and an awareness of the soil influence on the failure mode and magnitude of energy absorption may result in an effective timber post energy absorbing protective barrier.

Additional information concerning this test can be found in Technical Memorandum 505-5 which is included in Appendix F.

Part 1. D. --- CONCRETE PIPE IMPACT SYSTEMBARRIER DESCRIPTION

Sixteen reinforced concrete sewer pipes were arranged in five rows (3 rows, 4 pipes wide; and 2 rows, 2 pipes wide) as shown in Figure IV.1.D.1. The first 4 rows were 10 ft apart (center to center). The last row was only 5 ft behind the row preceding it. The pipes were spaced 4 ft apart (center to center) within each row. These reinforced concrete pipes had an outside diameter of 30 in. and a length of 75 in. The reinforcement was 3 x 8-6/8 welded wire fabric. The pipes were embedded 4 ft 3 in. in the soil and the interior of the pipes was filled with soil to ground level. Details of a single pipe are shown in Figure IV.1.D.2.

TEST DESCRIPTION

Based on pendulum tests conducted by the Southwest Research Institute^{1*} on various transite, vitrified clay, and concrete pipes, it was decided to conduct a full-scale crash test on a reinforced concrete sewer pipe crash cushion, since it seemed apparent that this pipe would give the highest values of fracture energy. By starting with the highest value, it was assumed that some interpolation could be made in predicting the fracture characteristics of the smaller pipes.

A 3950 lb vehicle impacted the system head-on at a speed of 40.5 mph. After shattering the two pipes in the first row, the vehicle ramped, became airborne, and finally came to rest on top of the third row of pipes (see Figure IV.1.D.3.). The first row of pipes was completely shattered and the soil was disturbed when the pipes began to tilt in the ground, but the rest of the system remained in tact and sustained little damage.

*Superscript numbers refer to references at the end of this chapter.

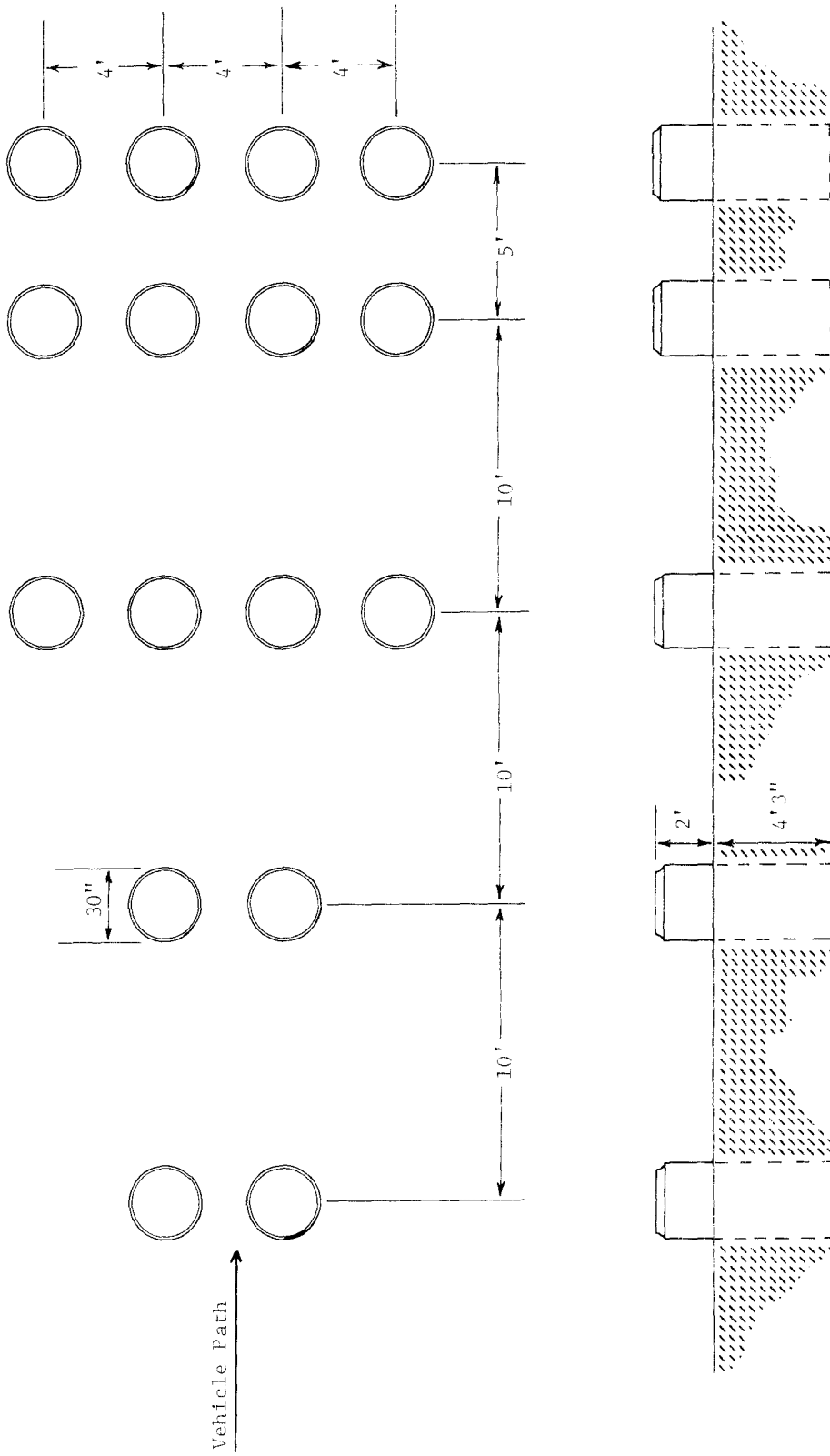


FIGURE IV. 1. D. 1. CONFIGURATION OF REINFORCED CONCRETE PIPE CRASH CUSHION

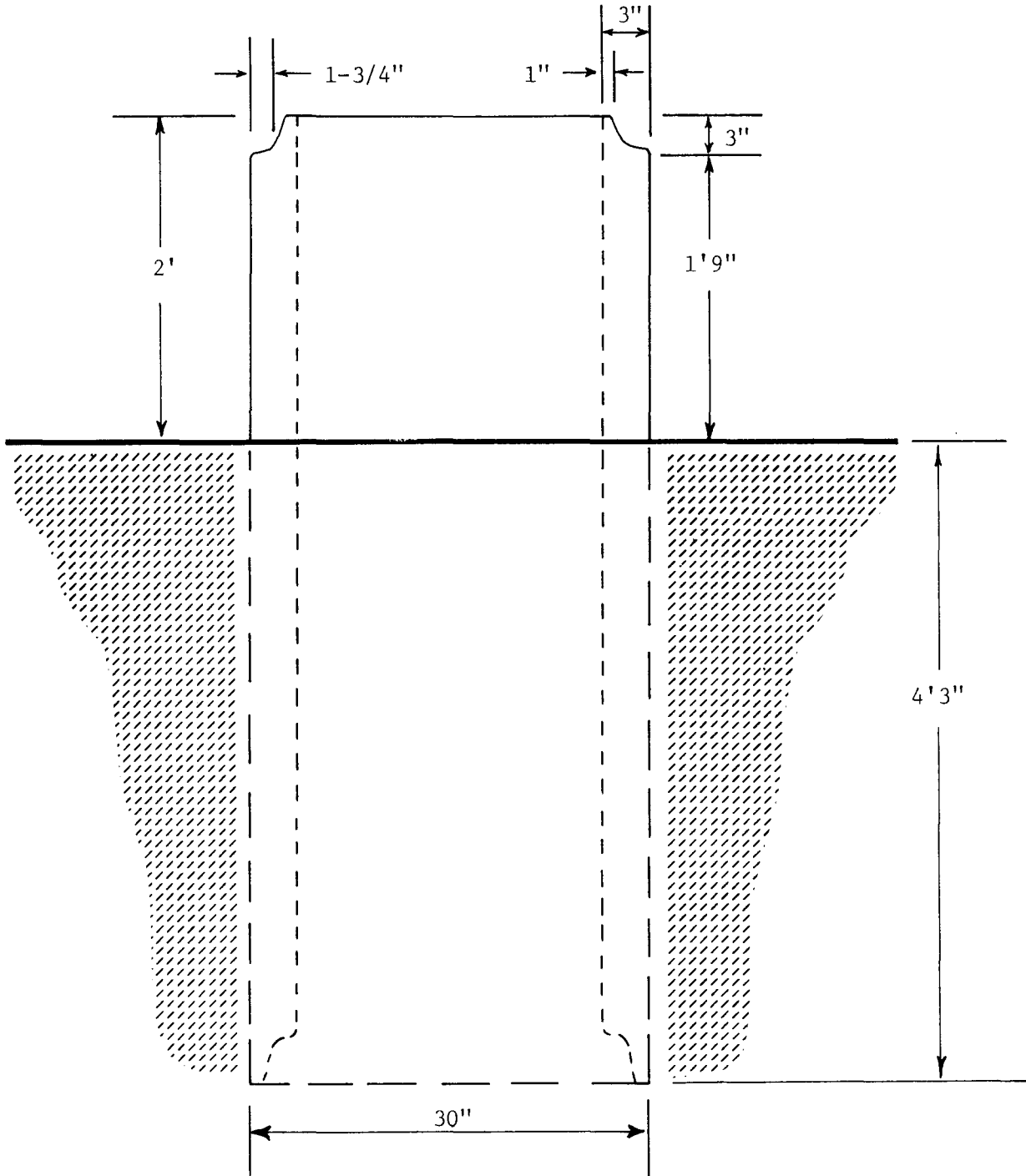


FIGURE IV.1.D.2. DETAILS OF ONE REINFORCED CONCRETE PIPE

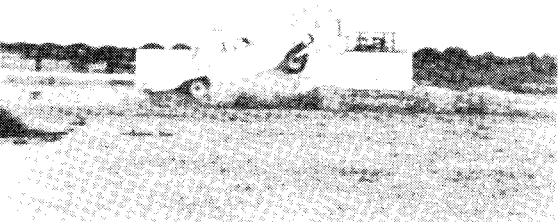
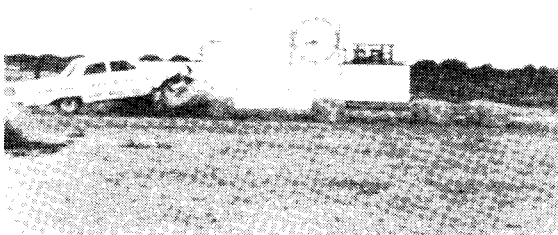


FIGURE IV.1.D.3. SEQUENCE PHOTOGRAPHS OF TEST 505 CP-A.

Average deceleration from the film was 9.2 g's over 4.3 ft of travel and 0.104 sec (accelerometer traces showed no more forces on the vehicle after this time). Vehicle damage was moderate, with a front-end deformation of 1.3 ft.

CONCLUSION

Since the reinforced concrete pipe tested gave a maximum deceleration of approximately 20 g's, and an average deceleration of approximately 9 g's, it would be desirable to reduce these deceleration levels in any subsequent tests. A better selection of pipe might be the transite 20 in. O.D. pipe which was used in Test #2 in the report by Michie and Bronstad.¹ This should reduce the deceleration levels to approximately 5 g's average and 10 g's maximum. By reducing the force level developed by each row of pipe, the ramping tendency should also be reduced. Whether or not this ramping tendency can be reduced to a level which would make this type of cushion feasible is a matter of speculation.

It was shown that concrete pipe crash cushions have the capability of absorbing enough kinetic energy to stop a vehicle in a reasonable distance, and thus should be considered a definite possibility for development.

Part 1. E. --- POLYURETHANE FOAM IMPACT ATTENUATION BARRIERBARRIER DESCRIPTION

The polyurethane foam barrier consisted of a mass of polyurethane foam surrounded by a sheet of 16-gage sheet steel. The barrier was held in place by 4 in. diameter wood posts. The entire barrier rested flush with the ground. Blocks of polyurethane foam were placed in the sheet steel form, and the upper surface was coated with water-proof mastic. The density of the foam in the front half of the barrier was 1.94 pcf with a crushing strength of approximately 20 psi; while that of the foam in the rear half was 2.72 pcf, with a crushing strength of approximately 35 psi. The barrier was 36 in. high by 66 in. wide by 20 ft long. Figure IV.1.E.1. is a photograph of the barrier prior to the crash test.

TEST RESULTS

A lightweight vehicle (2060 lb) was directed into the barrier head-on with an initial speed of 48.1 mph (see Figure IV.1.E.2.). During the collision, the vehicle's wheels lost contact with the ground, and the front portion of the barrier was slightly lifted. The wooden post in the barrier at the point of impact was completely severed, while four other posts were displaced by varying amounts. During the test, several large pieces of the polyurethane foam were propelled up and out of the barrier. The high-speed films show that this disintegration occurred just before the vehicle had been brought to a stop, and therefore it is unlikely that it had a significant effect on the outcome of this test. The vehicle was stopped 4.0 ft after impact, resulting in an average deceleration of 19.4 g's.

This particular barrier design was not satisfactory, especially for lightweight vehicles, due to the excessive stopping force and consequently

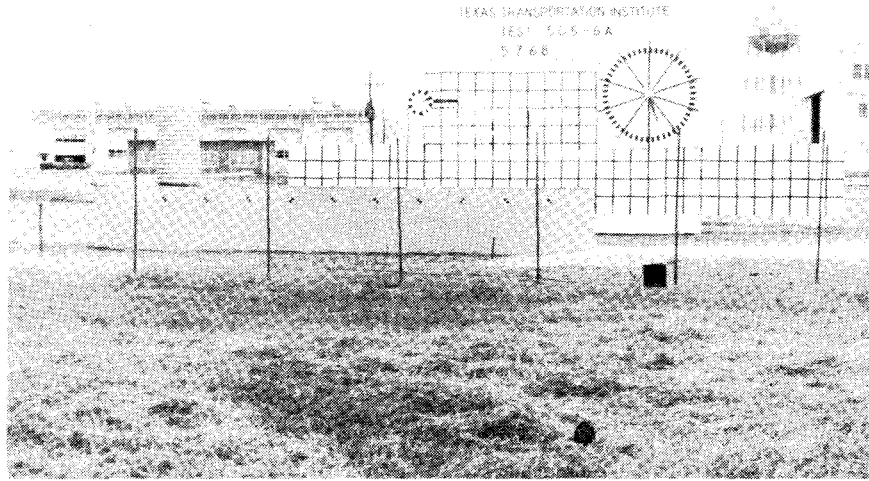


FIGURE IV.1.E.1. POLYURETHANE FOAM BARRIER BEFORE COLLISION. TEST 6A.

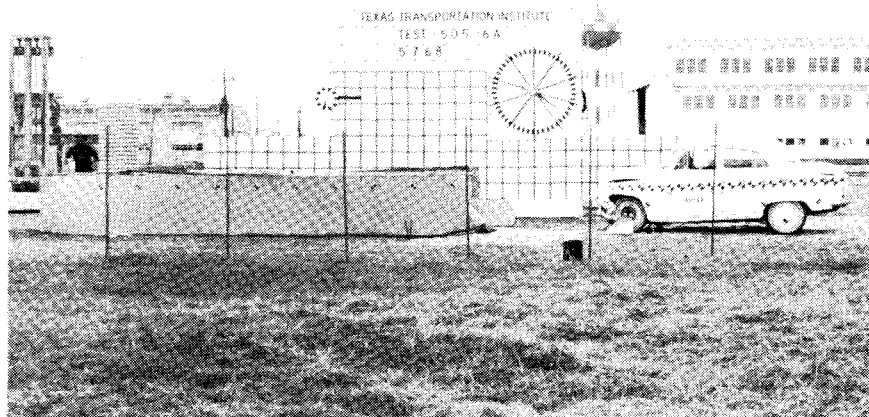


FIGURE IV.1.E.2. POLYURETHANE FOAM BARRIER AND VEHICLE AFTER COLLISION.

high deceleration levels that it produced. The post at the nose of the barrier seemed to contribute significantly to the damage sustained by the vehicle, since the force exerted by the post was concentrated on a small area of the vehicle's front end.

The authors believe that certain modifications to this type of barrier could result in an adequate impact attenuator. The following modifications should be considered:

1. Decrease the strength of the barrier by decreasing the strength of the polyurethane foam, reducing frontal area of the foam, or by incorporating voids in the barrier.

2. Omit the stabilizing posts and use a cable anchorage system. This would remove the semi-rigid areas from the periphery of the barrier. The cable system should provide the barrier with lateral stability for side or angled impacts, but have little effect on the longitudinal properties of the barrier.

3. Pour the polyurethane foam continuously using the sheet steel covering as the form. This should reduce or eliminate the tendency for large blocks to fly out during impact.

4. Elevate the barrier, or increase its overall height, to reduce the tendency of the vehicle to "ramp" during head-on collisions.

Technical Memorandum 505-6 contains an idealized theory for use in predicting stopping distances for head-on impacts of this system. Additional test data can also be found in the memorandum which is included in Appendix F of this report.

C H A P T E R I V --- Part 2

Vehicle Impact Attenuation Barriers
(Crash Cushions With Redirection Capabilities)

Part 2. A. --- MODULAR CRASH CUSHION (STEEL DRUMS)EARLIEST DESIGNS AND TESTS

Predecessors to the modern Modular Crash Cushion included such configurations as: burlap bags filled with empty beverage cans; eight 55-gallon steel drums filled with empty beverage cans; fifteen 55-gallon drums filled with empty beverage cans; and twenty-nine 55-gallon drums filled with empty beverage cans.

The first barrier (505-1A) consisted of 21 burlap bags filled with empty beverage cans and held together with poultry wire. The bags were arranged as shown in Figure IV.2.A.1. A 3500 lb Ford impacted the system head-on at a speed of 22 mph. The vehicle was stopped after traveling 6.3 ft at an average deceleration of 3.9 g's. Vehicle damage was very minor as shown in Figure IV.2.A.2.

The next design (505-1B) tested is shown in Figure IV.2.A.3. Eight 55-gallon steel drums filled with empty beverage cans were arranged between 7 in. diameter posts. The initial speed of the 3380 lb vehicle was 63 mph. Shortly after impacting the drums head-on, the vehicle ramped and came to a stop on top of the barrier. Average deceleration was 14.2 g's with a peak of 40.0 g's. The vehicle was damaged considerably and is shown in Figure IV.2.A.4.

In 505-1C, fifteen 55-gallon steel drums filled with empty beverage cans were arranged 3 drums wide and 5 drums deep. See Figure IV.2.A.5. A 3520 lb Plymouth impacted the barrier head-on at a speed of 59 mph. The vehicle received severe damage. The vehicle and barrier after the test are shown in Figure IV.2.A.6. The average deceleration was 14.2 g's over a distance of 7.1 ft.

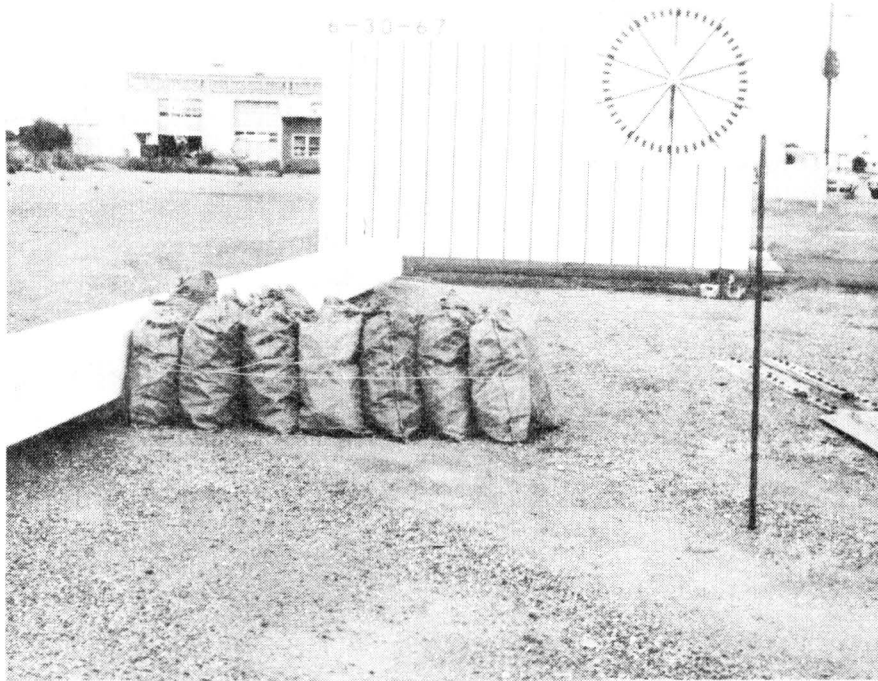


FIGURE IV.2.A.1. BURLAP BAGS FILLED WITH EMPTY BEVERAGE CANS BEFORE TEST 505-1A.



FIGURE IV.2.A.2. VEHICLE AFTER TEST 505-1A.

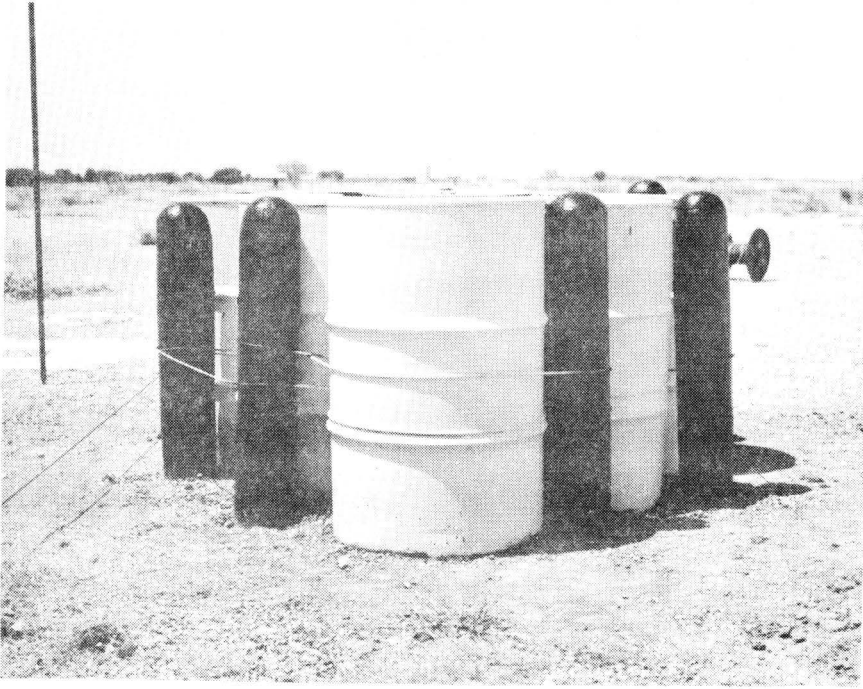


FIGURE IV.2.A.3. EIGHT 55-GALLON DRUMS FILLED WITH EMPTY BEVERAGE CANS BEFORE TEST 505-1B.



FIGURE IV.2.A.4. VEHICLE AND BARRIER AFTER TEST 505-1B.



FIGURE IV.2.A.5. FIFTEEN 55-GALLON STEEL DRUMS FILLED WITH EMPTY BEVERAGE CANS BEFORE TEST 505-1C.



FIGURE IV.2.A.6. VEHICLE AND BARRIER AFTER TEST 505-1C.

The barrier for the next test (505-1D) consisted of twenty-nine 55-gallon drums filled with empty beverage cans with nine rows of 3 drums wide and the first row was 2 drums wide. See Figure IV.2.A.7. This cushion was hit head-on by a 4480 lb vehicle traveling 67 mph. The vehicle was stopped after 10.4 ft of travel with an average deceleration of 16.7 g's. The vehicle sustained considerable damage as shown in Figure IV.2.A.8. Additional information on these tests can be found in Technical Memorandum 505-19, included in Appendix F of this report.

These four tests clearly indicated that the crushing strength of the barrels had to be decreased and the empty beverage cans had to be removed in order to reduce the g levels encountered and to minimize vehicle damage. Static crush tests were conducted on uncut, tight-head 55-gallon steel drums and on 55-gallon steel drums with four elliptical holes cut in the top and bottom of the barrel. Results of these static tests indicated the importance of removing some of the metal from the top and bottom of the drum in order to reduce the crushing strength of the barrel. The uncut barrels generated approximately 3 times as much stopping force as the barrels with the elliptical holes. Details of these static tests can be found in Technical Memorandum 505-1, contained in Appendix F.

The next barrel system which was tested (505-1E) incorporated the cutting of elliptical holes in the top and bottom of the barrels, and the system and the test results are described below. Two other head-on crash tests and three angle impact crash tests have been conducted on modified versions of this early Modular Crash Cushion and they are also described. Also discussed are three tests conducted on a combination Modular Crash Cushion--concrete median barrier.

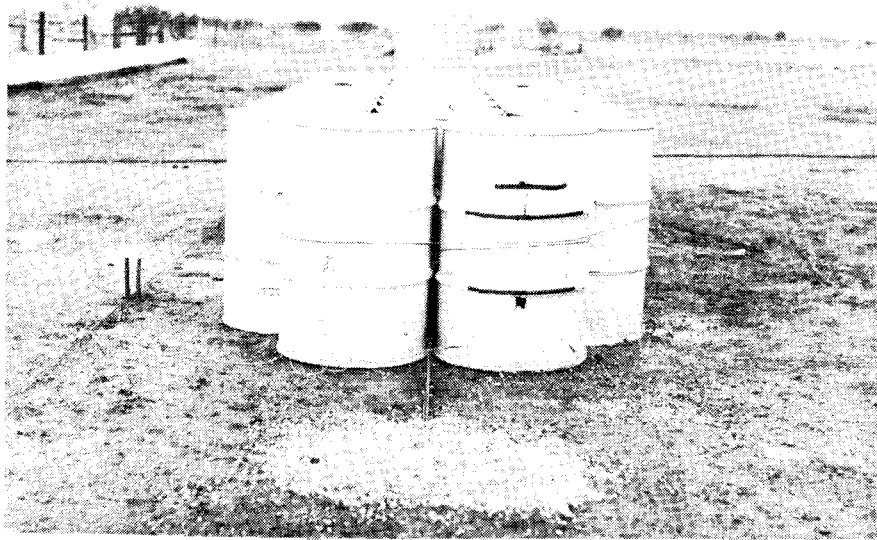


FIGURE IV.2.A.7. TWENTY-NINE 55-GALLON DRUMS FILLED WITH EMPTY BEVERAGE CANS BEFORE TEST 505-1D.

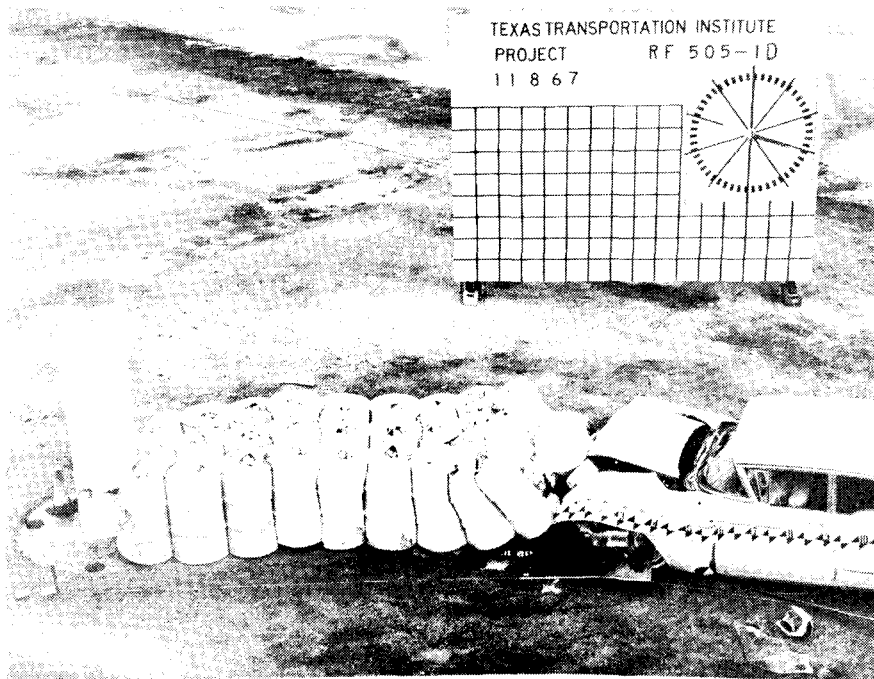


FIGURE IV.2.A.8. VEHICLE AFTER TEST 505-1D.

BARRIER DESCRIPTIONS

The 505-1E crash cushion which was tested consisted of twenty-nine 55-gallon, 16-gage steel drums. This system is illustrated in Figures IV.2.A.9-11. These barrels had four elliptical holes cut in the top and bottom of each barrel. There were 9 rows of barrels 3 drums wide and a front row of 2 drums wide. The top and bottom rims of the drums were welded together at all points of contact between adjacent barrels. One-half in. cables were threaded between the rows of barrels, supported on the rolling hoops, and tied off to a reinforced concrete anchor shaft located flush with the ground in front of the nose of the barrier. The 1/2 in. cables were designed to give the barrier lateral stability in the case of an angle hit by a vehicle and also to hold the barrels on the ground during vehicle impact. The barrels were not attached to the cable in any manner in order for them to remain free to slide down the cable during vehicle impact.

In a later test series, 505-B, head-on and angled impact tests were conducted on three other Modular Crash Cushion designs. These three designs used 20-gage steel tight-head drums, with 7 in. diameter holes centered in the top and bottom of each, as the basic energy absorbing modules. The first configuration in this later series was tested under an angle impact only (Test B-A). The system is shown in Figure IV.2.A.12. The columns of modules were separated by plywood inserts, and the two support cables ran between the columns of drums in a path as shown in Figure IV.2.A.12. Overlapping redirection panels were attached to the sides of the crash cushion. These panels overlapped approximately 11 in. and were made of 3/4 in. plywood covered with fiberglass and then coated with a polyester resin. This gel coat was used to give more smoothness to the panel

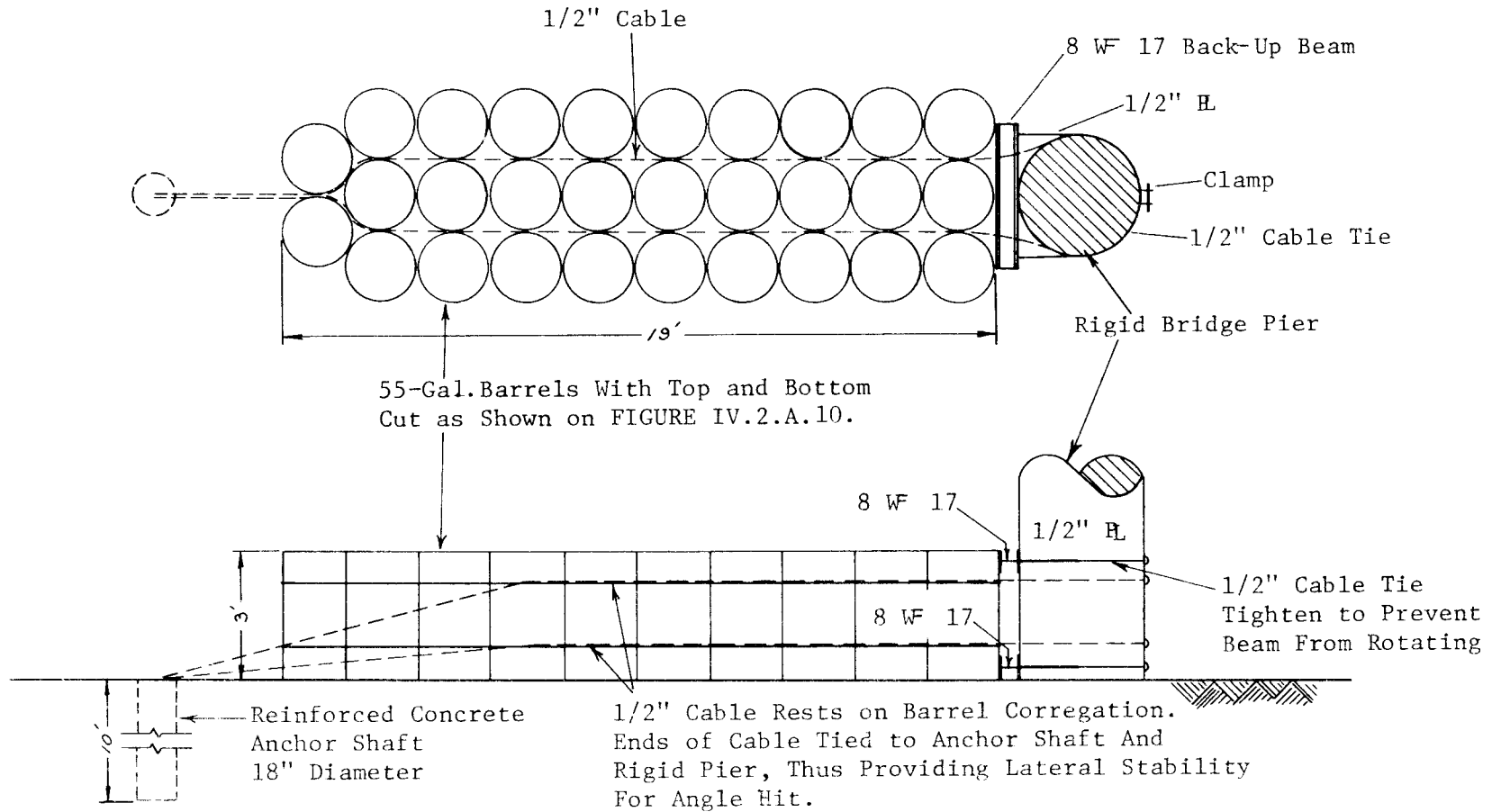


FIGURE IV.2.A.9. PROTECTIVE BARRIER (TEST 505-1E).

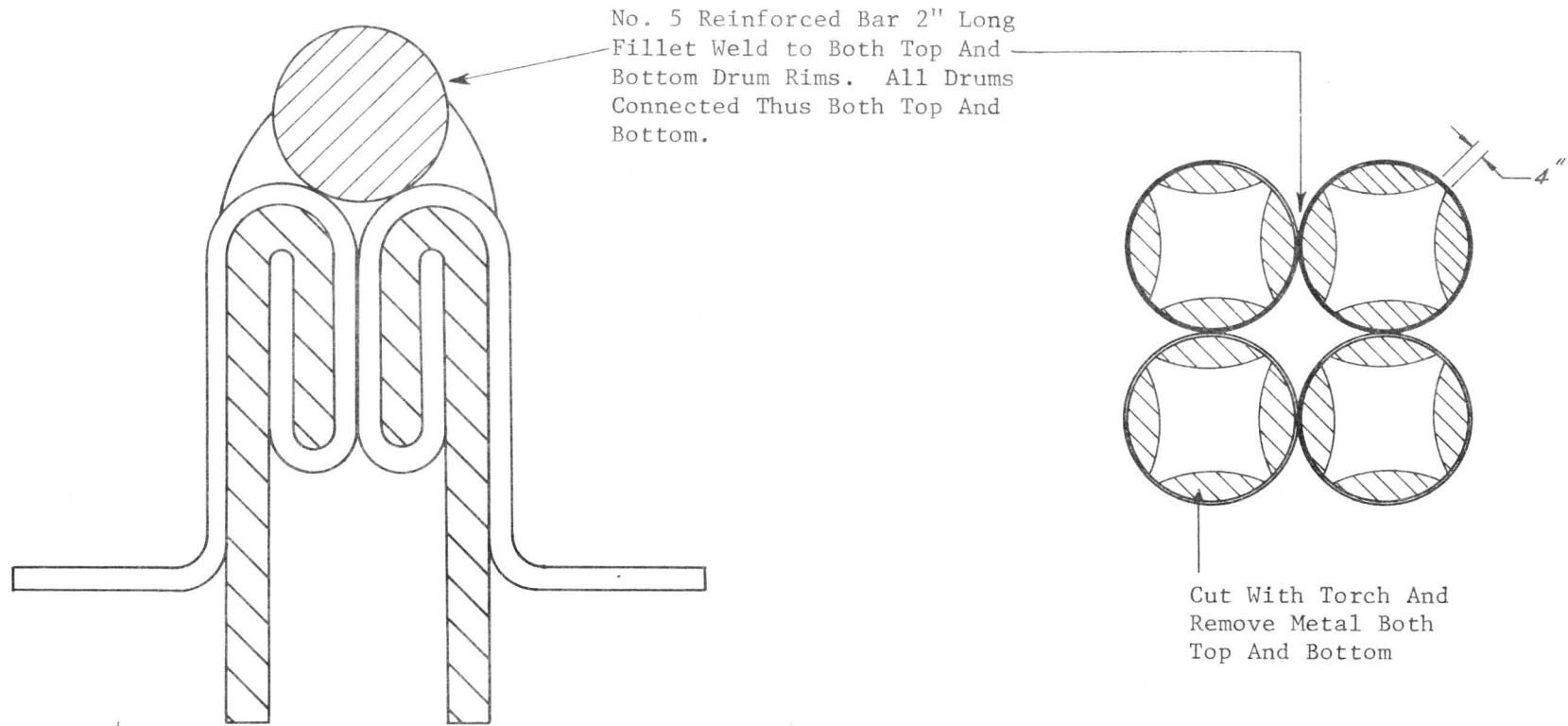


FIGURE IV.2.A.10. DETAIL OF TOP OR BOTTOM OF 55-GAL. TIGHT-HEAD UNIV. DRUM, 16-GAGE STEEL (TEST 505-1E).



FIGURE IV.2.A.11. BARREL PROTECTIVE BARRIER INSTALLED IN FRONT OF 30-IN. DIAM. SIMULATED BRIDGE PIER. (TEST 505-1E)

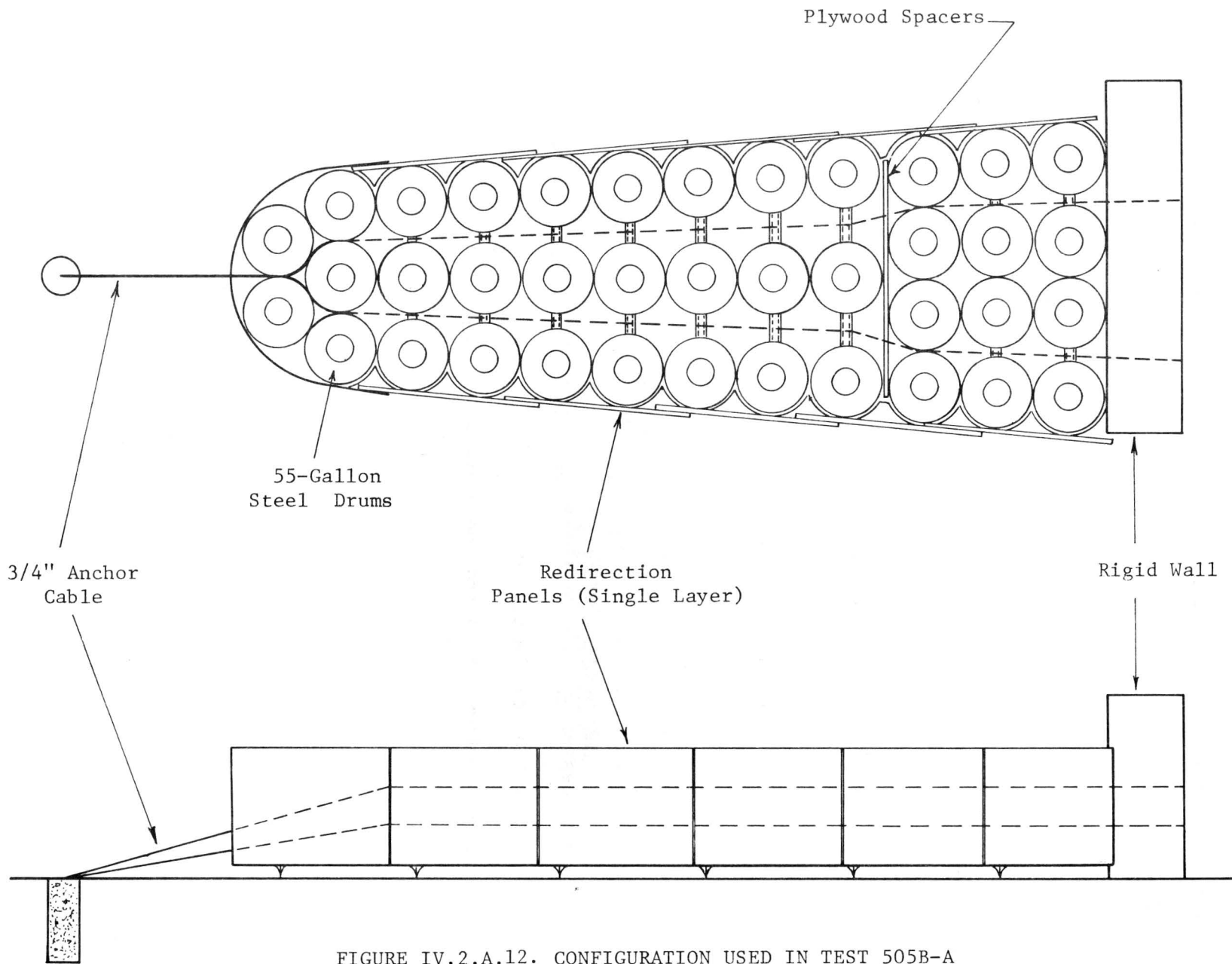


FIGURE IV.2.A.12. CONFIGURATION USED IN TEST 505B-A

surfaces and to improve the appearance of the barrier. The front edges of the panels were hinged so that the back edges could telescope or swing out, allowing free crushing of the barrier during head-on collisions.

The second barrier tested (shown in Figure IV.2.A.13) was impacted both head-on and at an angle. The basic drum arrangement was the same as before, but the support cables were moved to run in a straight line between the outer modules and the redirection panels to reduce vehicle pocketing. An angle-iron "truss" was welded to the tops of the modules to increase the lateral strength and stiffness.

The final system constructed for testing in this series (shown in Figure IV.2.A.14) was also impacted head-on and at an angle. Angle-iron spacers were used here, and the module arrangement was modified to reduce the stopping force at the onset of the collision. This modification is especially desirable when the colliding vehicle is small and lightweight. Also, the rear of the barrier was widened to provide a cushion between the end redirection panels and the rigid wall. Again, cables inside the redirection panels were used to give lateral stability without rigidity.

In another series, 505-M, two angle impacts and one head-on were conducted on a combination of a reinforced concrete median barrier and a variation of the Modular Crash Cushion. This system was installed around two simulated concrete bridge piers. The installation is shown in Figures IV.2.A.15-16 and consisted of 55-gallon steel drums with holes in the top and bottom. Redirectional panels were attached to the side of the crash cushion and steel cables gave the cushion lateral stability.

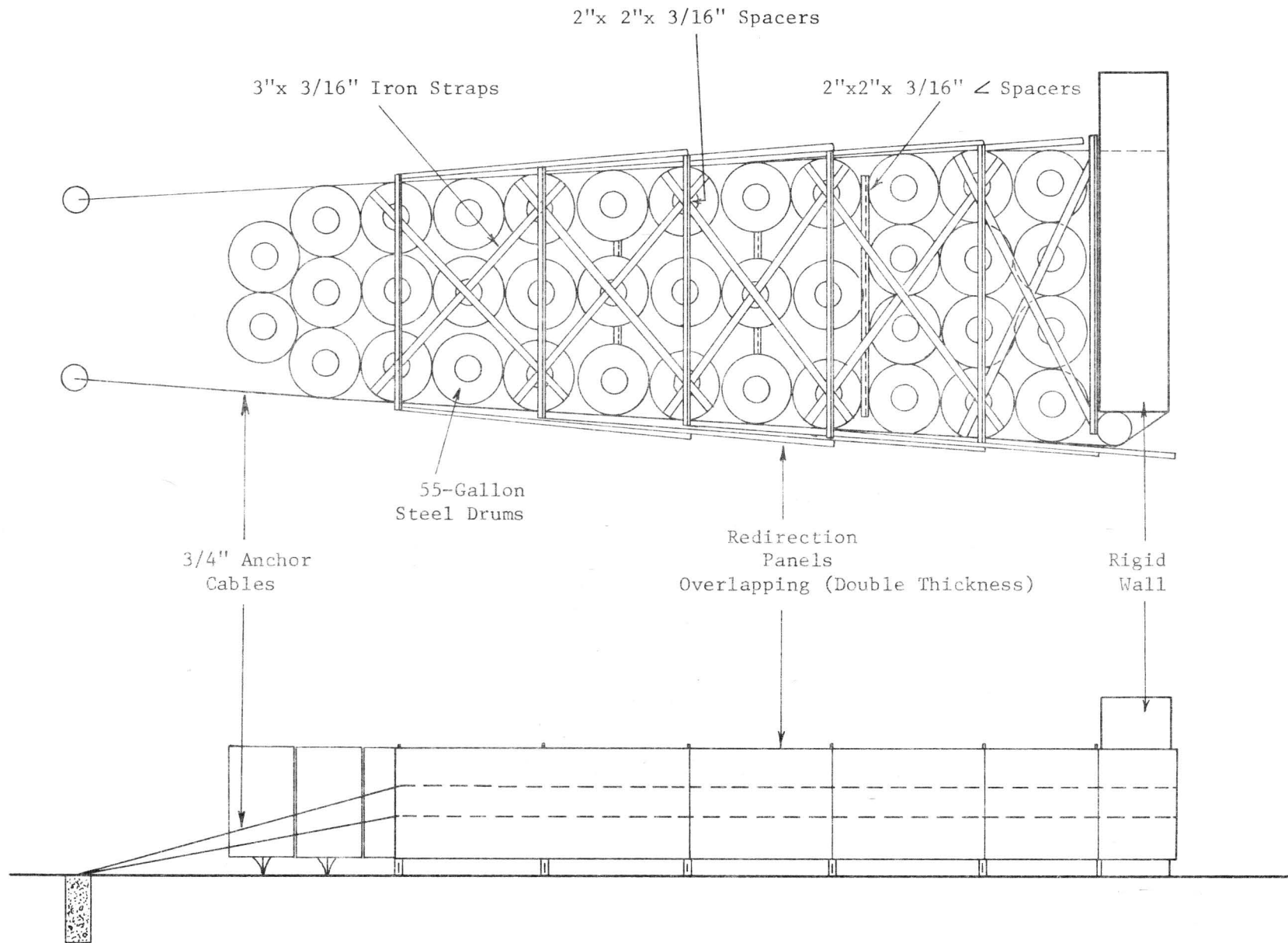


FIGURE IV.2.A.13. CONFIGURATION USED IN TESTS 505B-B AND 505B-C

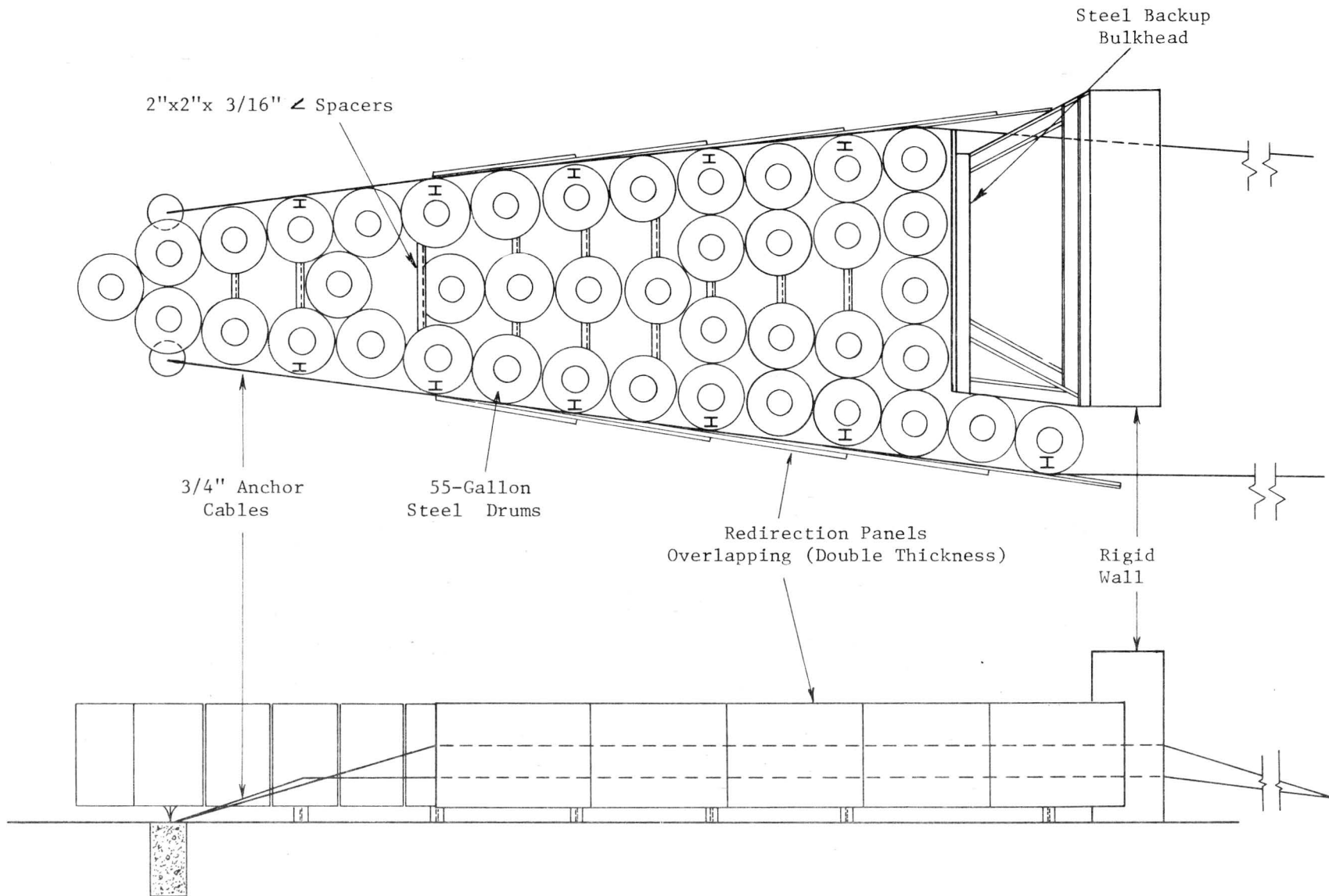


FIGURE IV.2.A.14. CONFIGURATION USED IN TESTS 505B-D AND 505B-E

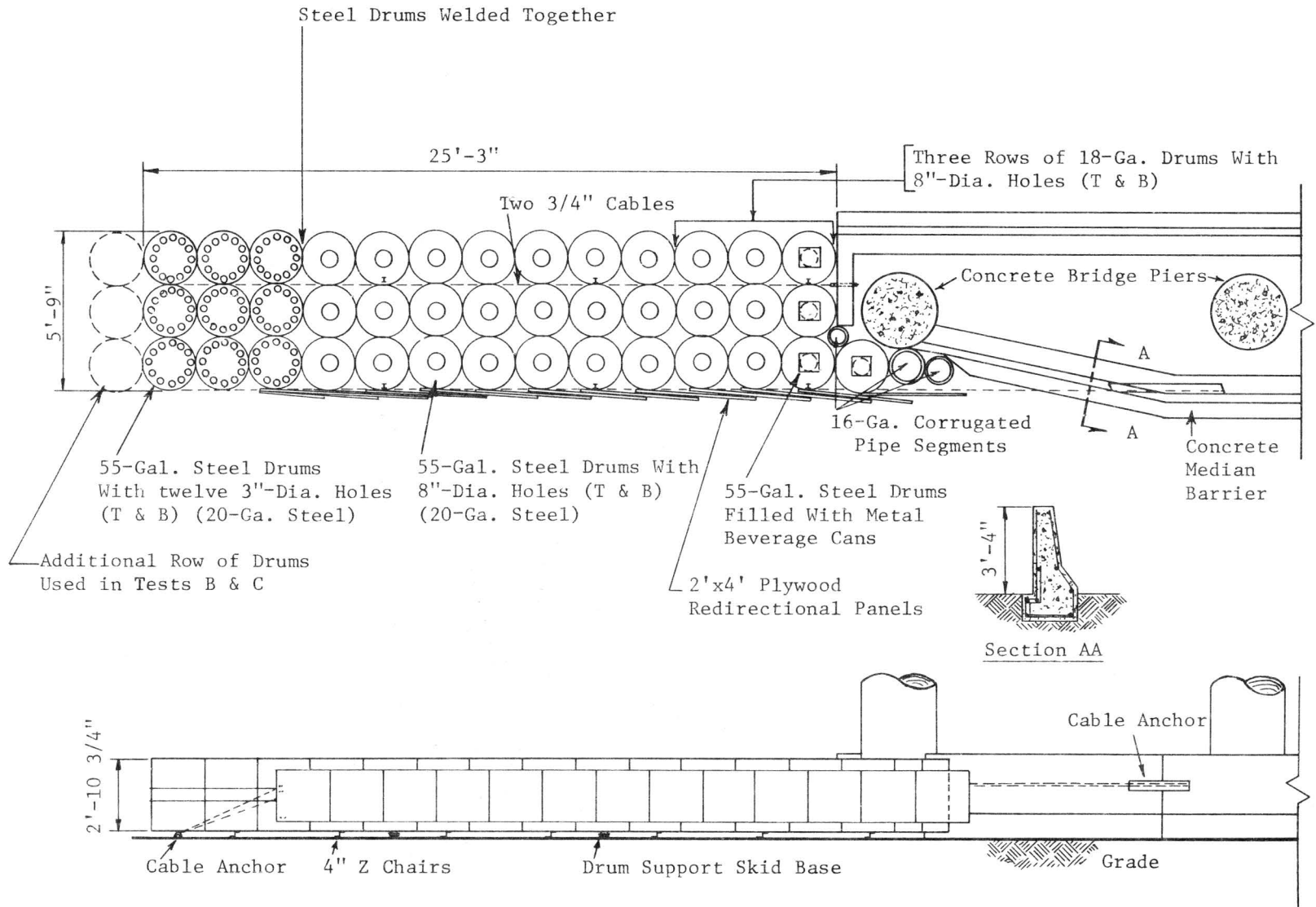


FIGURE IV.2.A.15. CRASH CUSHION-MEDIAN BARRIER SYSTEM (505 M-A, M-B, & M-C).

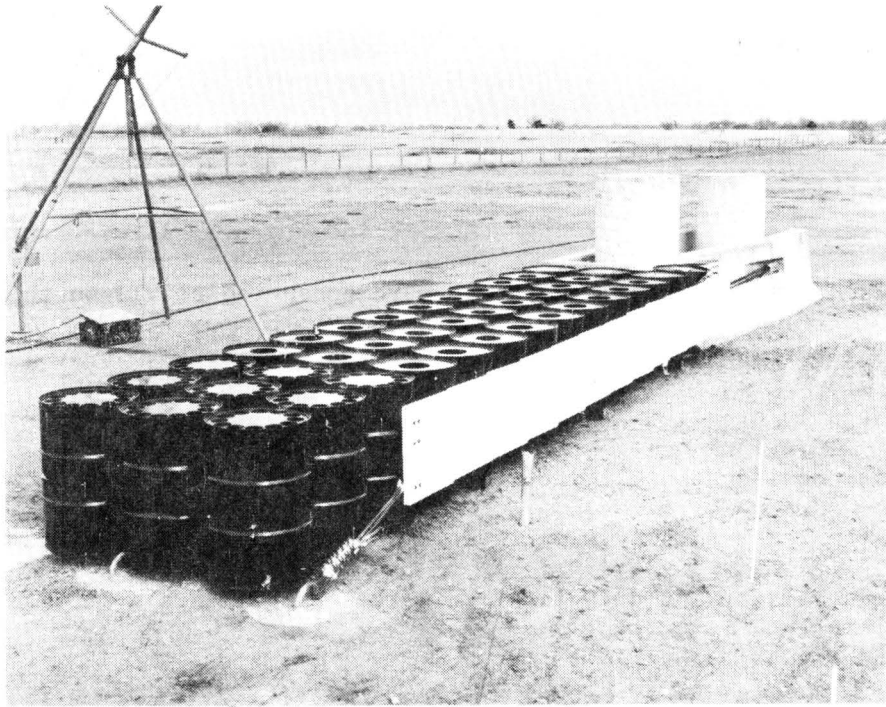


FIGURE IV.2.A.16. MODULAR CRASH CUSHION--CONCRETE MEDIAN BARRIER BEFORE TEST 505 M-A.

In previous steel drum crash cushion tests, all drums used in a given design had the same crushing strength (same gage and hole cut-out pattern). These drums could be referred to as mono-modular in design concept. The Modular Crash Cushion - median barrier system design could best be termed poly-modular, since drums having three different crush strengths were used. Relatively "soft" drums were used on the crash cushion nose, "medium stiff" drums in the center, and "stiff" drums in the rear of the crash cushion. This system was thus better adapted to stopping both lightweight and heavyweight vehicles with acceptable deceleration forces.

The concrete median barrier portion of this system is an adaptation of a design used in New Jersey. No tests were conducted at TTI on this portion since results of test on a similar median barrier have been reported by Nordlin, et al.²

Additional modifications and tests on the Modular Crash Cushion were sponsored by the Texas Highway Department in cooperation with the Federal Highway Administration, and details of this test program are available in Research Reports 146-1³ and 146-3⁴.

TEST RESULTS -- HEAD-ON

One test was conducted on the 505-1E system. A 3200 lb vehicle impacted the barrier head-on with an initial speed of 60.2 mph. The vehicle penetrated the barrier 13.3 ft over 0.346 sec. The average deceleration force on the vehicle was 9.1 g's. Only minor damage was inflicted on the vehicle, as shown in Figures IV.2.A.17 - 18.

One of the four headlights was broken and the front bumper and grillwork were deformed approximately 4 in. The vehicle was in running condition immediately after the impact. The vehicle stopping distance of 13.3 ft



FIGURE IV.2.A.17. VIEW OF MINOR VEHICLE DAMAGE. ONLY ONE OF FOUR HEADLIGHTS WAS BROKEN; BUMPER AND GRILL DEFORMED APPROXIMATELY 4 IN. (TEST 505-1E).

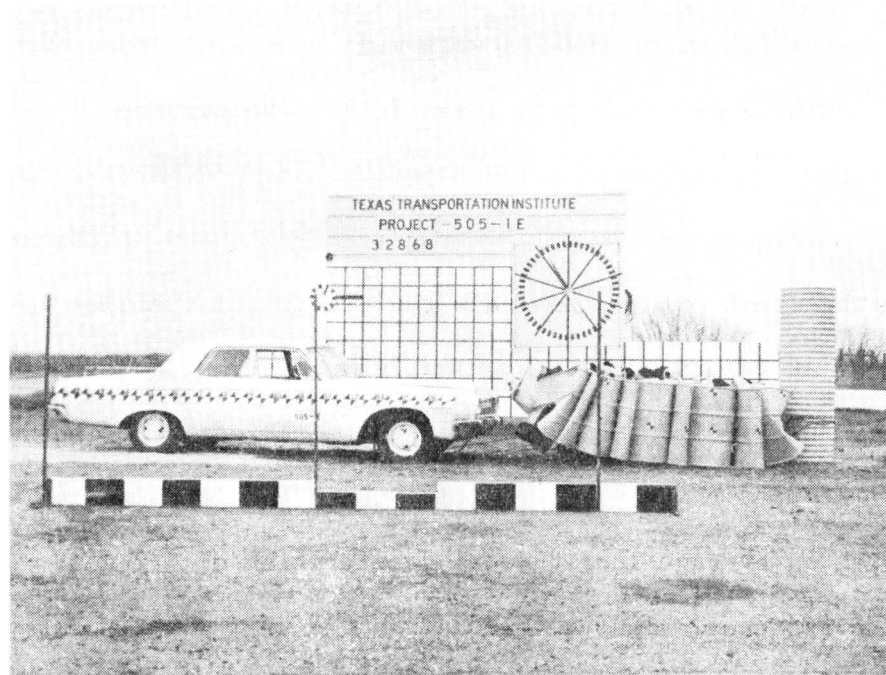


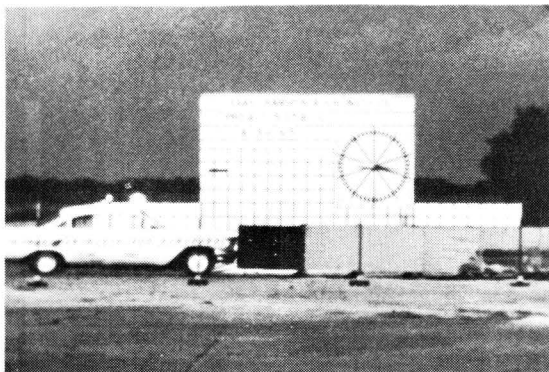
FIGURE IV.2.A.18. VIEW OF VEHICLE AND BARRIER AFTER IMPACT. (TEST 505-1E)

indicated that approximately 70% of the energy capacity of the barrier was used up. The vehicle had 387,000 ft-lbs of kinetic energy.

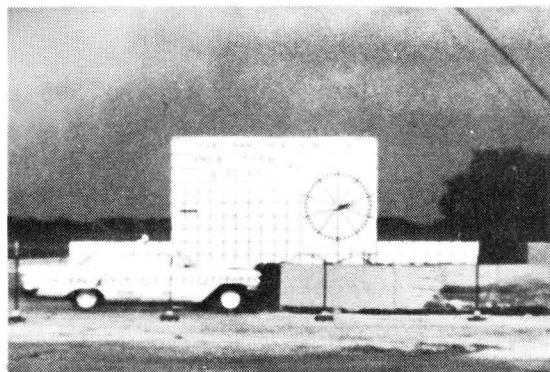
From an analysis of the high-speed film data, it was apparent that the crush strength of the total barrel system welded together was somewhat larger than that obtained from the sum of the individual barrels as indicated by static tests. This increase in the total barrier force was attributed to cable friction, ground friction, and lateral support provided to the barrels by adjacent barrels.

Based on this single test, the impact behavior of the system appeared very good. This barrel protective barrier appeared to be very effective, economical, and practical as a vehicle crash attenuator. Additional details of this test can be found in Technical Memorandum 505-1 in Appendix F.

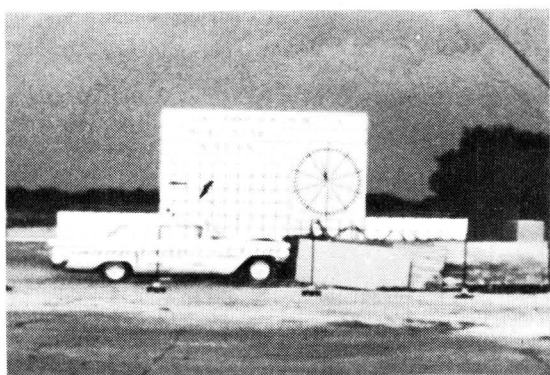
In the 505 B series, the second system was subjected to a 20° angle impact (Test B-B) which will be described in the next section of this report. After a few minor repairs were made, the same crash cushion was subjected to a head-on crash test (Test B-C). The purpose of this test was to evaluate the longitudinal response on the modified barrier to a head-on collision (see Figure IV.2.A.19). Lateral strength and stiffness had been built into the crash cushion for safe redirection of vehicles impacting at an angle. At the same time, however, this system had been designed to maintain its relatively soft, crushable characteristics for head-on impacts. The barrier stopped the 4180 lb vehicle, which was traveling 46.6 mph, in 11.7 ft, with an average longitudinal deceleration of 6.2 g's. The system performed as designed. The vehicle damage was very minor. Permanent vehicle front-end deformation was only 2 in. and the headlights were not broken.



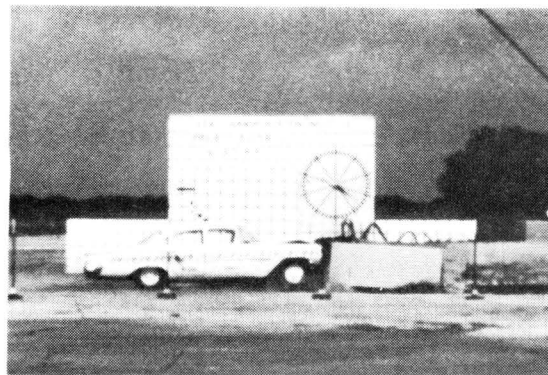
1



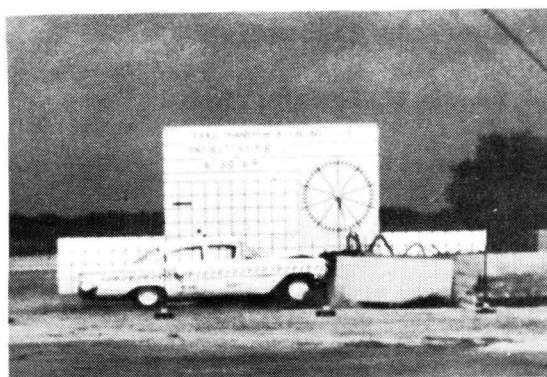
2



3



4



5

FIGURE IV.2.A.19. SEQUENTIAL PHOTOGRAPHS OF TEST 505 B-C. (SIDE VIEW).

The third system in the 505 B series was hit at a 20° angle (Test B-D), repairs were made, and the same cushion was hit by a 1500 lb vehicle at 58.2 mph (Test B-E) for the purpose of evaluating the effectiveness of the barrier in head-on impacts with small vehicles (see Figure IV.2.A.20). This lightweight vehicle was stopped in 12.4 ft with an average longitudinal deceleration of 9.1 g's. It was stopped smoothly, without tendency to roll or spin. The sheet metal portion of the front end of the vehicle was severely buckled, which would be expected in a lightweight, low front profile, rear-engine vehicle.

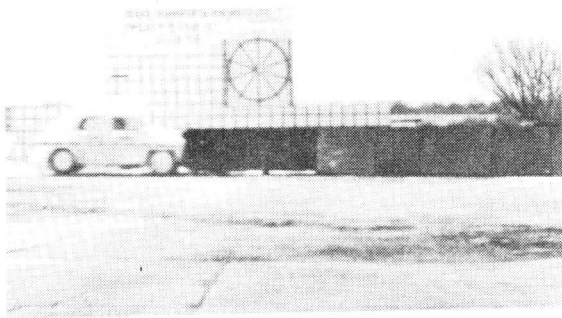
Additional information on these two tests can be found in Technical Memorandum 505-1S in Appendix F.

The system in the 505 M series was subjected to two angle impacts before a head-on test was conducted. (The two angle tests will be described in the next section). The crash cushion was not restored after the second angle test except for painting and reshaping of some of the fender panels. A 1790 lb Simca impacted the barrier head-on at a speed of 55.8 mph (Test M-C). The front end of the lightweight, rear-engine vehicle was deformed approximately 1 ft at the bumper level. The average deceleration (film) over 0.257 sec and 11.3 ft of travel was 9.2 g's. See Figure IV.2.A.21.

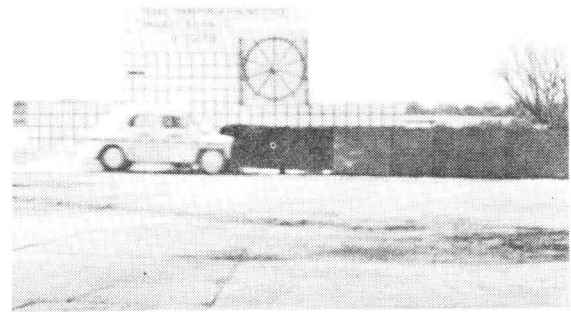
Additional information on this test can be found in Technical Memorandum 505-15 in Appendix F.

TEST RESULTS -- REDIRECTIONAL

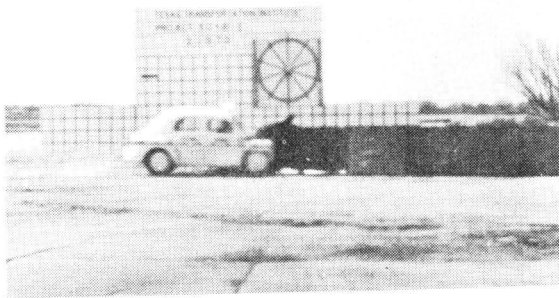
The first crash cushion described in the 505 B series was tested with a 3000 lb vehicle impacting the Modular Crash Cushion at 56.9 mph (Test B-A). The vehicle centerline made a 20° angle with the centerline of the barrier at impact. (See Figure IV.2.A.22.) After initial contact, the lateral



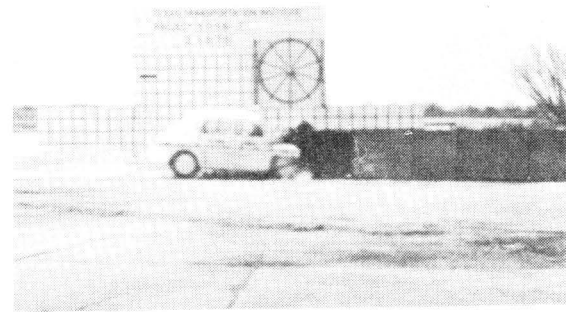
1



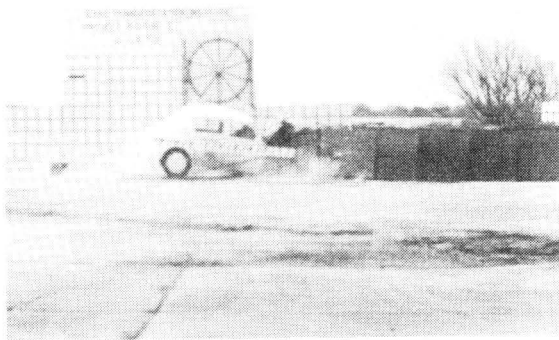
2



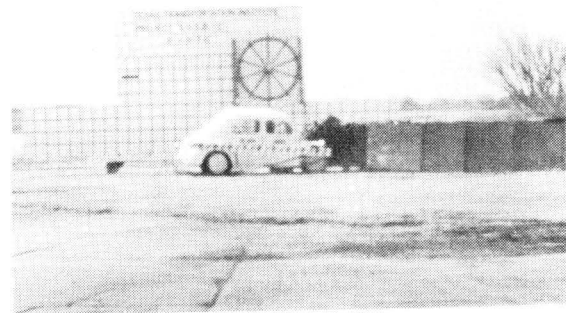
3



4

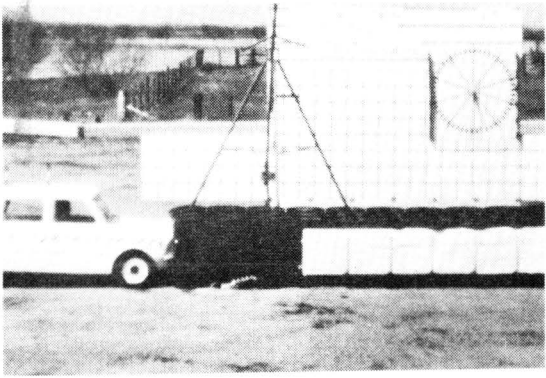


5

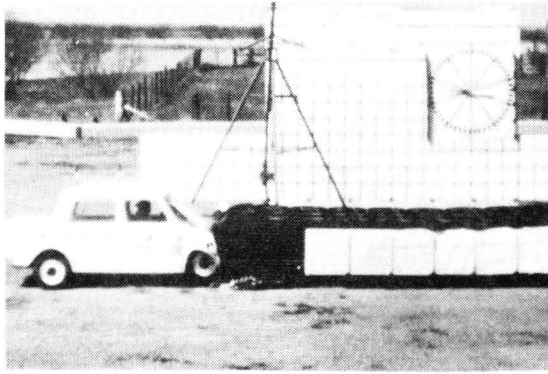


6

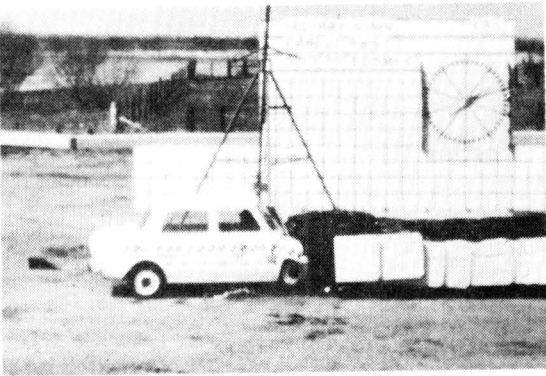
FIGURE IV.2.A.20. SEQUENTIAL PHOTOGRAPHS OF TEST 505 B-E.
(SIDE VIEW).



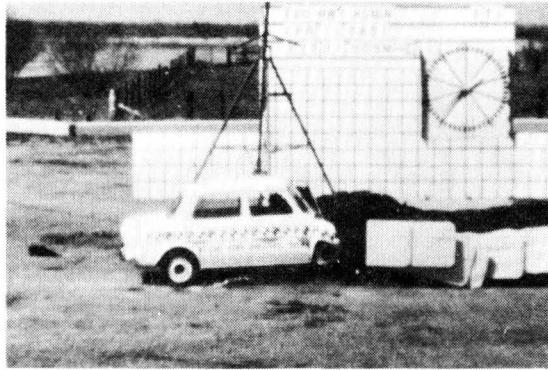
1



2



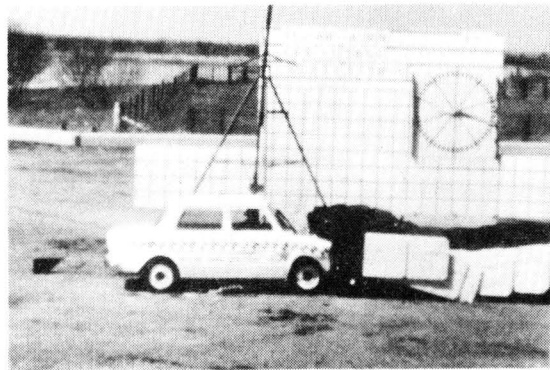
3



4

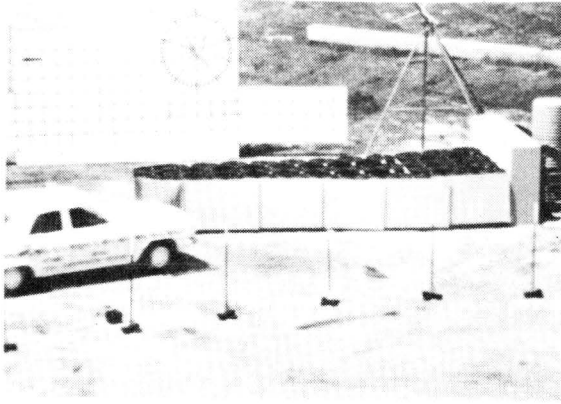


5

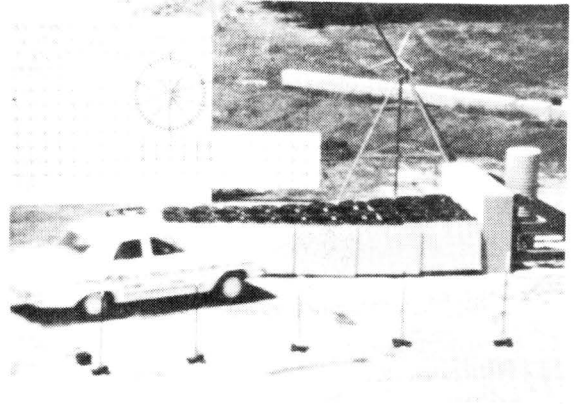


6

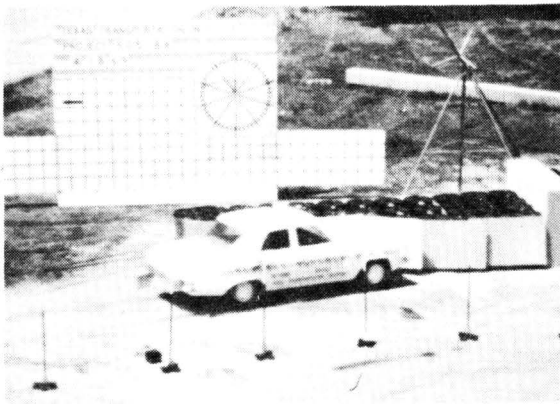
FIGURE IV.2.A.21. SEQUENTIAL PHOTOGRAPHS OF TEST M-C.
(SIDE VIEW)



1



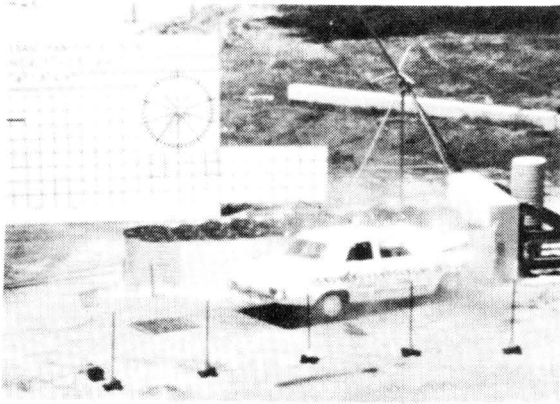
2



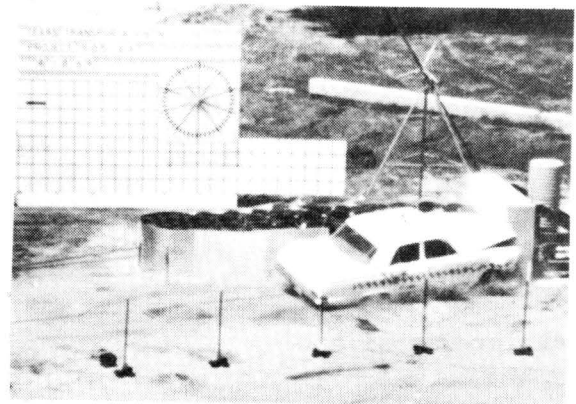
3



4



5



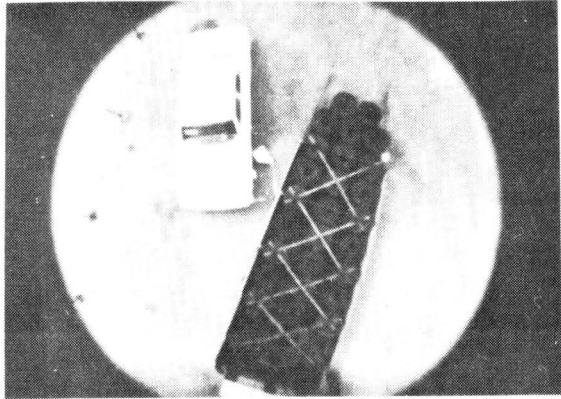
6

FIGURE IV.2.A.22. SEQUENTIAL PHOTOGRAPHS OF TEST 505 B-A. (SIDE VIEW).

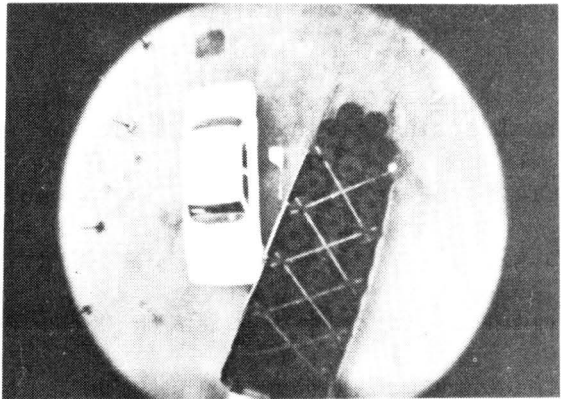
stability of the redirection panels was not sufficient to prevent the vehicle from "pocketing" and crushing several barrels into the rigid wall. This was the reason for the high maximum longitudinal deceleration of 53 g's. Analysis of the accelerometer traces showed the average deceleration to be 10.8 g's longitudinally and 1.1 g's laterally. Damage to the vehicle was rather severe due to the impact with the rigid wall. The insufficient lateral stability was attributed to the position of the anchor cable and to inadequate overlapping of the redirection panels.

In order to provide acceptable redirection capabilities during angled hits, the basic system previously tested was modified. Instead of the plywood spacers between the barrels, metal straps were welded across the top of the barrels. In addition, the anchor cables were placed just inside the deflection panels and were aligned straight and taut. Also, the redirection panels were positioned to overlap each other four feet, creating a double thickness of plywood along the impact area. This second barrier in the 505 B series was impacted by a 3080 lb vehicle, traveling at 59.3 mph and hitting at an angle of 20° (Test B-B). The vehicle was redirected, leaving the barrier at 26.7 mph after 0.210 sec (see Figure IV.2.A.23). The average longitudinal deceleration during this time was 7.4 g's, and the average transverse deceleration was 3.2 g's. The left front end of the vehicle was deformed about 1.5 ft. Damage to the barrier was slight.

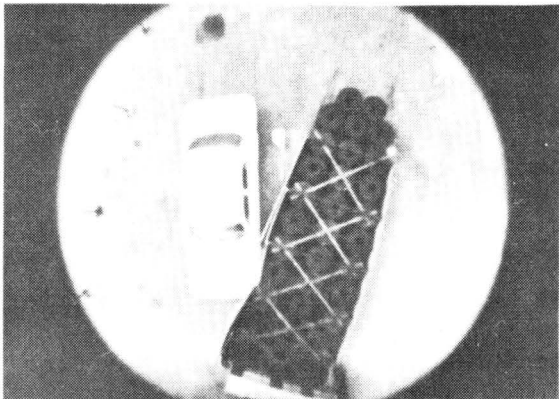
In the third configuration of the 505 B series, the barrel modules were arranged in a more triangular shape to provide a softer nose for better head-on attenuation of small, lightweight vehicles. The straight, taut cables and overlapping plywood panels were believed to be sufficient for



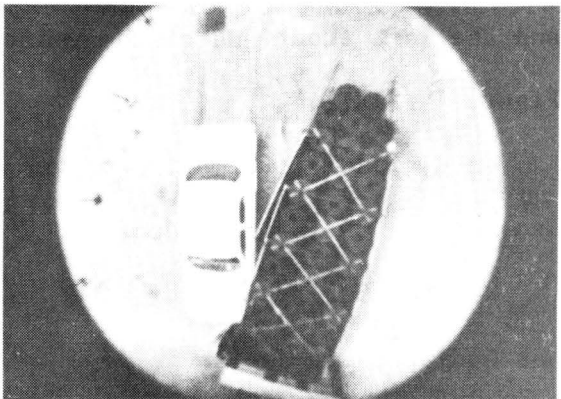
1



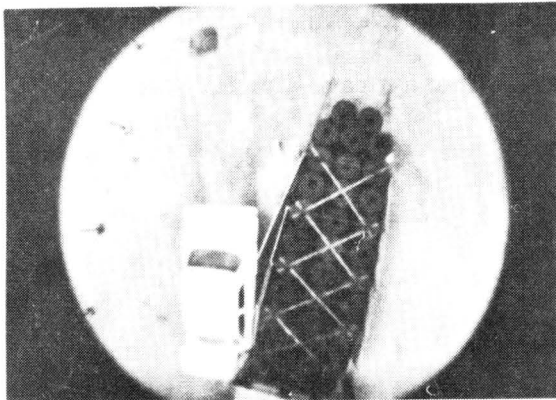
2



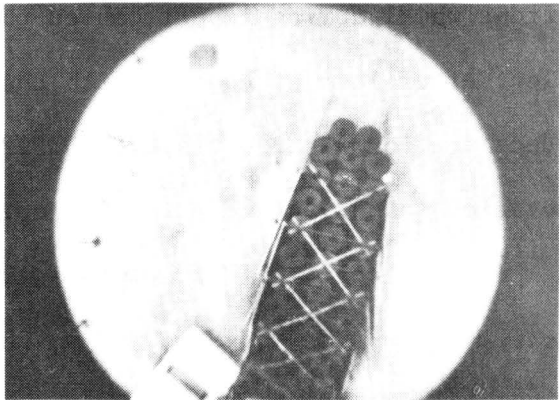
3



4



5



6

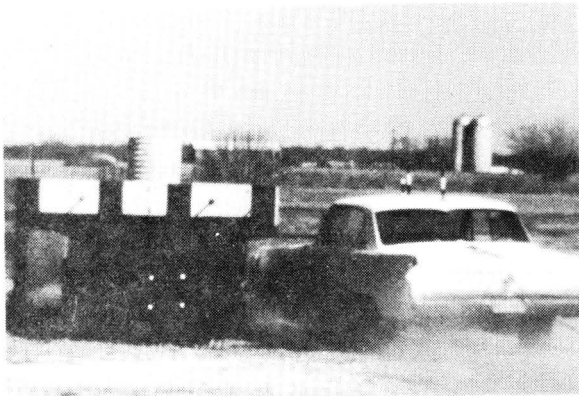
FIGURE IV.2.A.23. SEQUENTIAL PHOTOGRAPHS OF TEST 505 B-B. (OVERHEAD VIEW).

redirecting a vehicle without the use of the metal "truss" as used in the previous angle hit. A 4350 lb vehicle impacted the crash cushion at an angle of 20° (Test B-D). The initial speed was 56.8 mph and the vehicle remained in contact with the barrier for 0.624 sec. A slight "ramping" tendency was observed, but the test vehicle remained upright throughout the test. The average longitudinal deceleration was 4.0 g's and the average transverse deceleration was 0.6 g's. The barrier was damaged moderately, and the left front end of the vehicle was deformed 3.25 ft. See Figure IV.2.A.24.

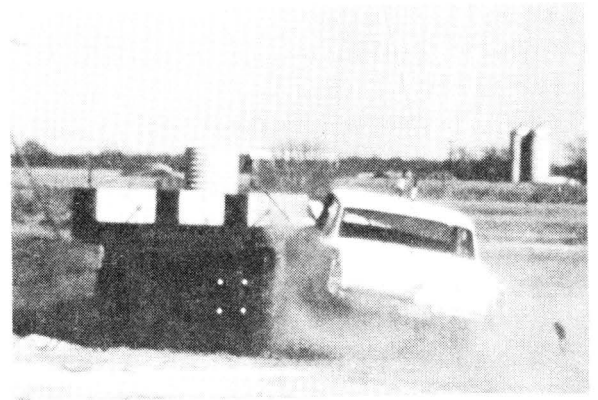
Additional information on the 505 B series can be found in Technical Memorandum 505-1S in Appendix F.

In the 505 M series, the Modular Crash Cushion--concrete median barrier was subjected to two angle impacts. For test M-A, a 4150 lb Ford traveling 56.7 mph impacted the system at an angle of 20° to the centerline of the crash cushion. The vehicle was smoothly redirected. Damage to the left front wheel during impact caused the vehicle to swerve in an arc to the left after loss of contact with the barrier. The average longitudinal deceleration was 2.6 g's over 0.513 sec, and the average transverse deceleration was 3.9 g's over 0.513 sec. See Figure IV.2.A.25.

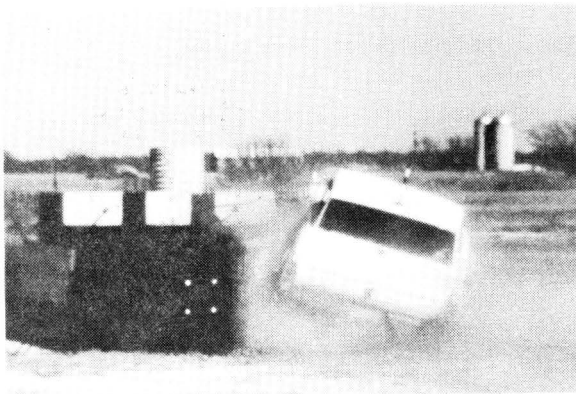
The second angle test was a 10° angle to the barrier centerline (Test M-B). The Dodge sedan, weighing 3990 lb, was traveling 62.3 mph at impact. The crash cushion had been restored to its original condition after the first test except for one corrugated steel pipe at the edge of the concrete back-up wall which was not replaced. In addition, another row of barrels was added to the front of the crash cushion. The damage



1



2



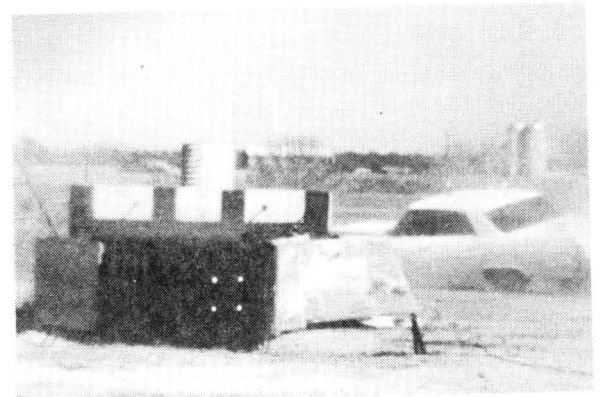
3



4

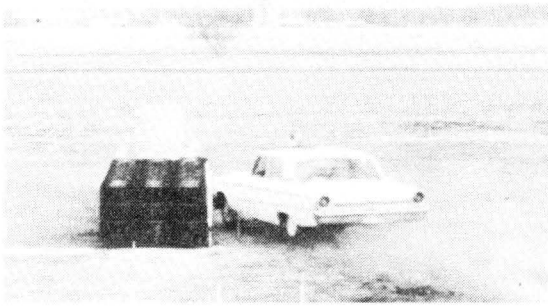


5



6

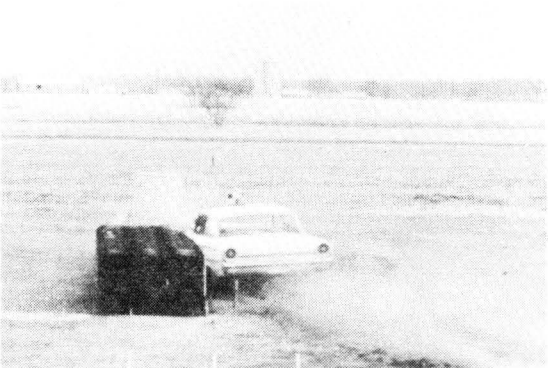
FIGURE IV.2.A.24. SEQUENTIAL PHOTOGRAPHS OF TEST 505 B-D.
(END VIEW).



1



2



3



4



5

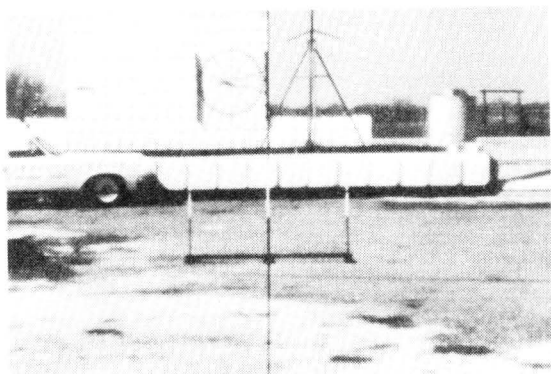


6

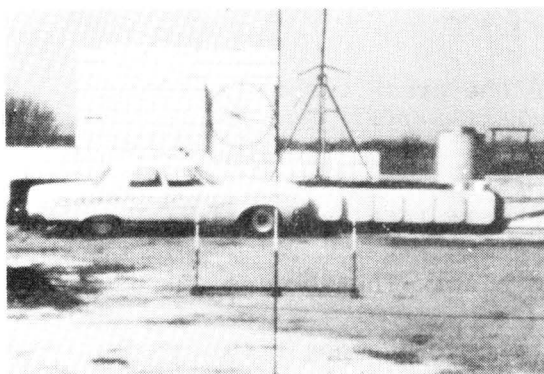
FIGURE IV.2.A.25. SEQUENTIAL PHOTOGRAPHS OF TEST M-A.

to the crash cushion was slight. The redirection was very smooth, with only a slight ramping of the left front end of the vehicle observed. The vehicle left the barrier at an angle of 5° to the centerline of the crash cushion. The vehicle was driven away from the site after the test, which indicates, along with the small angle of departure, that a driver could have maintained control after impact. Analysis of high-speed films showed an average longitudinal deceleration of 1.3 g's and an average deceleration perpendicular to the crash cushion of 3.0 g's. See Figure IV.2.A.26.

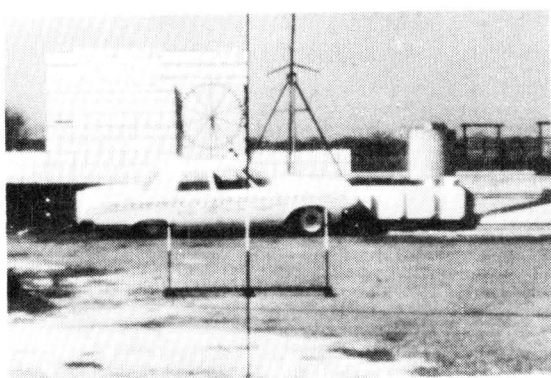
Additional information on these two tests can be found in Technical Memorandum 505-15 in Appendix F.



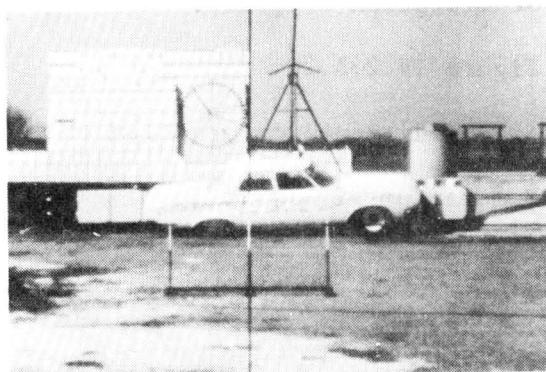
1



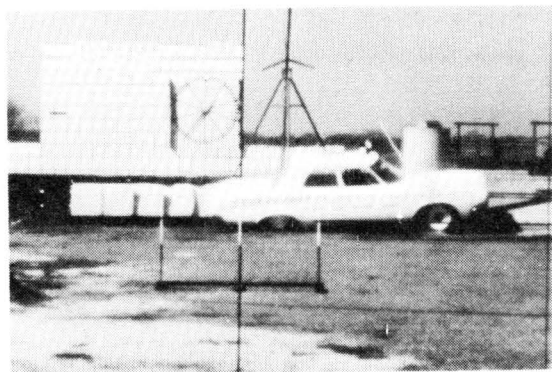
2



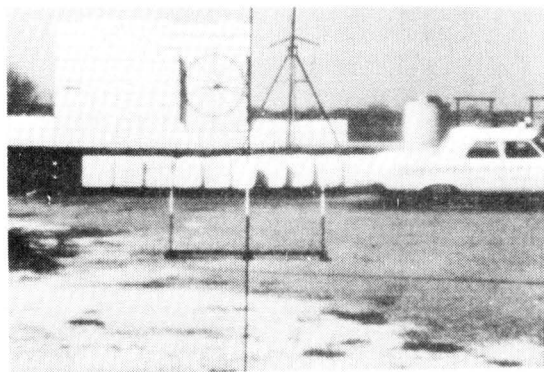
3



4



5



6

FIGURE IV.2.A.26. SEQUENTIAL PHOTOGRAPHS OF TEST M-B.

Part 2. B. --- THE HI-DRO CUSHION VEHICLE IMPACT ATTENUATOR

BARRIER DESCRIPTION

The basic unit of the crash cushion is the Hi-Dro Cushion Cell which is a hollow cylinder or envelope made of plastic material. The cap contains orifices through which the water in the cell can be expelled (see Figure IV.2.B.1.). The "stiffness" of the cell is determined by the orifice areas. These cells were assembled as shown in Figures IV.2.B.2. and IV.2.B.3. When the Hi-Dro cell barrier is struck by a vehicle, the water in the tubes is forced out the orifices. This reaction of individual tubes results in a predictable barrier deformation force characteristic. Augmenting the vehicle stopping force is the barrier inertia.

The 138 cells were divided among eight "bays" separated by diaphragms as shown in Figure IV.2.B.2. The third "bay" from the front was void of cells due to design factors concerning the profile of the acceleration pulse produced during impact. The diaphragms separating the "bays" were made of 1-1/2 in. fibreglassed plywood. The rows of cells in each "bay" were separated by 1/4 in. Duraply interior panels. The three diaphragms closest to the rigid barrier each had two 1/4 in. steel plates attached.

The "fish-scale" fender panels were designed to provide redirectional ability during angled impacts, while providing minimal interference during head-on crashes. These panels were hinged to the transverse diaphragms and were made of 1-1/4 in. fibreglassed plywood.

Some modifications were made to the crash cushion for the last head-on and angled impacts. The five front fender panels on the impacted side were made of fibreglassed Hexcel, which is a lightweight, high-strength

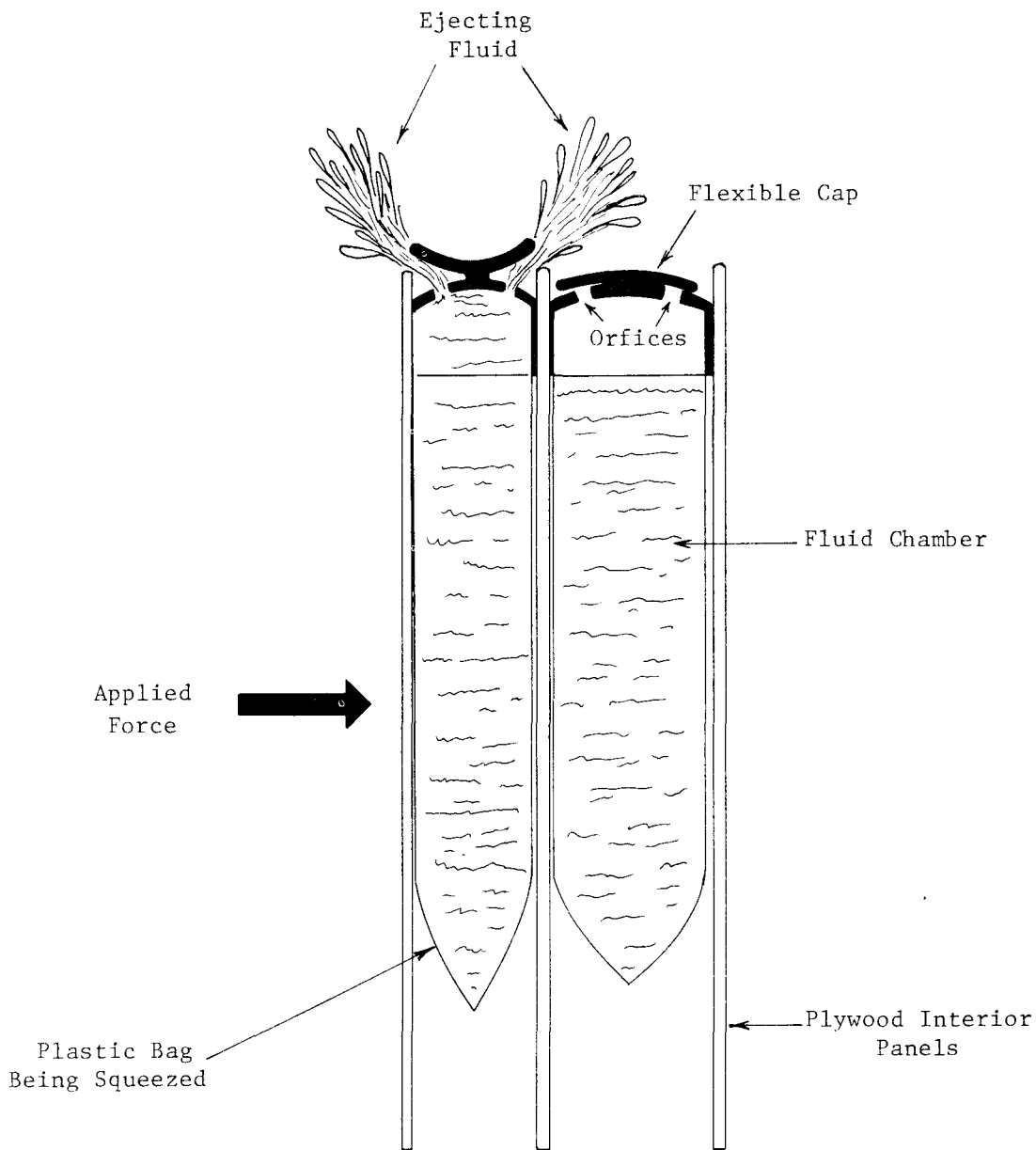
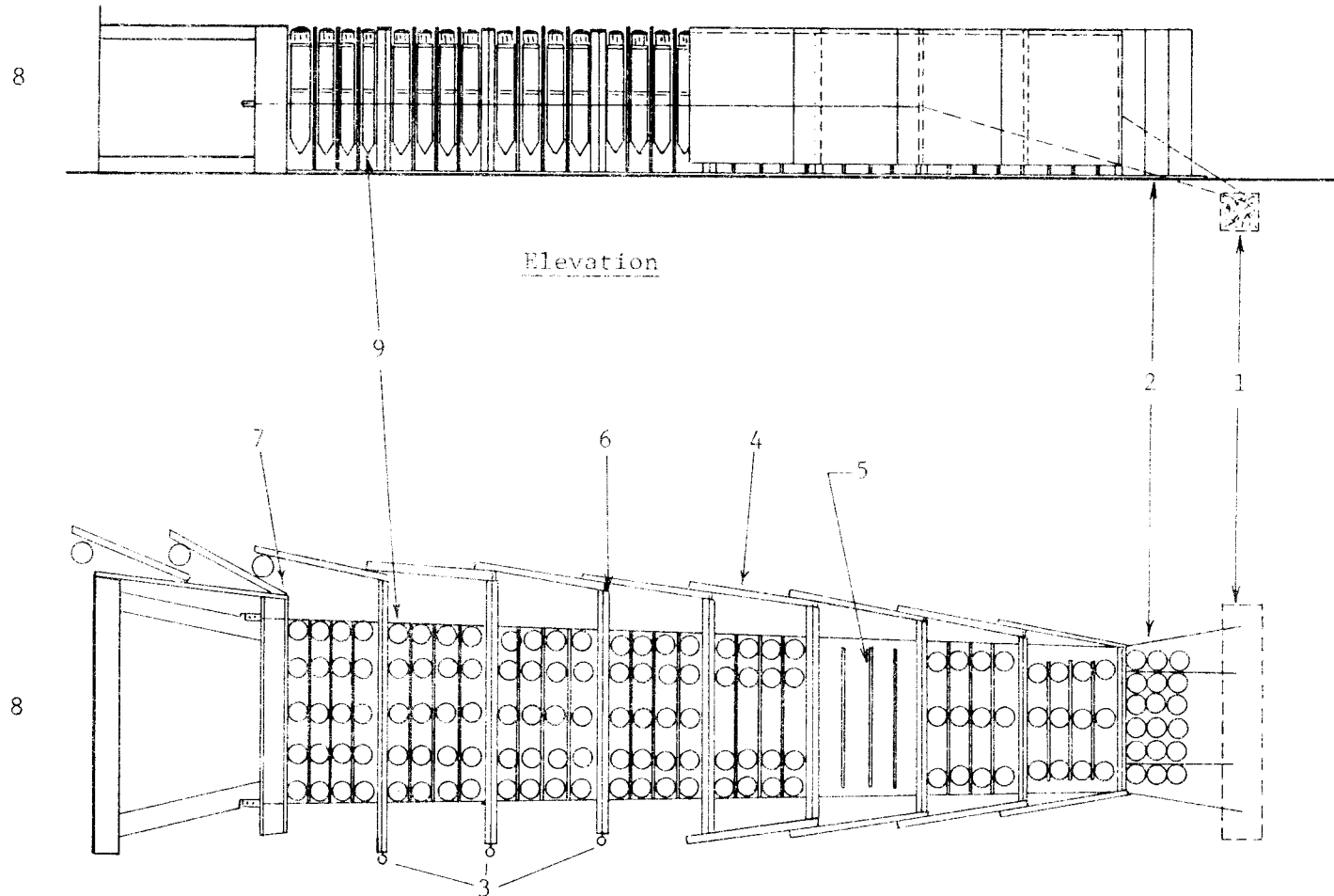


FIGURE IV.2.B.1. FUNCTION OF HI-DRO CELL



- | | | | |
|---|---|---|----------------------|
| 1 | Front Anchor | 7 | Steel Back Up Plate |
| 2 | Main Restraining Cables | 8 | Rigid Concrete Wall |
| 3 | Steel Bars to Simulate Weight of Side Deflection Panels | 9 | Hi-Dro Cushion Cells |
| 4 | Deflection Panels | | |
| 5 | Interior Panels (This Bay Void of Cells) | | |
| 6 | Transverse Diaphragms | | |

FIGURE IV.2.B.2. TTI CONFIGURATION OF HI-DRO CELL SANDWICH UNIT

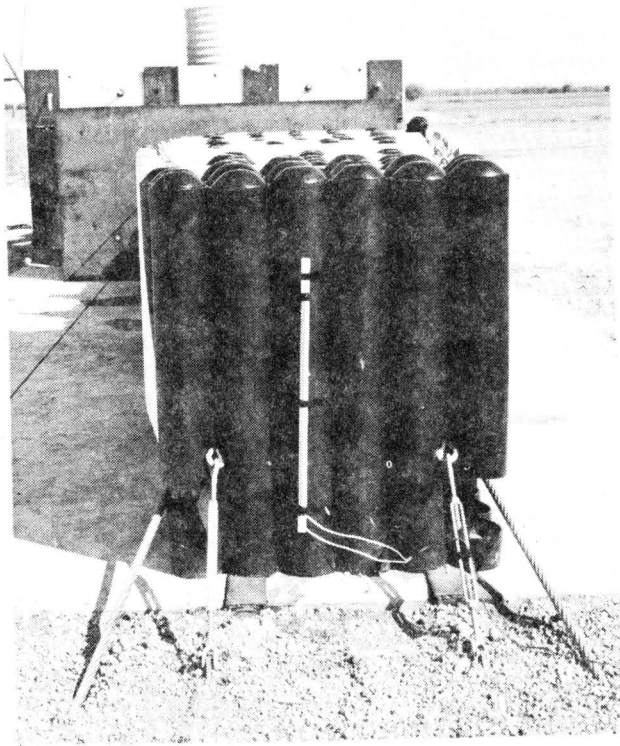
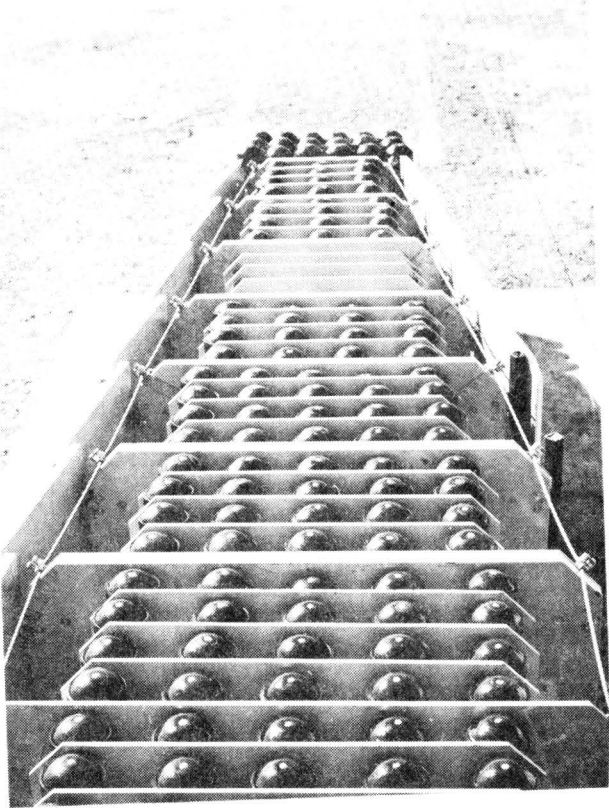


FIGURE IV.2.B.3. TOP AND FRONT VIEWS OF HI-DRO CUSHION ATTENUATOR.

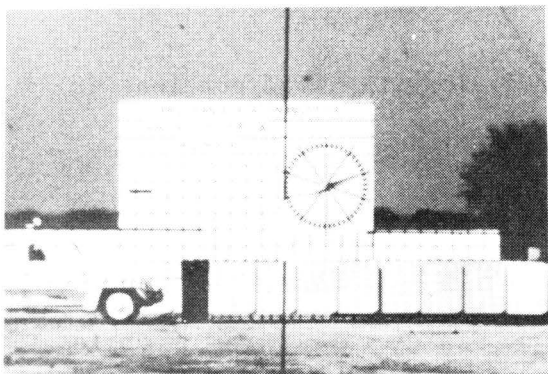
paper material resembling a honeycomb. In addition, the wood portions of the second and third diaphragms from the rear of the attenuator were removed and the 12-gage steel plate in the last diaphragm was eliminated in order to maintain the previous weight distribution after the modified fender panels had been installed. The 7/8 in. diameter restraining cables were increased to 1 in., and the last diaphragm was increased in width to provide a constant diverging side slope.

TEST RESULTS -- HEAD-ON

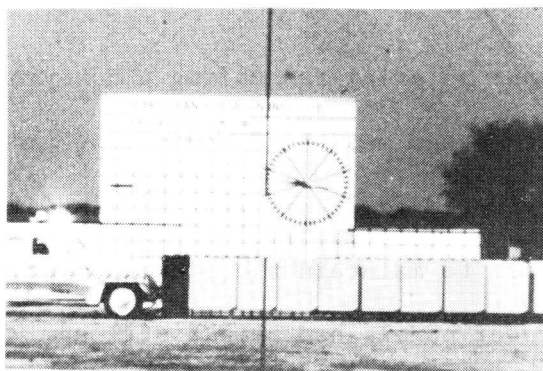
The first head-on test (Test 505 R-A) involved a light vehicle (1820 lb) traveling 42 mph (see Figure IV.2.B.4.). The vehicle was stopped in 13.2 ft with an average deceleration of 4.5 g's, and a peak deceleration of 14.6 g's. The vehicle damage was not severe; a deformation of 1.04 ft was measured.

Test R-B utilized a heavier vehicle (4650 lb) with an initial speed of 64 mph (see Figure IV.2.B.5.). The average deceleration over 17.3 ft and 0.340 sec was 7.9 g's, while the maximum deceleration of 13.4 g's was lower than that of the first test.

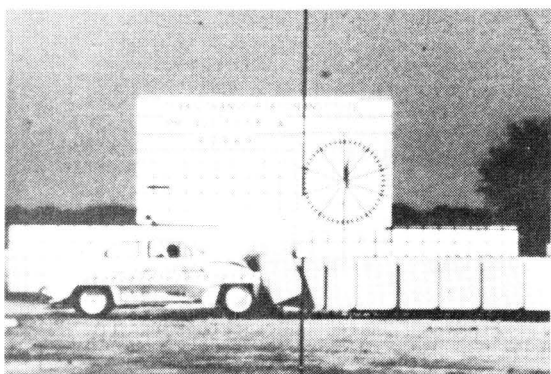
The third head-on test (Test R-D) was conducted on the modified system as described previously (see Figure IV.2.B.6.). In this test, a 1680 lb vehicle impacted the crash cushion at 59 mph. The stopping distance of 16.3 ft gave an average deceleration of 7.1 g's (over 0.580 sec), and the maximum deceleration was 15.6 g's. The vehicle apparently struck



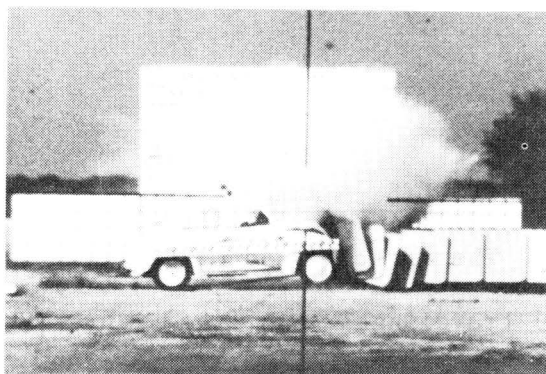
1



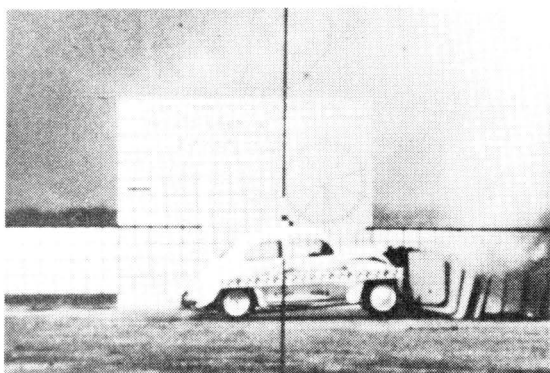
2



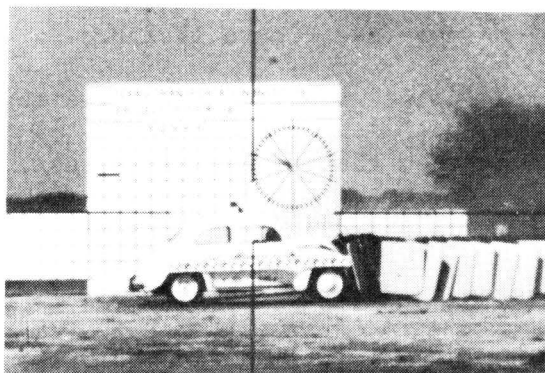
3



4

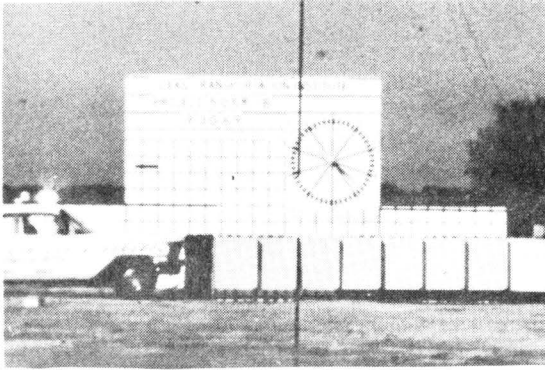


5

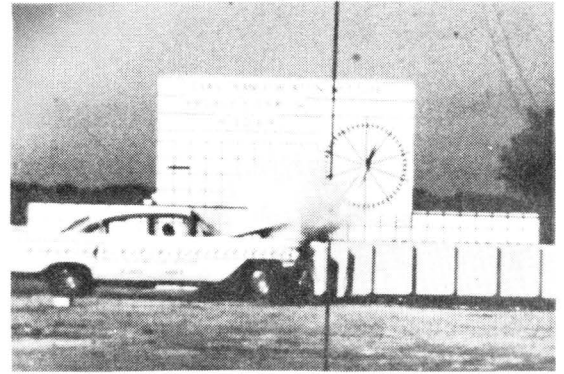


6

FIGURE IV.2.B.4. SEQUENTIAL PHOTOGRAPHS OF TEST R-A.



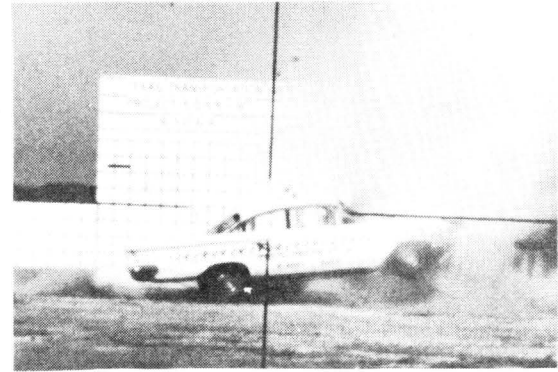
1



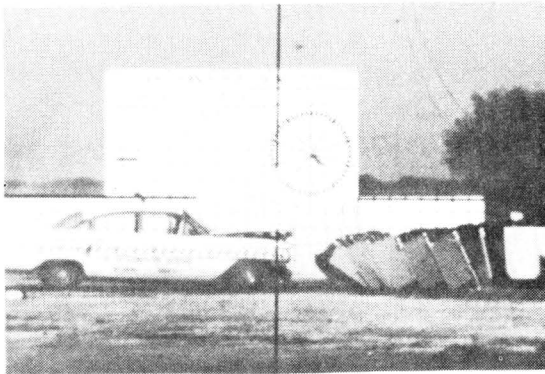
2



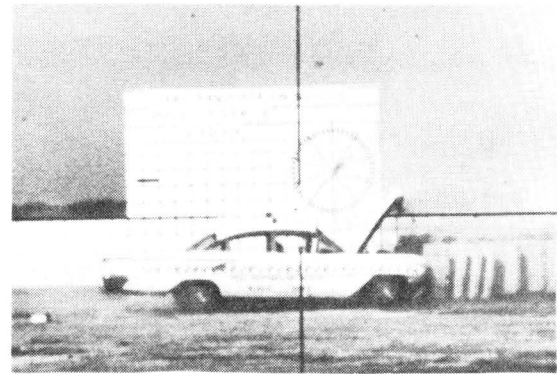
3



4

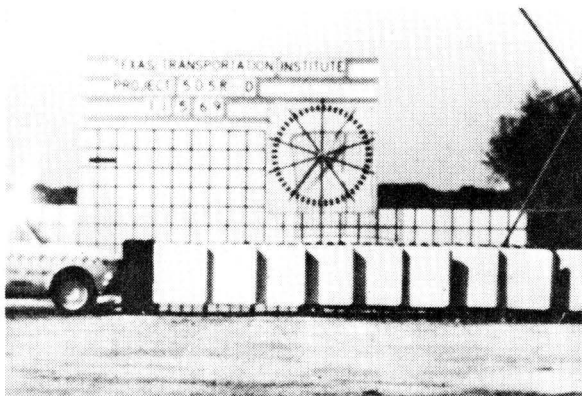


5

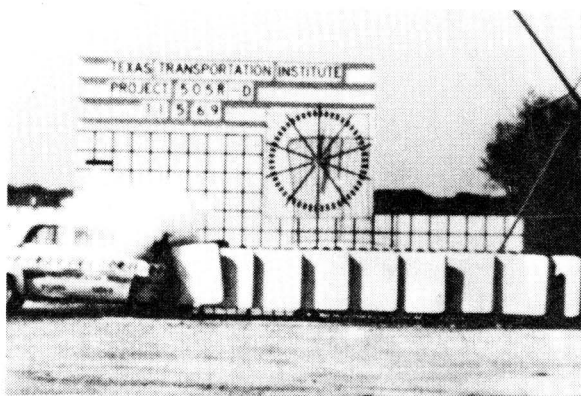


6

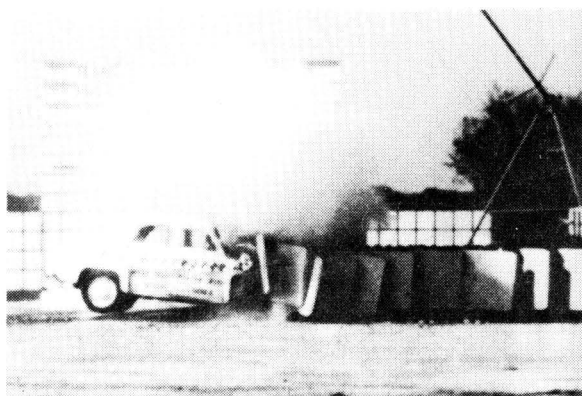
FIGURE IV.2.B.5. SEQUENTIAL PHOTOGRAPHS OF TEST R-B.



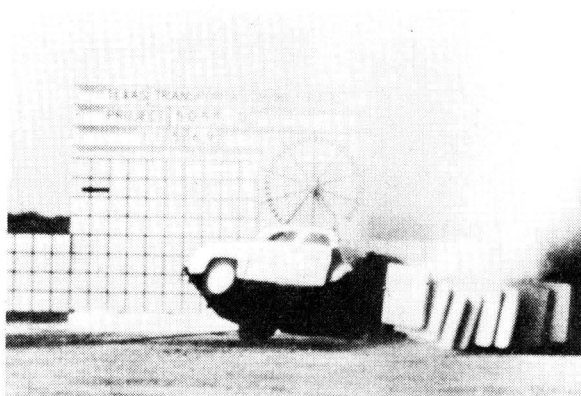
1



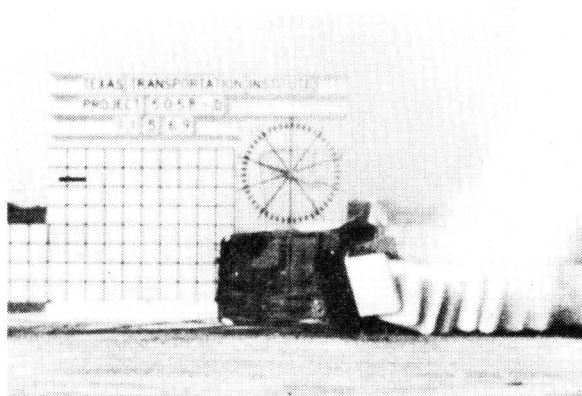
2



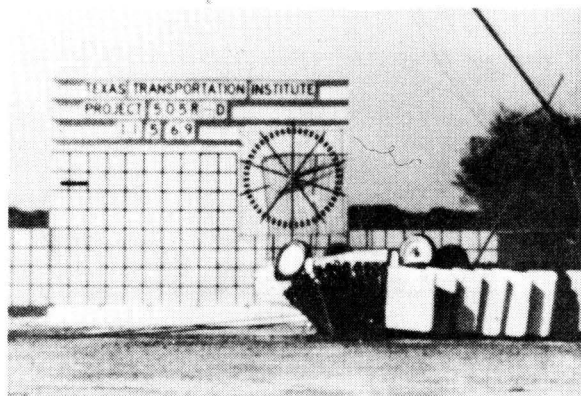
3



4



5



6

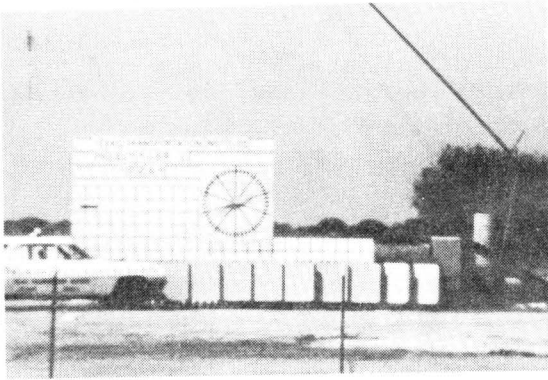
FIGURE IV.2.B.6. SEQUENTIAL PHOTOGRAPHS OF TEST R-D.

the front of the barrier about one foot off-center and started a yaw and roll motion, finally rolling over on its top after most of the kinetic energy had been absorbed.

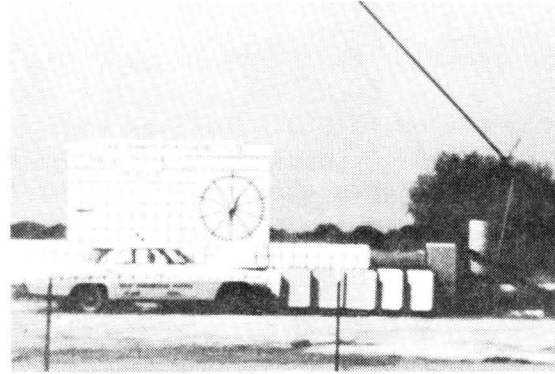
TEST RESULTS -- REDIRECTIONAL

The redirection capabilities of the unmodified crash cushion were tested under an impact at the angle of 20° with the barrier centerline in Test R-C. The 4410 lb vehicle struck the cushion at 54 mph (see Figure IV.2.B.7.). The vehicle had begun to redirect and had rotated approximately 5° when the main restraining cables pulled out of their front anchorage connections. The left front of the vehicle went head-on into the rigid barrier, and the vehicle rolled over on its right side. The cables pulled out of their connectors due to an improper installation procedure. Because of this installation error, this test cannot be judged representative of the performance of the barrier. In spite of this, the films showed a very tolerable average longitudinal deceleration of 5.8 g's over 16.7 ft and 0.340 sec.

A 20° impact test was also conducted on the modified system (Test R-E). A 3710 lb sedan impacted the barrier at 59 mph (see Figure IV.2.B.8.). This was the only test in which the vehicle left the barrier with significant speed. After impact, the vehicle began to ramp, or climb up the side of the barrier. It became completely airborne by as much as 1.5 ft for about 20 ft. Upon recontacting the ground, it rolled over on its left side before coming to rest upright. Examination of the vehicle and barrier indicate that a slight contact was made with the upper corner of the rigid steel wall. The average longitudinal deceleration during distance in contact (19.4 ft) was 4.9 g's. The maximum deceleration was 8.9 g's.



1



2



3



4

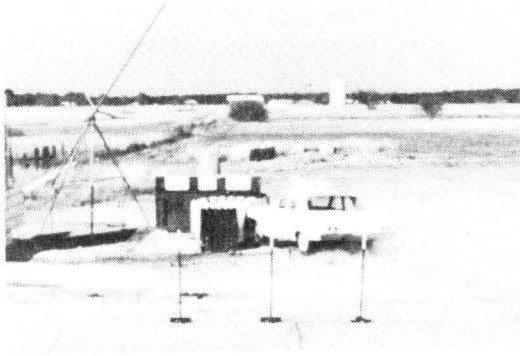


5

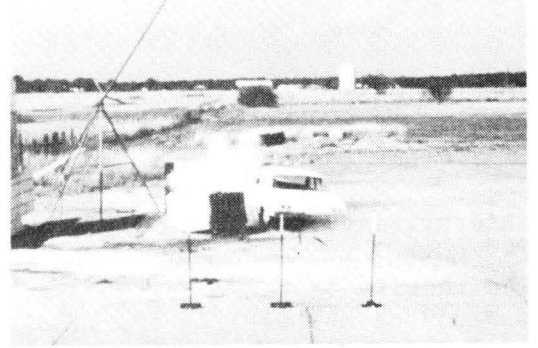


6

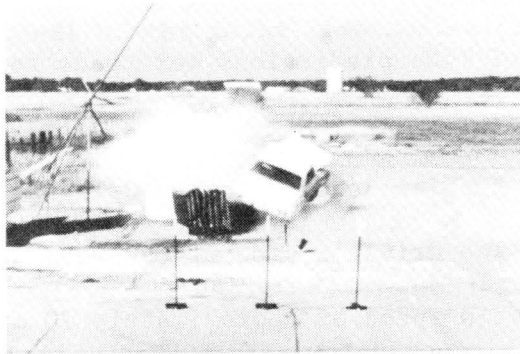
FIGURE IV.2.B.7. SEQUENTIAL PHOTOGRAPHS OF TEST R-C.



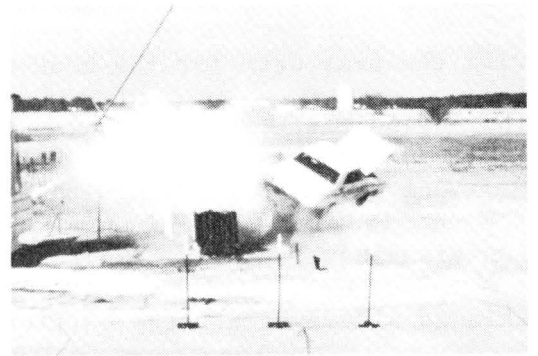
1



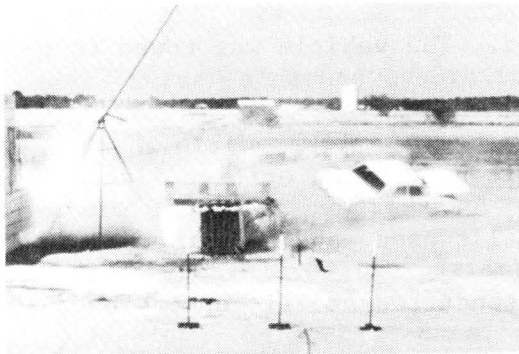
2



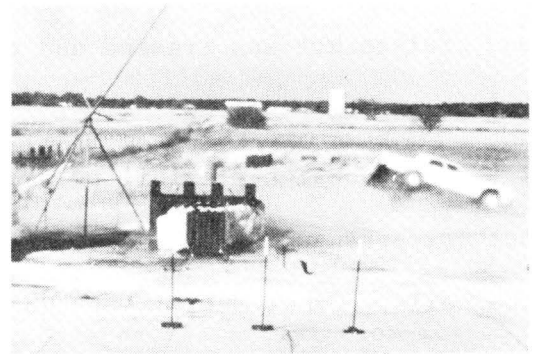
3



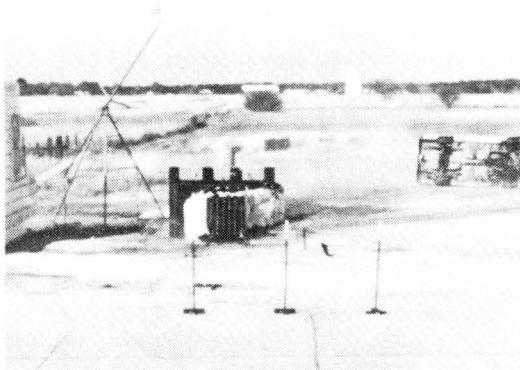
4



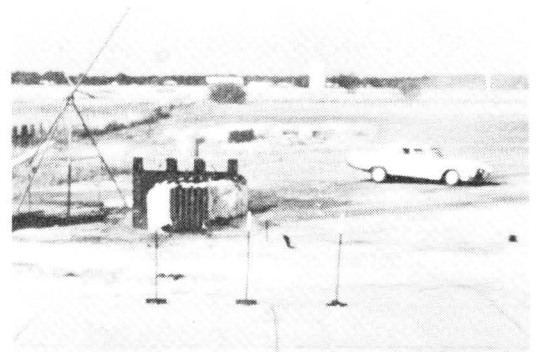
5



6



7



8

FIGURE IV.2.B.8. SEQUENTIAL PHOTOGRAPHS OF TEST R-E.

CONCLUSIONS

Other tests on this type of barrier have been conducted by Rich Enterprises, California Division of Highways, and Brigham Young University. The results of these tests have, in general, shown acceptable performance of this vehicle impact attenuator. The predictions of the mathematical model developed at Brigham Young University showed very good agreement with the test data for the head-on tests.⁵ No predictions were made for the angled tests.

One severe collision with a Hi-Dro cushion located in New Orleans, Louisiana has recently been reported.⁶ The driver's side of the vehicle skidded sideways into the barrier nose at a speed of approximately 70 mph on rain-slick pavement. The driver, who was unrestrained, suffered cuts and bruises but was treated and released. The vehicle was towed to a garage and then driven inside.

Great design flexibility is possible by varying orifice size and number, arrangement of cells, size of cells used, and amount of fluid in the cells. Other details of the tests conducted at TTI can be found in Technical Memorandum 505-11 which appears in Appendix F.

Part 2. C. --- TOR-SHOK ENERGY ABSORBING PROTECTIVE BARRIERBARRIER DESCRIPTION

The TOR-SHOK energy absorbing barrier was developed by ARA, Inc., under a contract with the Federal Highway Administration. The barrier was fabricated, delivered, and installed by ARA; and the vehicle crash tests were conducted by personnel of the Texas Transportation Institute. This highway protective system (see Figure IV.2.C.1.) is constructed of high-strength, lightweight elliptical steel tubes (4 in. x 7 in.) which are supported from the fixed object by a number of TOR-SHOK attenuators. At impact, the protective barrier tubes transmit the impact forces axially to the cylindrical TOR-SHOK arms which contain a large number of stainless steel "torus" elements that are squeezed between two cylindrical tubes. At impact, these "torus" elements absorb the energy by rolling between the cylinders. Eight of the twelve TOR-SHOK arms are acting in tension while four others are acting in compression. These TOR-SHOK arms exert a stopping force on the vehicle as the barrier deforms under the vehicle collision.

Design drawings, parametric data, and performance characteristics for the TOR-SHOK energy absorbing system are presented in Technical Memoranda 505-2 and 505-2S of Appendix F. This information was provided by ARA, Inc. Drawings B1450 and B1449 in Technical Memorandum 505-2 show the dimensions and configuration of the barrier tested. The barrier tested by TTI had a nose angle of 15°, a nose radius of 31 in., and the weight of the tubular nose was 845 lb.

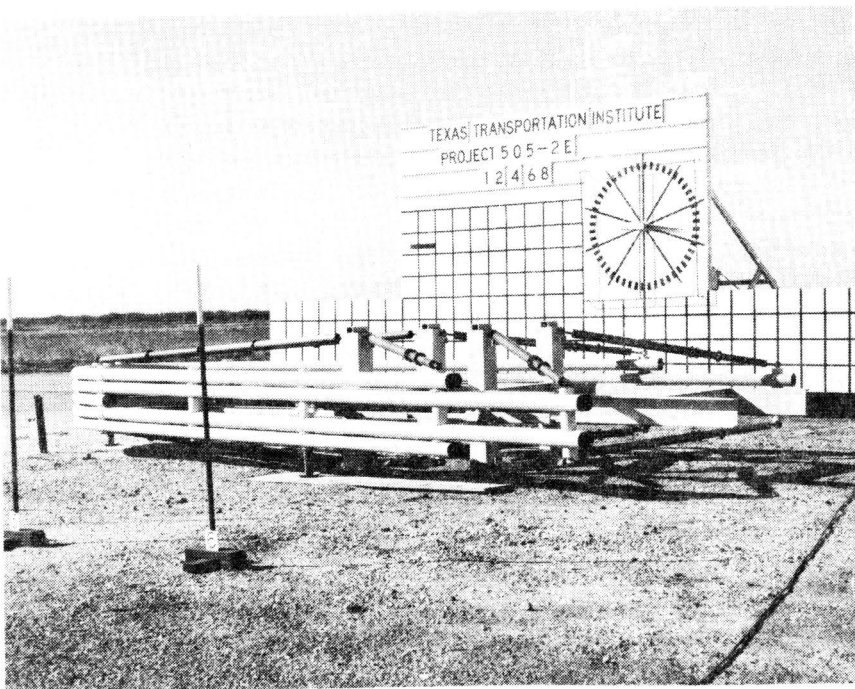


FIGURE IV.2.C.1. TOR-SHOK PROTECTIVE BARRIER
BEFORE TEST 505-2E.

TEST RESULTS

Detailed descriptions of the five crash tests conducted by TTI are given in Technical Memoranda 505-2 and 505-2S in Appendix F. One of the most successful tests conducted on the TOR-SHOK attenuator was Test 505-2A, which involved a 4600 lb vehicle impacting the TOR-SHOK head-on at a speed of 34.1 mph (see Figure IV.2.C.2.). The vehicle deformed the barrier 4.48 ft. The maximum TOR-SHOK stopping force was thus approximately 48 kips. The TOR-SHOKs absorbed 163 kip-ft of the vehicle kinetic energy (approximately 91%). The average deceleration during this impact was 6.6 g's. Vehicle deformation was 1.42 ft. The TOR-SHOK barrier performed as designed, with minor vehicle and barrier damage and a moderate deceleration level.

The third test on this system (Test 2C) was conducted with a heavier vehicle (4940 lb) at a higher speed (59.4 mph) and also resulted in vehicle arrestment (see Figure IV.2.C.3.). However, barrier deformation (11.12 ft) and vehicle deformation (1.75 ft) were greater than those in the first test. Average deceleration was 9.9 g's, and damage to the barrier was severe.

Other tests conducted on this system are described in Technical Memoranda 505-2 and 505-2S in Appendix F. For head-on collisions, the TOR-SHOK system provided reasonable impact attenuation when struck by heavy vehicles (4000 lb or more). When the kinetic energy of the vehicle exceeds about 425,000 ft-lb, considerable damage to the barrier and TOR-SHOKs can be anticipated. For the angled collisions conducted (Tests 2D and 2E), the performance of the system was unsatisfactory. Modifications of the system to insure proper activation of the TOR-SHOK arms under angle hits should minimize or correct this deficiency. Modifications are being made by the designers.

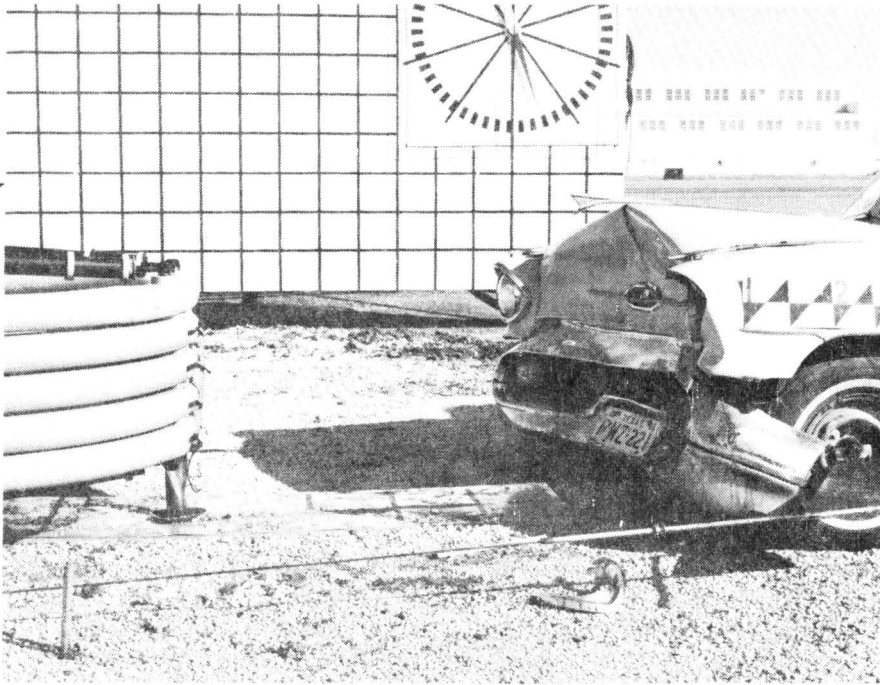


FIGURE IV.2.C.2. TOR-SHOK AND VEHICLE AFTER COLLISION, TEST 505-2A.

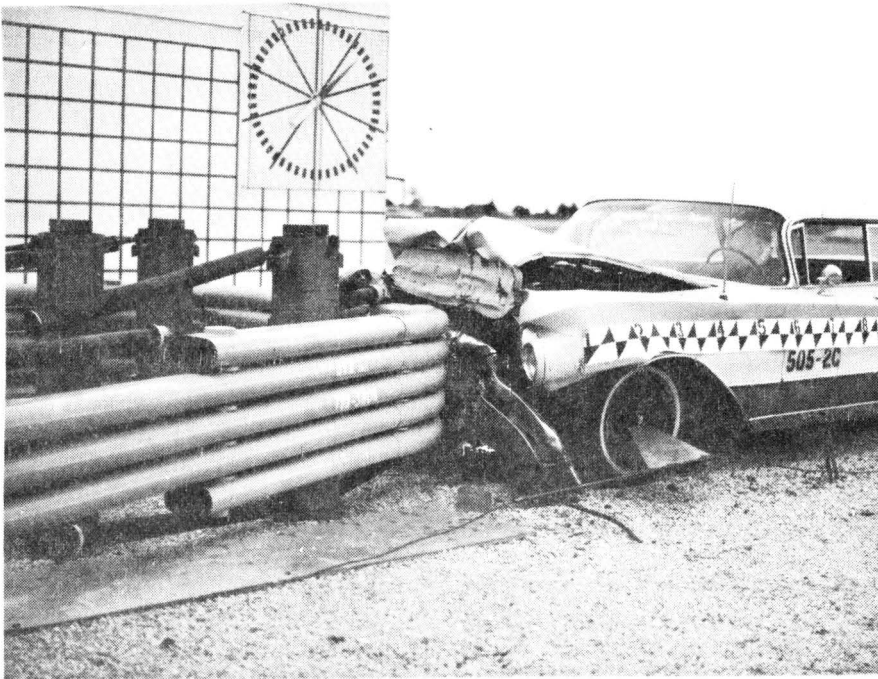


FIGURE IV.2.C.3. VEHICLE AND BARRIER AFTER TEST 505-2C.

Part 2. D. --- LIGHTWEIGHT CELLULAR CONCRETE VEHICLE CRASH CUSHIONBARRIER DESCRIPTION

Six vehicle crash tests on a lightweight cellular concrete crash cushion have been conducted under this project with very favorable results. The crash cushion is composed of vermiculite concrete with hollow cardboard Sonotubes (23 in. in diameter) spaced throughout to provide the necessary voids. Lightweight welded wire fabric was used as reinforcement for the vermiculite.

The concrete used for the crash cushions in this study was composed of cement, water, and a commercial grade of vermiculite. Vermiculite is a kiln-expanded mica and this vermiculite aggregate was very uniform in gradation. The extreme light weight (per bulk volume) of this aggregate in combination with a high degree of air entrainment produces a very lightweight, low-strength concrete.

The evolution of the cellular concrete crash cushion is shown graphically in Figure IV.2.D.1. The first step in the evaluation of this newly designed system was the feasibility testing of a prototype cushion which was only one-half the length (12 ft) of the proposed full-size crash cushion (24 ft). With encouraging results from the first test, full-scale, head-on testing was conducted on two cushions incorporating design modifications and different construction techniques. Because of the excellent performance of the concrete crash cushion in the first three tests conducted, it was decided to take step three in the evaluation of the system-- side angle testing. Side fender panels which were previously tested as part of the Modular Crash Cushion were added to the concrete crash cushion,

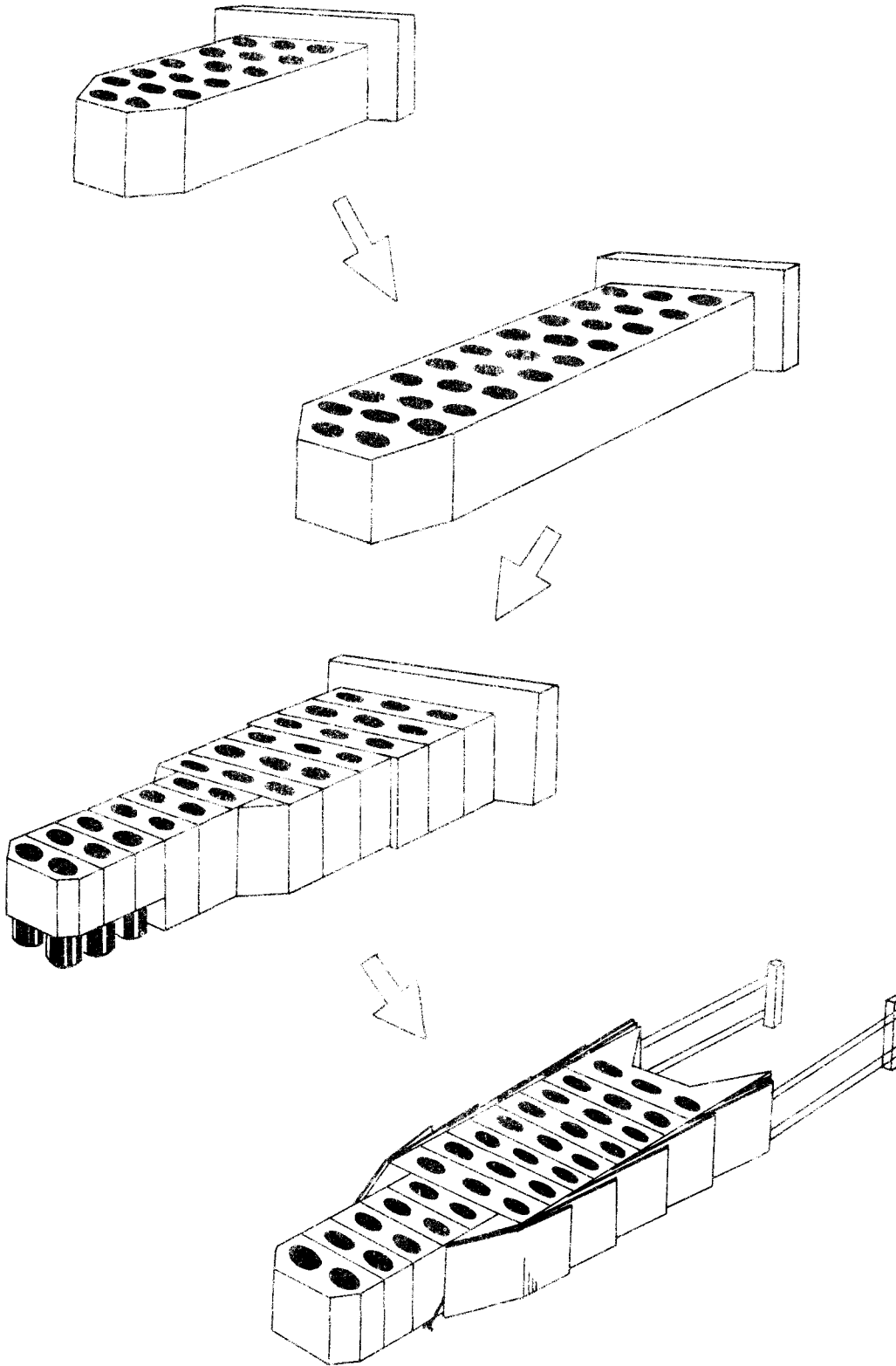


FIGURE IV.2.D.1. THE EVOLUTION OF THE CELLULAR CONCRETE CRASH CUSHION.

and other modifications were made before two angle tests involving heavy vehicles and one head-on test involving a lightweight vehicle were conducted on the crash cushion.

The prototype crash cushion for Test V-A was cast as a single unit, then transported to the test site and installed (see Figure IV.2.D.2.). Folding cardboard carton forms were used to support the cushion 6 in. above ground level when installed at the test site. The crash cushion for Test V-B was cast in place at the test site. Figure IV.2.D.3. shows the configuration of this cushion. Cardboard carton forms again supported the cushion. The Sonotube spacing in the cushions is maintained with small wooden blocks.

The precast modular construction technique was used for the remaining four crash cushions and the barrier was put together in the field using three-tube and two-tube modules. One of the three-tube modules is shown in Figures IV.2.D.4. and IV.2.D.5. The cushion for Test V-C was supported on cardboard forms in the front and re-bar chairs in the back. The design of this cushion is shown by Figure IV.2.D.6. For Tests V-D, V-E, and V-F, redirection panels were attached to the sides of the crash cushion, the rear module voids were filled with vermiculite, I-beams mounted on skid plates were incorporated, re-bar chairs were used to support the cushions above the ground, the position of the cables and their anchors were changed, and other modifications were made. This configuration is shown in Figure IV.2.D.7.

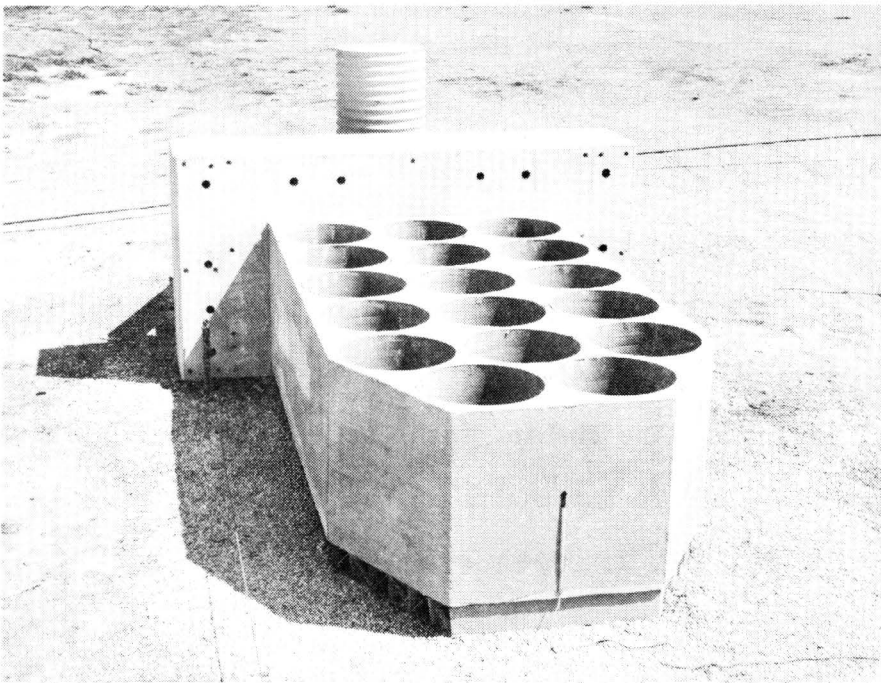


FIGURE IV.2.D.2. PROTOTYPE OF CONCRETE CRASH CUSHION.

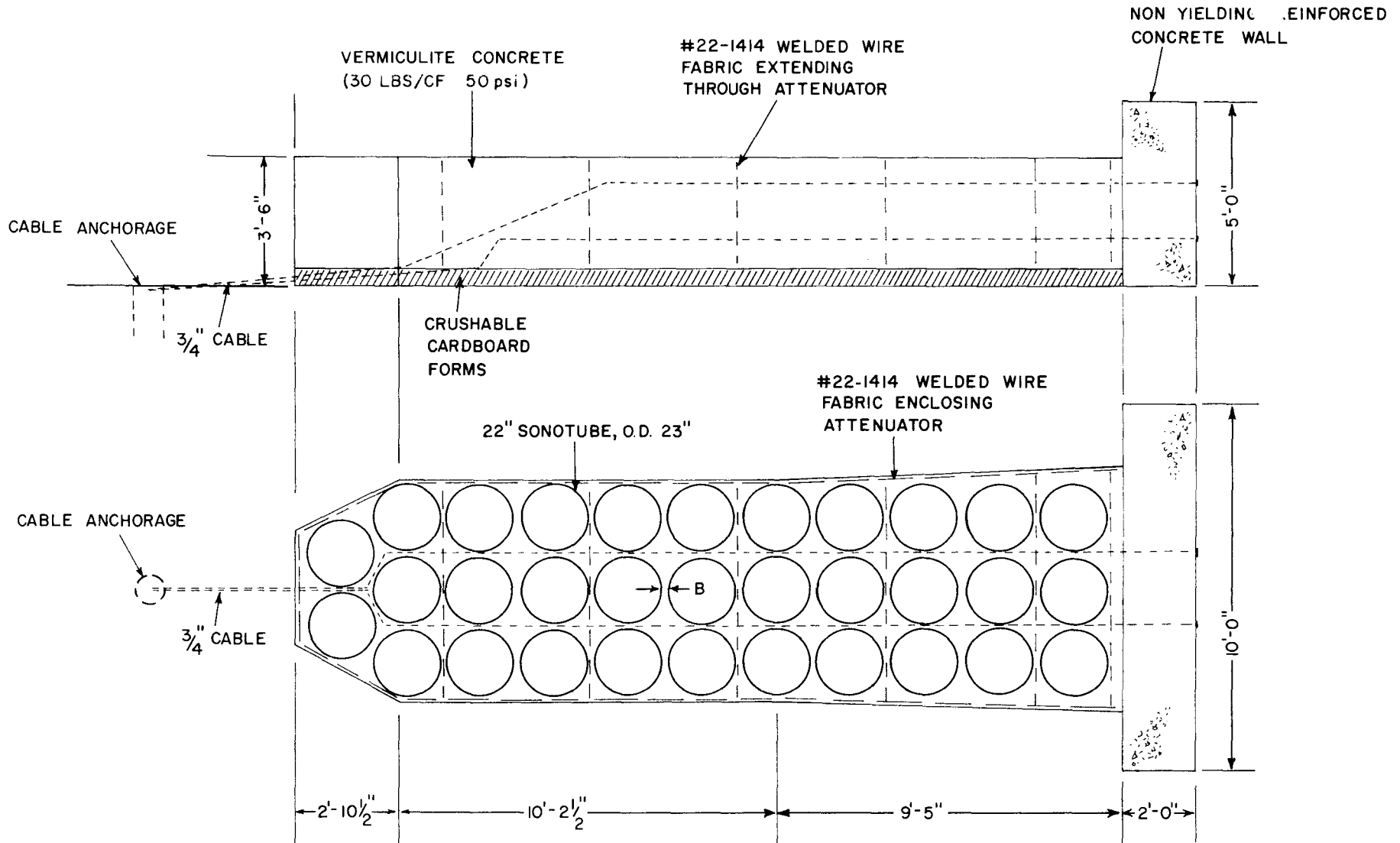


FIGURE IV.2.D.3 CONCRETE CRASH CUSHION, TEST 505 V-B

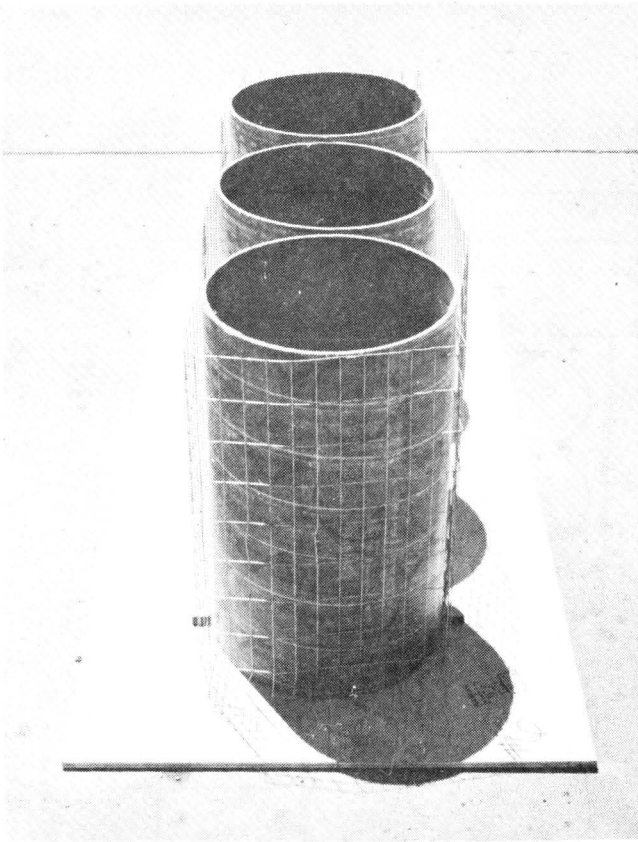


FIGURE IV.2.D.4. NONCONCRETE COMPONENTS OF PRECAST VERMICULITE MODULE.



FIGURE IV.2.D.5. PRECAST VERMICULITE MODULE.

NON-YIELDING
REINFORCED
CONCRETE WALL

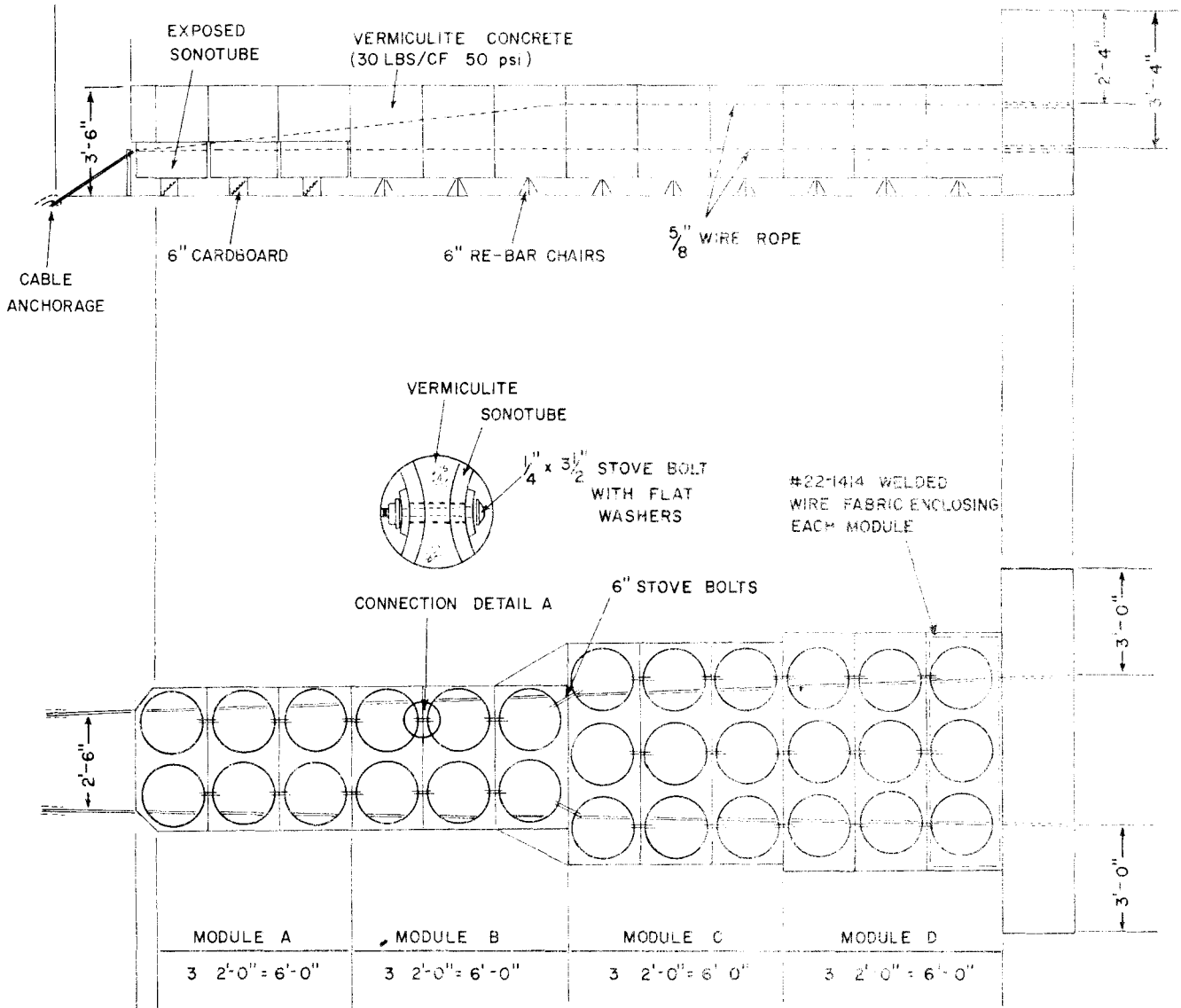


FIGURE IV.2.D.6. CONCRETE CRASH CUSHION, TEST 505 V-C

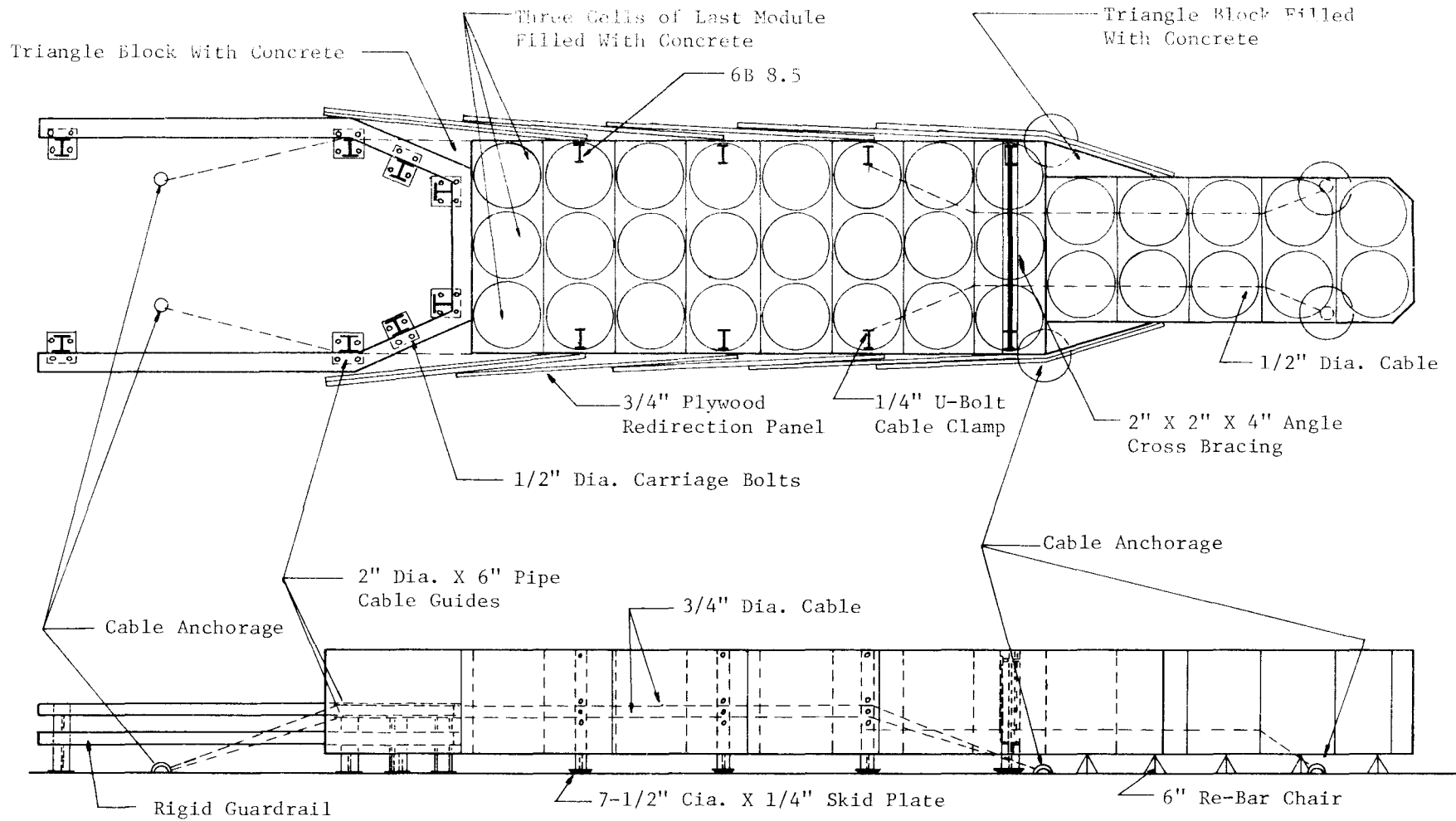


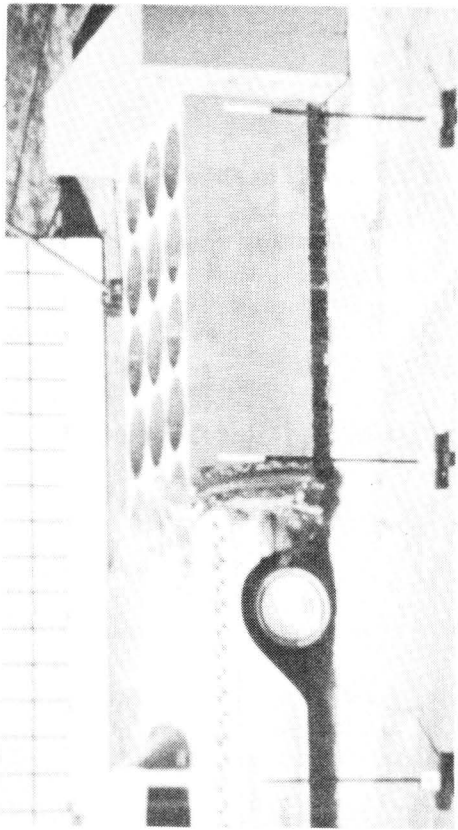
FIGURE IV.2.D.7. DETAILS OF CONCRETE CRASH CUSHION (TESTS 505 V-D, V-E, AND V-F).

TEST RESULTS

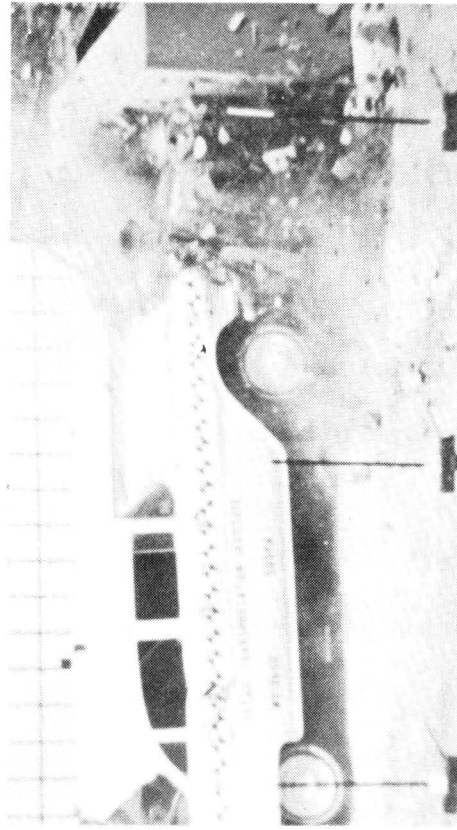
The prototype crash cushion was subjected to a low-speed, head-on test (41.1 mph) by a 3650 lb vehicle in Test V-A. The vehicle was stopped in 9.0 ft, with an average barrier force of 23,000 lb (see Figure IV.2.D.8.). The average deceleration was 6.3 g's and the maximum was 10.5 g's. Only superficial sheet metal damage was sustained by the vehicle (deformation was 7 in.).

Test V-B illustrated the importance of the control of certain parameters in the fabrication of lightweight cellular concrete crash cushions (see Figure IV.2.D.9.). The compressive strength of the vermiculite concrete was increased and the spacing between the Sonotubes was also increased. The welded wire fabric was placed in the top and bottom of this barrier to eliminate the tendency of some portions of the barrier to scatter on impact. Due to these differences, the barrier was significantly stiffer than the previous barrier tested and an average deceleration level of 10.3 g's was observed. This corresponds to an average stopping force of approximately 33,000 lb. The 3200 lb vehicle impacted the cushion at 58.8 mph. More sheet metal damage was done to this vehicle than the previous one. The entire front was deformed approximately 12 in.

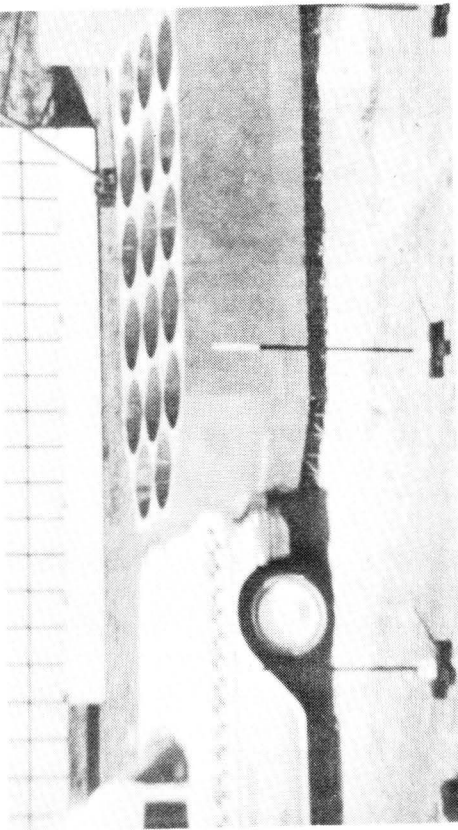
Based on the results of the first two tests, a third barrier was designed and tested with a 4560 lb vehicle traveling 63.6 mph. Test V-C was also a head-on impact (see Figure IV.2.D.10.). The vehicle was stopped in 21.4 ft and an average deceleration of 6.3 g's, which means an average stopping force of 28,700 lb. Predictions of stopping forces for this barrier had been made (see Technical Memorandum 505-9 in Appendix F) and estimated crushing force levels from photographic data showed the



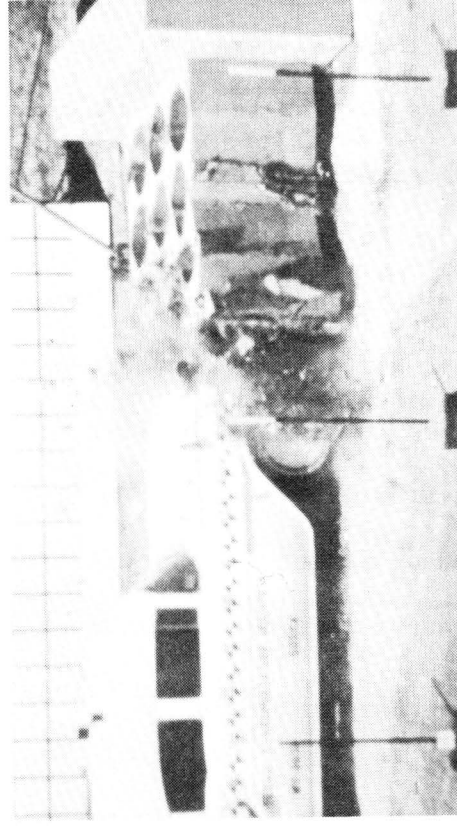
1



2

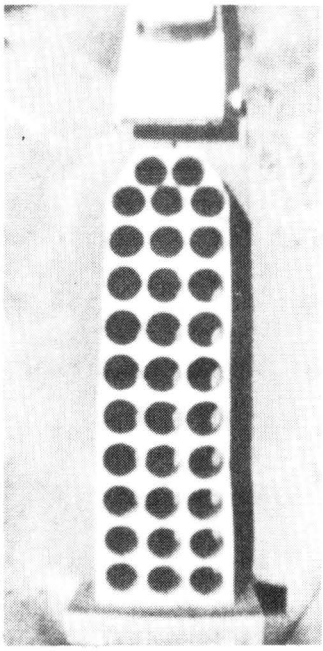


3

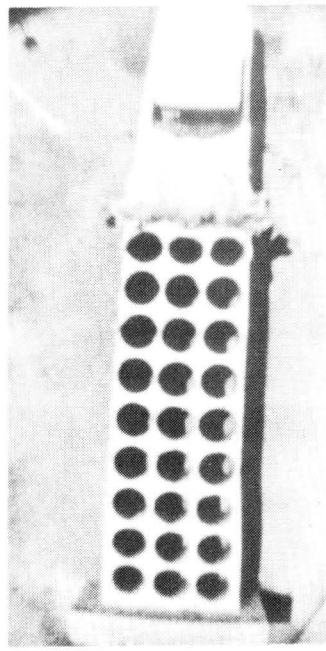


4

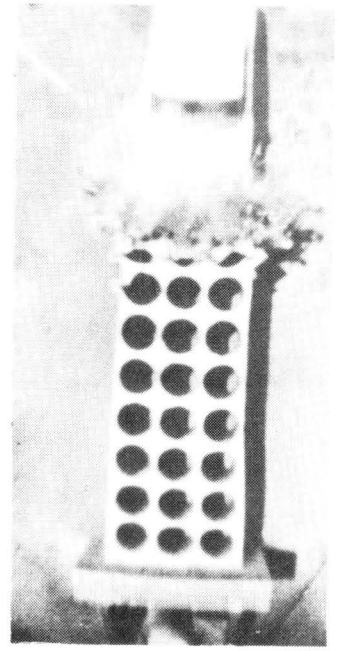
FIGURE IV.2.D.8. SEQUENTIAL PHOTOGRAPHS OF TEST V-A.



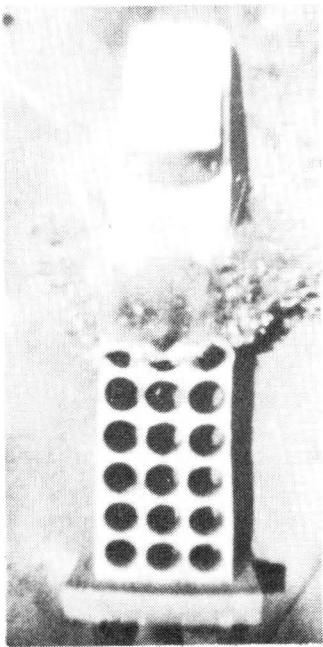
1



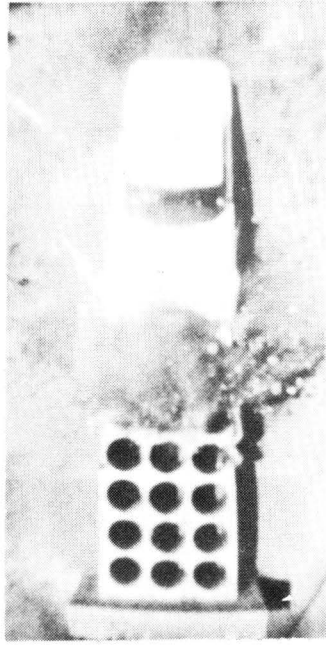
2



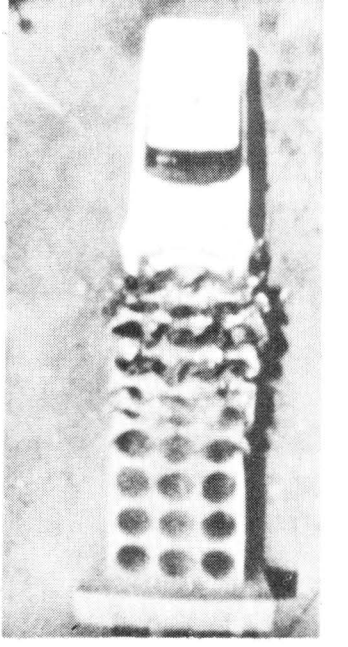
3



4

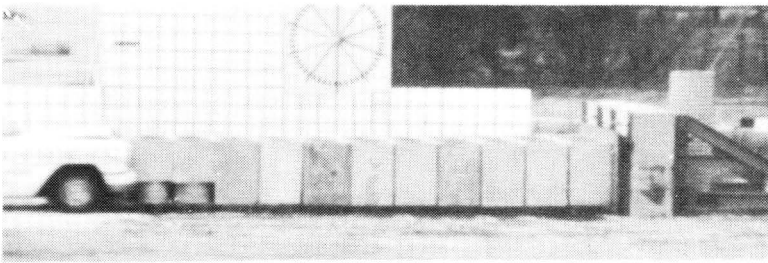


5

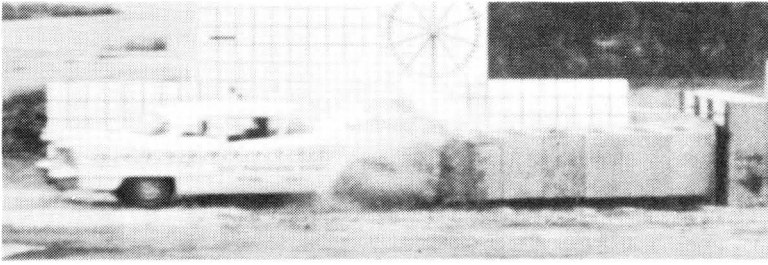


6

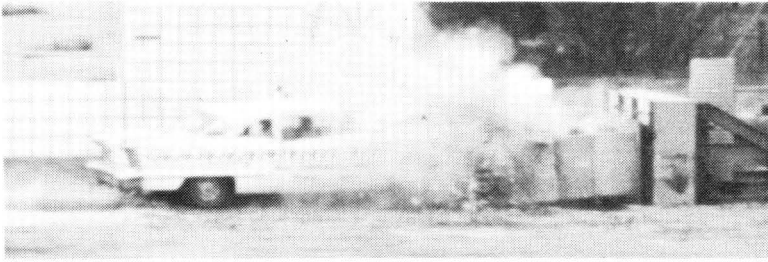
FIGURE IV.2.D.9. OVERHEAD SEQUENCE PHOTOGRAPHS OF TEST V-B.



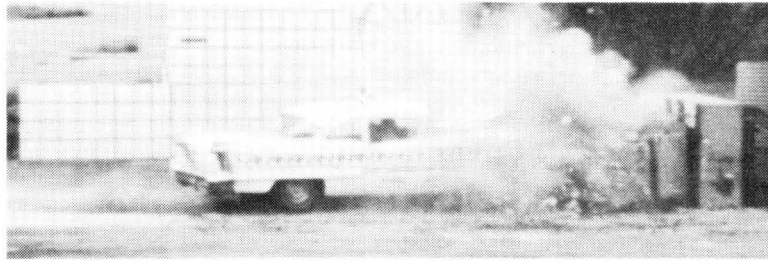
1



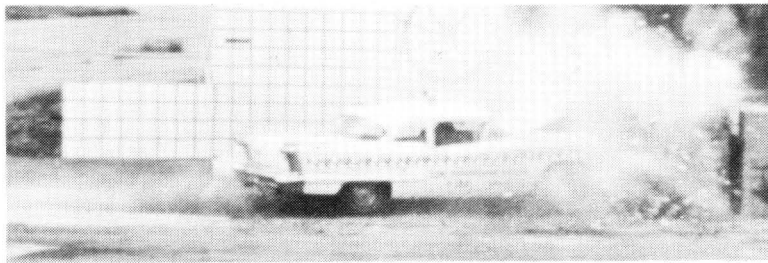
2



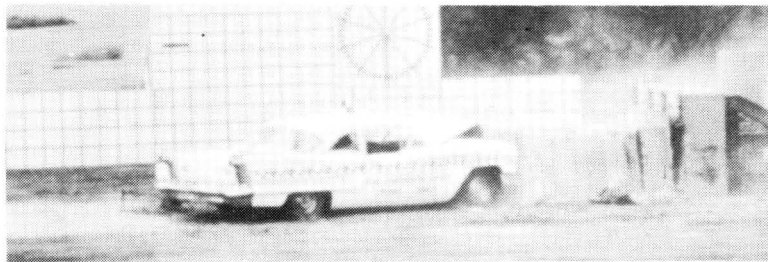
3



4



5



6

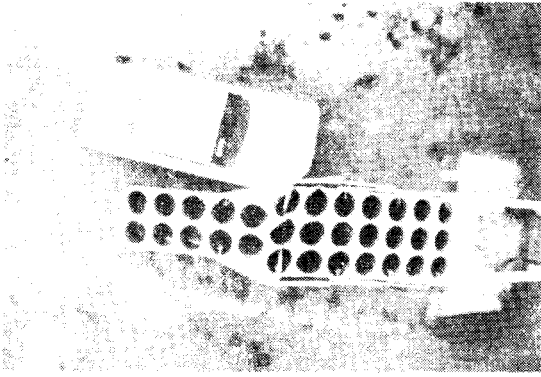
FIGURE IV.2.D.10. SEQUENTIAL PHOTOGRAPHS OF TEST V-C.

predictions to be fairly accurate. Again, only superficial sheet metal and some bumper damage was sustained.

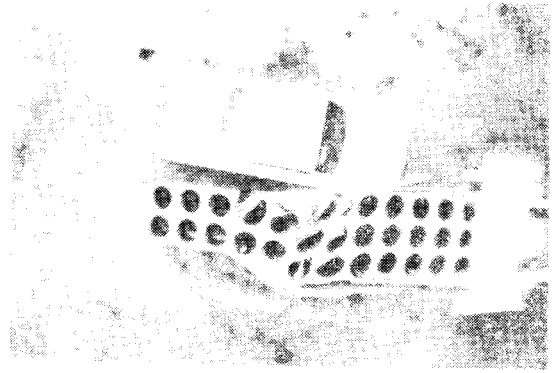
Test V-D was conducted to determine the redirection capabilities of the vermiculite crash cushion with redirection panels attached to the sides of the barrier. The 3790 lb vehicle was traveling 57.2 mph when it impacted the barrier at an angle of 10° at the point where the cables were anchored at the side of the cushion (see Figure IV.2.D.11.). The vehicle was smoothly redirected, with an average longitudinal deceleration of 1.3 g's and peak g's reaching 6.2 g's. The average transverse deceleration was 2.4 g's, with a peak of 9.8 g's. Vehicle damage was relatively light; only five modules of the cushion were significantly damaged and the cushion could probably have still sustained a head-on impact in its condition.

Test V-E represents the only test conducted to date in which an unacceptable reaction of the vehicle was found. The 3820 lb vehicle impacted the crash cushion at a 20° angle and speed of 59.7 mph (see Figure IV.2.D.12.). The average longitudinal deceleration was 5.6 g's. As the vehicle slid down the side of the cushion, a slight ramping tendency was observed which culminated in a high roll-initiating force as the vehicle reached the end of the cushion. The vehicle skidded on its left side after losing contact with the cushion, rolled upright, and then rolled over on its top. It came to rest approximately 80 ft past the barrier. An analysis of the factors which caused this roll and recommendations for modifications of the barrier to preclude such a situation can be found in Technical Memorandum 505-9S which appears in Appendix F.

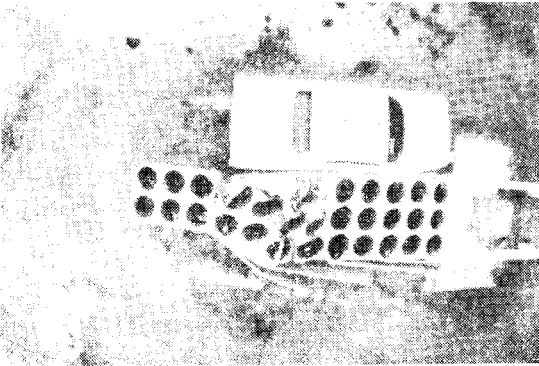
As a final test of the system, Test V-F was conducted to observe the reaction of the latest crash cushion design under a head-on collision



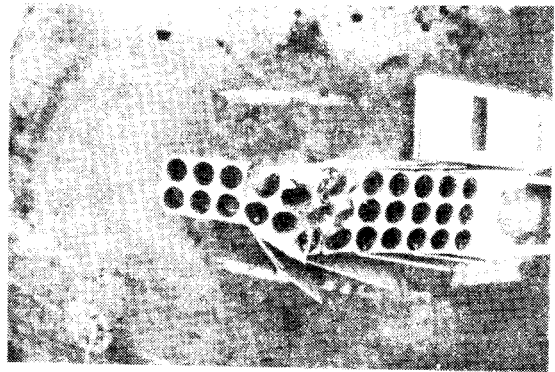
1



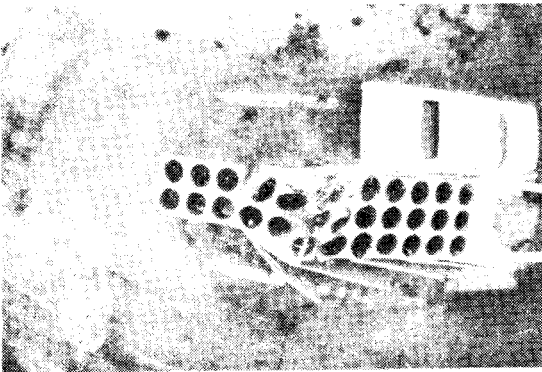
2



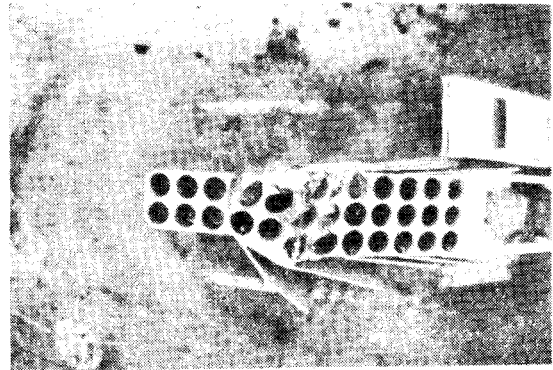
3



4

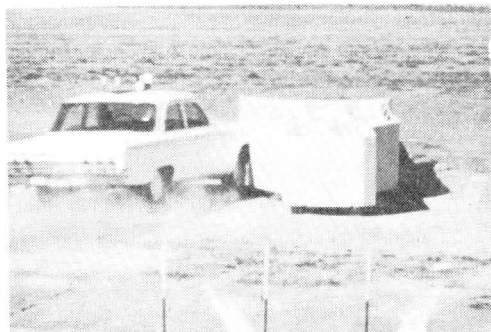


5

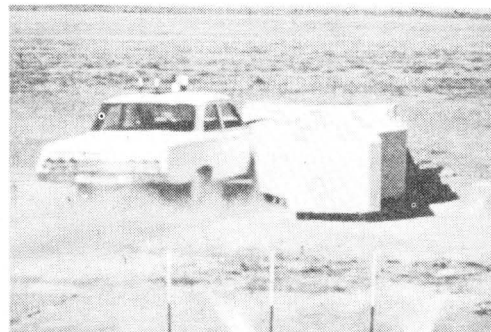


6

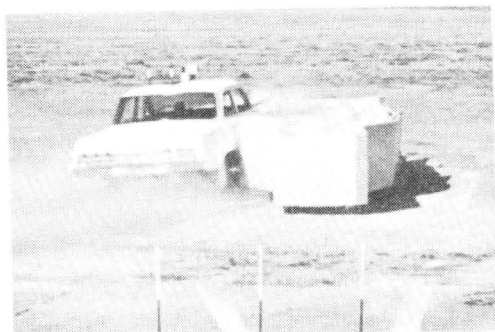
FIGURE IV.2.D.11. SEQUENTIAL PHOTOGRAPHS OF TEST V-D.



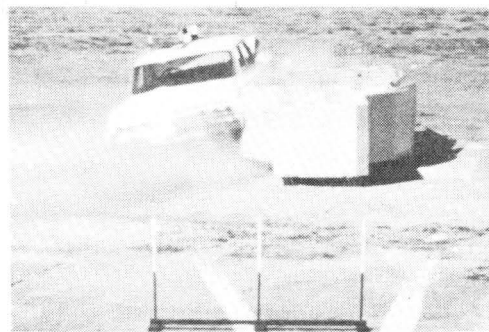
1



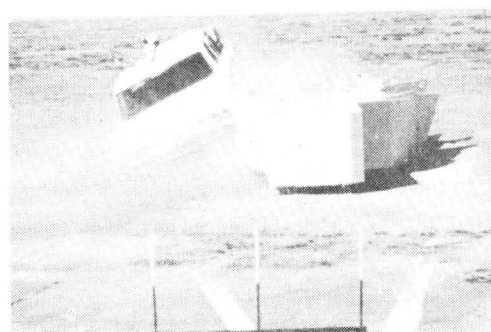
2



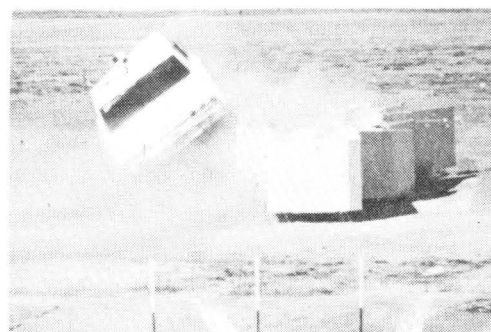
3



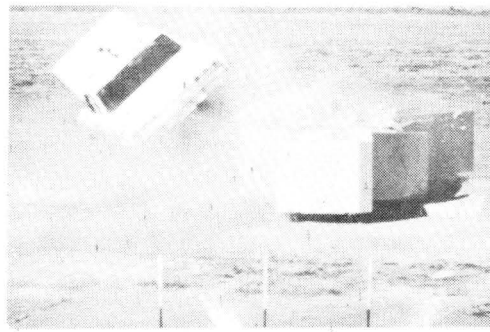
4



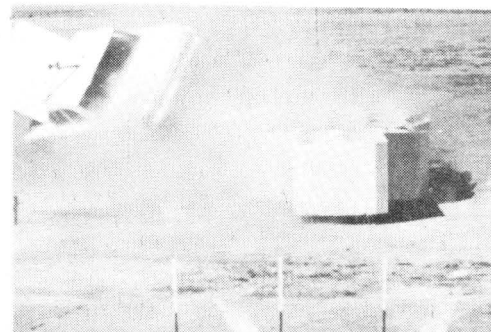
5



6



7



8

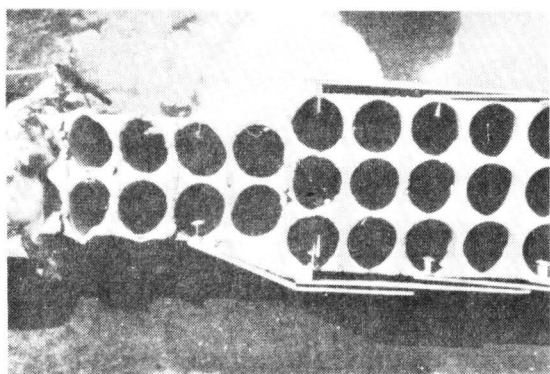
FIGURE IV.2.D.12. SEQUENTIAL PHOTOGRAPHS OF TEST V-E.

using a very lightweight vehicle. The 2210 lb vehicle impacted the crash cushion with a speed of 61.2 mph (see Figure IV.2.D.13.). The average longitudinal deceleration was 10.2 g's. The interaction of the vehicle and cushion was considered extremely good and the vehicle damage was moderate.

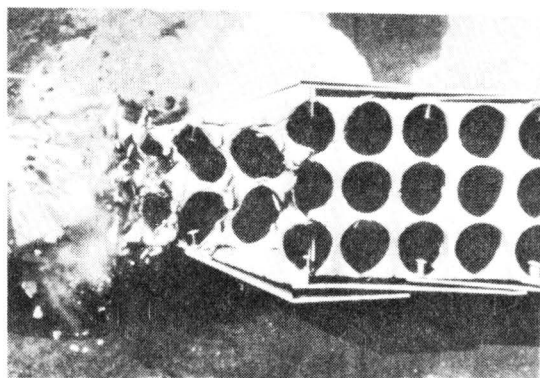
CONCLUSIONS

The cellular concrete crash cushion has now shown a capability to perform effectively in decelerating a vehicle for both the head-on and side-angle crash conditions. Close quality control should be exercised on the geometry of the module and on the vermiculite concrete. Control of batch proportions and unit weight will give predictable crushing strengths. Replacement of segments of the crash cushion can be easily accomplished after a collision.

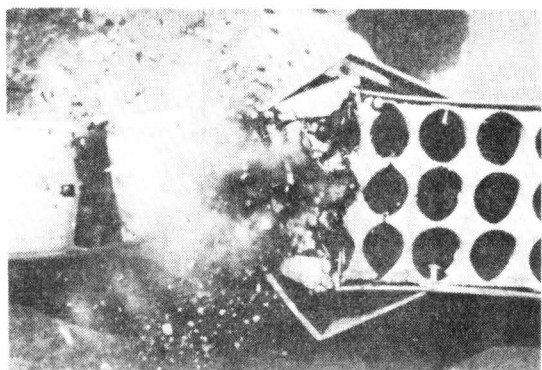
Modifications are continually made in order to design the best possible crash cushion. Cellular Concrete Crash Cushions will be appearing on Florida highways soon and many applications for use of this cushion are being investigated. For details on the predicted stopping forces, construction of the crash cushions, and data from the model study and durability tests of vermiculite, consult Technical Memoranda 505-9 and 505-9S which appear in Appendix F.



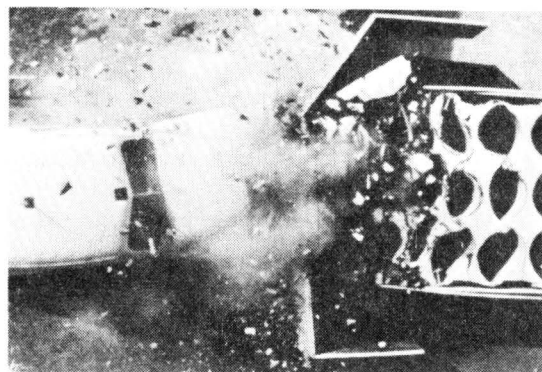
1



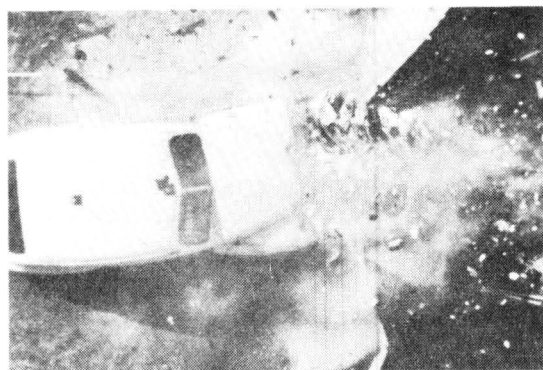
2



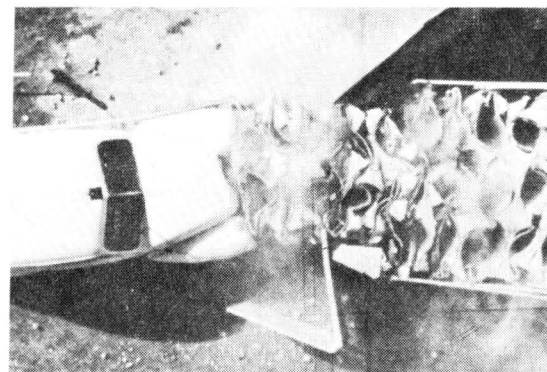
3



4



5



6

FIGURE IV.2.D.13. SEQUENTIAL PHOTOGRAPHS OF TEST V-F.

Part 2. E. --- CORRUGATED METAL PIPE CRASH CUSHIONBARRIER DESCRIPTION

Three experimental crash tests were conducted on two crash cushion designs of corrugated steel pipes. The cushion for Test 505 CSP-1 consisted of fifteen rows of 15 in. diameter pipes of 16- and 14-gage metal (see Figure IV.2.E.1.). This test was conducted to observe the overall dynamic interaction of the vehicle and crash cushion. The cushion installation for tests CSP-2 and CSP-3 consisted of nine rows of 24 in. diameter pipes of 16- and 14-gage metal and eight rows of 18 in. diameter pipes of 16- and 14-gage metal. Flexbeam panels were attached to the front and sides of the cushion to give it redirection capability (see Figure IV.2.E.2.). Test CSP-2 was an angle test conducted to evaluate the redirection capability of the flexbeam panels. The objective of the head-on test, CSP-3, was to determine if the addition of the flexbeam on the nose and the more numerous and stronger support posts would eliminate the ramping tendency observed in test CSP-1.

TEST RESULTS

The head-on test of the first cushion (CSP-1) involved a 3750 lb vehicle traveling 58.4 mph. After the first seven rows of pipes had crushed, the vehicle ramped upward and became airborne. The front portion of the barrier pivoted upward and the first 5 rows of pipes became detached in a group and rotated through 360° in the air before coming to rest on top of the rear portion of the barrier near the backup wall (see Figures IV.2.E.3. & 4.). Little vehicle damage resulted (0.5 ft) despite an average longitudinal deceleration of 10.2 g's during the 89 msec before ramping.

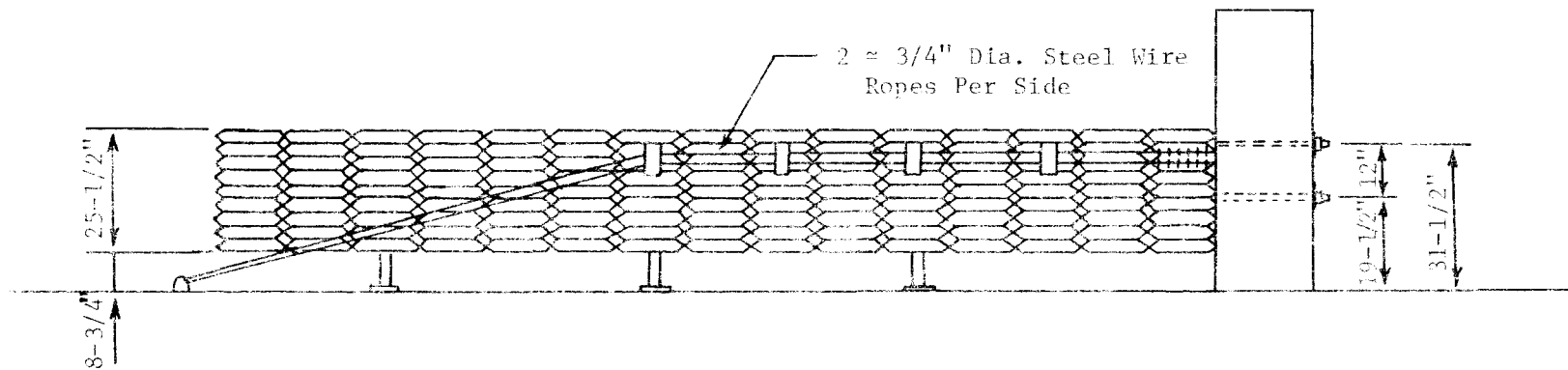
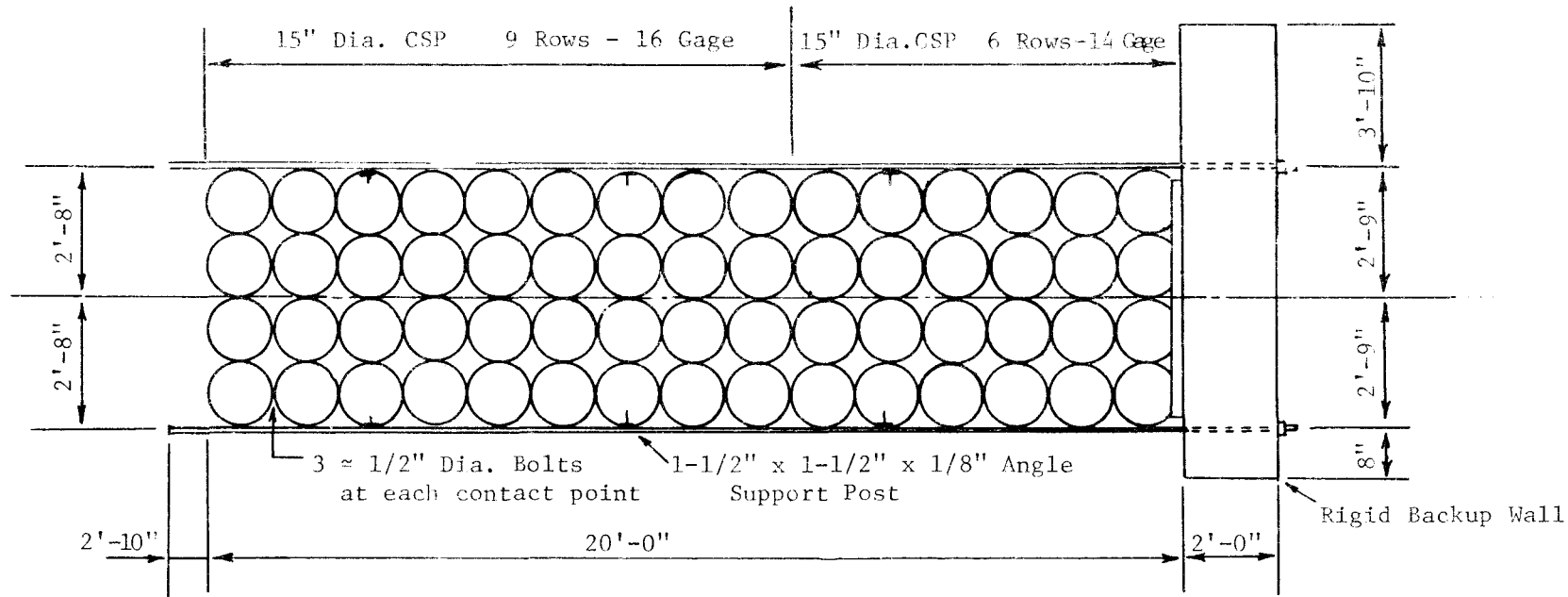
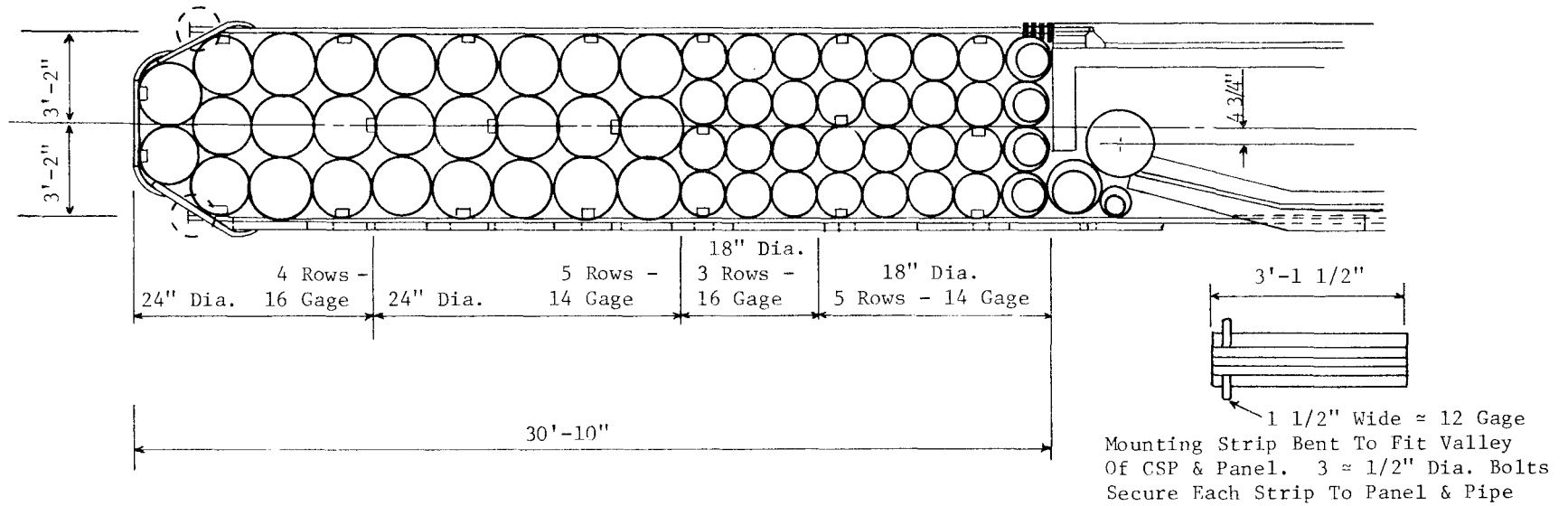


FIGURE IV.2.E.1. CORRUGATED STEEL PIPE CRASH CUSHION USED FOR FPST 505 CSP-1.



FLEXBEAM PANEL DETAIL

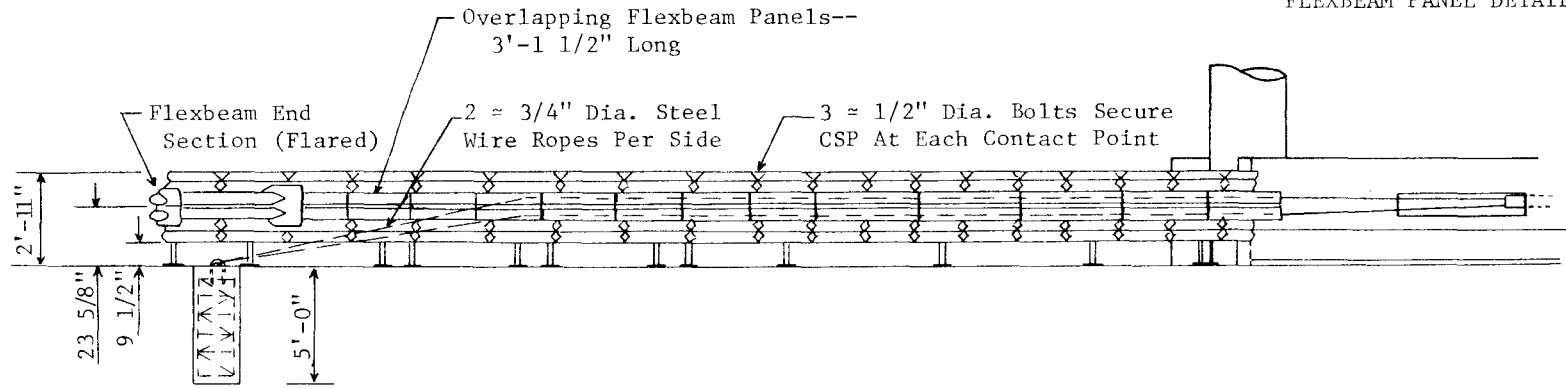


FIGURE IV.2.E.2. CORRUGATED STEEL PIPE CRASH CUSHION USED FOR TESTS 505 CSP-2 & -3.

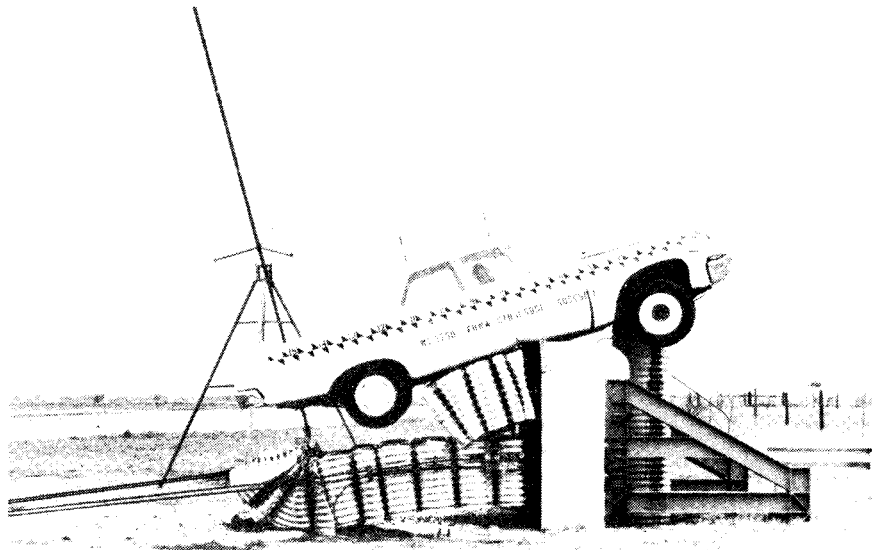
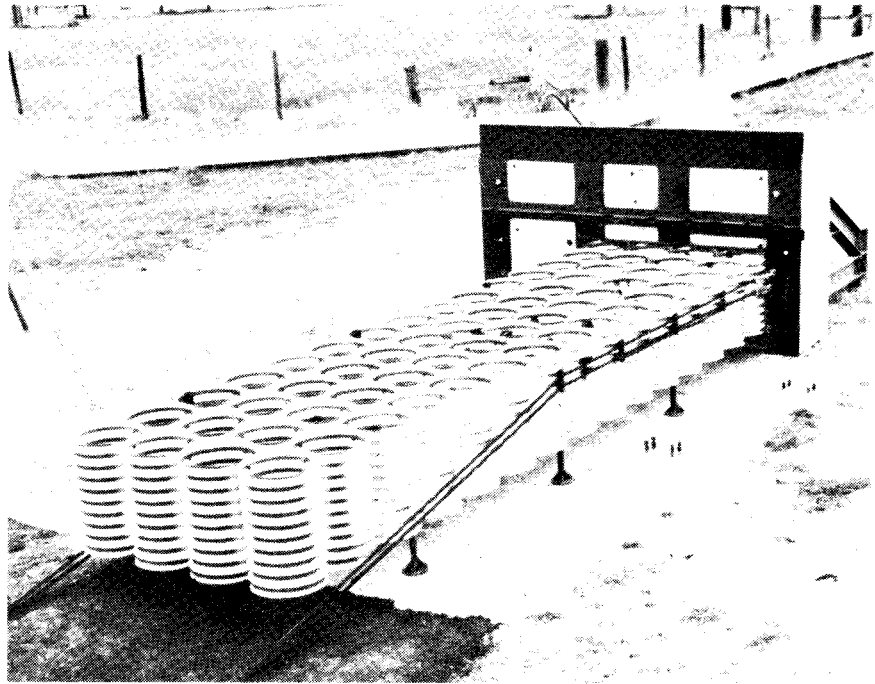


FIGURE IV.2.E.3. CRASH CUSHION BEFORE AND AFTER TEST 505 CSP-1.

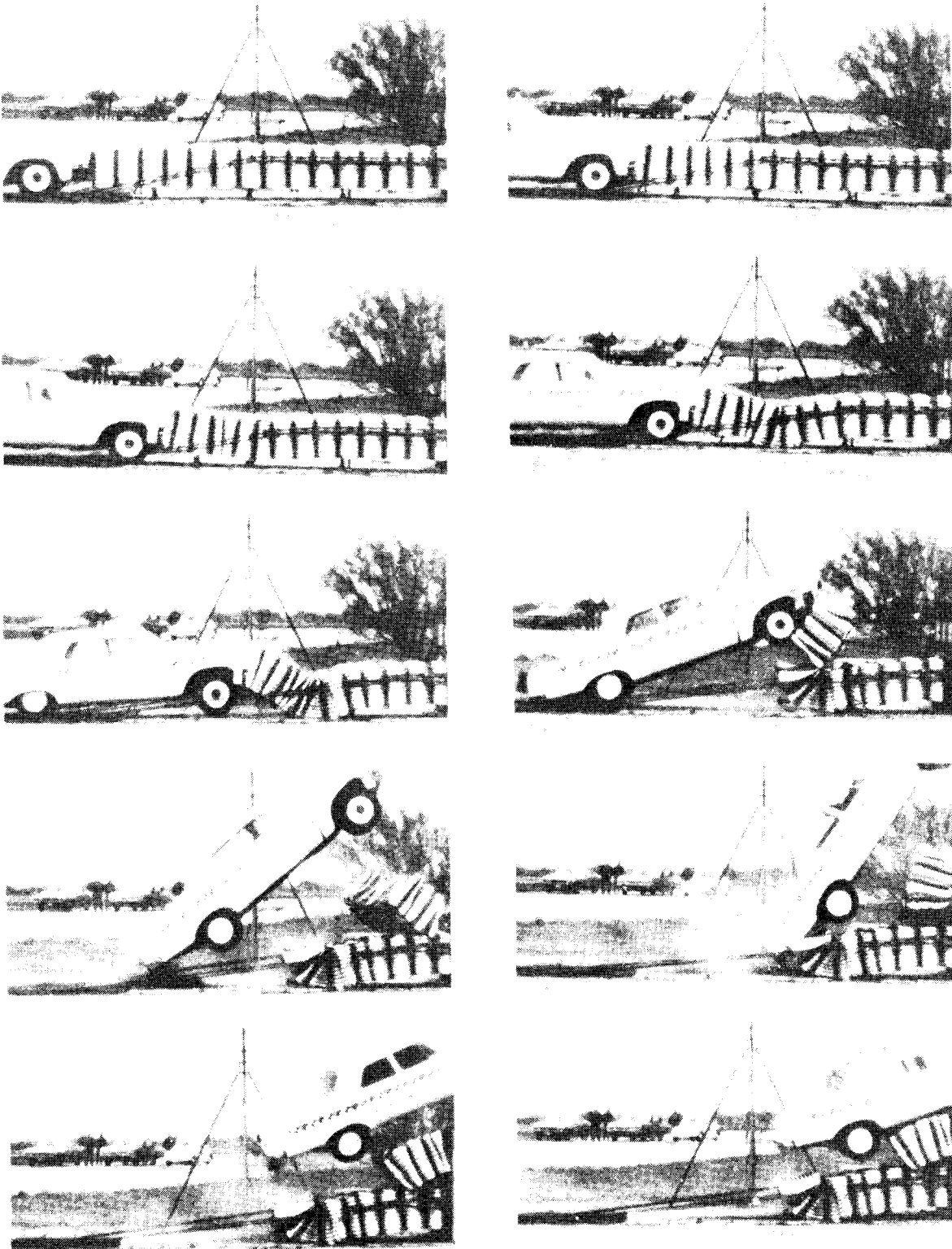


FIGURE IV.2.E.4. SEQUENTIAL PHOTOGRAPHS OF TEST 505 CSU-1.

In test CSP-2 a 3810 lb vehicle traveling 59.8 mph impacted the barrier at an angle of 20°. Dynamic lateral deformation of the barrier reached a maximum of 1.0 ft, residual lateral deformation was 0.4 ft. Damage to the left front quarter of the vehicle was considerable (see Figure IV.2.E.6.). Damage to the barrier was much less severe (see Figure IV.2.E.5.) and with only minor repairs it was used again for test CSP-3. The vehicle redirected smoothly, with an average longitudinal deceleration of 2.2 g's and an average transverse deceleration of 3.4 g's (see Figure IV.2.E.7.).

The vehicle in test CSP-3 weighed 3880 lbs and impacted the cushion head-on at 62.3 mph. The barrier-vehicle interaction was similar to that of test CSP-1 (see Figure IV.2.E.8. & 9.). The first six rows of the barrier were crushed and bent downward, then pivoted upward. The front of the vehicle was lifted upward by one of the flexbeam panels which dug into the ground. The vehicle continued to ramp upward, pushing the first four rows of pipes, which had become detached, over the right side of the barrier. When the vehicle came to rest, it was suspended by the barrier and support cables. The average longitudinal deceleration during the 93 msec before ramping was 9.3 g's.

CONCLUSIONS

The corrugated steel pipe crash cushion did not perform as intended during the two head-on tests. It is believed that the strength distribution of the pipe contributed to the ramping, i.e., the pipe is weaker at the top and bottom and stronger in the midsection, thus tending to deform first at one of the weaker points and allowing the vehicle to ramp. It

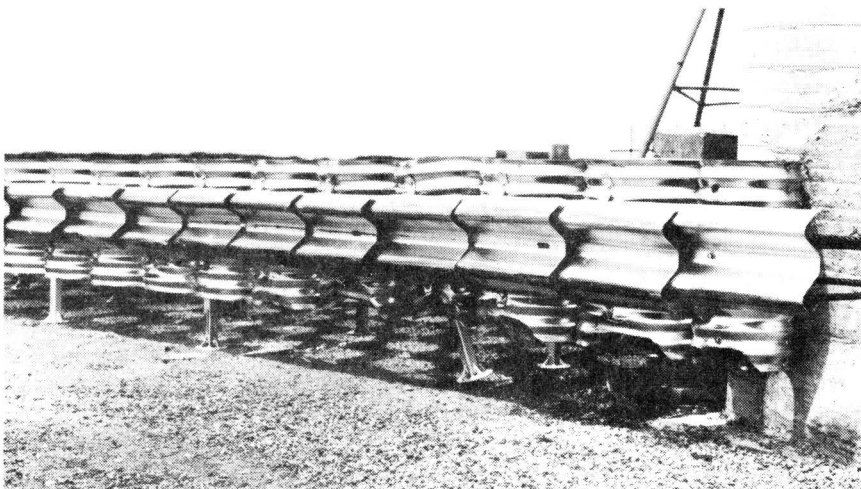
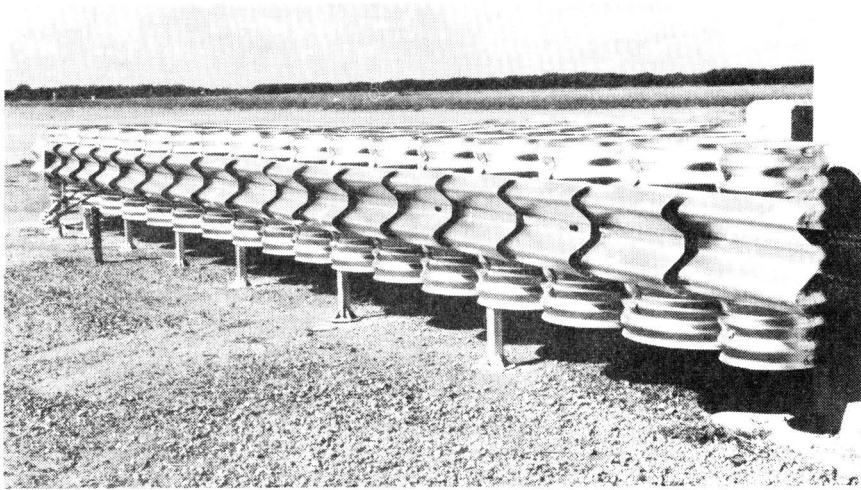
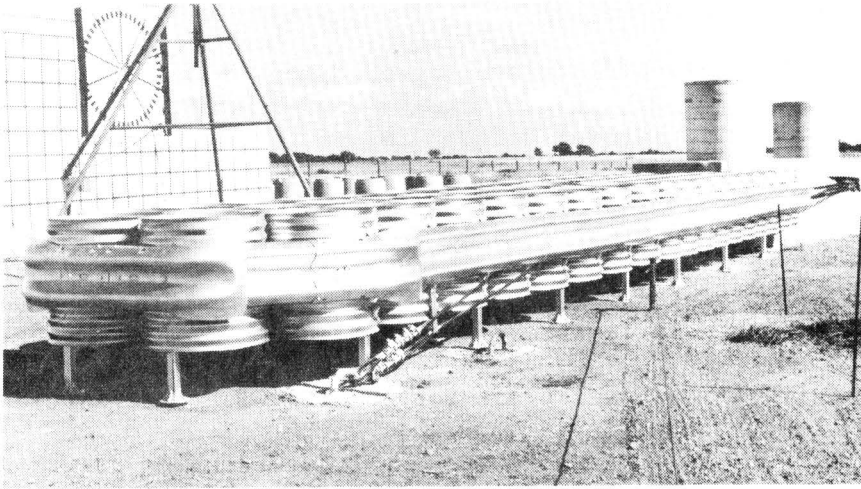


FIGURE IV.2.E.5. CRASH CUSHION BEFORE AND AFTER TEST 505 CSP-2.



FIGURE IV.2.E.6. VEHICLE AFTER TEST 505 CSP-2.

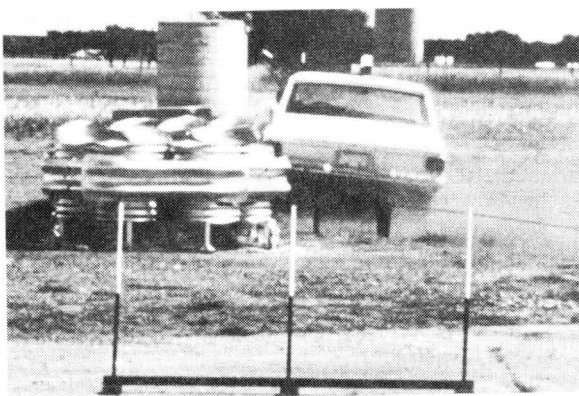
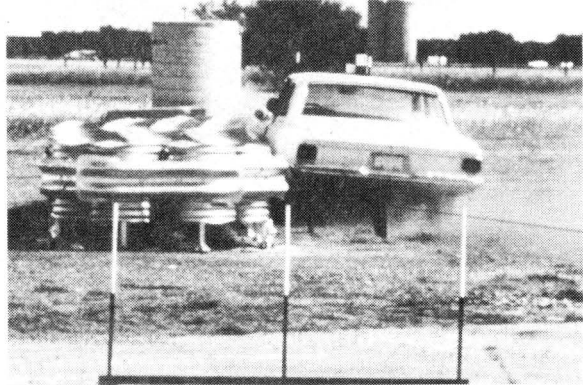
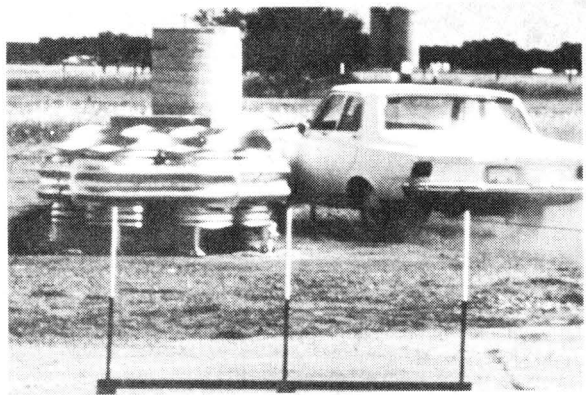


FIGURE IV.2.E.7. SEQUENTIAL PHOTOGRAPHS OF TEST 505 CSP-2.

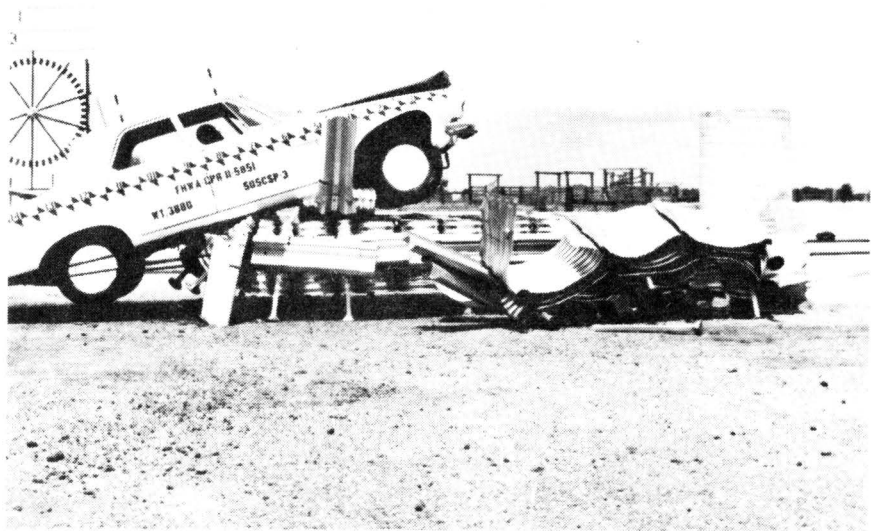
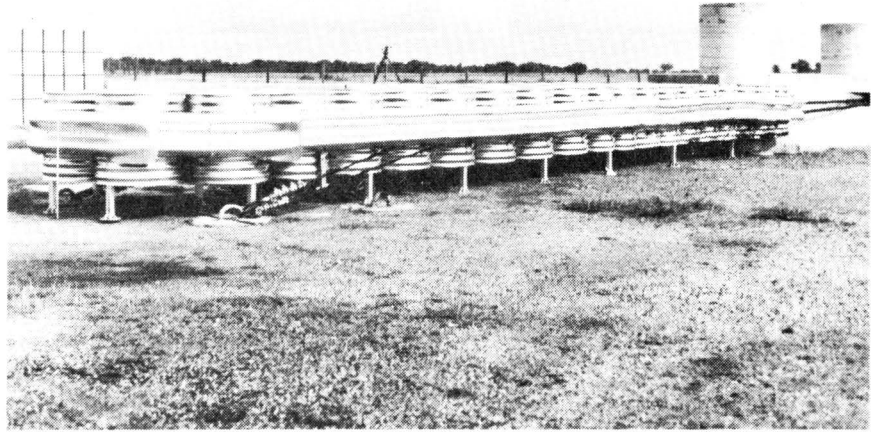


FIGURE IV.2.E.8. CRASH CUSHION BEFORE AND AFTER TEST 505 CSP-3

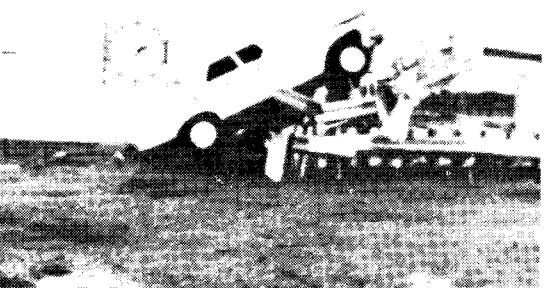
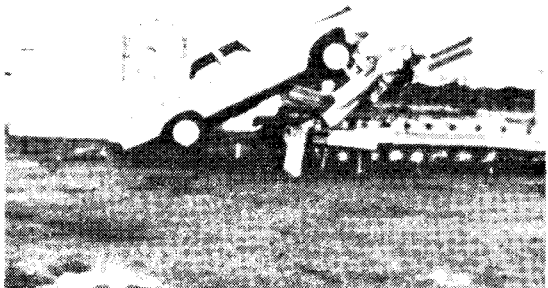
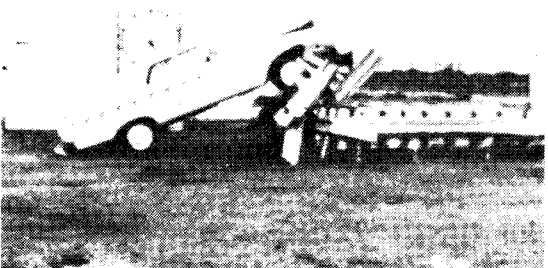
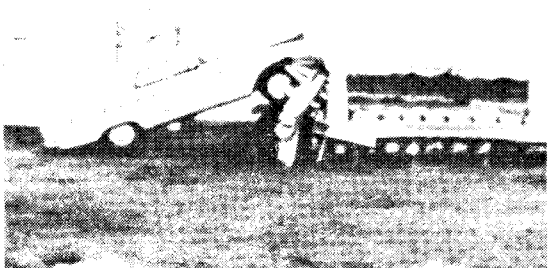
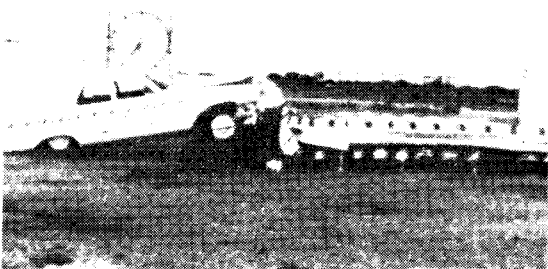
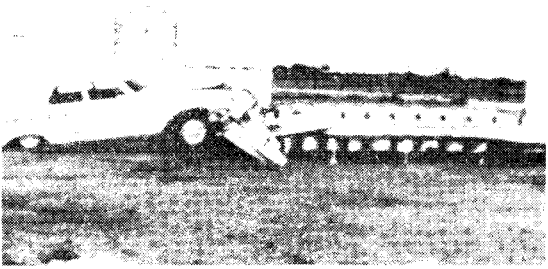
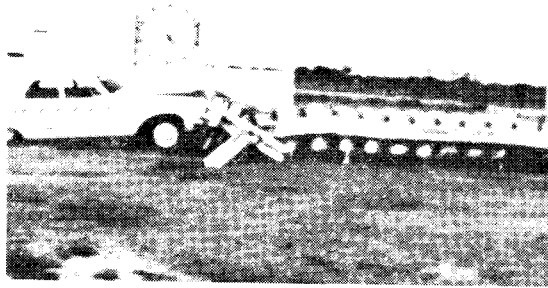
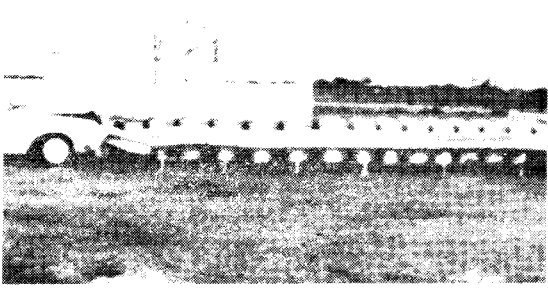


FIGURE IV.2.E.9. SEQUENTIAL PHOTOGRAPHS OF TEST 505 CSP-3.

also appears that the frictional forces on the support legs and the length-to-height ratio of the cushion work in combination with the strength distribution of the pipe to cause a vertical force to be applied to the vehicle, causing it to ramp.

Recommendations for possible remedies to the ramping problem, as well as other detailed information concerning these tests can be found in Technical Memorandum 505-18 which appears in Appendix F.

CHAPTER IV --- Part 3

Longitudinal Redirection Barriers

Part 3. A. --- ONE-WAY ENTRAPMENT GUARDRAIL AND MEDIAN BARRIERBARRIER DESCRIPTION

The One-Way Guardrail vehicle arresting system was developed by the Martin Marietta Corp. under a contract with the FHWA. The arresting system was fabricated and delivered by Martin Marietta to TTI. The system was installed and the vehicle crash tests were conducted by personnel of TTI. The system consists of two continuous parallel lengths of guardrail which would be installed approximately 12 ft apart on a highway median. The function of the installation is shown by Figure IV.3.A.1. The guardrail was composed of the standard 12-gage W-section guardrail on the inward side and a 12-gage steel bumper plate on the outward side. These W-section beams and bumper plates were bolted to 4-in. wide-flange posts which were installed so that the entire guardrail leaned at an angle of 15° toward the middle of the median. The web and outward flange of each post was precut at the ground line so that it would bend inward (only) under a rather minimal force. Details of these components are given in Figures IV.3.A.2. & 3.). This allows a vehicle which is out of control to lay down the first guardrail it encounters when driving into the median. Once the vehicle crosses the first guardrail, it is trapped between the rigid faces of guardrail on both sides and cannot re-enter the highway it has left or cross the median strip into the opposing traffic.

TEST RESULTS

For Test 505-7A, a small vehicle weighing 1600 lb was directed into the guardrail arresting system at an attack angle of 30° and a speed of 47 mph. The arresting system performed as designed, redirecting and

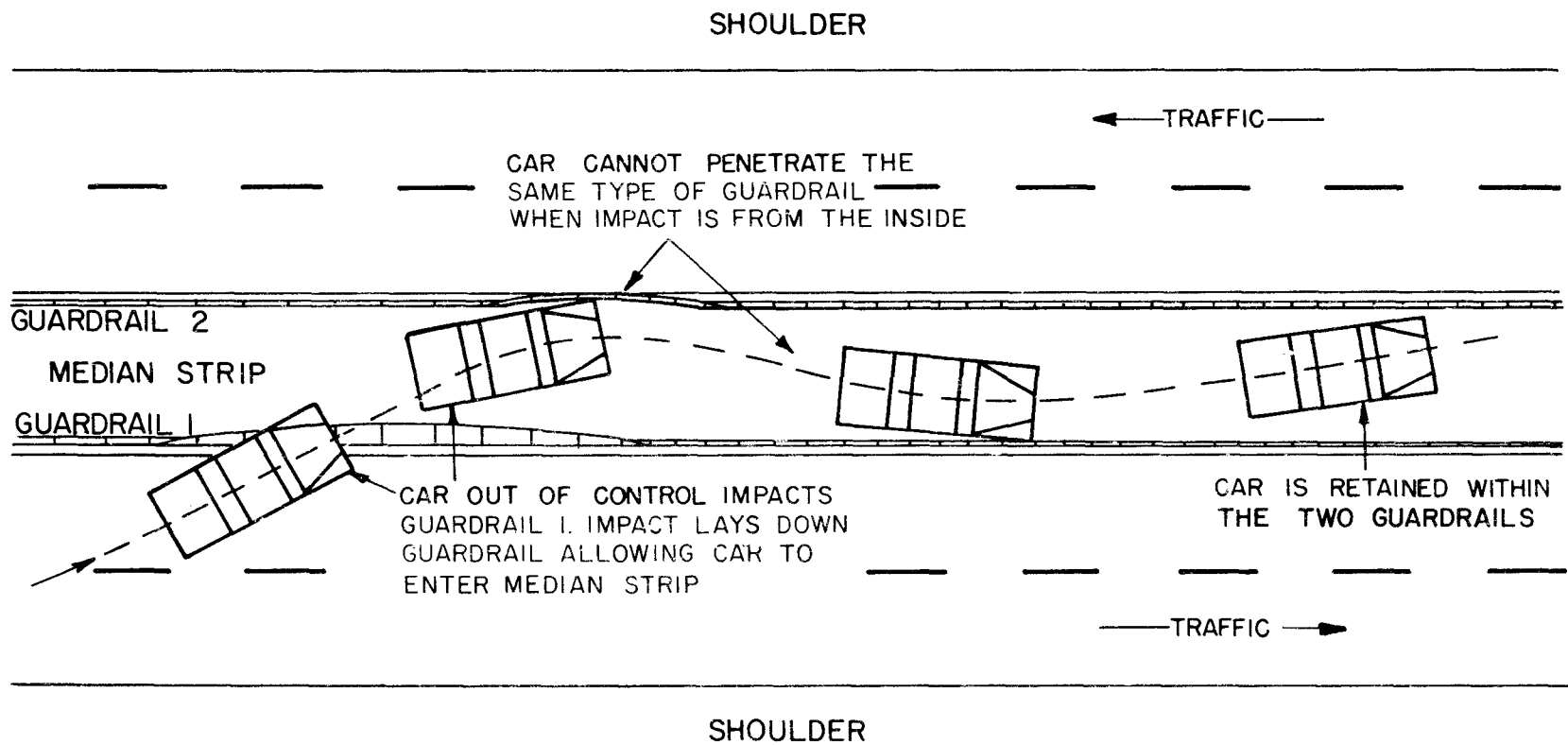


FIGURE IV.3.A.1. IDEALIZED FUNCTION OF ONE-WAY GUARDRAIL INSTALLATION

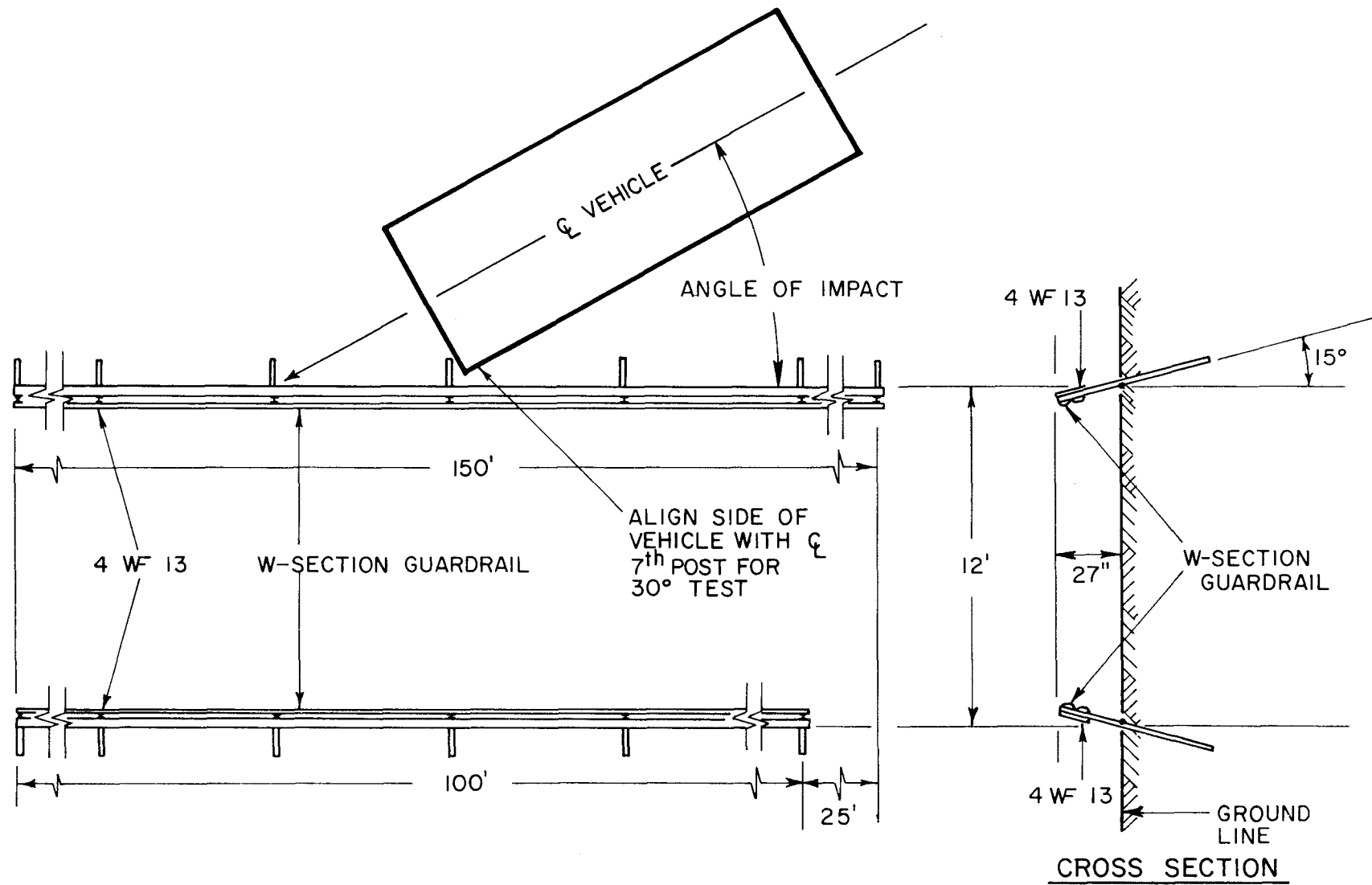


FIGURE IV.3.A.2. PLAN VIEW OF ONE-WAY GUARDRAIL ARRESTING SYSTEM

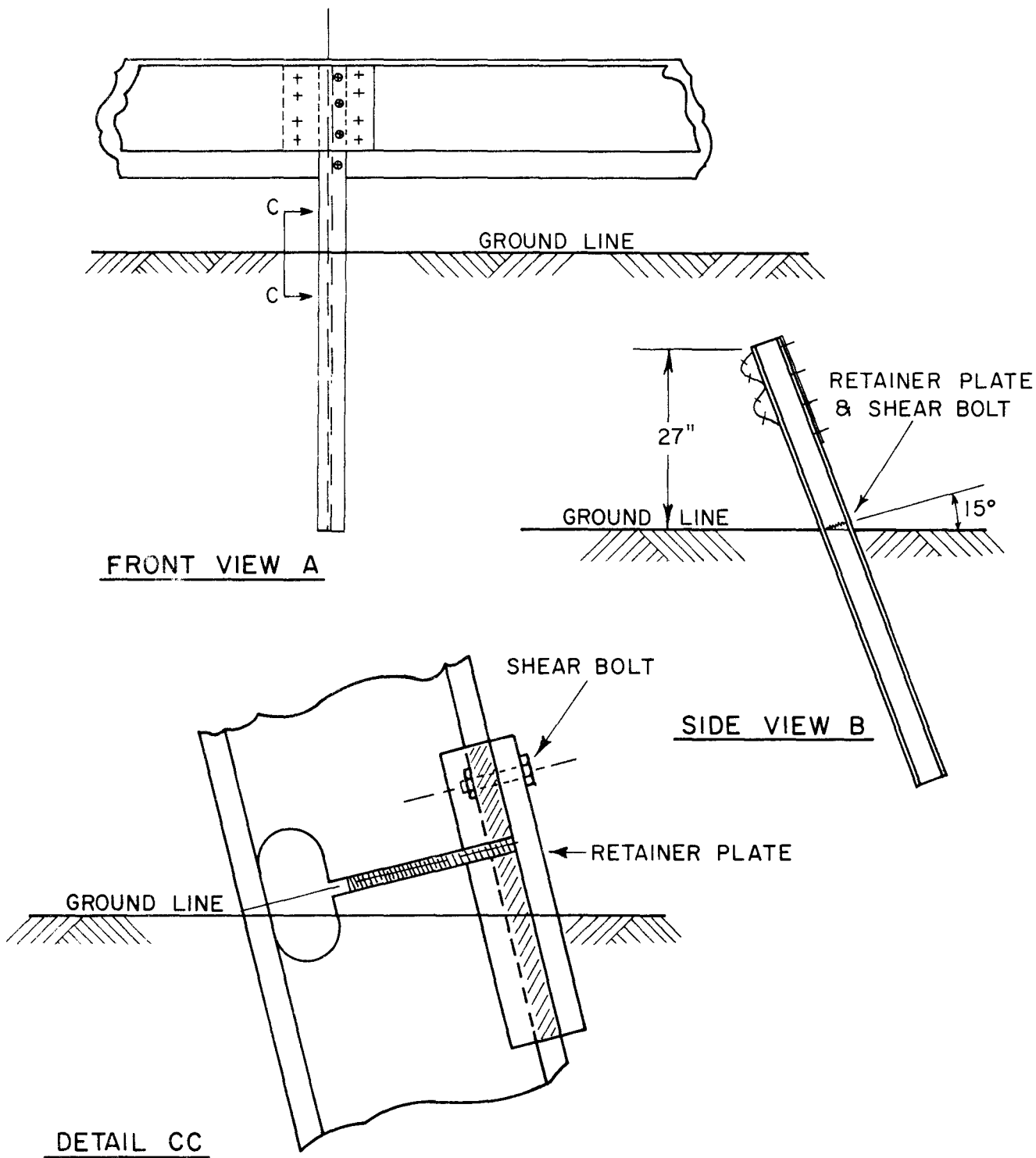


FIGURE IV.3.A.3. DETAIL OF ONE-WAY GUARDRAIL SYSTEM

containing the vehicle (see Figure IV.3.A.4.). A comparison of the vehicle and guardrail before and after the test indicated that the damage to both was minor. Figure IV.3.A.5. shows the point of impact with the first guardrail and demonstrates proper performance of the "one-way" design.

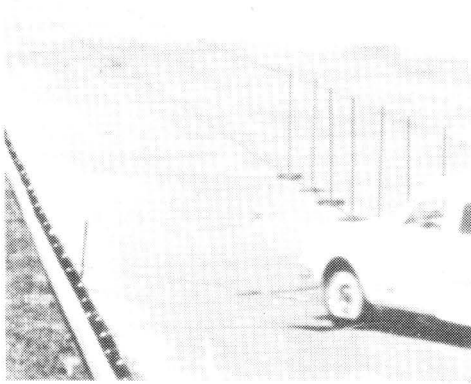
Calculated average decelerations in the longitudinal and transverse directions were below 2.5 g's throughout the test, an extremely acceptable level.

Another successful test was Test 9A, conducted with a 4180 lb vehicle traveling 64 mph and impacting the guardrail at an angle of only 20°. This lower impact angle reduced the kinetic energy perpendicular to the guardrail to 197 kip-ft and allowed the vehicle to be successfully contained (see Figure IV.3.A.6.). The vehicle recontacted the first guardrail from inside of the system after being redirected by the second guardrail. The critical point was during contact with the second guardrail. The sequence photographs of Figure IV.3.A.6. indicate that the vehicle came very close to jumping the second guardrail. Considerable damage was done to the vehicle suspension at that point.

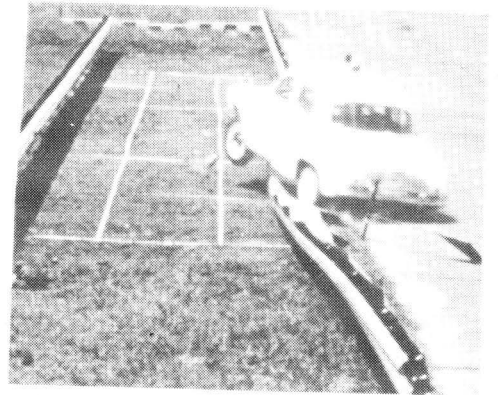
The left front of the vehicle contacted the ground when the first guardrail was recontacted. This probably contributed significantly to the decelerations experienced at that point. The average decelerations at the various contact points were all below 2.3 g's, which is a very moderate level.

CONCLUSIONS

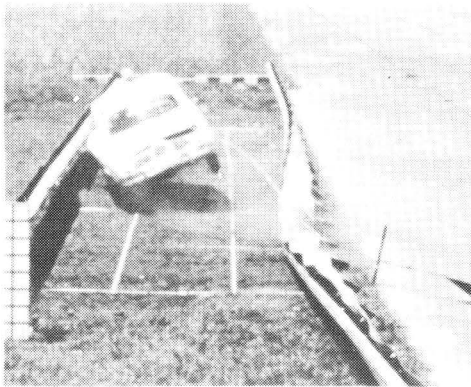
The One-Way Guardrail vehicle arresting system performed as designed in three of the four tests conducted. The system should be effective for



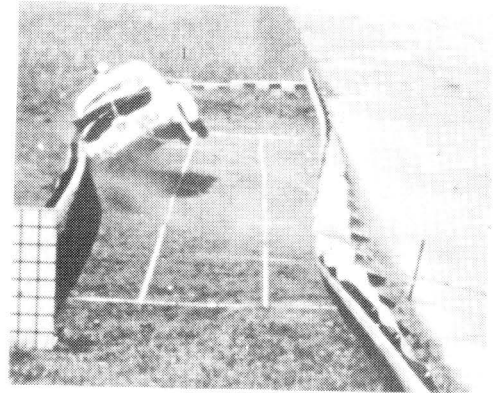
1



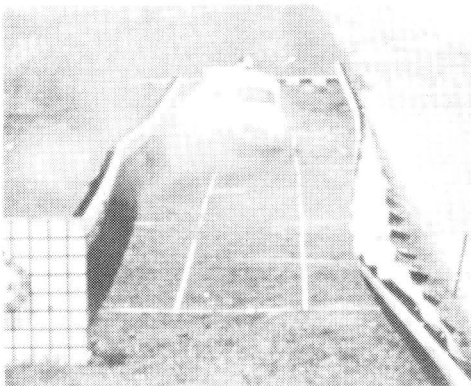
2



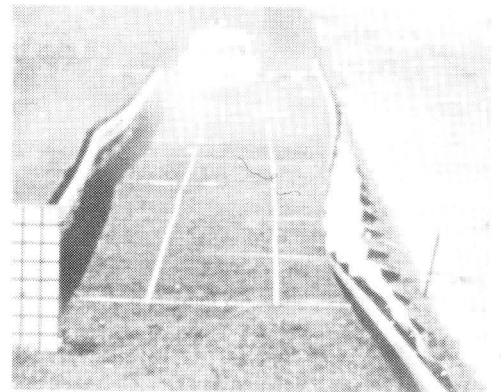
3



4



5



6

FIGURE IV.3.A.4. SEQUENTIAL PHOTOGRAPHS OF TEST 505-7A.

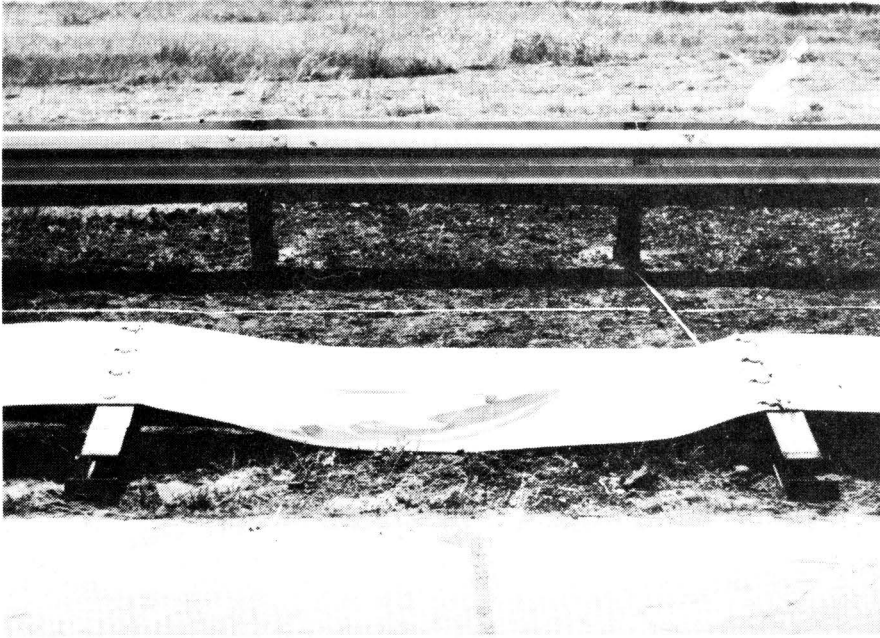
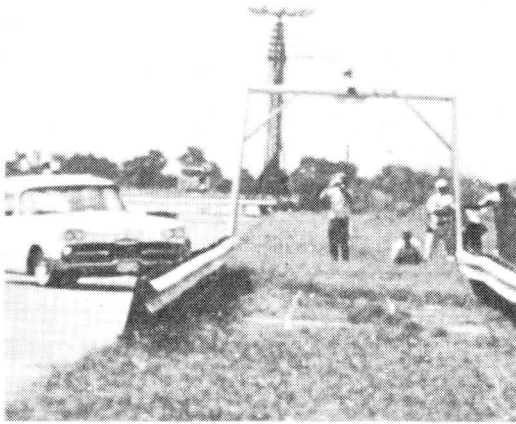
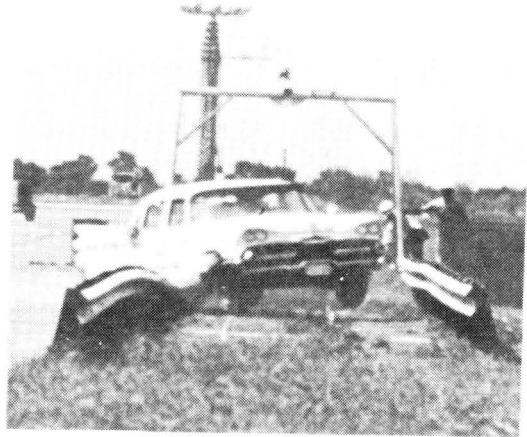


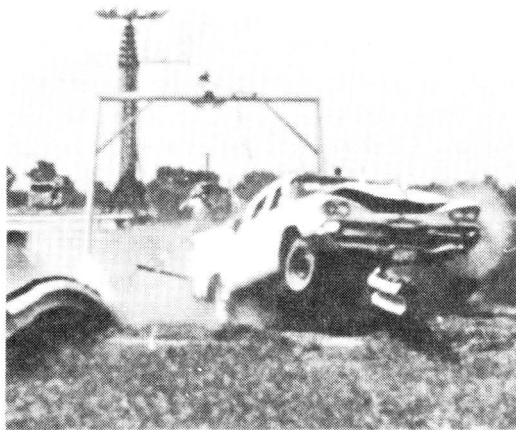
FIGURE IV.3.A.5. FIRST GUARDRAIL WAS LAID DOWN AS DESIGN PREDICTED. TREAD MARK SHOWS POINT OF VEHICLE CONTACT (TEST 505-7A).



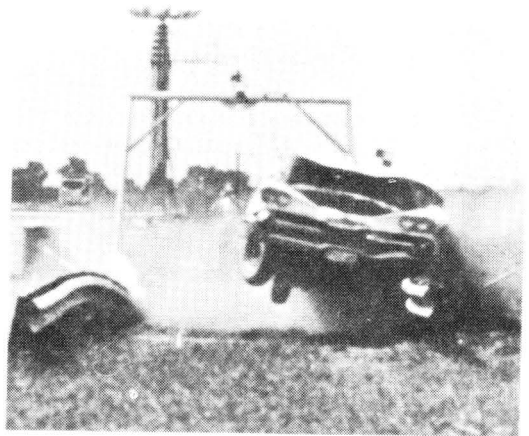
1



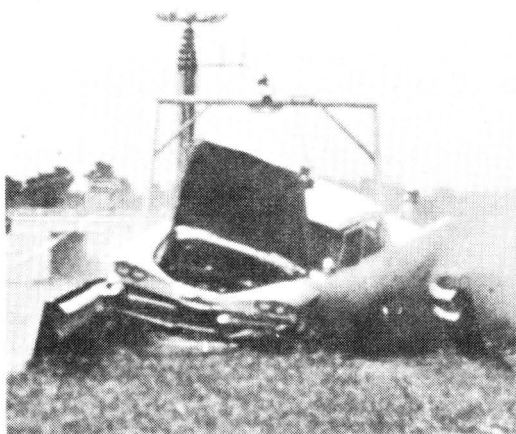
2



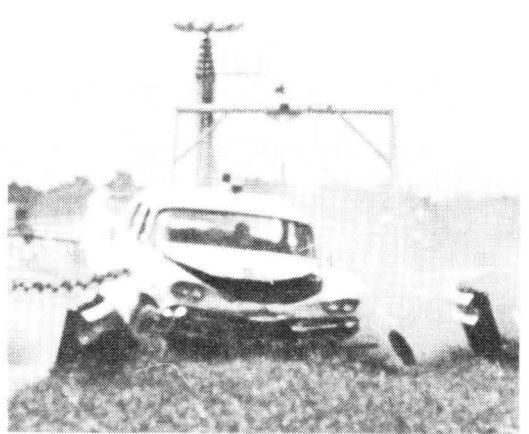
3



4



5



6

FIGURE IV.3.A.6. SEQUENTIAL PHOTOGRAPHS OF TEST 505-9A.
(FRONT VIEW).

vehicle speeds somewhat less than 60 mph or angles of attack slightly less than 30°. All tests where the vehicle was contained show deceleration levels well within the tolerance limits of restrained humans.

It should be emphasized that the functioning of this system is dependent to some degree on the properties of the soil surrounding the guardrail support posts. If a low cohesion soil is not avoidable in a given location, the guardrail system could be made to function properly by increasing the embedment length or the bearing area or by placing concrete around the wide-flange support posts.

Other tests conducted on this system (at various impact angles and speeds) are described in detail in Technical Memorandum 505-3 in Appendix F.

Part 3. B. --- ENERGY ABSORBING BRIDGE RAIL (FRAGMENTING TUBE)BARRIER DESCRIPTION

A series of four vehicle crash tests was conducted to evaluate an energy absorbing bridge rail which was designed in a joint effort by engineers of the Federal Highway Administration and those of the Southwest Research Institute. This bridge rail was designed to have sufficient strength to retain heavy vehicles, and also to be sufficiently flexible in order to lower deceleration forces on vehicle passengers.

This energy-absorbing system is a blocked-out 6 in. by 6 in. box-beam guardrail, attached to 6 WF25 support posts as shown in Figure IV.3.B.1. The blocking out of the box beam is accomplished at each WF support point by a guide tube and a fragmenting (energy-absorbing) tube. The thin aluminum fragmenting tube is rigidly connected to the 6 in. by 6 in. box beam. It is not rigidly connected to the WF post, but fits into a die which is attached to the post. Under lateral load, the fragmenting tube is forced onto the die and progressively breaks into small segments at a predictable load level. The bridge guide tube acts to prevent movement of the box beam in a longitudinal and vertical direction, but slips through its support on the WF post to allow lateral movement of the box beam. The box beam is then capable of lateral deformation (up to a distance of approximately 18 in.) under the loads imposed by an impacting vehicle. After 18 in. of lateral movement, the box beam comes into contact with the rigid WF support posts which develop a high level of lateral restraint.

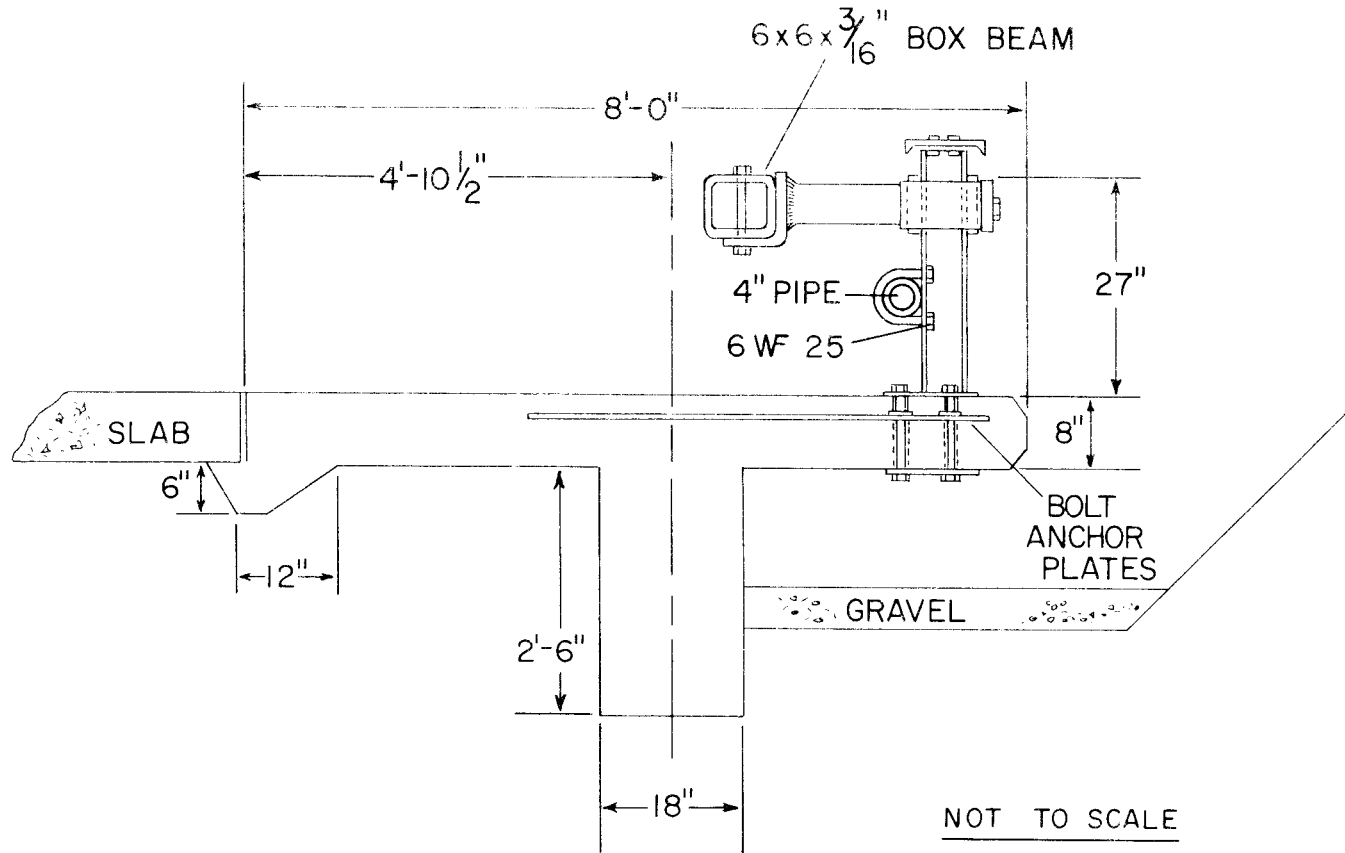


FIGURE IV. 3. B. I. CROSS SECTION OF BRIDGE DECK AND BRIDGE RAIL

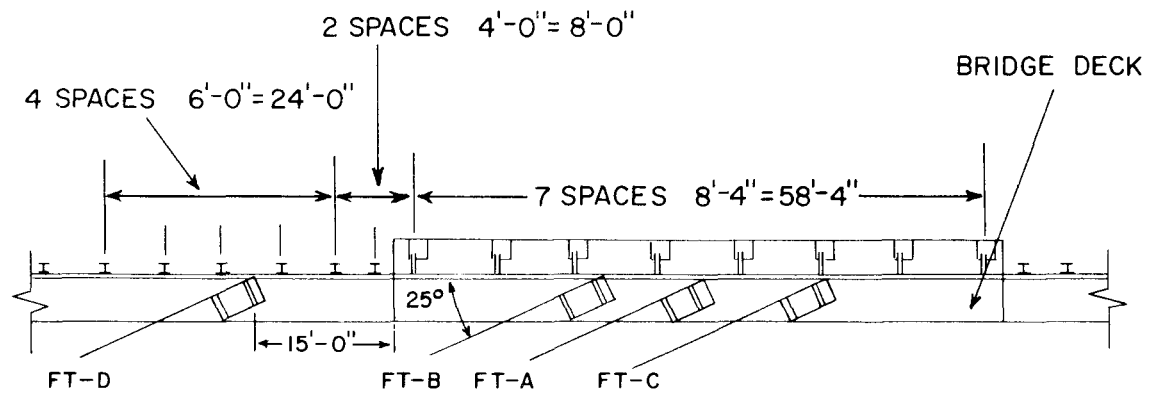


FIGURE IV.3.B.2. LOCATION OF VEHICLE IMPACTS

TEST RESULTS

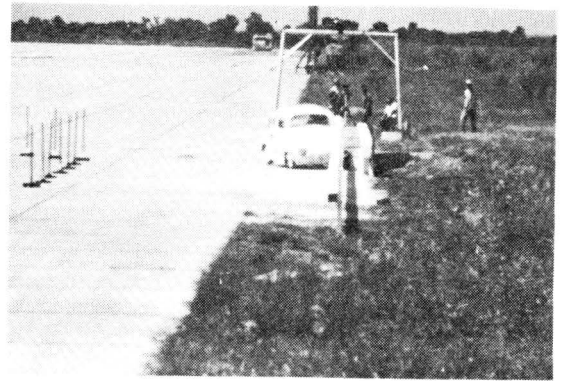
The smoothest redirection occurred in test FT-C with a 1560 lb Volkswagen impacting the bridge rail at an angle of 25° and a speed of 46.1 mph (see Figure IV.3.B.3.). There was no measurable tube deformation due to the impact, though one tube was partially activated. After impact, the vehicle followed the rail at a distance of from one to two feet (some 120 ft from point of impact), brushed the end in a long left turn, and came to rest in an open field. Though the left side of the vehicle was dented from front to rear, there was no significant encroachment of the vehicle compartment.

Another test (FT-B), using a heavy vehicle (4720 lb), also showed good redirection capabilities of the bridge rail system. Impact speed was 54.8 mph and the angle of attack was 25° (see Figure IV.3.B.4.). The point of impact was chosen at a point on the rail halfway between two posts in an effort to test the weakest point of the box beam. After impact, the vehicle left the rail at an angle of approximately 30° , moved to a position some 5 ft from the original rail position, followed the rail, and then turned back into the guardrail due to left front drag caused by wheel damage. After tearing down four guardrail line posts, the vehicle came to rest at an angle of approximately 45° to the rail, some 100 ft from the point of impact. No visible vehicle compartment encroachment was noted.

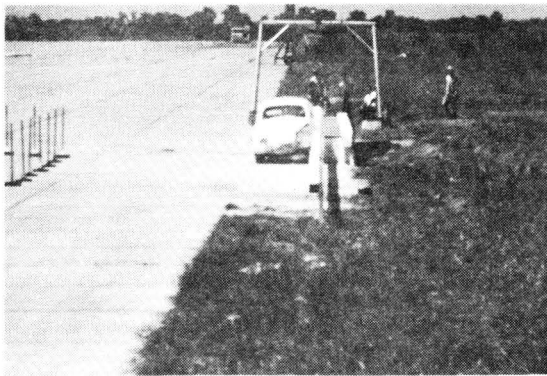
The final test in this series (FT-D) was designed to test the transition area between the bridge rail and guardrail (see Figure IV.3.B.5.). A point 15 ft upstream from the bridge deck (17 ft from the first bridge rail post) was chosen for the impact point. The test was run with



1



2

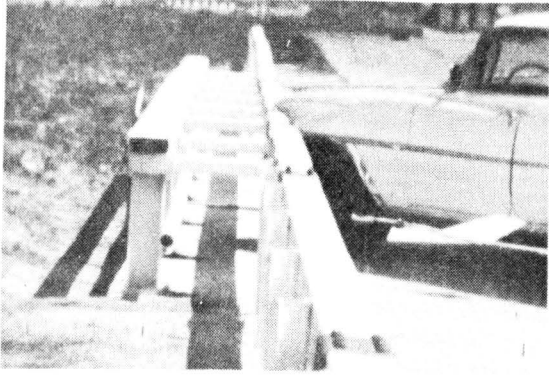


3



4

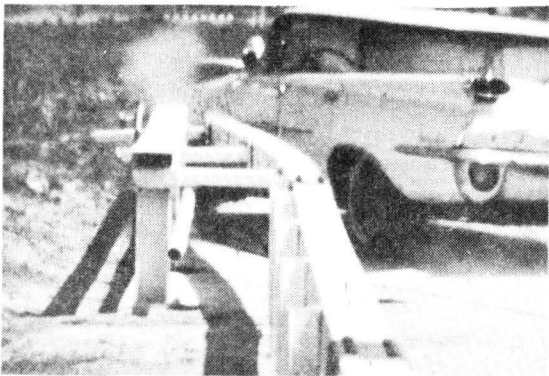
FIGURE IV.3.B.3. SEQUENTIAL PHOTOGRAPHS OF TEST (FT-C).



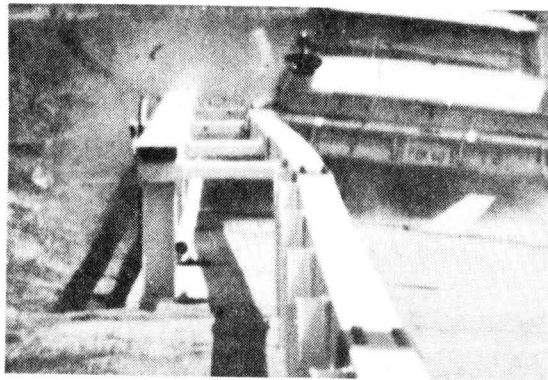
1



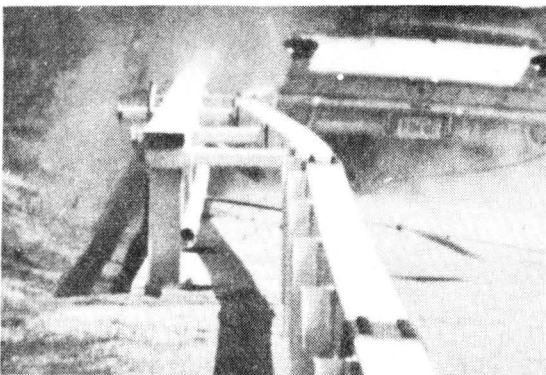
2



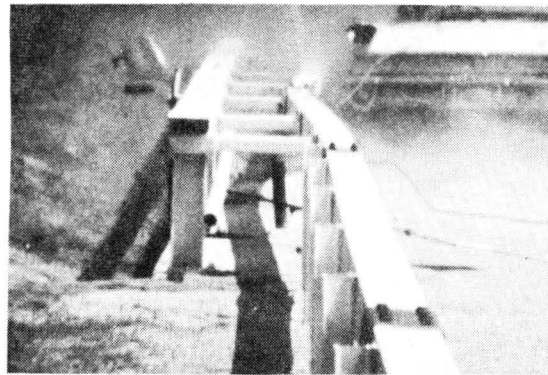
3



4

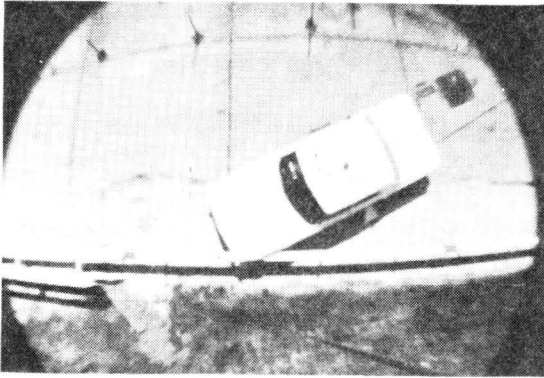


5



6

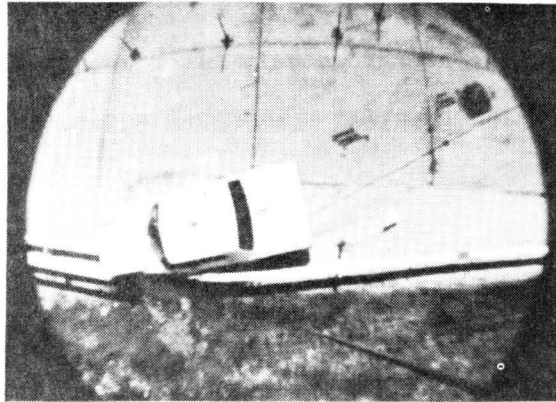
FIGURE IV.3.B.4. SEQUENTIAL PHOTOGRAPHS OF TEST (FT-B).



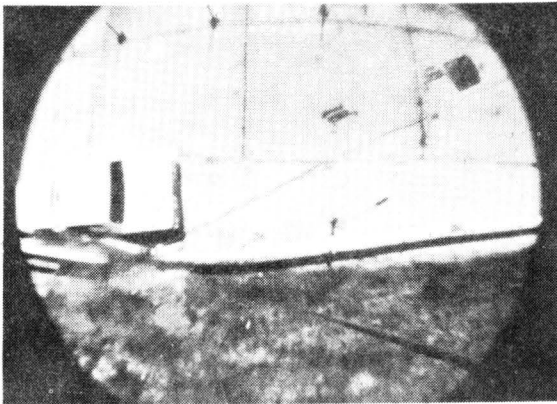
1



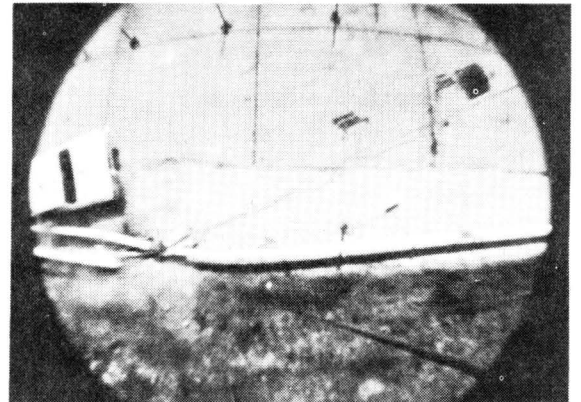
2



3



4



5

FIGURE IV.3.B.5. SEQUENTIAL PHOTOGRAPHS OF TEST (FT-D).

a 3270 lb vehicle. Impact speed was 61.8 mph and the angle of attack was 25°. The vehicle was successfully redirected though there was considerable damage to the installation and the vehicle. After traveling approximately 80 ft from the point of impact, the vehicle came to rest in the guardrail system just downstream from the bridge. The left front door was torn off at the point of impact, however there was no significant vehicle compartment encroachment.

In all tests in this series, the vehicles were redirected and came to rest without rolling over. A properly seatbelted, shoulder-harnessed passenger would probably have sustained only minor injuries in each test. Additional data are given in Technical Memorandum 505-8 found in Appendix F.

Part 3. C. --- TEXAS T1 BRIDGE RAIL-GUARDRAIL SYSTEMBARRIER DESCRIPTION

This bridge rail system consisted of 12-gage W-section guardrail bolted to W posts on the bridge deck and to 7 in. timber posts on the approach and exit of the bridge deck. The barrier system tested consisted of 75 ft of approach guardrail, 58 ft of T1 bridge rail, and 75 ft of exit guardrail. This T1 system is shown in Figure IV.3.C.1. The modified T1 system included an additional W-section guardrail which overlapped the bottom half of the existing bridge rail only. Three tests were run on the unmodified T1 bridge rail and a final test was conducted on the slightly modified version of the T1 system.

TEST RESULTS

Test 505 T1-A was conducted with an 1860 lb vehicle traveling 44.5 mph and impacting the bridge rail section at an angle of 25° (see Figure IV.3.C.2.). The bridge rail contained and redirected the vehicle, imparting an average longitudinal deceleration of 2.2 g's and an average lateral deceleration of 4.7 g's. While in contact with the rail, the vehicle's speed decreased 17.8 mph. Photographs indicate the impact attenuation was provided by the vehicle, since the barrier was not significantly displaced during the collision incident. Snagging of the left front wheel on a bridge rail post caused extensive suspension damage.

Test T1-B of this bridge rail involved a heavier vehicle (3920 lb) traveling 56.4 mph (see Figure IV.3.C.3.). Under the force of impact, the 12-gage W-section was deformed considerably, permitting the vehicle to snag on a bridge post and producing a greater longitudinal component of

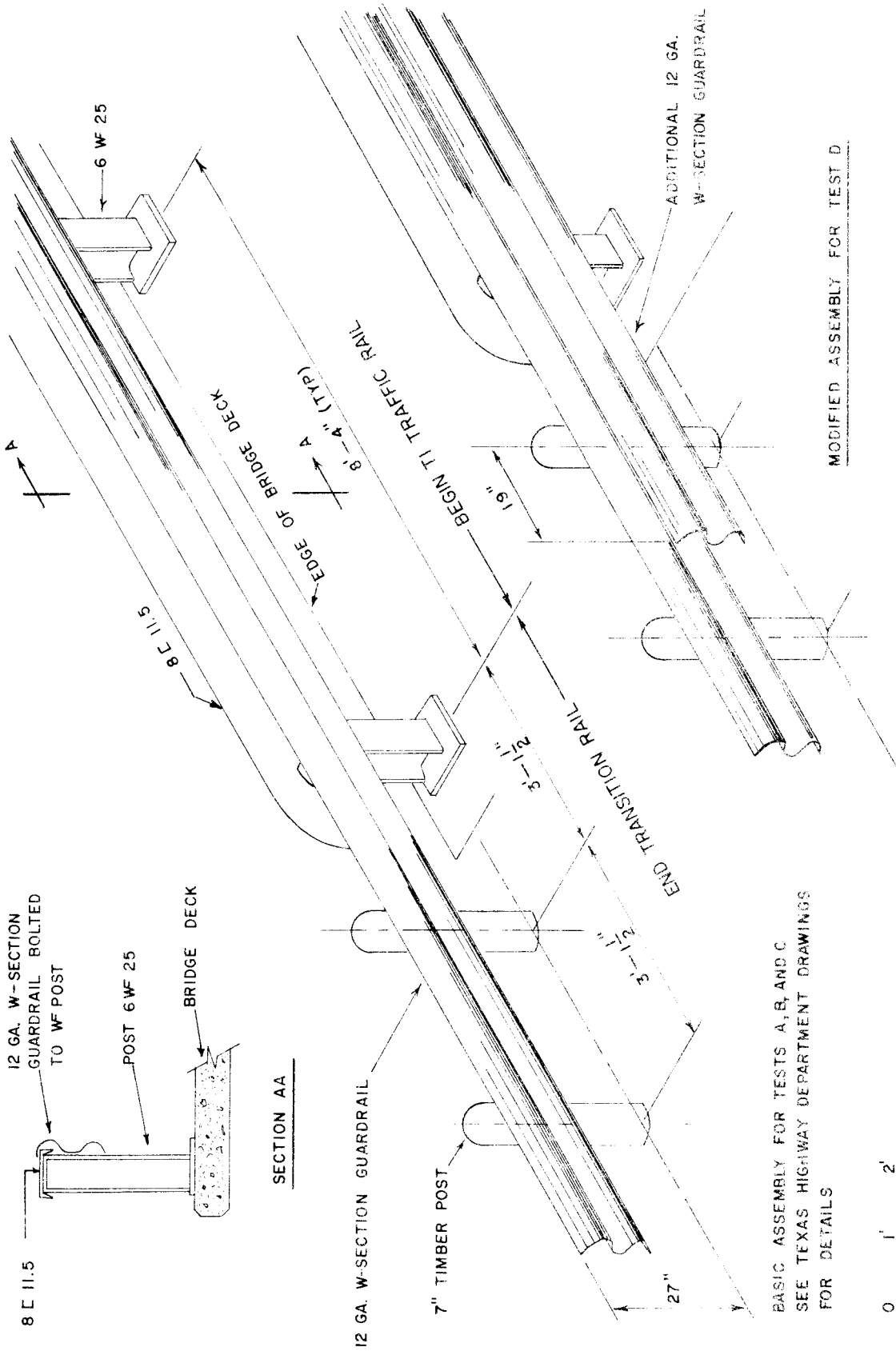


FIGURE IV.3.C.1. TEXAS TI PROTECTIVE BARRIER.



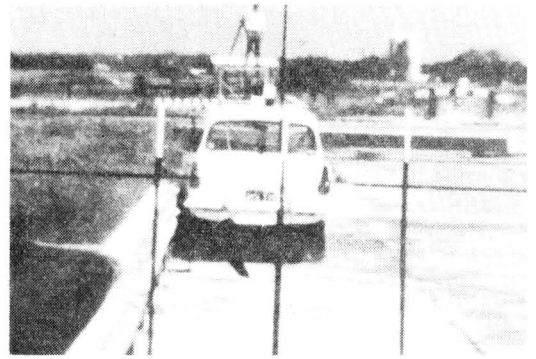
1



2



3



4



5



6



7



8

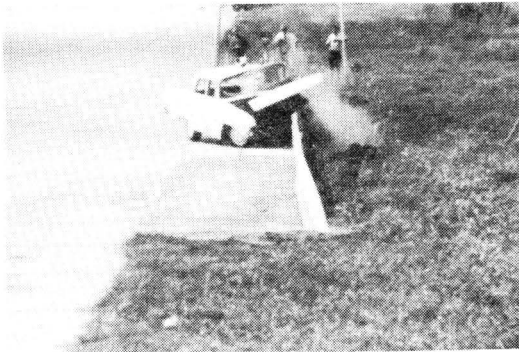
FIGURE IV.3.C.2. SEQUENTIAL PHOTOGRAPHS OF TEST T1-A.



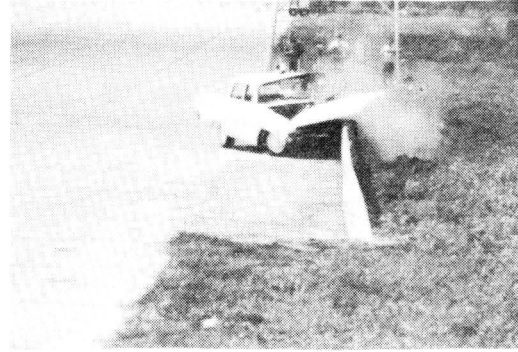
1



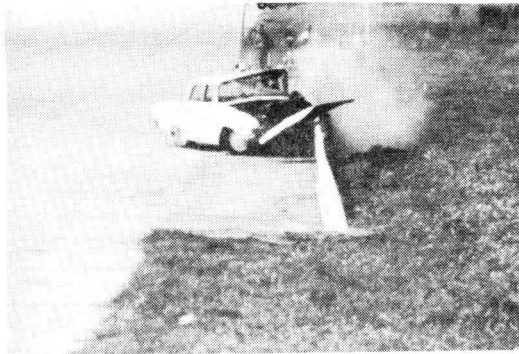
2



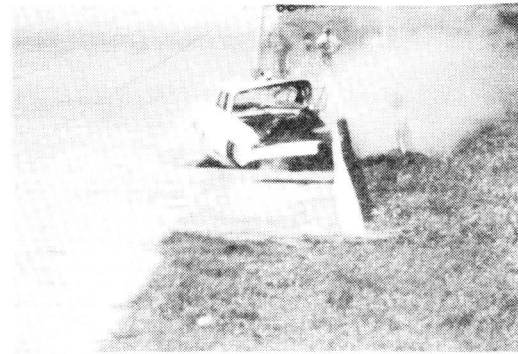
3



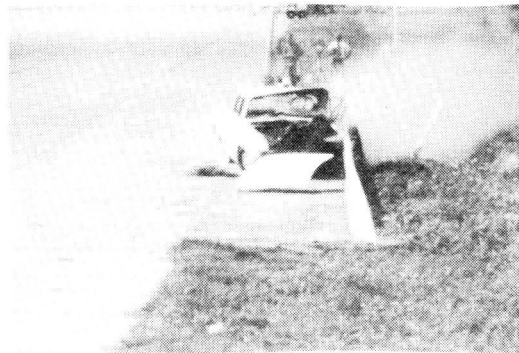
4



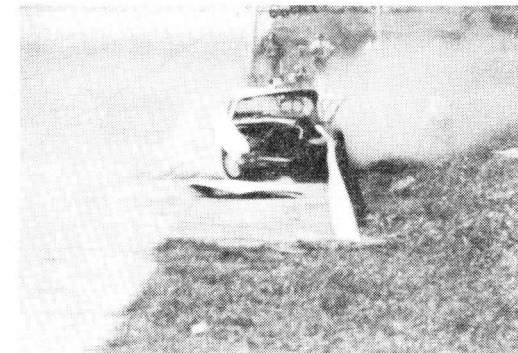
5



6



7



8

FIGURE IV.3.C.3. SEQUENTIAL PHOTOGRAPHS OF TEST T1-B.

deceleration than was calculated in the above test. Also, the average deceleration perpendicular to the rail increased about 30%. Vehicle damage was rather severe.

Test T1-C of this system was designed to test the transition area of the guardrail-bridge rail (see Figure IV.3.C.4.). The 3670 lb vehicle, traveling 58.0 mph, contacted the guardrail 15 ft in advance of the guardrail-bridge rail interface at an impact angle of 25°. The guardrail contained and redirected the vehicle as intended. The average deceleration perpendicular to the rail was smaller in this test than in all previous tests. The transition rail to bridge rail connection was adequate to provide structural continuity between the two systems. The vehicle sustained moderate damage.

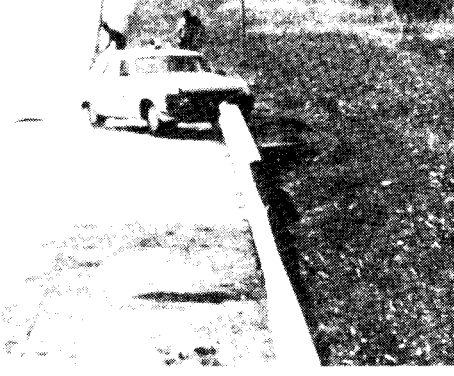
For the last test in this series (T1-D), the bridge rail section of the barrier system was modified as described earlier. The 3620 lb vehicle, traveling 61.4 mph, collided with the bridge rail section at an angle of 25° (see Figure IV.3.C.5.). Good redirection was noted and the vehicle had no tendency to snag. The overlapped 12-gage W-section provided a stronger system between posts, thus the average deceleration perpendicular to the rail was larger than in the previous test. However, the longitudinal component was smaller. Vehicle damage was considered moderate.

CONCLUSIONS

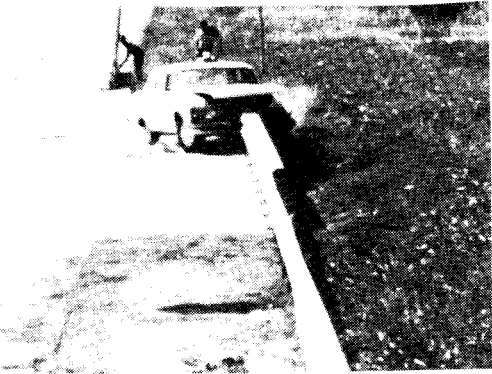
On the basis of the tests conducted, it appears that maintenance costs of the T1 Bridge Rail System should be rather nominal. The usual damage in a high-speed hit consists of localized deformations to one W-section, and cracking of the bridge slab. The bridge slab cracking



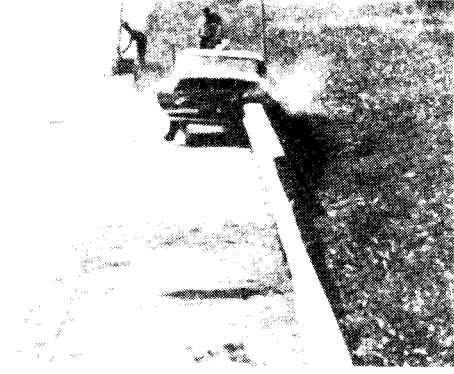
1



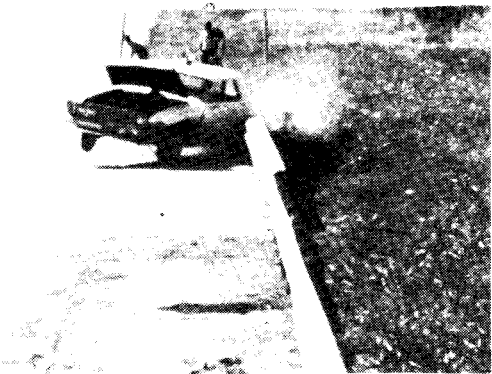
2



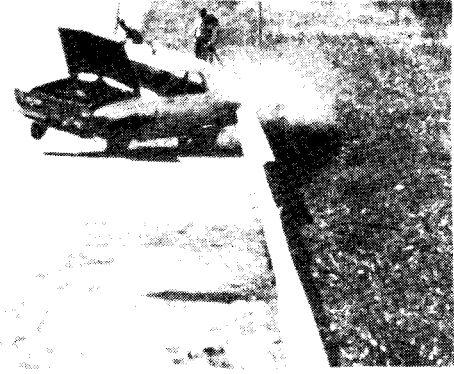
3



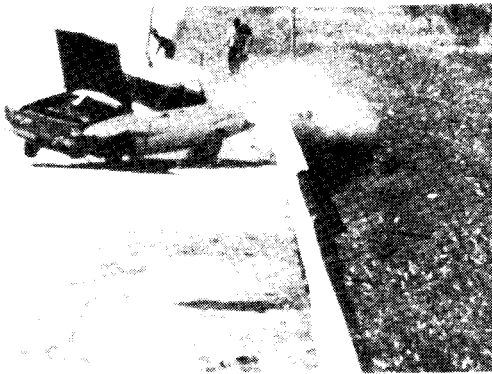
4



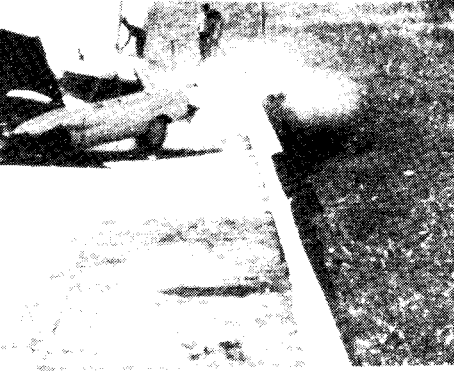
5



6

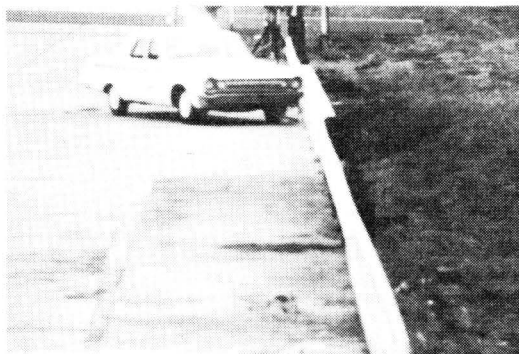


7

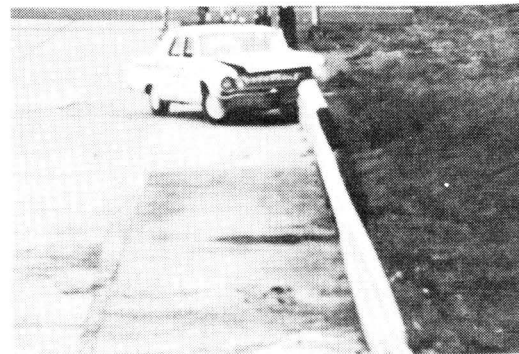


8

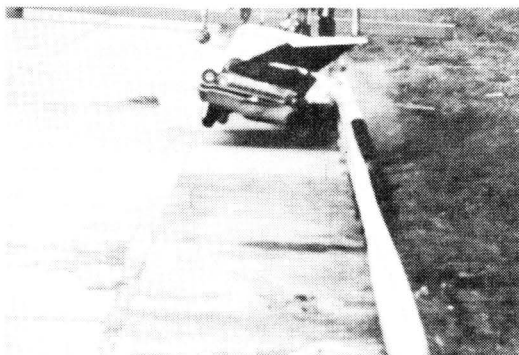
FIGURE IV.3.C.4. SEQUENTIAL PHOTOGRAPHS OF TEST T1-C.



1



2



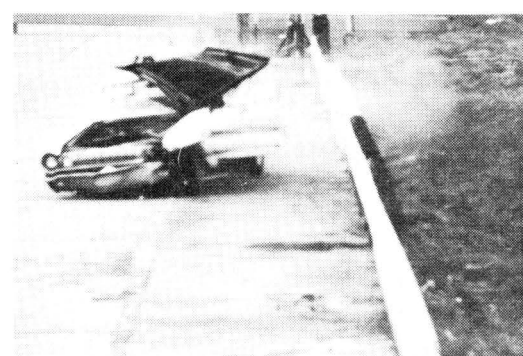
3



4



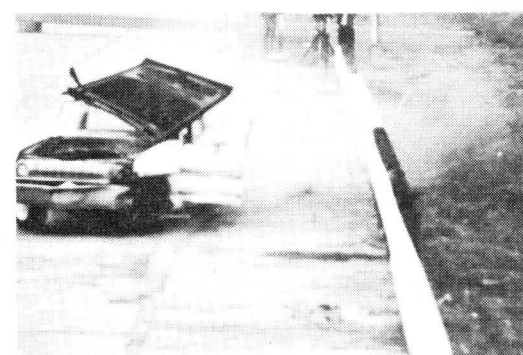
5



6



7



8

FIGURE IV.3.C.5. SEQUENTIAL PHOTOGRAPHS OF TEST T1-D.

appears to be a diagonal tension-type crack which results from the punching shear load generated by the base plate of the bridge rail support post. Although the concrete cracks in the collision area appear rather severe, the structural integrity of the slab is maintained by the steel reinforcement. In only the higher speed hits does yielding of this steel reinforcement appear likely.

Additional information and test data can be found in Technical Memorandum 505-10 which appears in Appendix F.

Part 3. D. --- NEW YORK BOX BEAM BRIDGE RAIL-GUARDRAIL SYSTEMBARRIER DESCRIPTION

The bridge rail portion of this system was 62 ft 4 in. in length. On each side of the bridge rail was a 54 ft 2 in. guardrail section. The bridge rail section consisted of 6 in. by 6 in. by 3/8 in. box beam attached to I-beam posts. The posts were securely anchored to the bridge deck by 10 in. by 9-1/2 in. by 1 in. base plates. The guardrail section consisted of 6 in. by 6 in. by 3/16 in. box beam also attached to I-beam posts. These guardrail posts were securely embedded in 3 ft of soil. Figures IV.3.D.1.-5. illustrate the box-beam bridge rail-guardrail.

TEST DESCRIPTION

Two 25° angle impact crash tests were conducted on this barrier. In Test NY-A, a 1964 Dodge weighing 3800 lb impacted the bridge rail at a speed of 55.4 mph (see Figure IV.3.D.6.). Average longitudinal deceleration calculated from high-speed films was 1.3 g's. Deceleration perpendicular to the rail, from high-speed film, was 4.8 g's. Approximately 50 ft of bridge rail and guardrail were damaged in the crash, and 12 bridge posts and guard posts were destroyed or damaged to some extent. Damage to the left front side of the vehicle was moderate.

The second angle test (NY-B) was conducted on the guardrail-bridge rail transition (see Figure IV.3.D.7.). A 1964 Dodge weighing 3670 lb impacted the transition area at a speed of 57.9 mph. Average longitudinal deceleration calculated from film data was 2.1 g's. Average deceleration perpendicular to the bridge rail was calculated from high-speed film to be

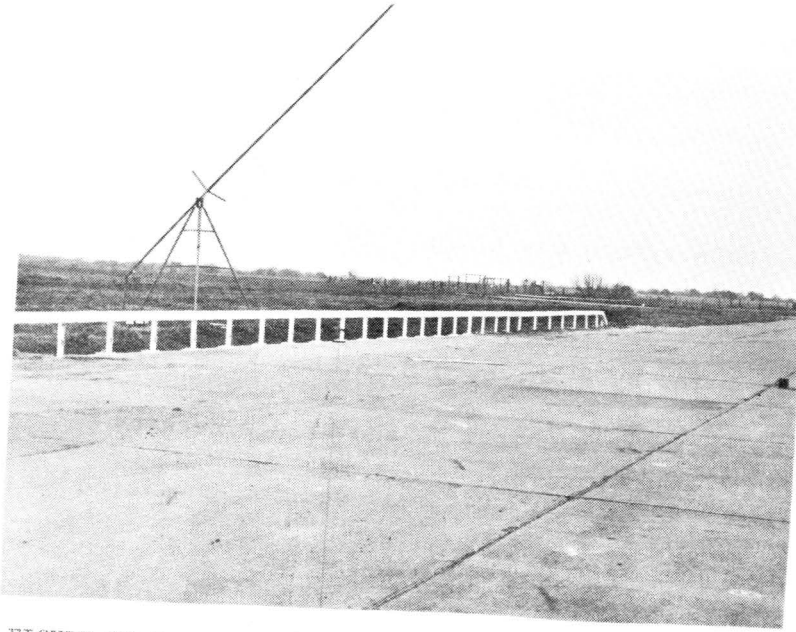


FIGURE IV.3.D.1. OVERALL VIEW OF BRIDGE RAIL-GUARDRAIL



FIGURE IV.3.D.2. BRIDGE POST

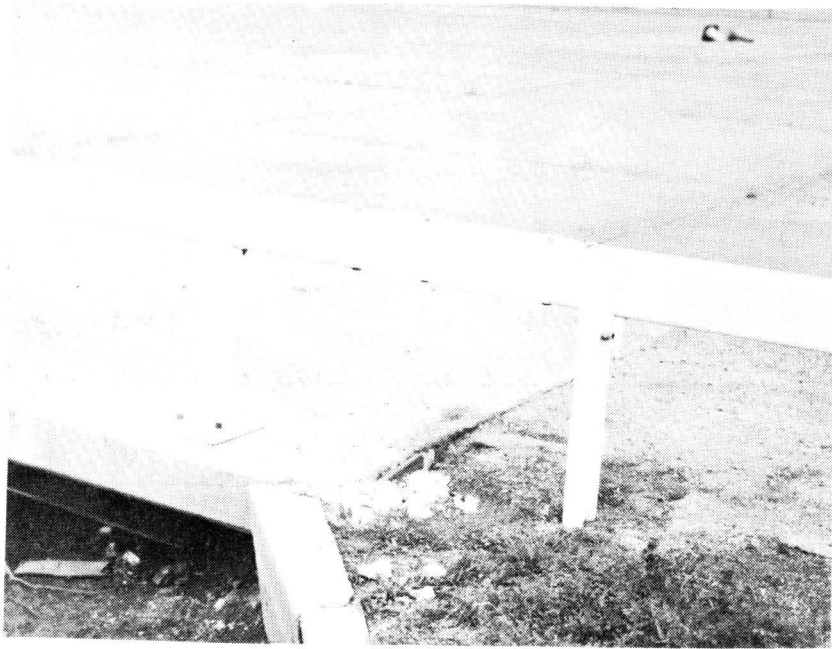


FIGURE IV.3.D.3. BRIDGE RAIL-GUARDRAIL TRANSITION

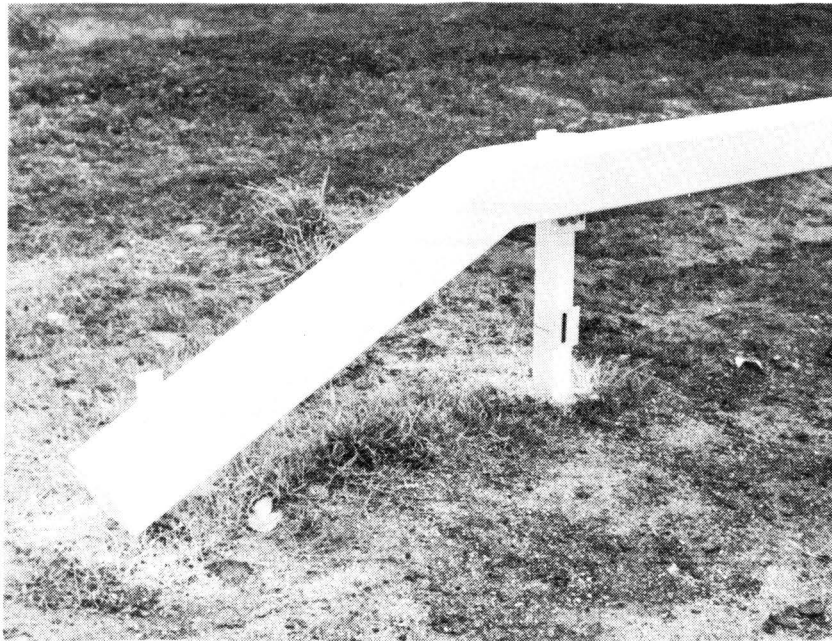


FIGURE IV.3.D.4. DETAIL OF END ANCHORAGE

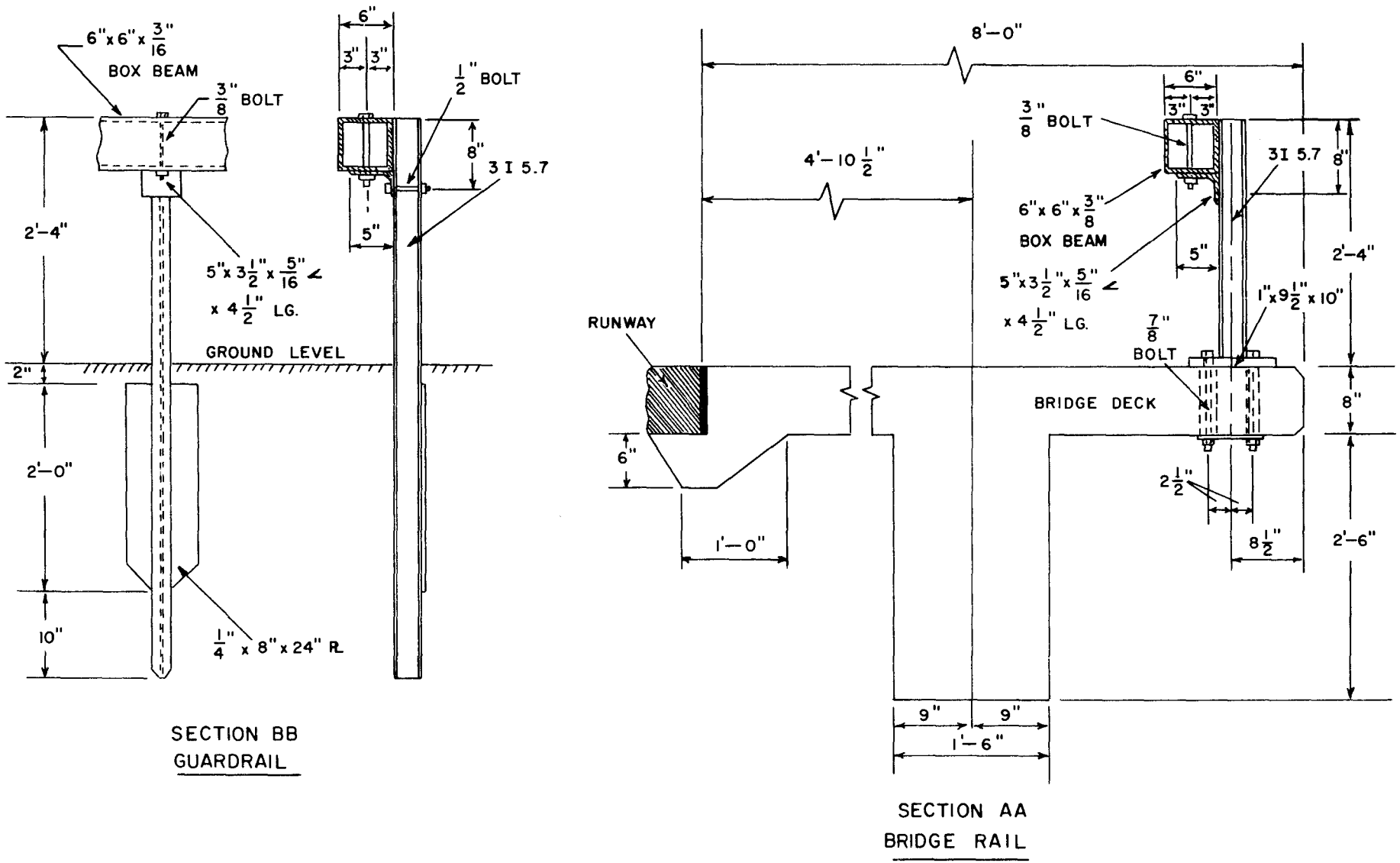


FIGURE IV.3.D.5. BRIDGE RAIL AND GUARDRAIL SECTIONS



1



2



3



4



5

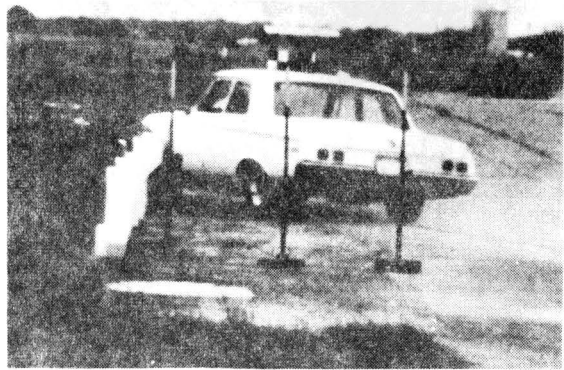


6

FIGURE IV.3.D.6. SEQUENCE PHOTOGRAPHS OF TEST NY-A
(VIEW PARALLEL TO BRIDGE RAIL).



1



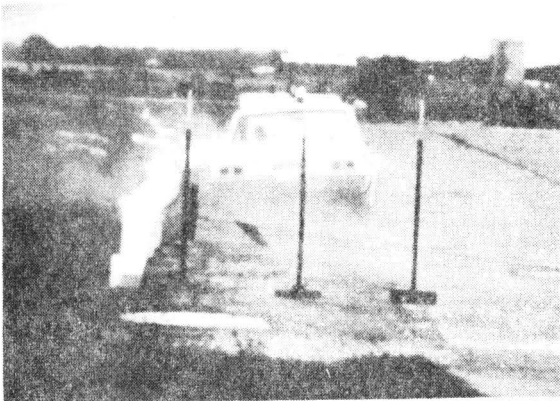
2



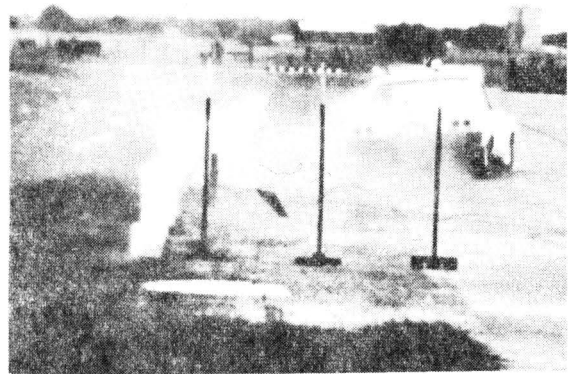
3



4



5



6

FIGURE IV.3.D.7. SEQUENCE PHOTOGRAPHS OF TEST NY-B
(VIEW PARALLEL TO BRIDGE RAIL).

5.1 g's. Damage was incurred on approximately 60 ft of the barrier, with some 11 bridge and guard posts bent or broken. The vehicle incurred moderate damage to its left front quarter.

CONCLUSIONS

In both tests, the barrier installation contained and redirected the vehicles. Vehicle compartment encroachment was negligible in each test. In Test NY-B an excellent transition between guardrail and bridge rail was achieved by this strong beam-weak post system.

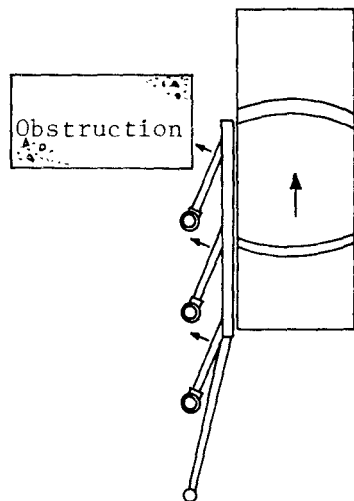
Additional information and data can be found in Technical Memorandum 505-12 which appears in Appendix F.

Part 3. E. --- ROTO-SHOK ENERGY-ABSORBING BARRIERBARRIER DESCRIPTION

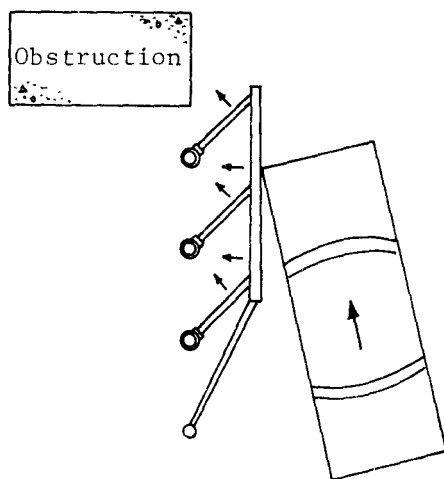
The ROTO-SHOK protective system consists of a series of straight sections of elliptical tubes rigidly supported from the ROTO-SHOKs by another system of elliptical tubes. Figures IV.3.E.2.-3. show the installation which was tested. The ROTO-SHOKs were mounted by their inner drums on posts. When the vehicle impacts the series of straight sections, the protective barrier tubes transmit the impact forces to the elliptical tubes which initiate the angular dissipation of energy in the ROTO-SHOKs. The ROTO-SHOKs contain small diameter tubes positioned with an interference fit in the annulus of two concentric drums. At impact, the rotation of the drums relative to one another provides the energy absorption mechanism in terms of cyclic bending strain around the circumference of the small diameter tubes. The resistance to torque provided by the ROTO-SHOK exerts a resisting force on the vehicle as the barrier deforms. This rotation of the ROTO-SHOK arms with resulting lateral translation of the impact section allows the vehicle to be redirected with nominal transverse decelerations.

TEST RESULTS

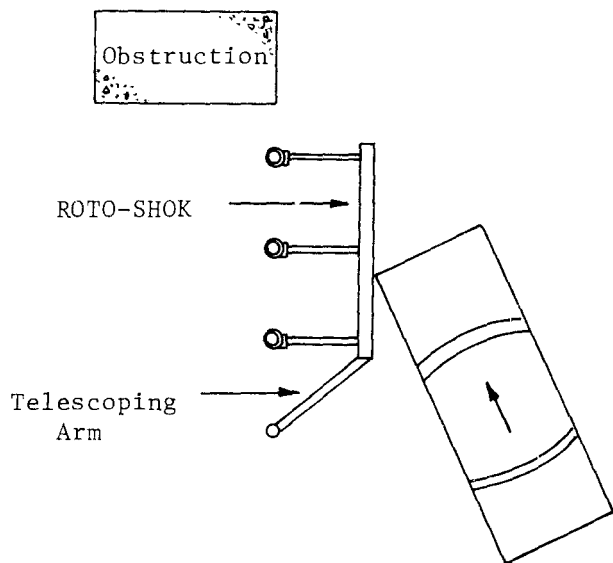
The only test conducted on this system (Test 505-2F) involved a 4290 lb vehicle traveling 46.0 mph and striking the barrier at an angle of 25° (see Figure IV.3.E.4.). Vehicle change in speed during contact was 11.4 mph. The barrier performed as intended, redirecting the vehicle with only superficial damage to it and moderate damage to the ROTO-SHOK.



(3) Vehicle is Redirected To Miss Obstruction



(2) ROTO-SHOK Rotates And Begins Redirecting Vehicle



(1) Vehicle Contacts ROTO-SHOK

FIGURE IV.3.E.1. IDEALIZED FUNCTION OF ROTO-SHOK

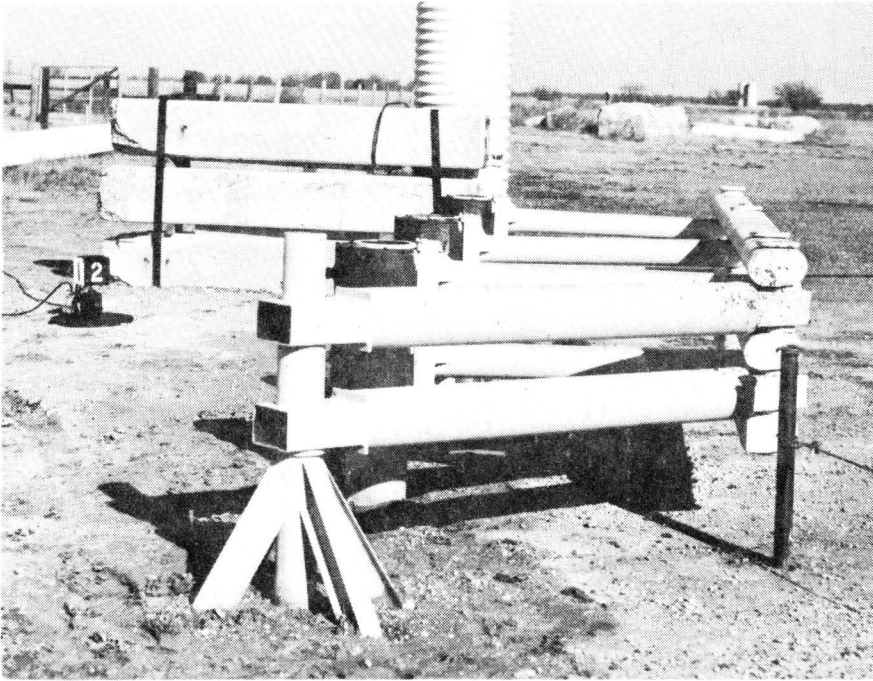
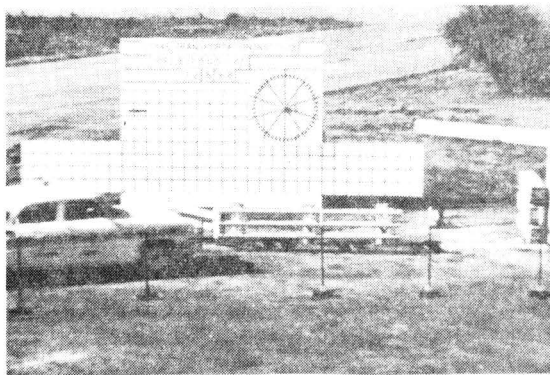


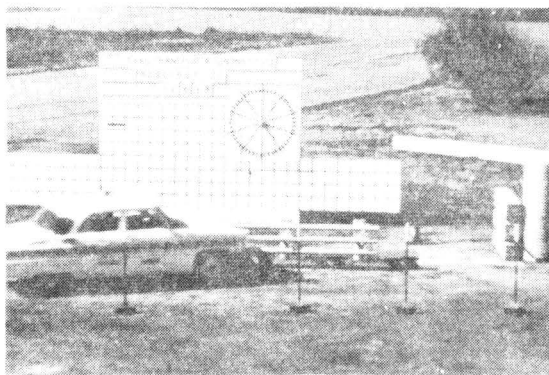
FIGURE IV.3.E.2. ROTO-SHOK BEFORE TEST.



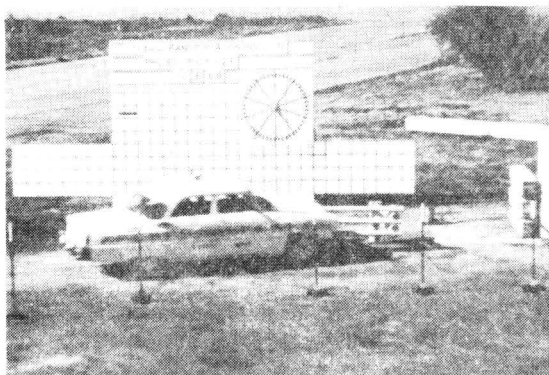
FIGURE IV.3.E.3. DETAILS OF ROTO-SHOK FROM REAR.



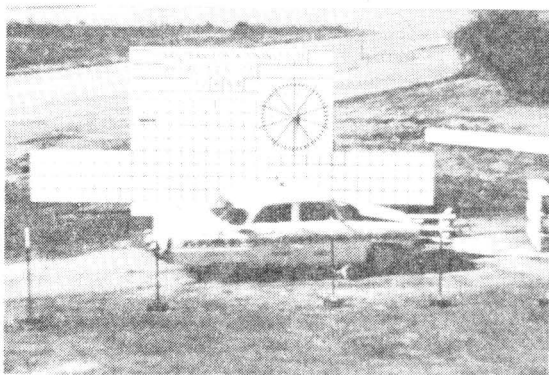
1



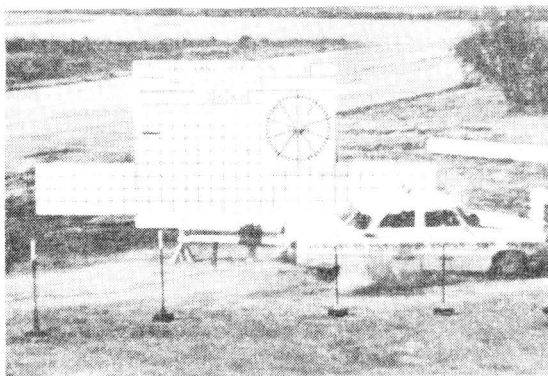
2



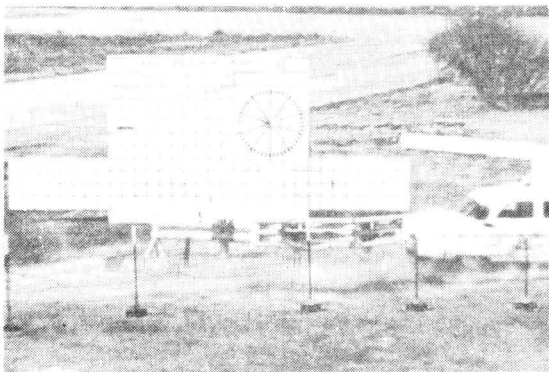
3



4



5



6

FIGURE IV.3.E.4. SEQUENTIAL PHOTOGRAPHS ROTO-SHOK, TEST 2F.

The total energy absorbed by the ROTO-SHOK was approximately 118 kip-ft (40% of the vehicle kinetic energy). Vehicle deformation was 0.83 ft; barrier deformation was 4 ft. The average longitudinal deceleration was 1.1 g's over 0.500 sec.

Additional test data are available in Technical Memorandum 505-2S which can be found in Appendix F.

Part 3. F. --- FIBERGLAS MEDIAN BARRIER (FLOWER POT CONCEPT)BARRIER DESCRIPTION

This median barrier consisted of a fiberglass trough containing fill material. Ten-foot sections were bolted together to form the trough. Figure IV.3.F.1. is a drawing of a section of the barrier. A fiberglass guardrail or rubrail was attached to the outside of the barrier to form a vehicle redirection surface. The lower portion of the barrier rested in a 10 in. wide by 11 in. deep trench parallel to the roadway. Pea gravel was used as fill material for the test conducted by TTI. A 150 ft length of this median barrier was installed adjacent to a concrete vehicle-approach area for this test.

TEST RESULTS

The only test conducted on this median barrier (Test 505 FG-A) involved a 1966 Chevrolet sedan weighing 4150 lb. The vehicle impacted the fiberglass barrier at a speed of 54.0 mph and an angle of 25°. The vehicle shattered a 12 ft segment of the fiberglass trough and rubrail, allowing it to penetrate the barrier. The vehicle then ramped on the barrier and came to rest astride the median barrier (see Figure IV.3.F.2.). The back wall of the trough collapsed when the front was shattered. The average longitudinal deceleration of the vehicle was 2.6 g's and the average transverse deceleration was 2.2 g's. The vehicle damage was severe, as evidenced by a right front fender deformation of 3.1 ft.

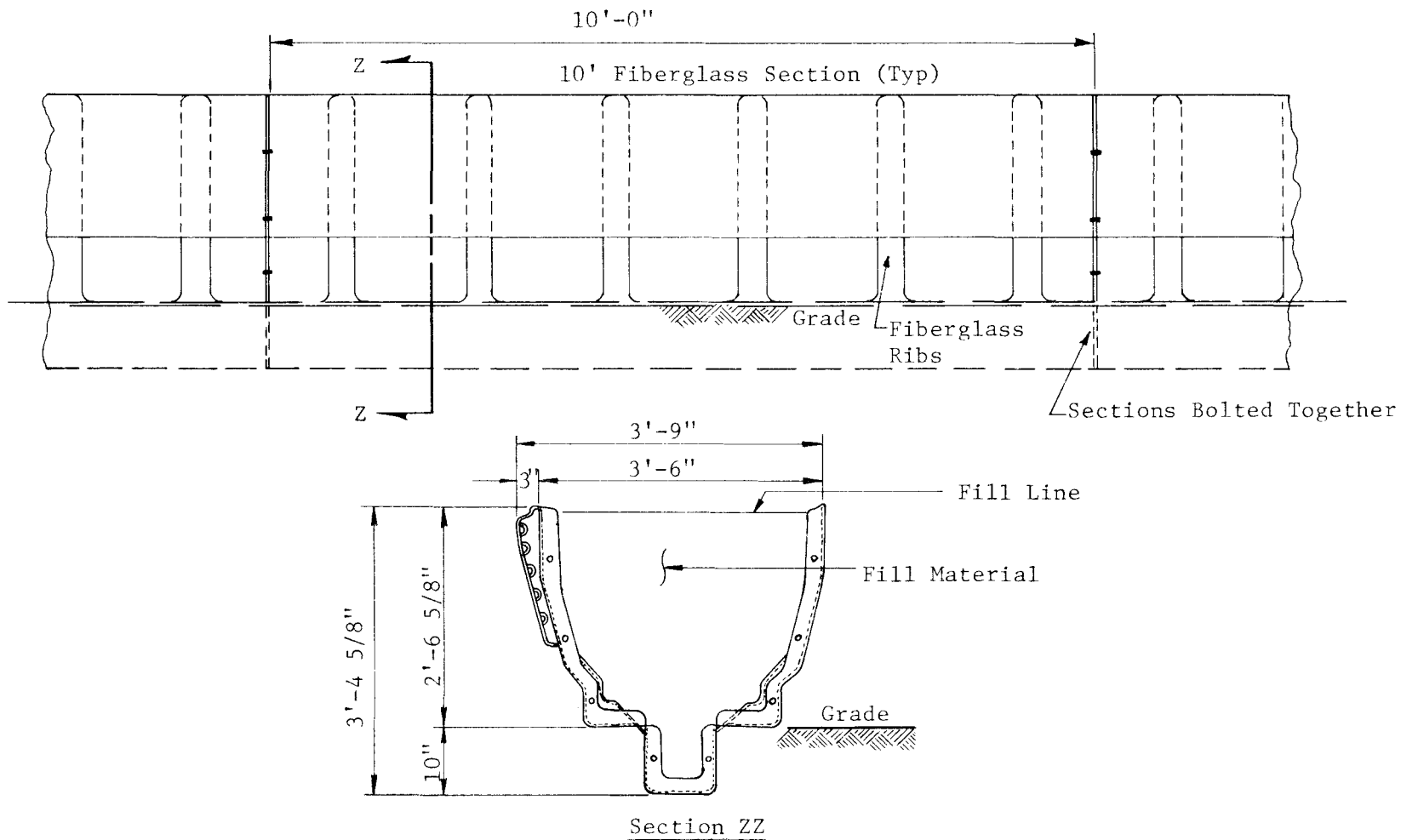
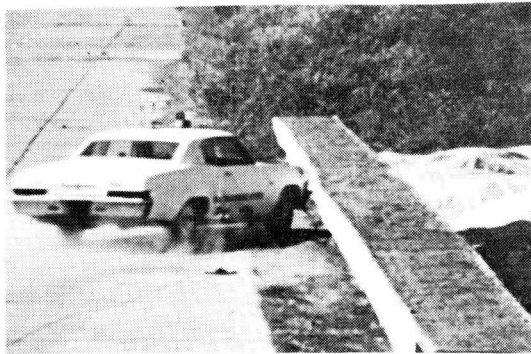


FIGURE IV.3.F.1. DETAIL OF FIBERGLASS SECTION



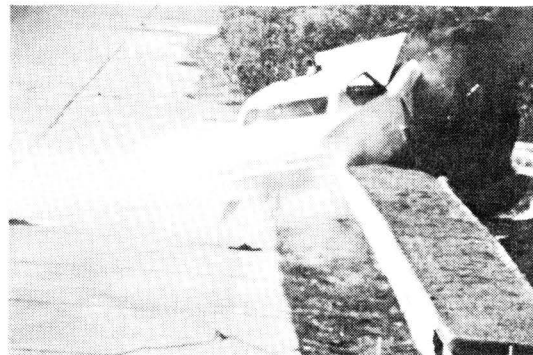
1



2



3



4



5



6



7



8

FIGURE IV.3.F.2. SEQUENTIAL PHOTOGRAPHS OF TEST FG-A.

CONCLUSIONS

Although a structural failure by the fiberglass median barrier precluded its proper functioning as a redirection device, the concept did function to attenuate the impact. The fiberglass barrier lacked strength and roughness to prevent the vehicle from penetrating it. The barrier contact surfaces and connections could possibly be altered to prevent disintegration of the side of the barrier under vehicular impact. This might be accomplished by replacing the fiberglass guardrail or rubrail with the common metal W-section flexbeam railing. However, further design modifications would probably be necessary for eliminating vehicle penetration into the median barrier.

Additional information can be found in Technical Memorandum 505-14 which appears in Appendix F.

CHAPTER IV REFERENCES

1. Michie, J. D. and Bronstad, M. E., "Impact Tests Of Nonmetallic Pipe Sections," report prepared for U.S. Department of Transportation, Federal Highway Administration on DOT Order No. 1-1-1360, April 1971.
2. Nordlin, Eric F. and Field, Robert N., "Dynamic Tests of Steel Box Beam and Concrete Median Barriers," Highway Research Record No. 222, 1968.
3. Hirsch, T. J. and Ivey, Don L., "Vehicle Impact Attenuation by Modular Crash Cushion," Research Report No. 146-1, Texas Transportation Institute, Research Study No. 2-8-68-146 sponsored by the Texas Highway Department in cooperation with the U.S. Department of Transportation, FHWA, June 1969.
4. Hayes, Gordon G., Ivey, Don L., and Hirsch, T. J., "Flexbeam Redirectional System for the Modular Crash Cushion," Research Report No. 146-3, Texas Transportation Institute, Research Study No. 2-8-68-146 sponsored by the Texas Highway Department in cooperation with the U.S. Department of Transportation, FHWA, 1971.
5. "Development of a Hydraulic-Plastic Barrier for Impact-Energy Absorption," Final Report on FHWA-DOT Contract No. FH-11-6909, Department of Mechanical Engineering, Brigham Young University.
6. Walters, William C. and Bokun, Steve G., "Performance Report of the HIDRO Cushion Crash Attenuation Devices," Highway Research Report, Louisiana Department of Highways, June 1970.

CHAPTER V

SUMMARY AND CONCLUSIONS

INTRODUCTION

The vehicle impact attenuation devices discussed in Parts 1 and 2 of Chapter IV (Vehicle Impact Attenuation Barriers without and with Redirection Capabilities) basically employ one or both of the following two concepts for stopping a speeding vehicle before it strikes a rigid hazard.^{1*}

ENERGY ABSORPTION BARRIERS

The first concept involves absorption of the kinetic energy of the speeding vehicle by use of "crushable" or "plastically" deformable materials or structures or by use of hydraulic "dashpots" or energy absorbers placed in front of the hazard. Devices of this type need a rigid backup or support to resist the vehicle impact force and deform the energy absorbing material or structure. Figures V.1 and V.2 illustrate this principle applied to a compression type barrier and a tension net (or snagging) device, respectively.

In Figure V.1 the stopping force (F) need not be constant, but the area under the force (F) vs deformation (D) graph of the crash cushion should equal the kinetic energy of the impacting vehicle. The crash cushion should be designed so that it will stop a small 2,000 lb vehicle traveling at 60 mph with D equal to or greater than the minimum required stopping distance of 10 ft. Additional material and distance should also be provided so that the device will also be capable of stopping a 4,500 lb vehicle traveling 60 mph.

*Superscript numerals refer to corresponding numbers in the References at the end of this section.

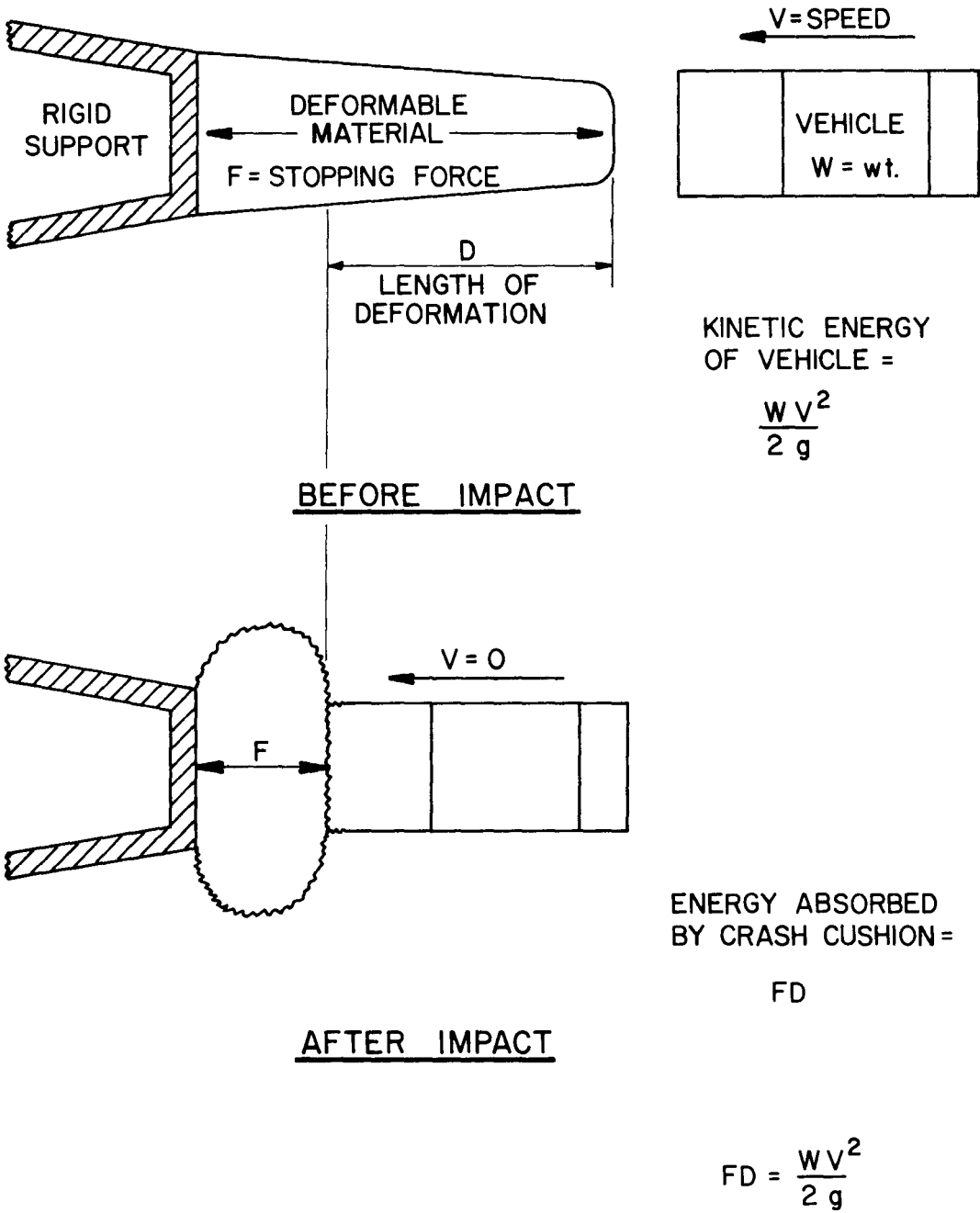


FIGURE V.1. PRINCIPLE OF ABSORBING VEHICLE KINETIC ENERGY — COMPRESSION DEVICE

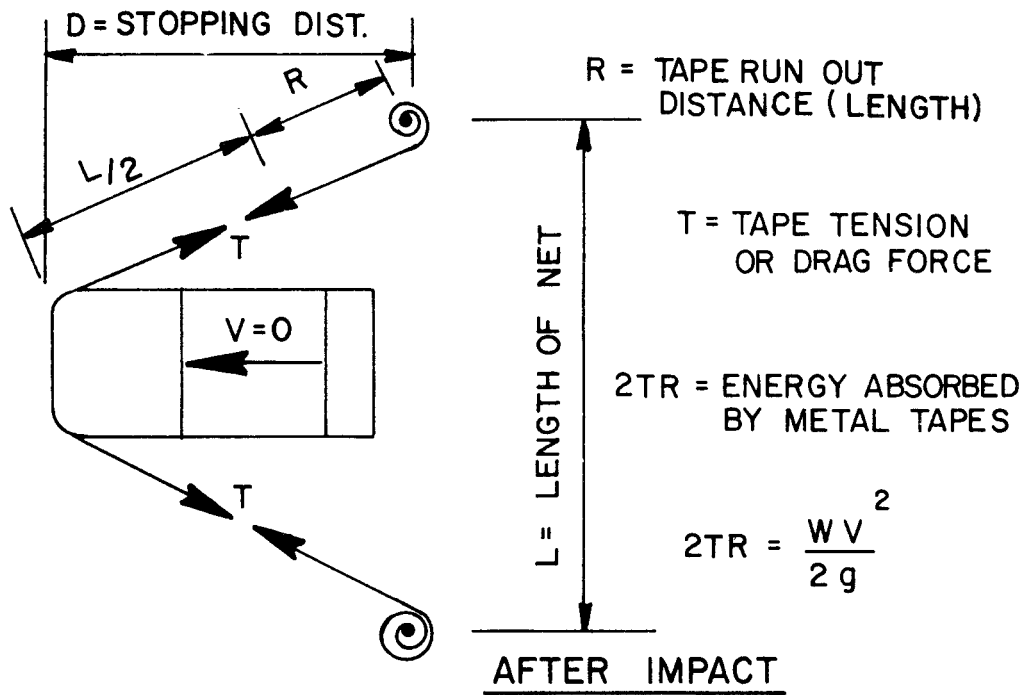
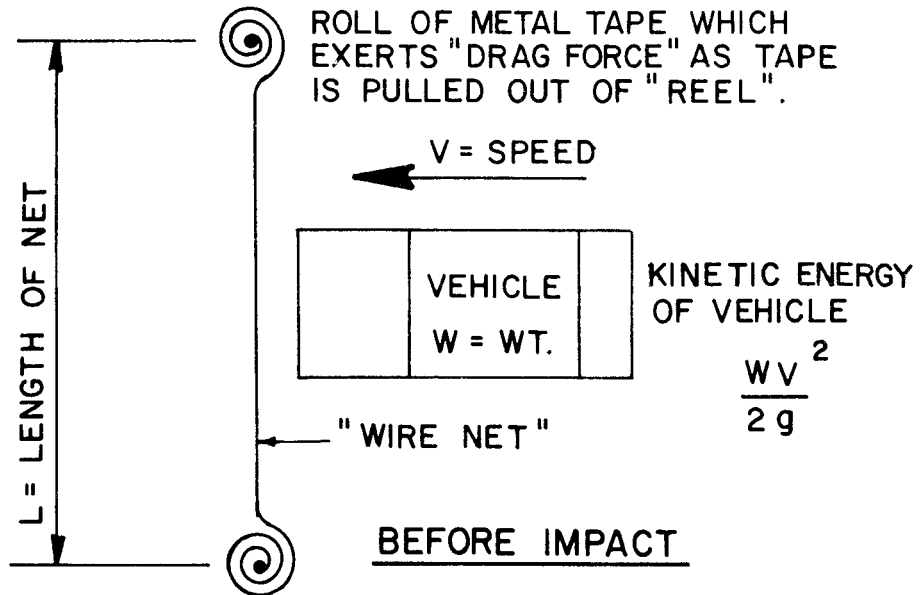


FIGURE V.2. PRINCIPLE OF ABSORBING VEHICLE KINETIC ENERGY - NETS OR SNAGGING DEVICES.

In Figure V.2 the metal tape tension or "drag force" (T) will usually be constant. The designer must select the proper combination of "drag force" (T) and tape run-out distance (R) so the device will stop a small 2,000 lb vehicle traveling 60 mph with a stopping distance (D) equal to or greater than the minimum required stopping distance of 10 ft. Additional tape run-out capacity (R) should be provided so the device will also be capable of stopping a 4,500 lb vehicle traveling at 60 mph. It should be noted that from simple geometry of Figure V.2 the relationship between stopping distance (D) and tape run out (R) is

$$D = \sqrt{R^2 + RL} \quad \text{or} \quad R = \frac{-L + \sqrt{L^2 + 4D^2}}{2} \quad (\text{approx.})$$

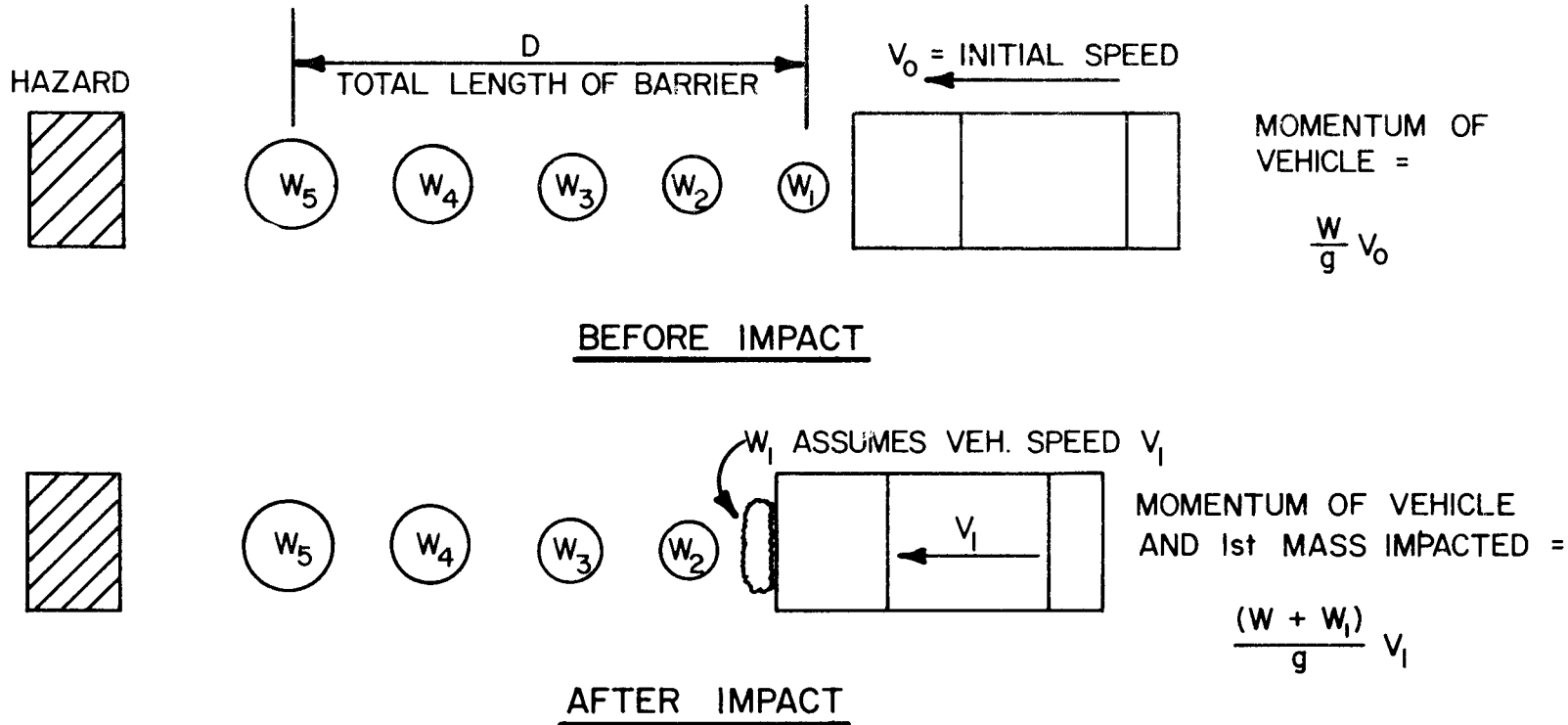
MOMENTUM TRANSFER OR INERTIA BARRIERS

The second concept involves transfer of the momentum of the speeding vehicle to some expendable masses of material located in the path of the vehicle. The expendable masses (or weights) are usually containers filled with sand although water and other materials can be used. Devices of this type need no rigid backup or support to resist the vehicle impact force since the kinetic energy of the vehicle is not absorbed but merely transferred to the other masses. This type of crash cushion is sometimes referred to as an "Inertia Barrier".

Figure V.3 illustrates this principle applied to a speeding vehicle impacting a series of five masses or containers filled with sand.

By the Law of Conservation of Momentum, the vehicle speed after first mass impact (assuming rigid body plastic impact) is

$$V_1 = V_o \left(\frac{W}{W + W_1} \right) .$$



MOMENTA BEFORE IMPACT = MOMENTA AFTER IMPACT

$$W V_0 = (W + W_1) V_1$$

$$V_1 = V_0 \left(\frac{W}{W + W_1} \right)$$

FIGURE V.3. PRINCIPLE OF TRANSFERRING VEHICLE MOMENTUM TO EXPENDABLE MASSES — ASSUMING PLASTIC RIGID BODY IMPACT

The vehicle speed after second mass impact is

$$V_2 = V_1 \left(\frac{W}{W + W_2} \right) \cdot$$

The final speed after fifth mass impact will be

$$V_5 = V_4 \left(\frac{W}{W + W_5} \right) \cdot$$

To obtain a constant change in speed as the vehicle strikes each container (W_1 through W_5) it can be seen that containers must increase in weight (or mass) as they get closer to the hazard.

Thus

$$\Delta V_1 = V_0 - V_1 = V_0 \left(1 - \frac{W}{W + W_1} \right)$$

and

$$\Delta V_2 = V_1 - V_2 = V_1 \left(1 - \frac{W}{W + W_2} \right)$$

and so forth. It is apparent that theoretically the vehicle cannot be stopped completely by this principle. Practically, however, it is usually adequate to design the Inertia Barrier to reduce the vehicle speed to 10 mph after the final container is impacted.

As in the design of any vehicle crash cushion, the weight and number of containers and length of the barrier should be proportioned to stop a small 2,000 lb vehicle traveling at 60 mph with a stopping distance (D) equal to or greater than the minimum required distance of 10 ft. Additional containers and distance should be supplied so the device can also stop a 4,500 lb vehicle traveling 60 mph.

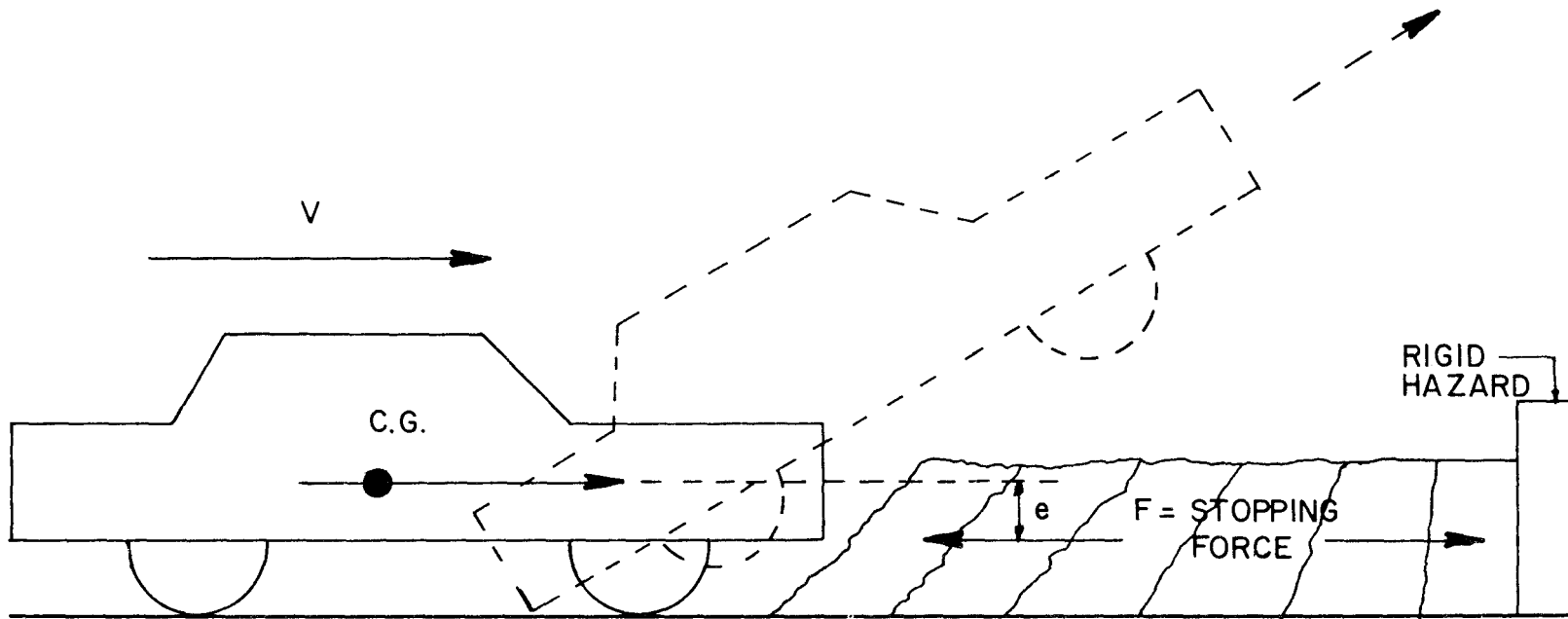
Basically, all the vehicle impact attenuation devices tested, evaluated, and reported herein principally employed the first concept (energy absorption) with the exception of the Fiberglass Median Barrier (a longitudinal barrier). All crash cushions have mass, of course, and thus some momentum transfer, but the mass alone is not sufficient to stop or significantly slow the vehicle as intended by the second inertia concept.

VEHICLE IMPACT ATTENUATION - GEOMETRIC AND DESIGN DETAILS

To make a crash cushion work as intended by the design concept, careful attention must be given to several other geometric and design details.

Figure V.4 illustrates how a vehicle may ramp and jump over the vehicle impact attenuation device if the resultant stopping force provided by the crash cushion is considerably lower than the vehicle center of gravity (C.G.). The energy-absorbing material may deform more at the top than at the bottom and thus form a ramp for the vehicle. Such behavior was observed in Tests 505-5A, 505 CSP-1, and 505 CSP-3. A tendency to do this was also observed in Test 505-1E. Figure V.5 illustrates how a vehicle may also flip end over end due to the couple formed by the eccentricity of the resultant stopping force and vehicle inertia force. This tendency was distinctly observed in Tests 505-4A, 505-4B, and 505-4E.

On the other hand, Figure V.6 illustrates how a vehicle may submerge under the vehicle impact attenuation device if the resultant stopping force is considerably higher than the vehicle center of gravity. This tendency was observed in Tests 505 M-C and 505 B-E. To



THE VEHICLE MAY RAMP AND JUMP OVER THE CRASH CUSHION.

FIGURE V.4. RESULTANT STOPPING FORCE LOWER THAN THE VEHICLE CENTER OF GRAVITY (C.G.). HEAD-ON IMPACT.

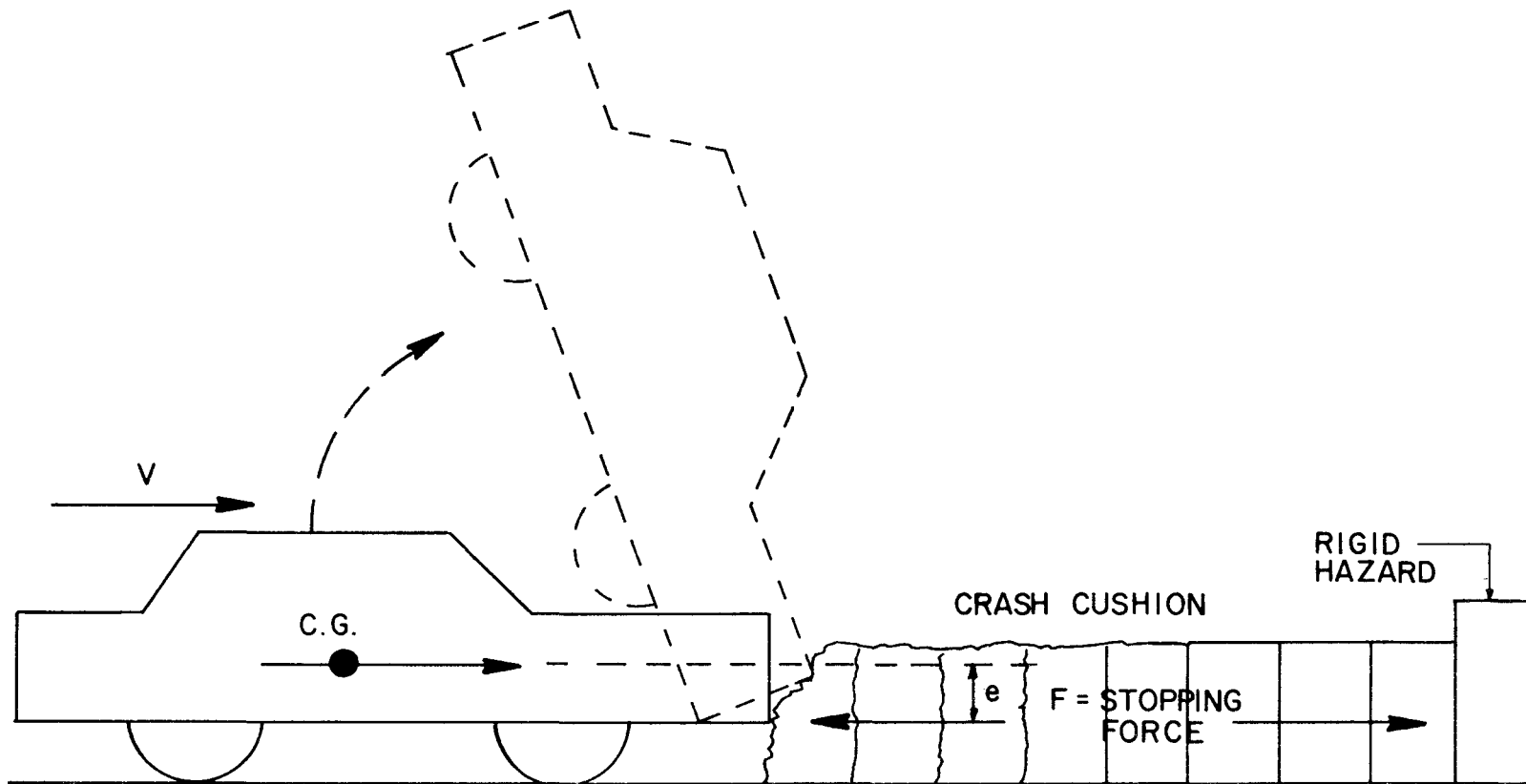
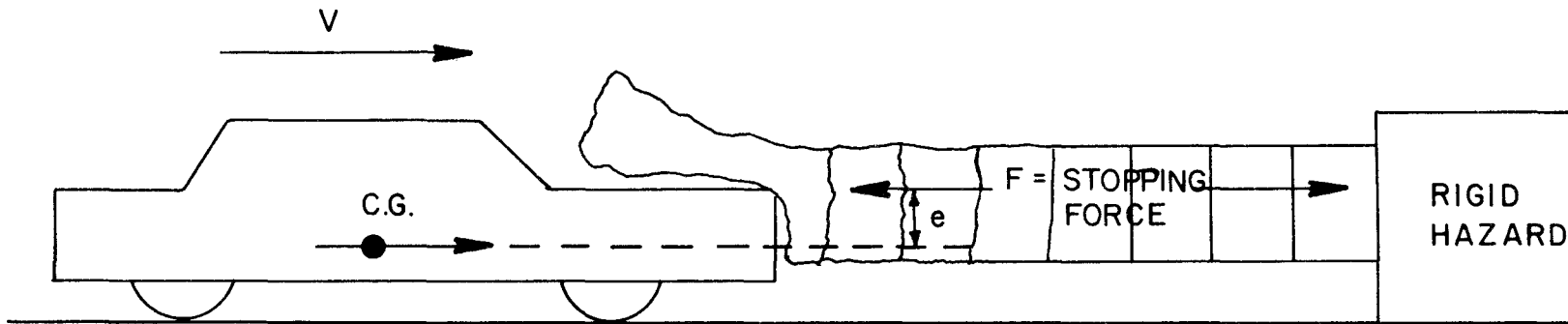


FIGURE V.5. RESULTANT STOPPING FORCE LOWER THAN THE VEHICLE CENTER OF GRAVITY (C.G.) HEAD-ON IMPACT.



THE VEHICLE MAY SUBMARINE UNDER THE CRASH CUSHION

FIGURE V.6. RESULTANT STOPPING FORCE HIGHER THAN THE VEHICLE CENTER OF GRAVITY (C.G.)

guard against such behavior as shown in Figures V.5 and V.6, the resultant stopping force provided by the energy absorbing material or inertia masses should be located approximately 22 to 24 in. above the roadway or ground. (This is the approximate location of a typical American passenger vehicle's center of gravity.) In addition, the energy absorbing crash cushion materials are usually stabilized by a cable or other anchoring system to prevent the material from moving up, down, or sideways during the collision.

Figure V.7 illustrates how a vehicle may "pocket", "spin out", and even "roll over" in a head-on off-center impact. This type behavior can occur if the vehicle crash cushion is extremely massive and/or stiff thus generating a large eccentric stopping force and rotation couple on the vehicle. Such behavior was observed in Tests 505-4C, 505-4D, 505-4F, and 505 R-D.

Thus far this discussion of Vehicle Impact Attenuators (VIA) has been limited to head-on or near head-on impacts. Of importance also is the behavior of these devices when the vehicle impacts them at an angle with respect to the VIA's longitudinal axis. Figure V.8 illustrates how a typical Vehicle Impact Attenuator without redirection capabilities will behave under an angle impact near the nose. In this case, sufficient distance and energy-absorbing material may be available between the point of impact and the rigid hazard to stop the colliding vehicle safely. In such cases, it is satisfactory to allow the vehicle to "pocket" and come to a complete stop short of the rigid hazard.

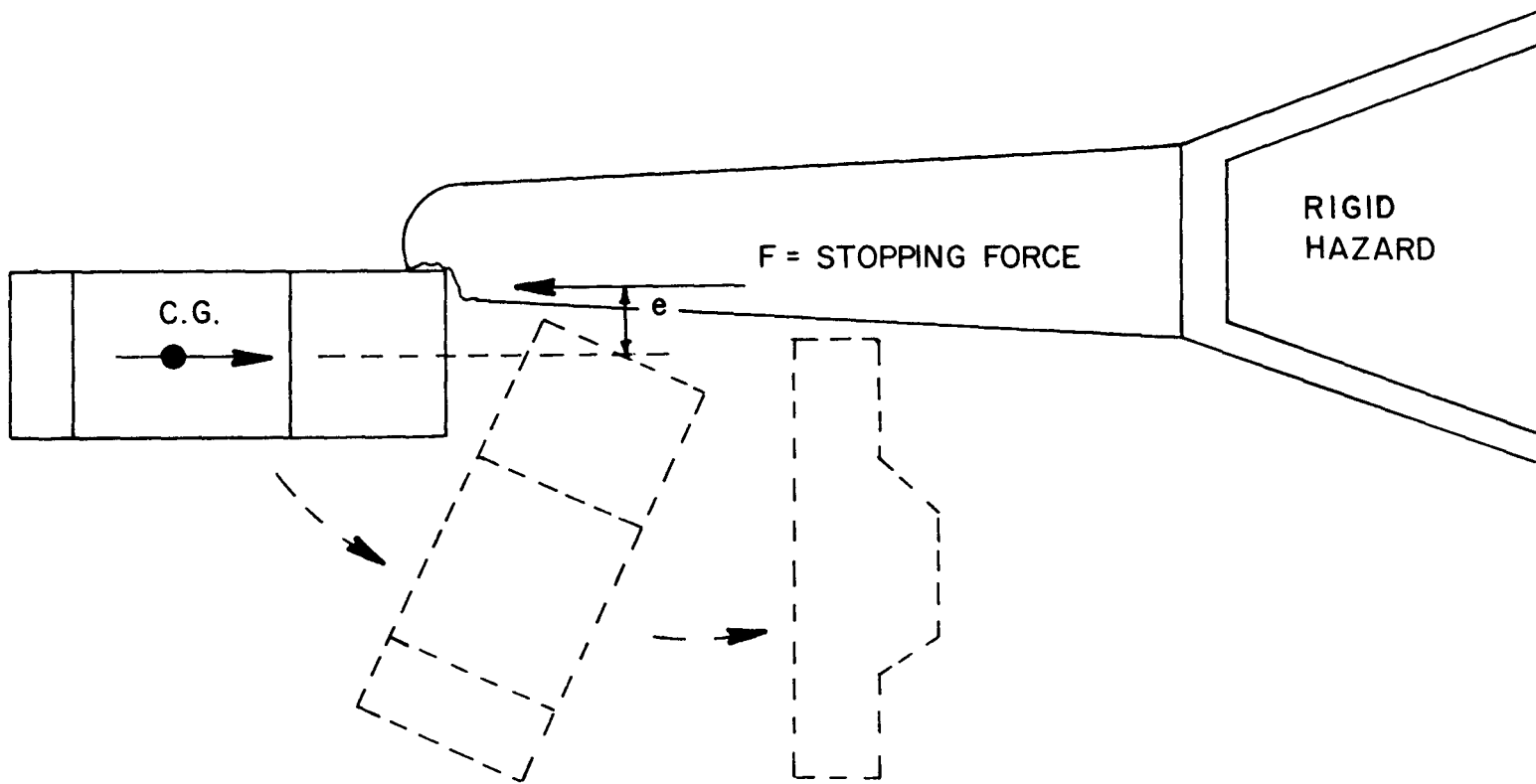


FIGURE V.7. VEHICLE IMPACT ATTENUATOR IS TOO MASSIVE AND STIFF (STOPPING FORCE TOO LARGE). AN OFF CENTER HIT MAY CAUSE THE VEHICLE TO "POCKET", "SPIN-OUT", AND "ROLL-OVER."

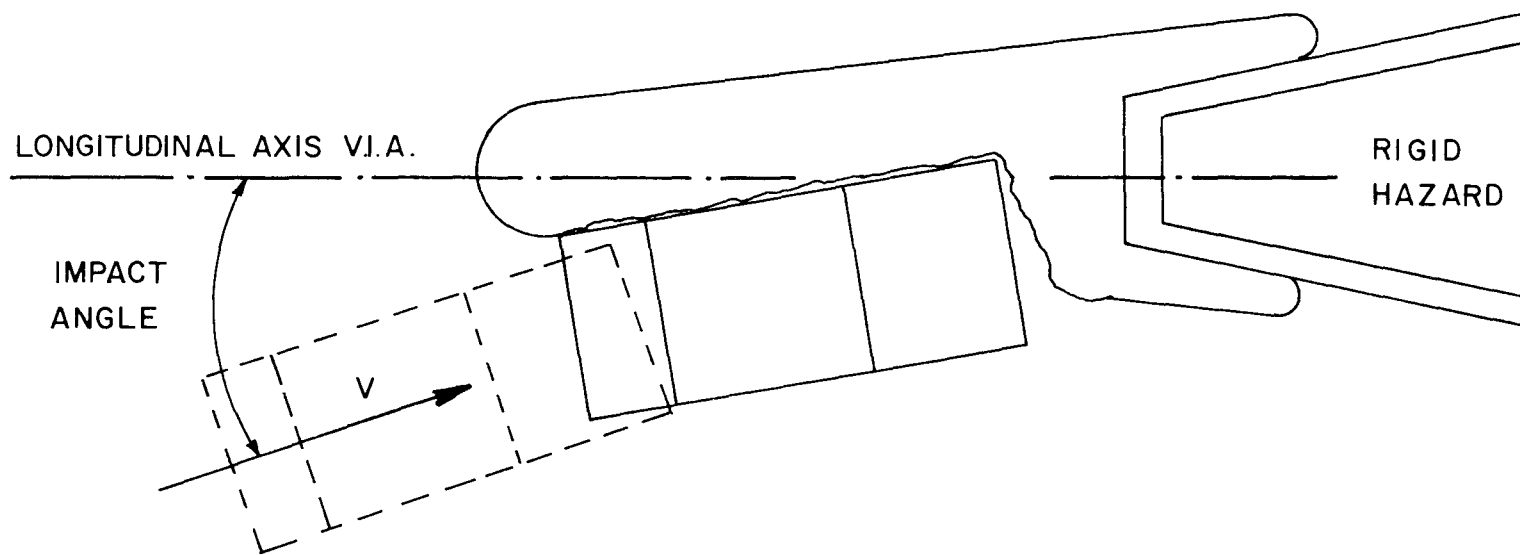


FIGURE V.8. VEHICLE ANGLE IMPACT NEAR THE NOSE OF THE IMPACT ATTENUATOR

Should the vehicle impact the VIA at an angle at a point near the rear of the VIA, a severe collision may occur when the vehicle strikes the rigid hazard. Figure V.9 illustrates this potential problem. In such a collision, distance and energy-absorbing material may be insufficient to stop the vehicle safely before it strikes the rigid hazard. Because of mechanical failures in the redirection system such behavior was observed in Tests 505 B-A, 505 R-C, 505-2D, and 505-2E. In an attempt to remedy this potential hazard, many VIA designers are cladding the sides of the vehicle impact attenuators with hard, stiff, and smooth panels which will prevent the vehicle from "pocketing" and thus redirect it as shown in Figure V.10. The provisions for redirection must be such that the VIA has lateral stability and still maintain the relatively "soft" crush characteristics under head-on impacts. Satisfactory behavior of such a redirection system is shown by Tests 505 M-A, 505 M-B, 505 B-B, and 505 B-D.

SUMMARY OF DESIRED VEHICLE IMPACT ATTENUATION BARRIER CHARACTERISTICS

The objective of this discussion was to briefly summarize some of the basic design concepts and desired behavior characteristics for vehicle impact attenuation devices.

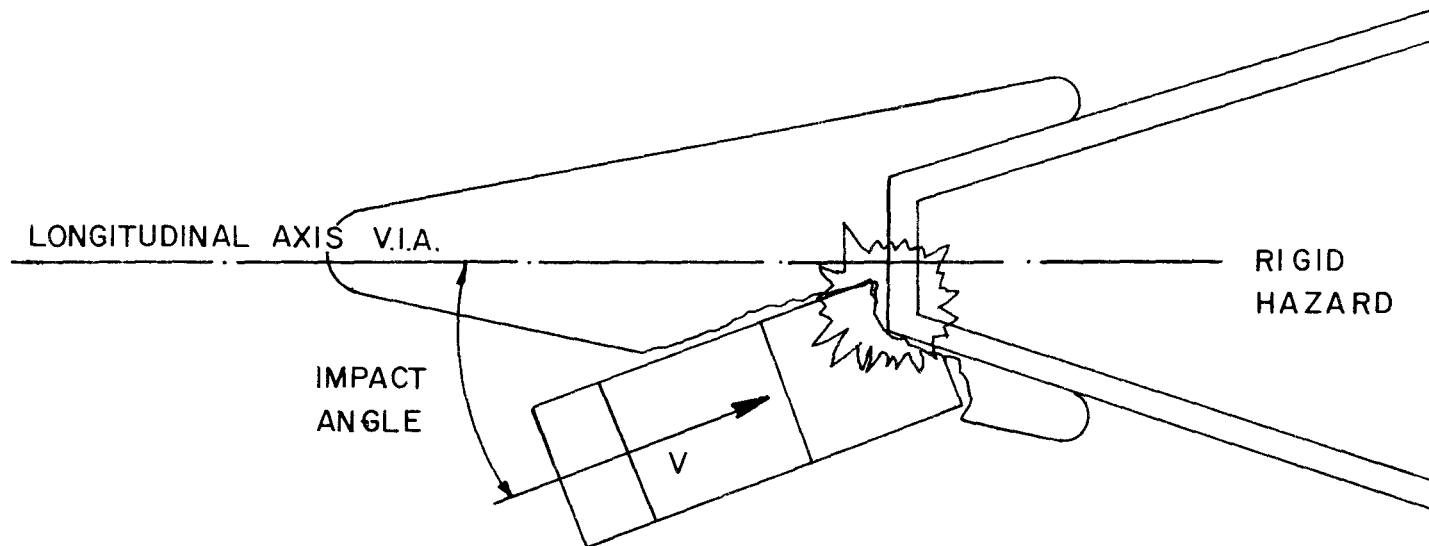


FIGURE V.9. VEHICLE ANGLE IMPACT NEAR THE REAR OF THE VEHICLE IMPACT ATTENUATOR

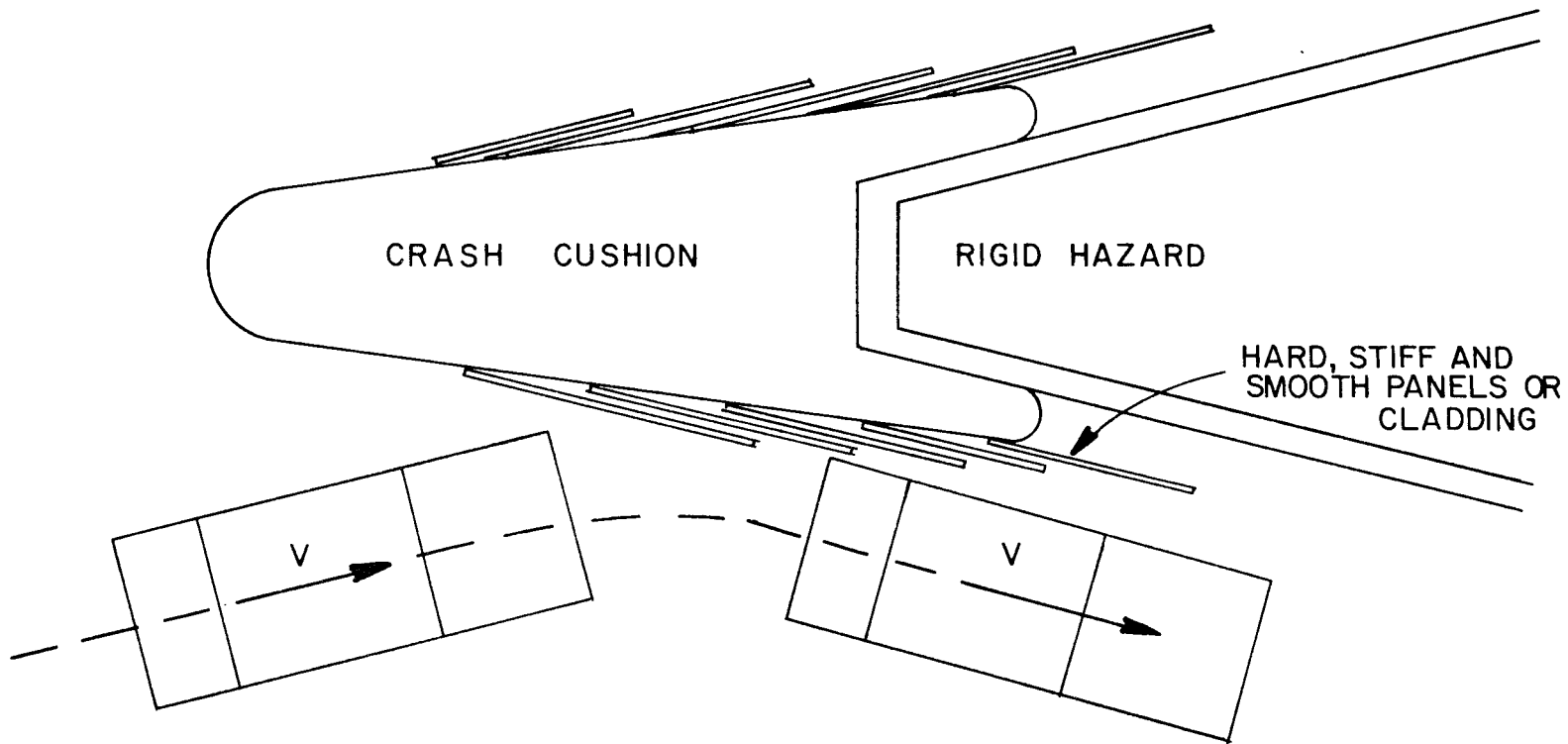


FIGURE V.10. VEHICLE ANGLE IMPACT INTO VEHICLE IMPACT ATTENUATOR DESIGNED TO REDIRECT VEHICLE RATHER THAN STOP IT.

For impact attenuation barriers to be effective and acceptable for use on our nation's highways, the test results and experience gained during this project indicate that it would be desirable for such barriers to have the following characteristics.

I. Vehicle Impact Attenuation Barriers (Crash Cushions without Re-direction Capability)

- A. A crash cushion should smoothly stop a selected vehicle impacting it head-on. The vehicle should not vault over the barrier and should not become unstable and roll over. (It would be desirable for simple crash cushions to have the capability of stopping a vehicle impacting anywhere along its length and at any angle up to the maximum design conditions of impact speed, vehicle weight, and impact angle.)
- B. A crash cushion should minimize vehicle decelerations in such a manner that occupants restrained by seat belts can survive, preferably uninjured.
- C. A crash cushion should remain essentially intact during and following a vehicle collision. A vehicle impact should not dislodge any hazardous elements into the travelway.
- D. A crash cushion should be compatible with the roadway and fixed object it is guarding. It should not protrude into the travelway or shoulders provided for emergency or evasive maneuvers by a vehicle.

- E. A crash cushion should be susceptible of quick repair. All elements of a barrier should be so designed that when repairs are necessary they can be done quickly and with a minimum of special equipment.
- F. A crash cushion should be mechanically reliable and dependable. It should be durable and stand up under extreme environmental exposure -- heat and cold, wet and dry, and corrosive elements expected under service conditions.
- G. The foregoing requirements should be met by giving emphasis first to safety, second to economics, and third to aesthetics.

II. Vehicle Impact Attenuation Barriers (Crash Cushions with Redirection Capabilities)

- A. A crash cushion with redirection capabilities should satisfy all the service requirements of a simple crash cushion of item I when a selected vehicle impacts it head-on.
- B. A crash cushion with redirection capabilities should restrain and smoothly redirect a selected vehicle which impacts it along its length or side. The impacting vehicle should not penetrate or vault over the barrier. The vehicle should not snag or pocket under side angle impacts.
- C. A crash cushion with redirection capabilities should be compatible with adjoining or abutting longitudinal barriers (guardrails, bridge rails, or median barriers) in order to prevent collisions with the ends of the adjoining or abutting barriers. A smooth redirection should be obtained at the transition point between the two barriers.

LONGITUDINAL BARRIERS (GUARDRAILS, BRIDGE RAILS, AND MEDIAN BARRIERS)

Basic design concepts and behavior characteristics for longitudinal barriers such as guardrails, bridge rails, and median barriers have been thoroughly covered by previous research (NCHRP Report 36, "Highway Guardrails - A Review of Current Practice," 1967; NCHRP Report 54, "Location, Selection and Maintenance of Highway Guardrails and Median Barriers," 1968; and NCHRP Report 86, "Tentative Service Requirements for Bridge Rail Systems," 1970).^{2,3,4}

SUMMARY OF DESIRED LONGITUDINAL BARRIER CHARACTERISTICS

As a result of the test results, experience gained during this project and information in the literature, it appears that longitudinal barriers should have the following characteristics:

III. Longitudinal Barriers (Guardrails, Bridge Rails, and Median Barriers)

- A. A longitudinal barrier should laterally restrain a selected vehicle. The impacting vehicle should not penetrate or vault the barrier.
- B. A longitudinal barrier should minimize vehicle decelerations.
- C. A longitudinal barrier should smoothly redirect a colliding vehicle. Vehicle progression should be smooth following impact; it should not snag or pocket or roll over.
- D. A longitudinal barrier should remain intact following a collision. Vehicle impact should not dislodge any hazardous elements into the travelway.

- E. A longitudinal barrier which serves vehicles and pedestrians should provide protection for both vehicle occupants and pedestrians. Sidewalks must be placed outboard of the vehicle-barrier railing.
- F. A longitudinal barrier should have a compatible transition between it and other adjoining or abutting barriers in order to prevent collisions with the ends of the adjoining barrier.
- G. A longitudinal barrier should have compatible beginning and end treatments. The end treatment should develop the required anchorage strength so the barrier can redirect colliding vehicles near the end. The end treatment should minimize the hazard of vehicles colliding with the ends.
- H. A longitudinal barrier should define the limits of the travelway yet provide adequate visibility. The driver's sight distance should not be obstructed on horizontal curves.
- I. A longitudinal barrier should be susceptible to quick repair.
- J. The foregoing requirements should be met by giving emphasis first to safety, second to economics, and third to aesthetics.

EVALUATION OF A CRASH CUSHION OR LONGITUDINAL BARRIER

A given barrier system can be objectively and subjectively evaluated from crash test data by using the foregoing desired characteristics. Table V.1 presents an example evaluation of the Texas T1 Bridge Rail-Guardrail System using the "Desired Longitudinal Barrier Characteristics". The evaluations of Tests 505 T1-A, 505 T1-B, 505 T1-C, and 505 T1-D were made using information from high-speed films, a National Safety Council

Service Requirement	T-1 Bridge Rail Test 505-T1 A	T-1 Bridge Rail Test 505-T1 B	Transition Rail Test 505-T1 C	Modified T-1 Bridge Rail Test 505-T1 D
III. A	Adequate lateral restraint is provided by each of these barriers; penetration and vaulting do not occur.			
III. B	$G_{TOTAL} = 5.2$ Vehicle Damage Rating: R = 4.9 Probability of Injury: 50%	$G_{TOTAL} = 7.2$ Vehicle Damage Rating: R = 6.4 Probability of Injury: 85%	$G_{TOTAL} = 4.5$ Vehicle Damage Rating: R = 3.9 Probability of Injury: 30%	$G_{TOTAL} = 6.8$ Vehicle Damage Rating: R = 4.5 Probability of Injury: 45%
III. C	Good redirection, slight snagging. See Figure 4.	Poor redirection, severe snagging. See Figure 10.	Good redirection. See Figure 16.	Fair redirection. See Figure 22.
III. D	Each barrier remained intact following the collision.			
III. E	Not applicable.	Not applicable.	Not applicable.	Not applicable.
III. F	Yes	Yes	This approach rail is compatible geometrically and has adequate connection to bridge rail.	Yes
III. G	Yes	Yes	Yes - rail end turned down and anchored.	Yes
III. H	Each barrier satisfies the requirement for delineation, and does not obstruct driver's sight distance.			
III. I	No repairs required.	Replaced W-section	Replaced posts and W-section.	No repairs required.
III. J	SAFETY: 3rd ECONOMICS: Vehicle Repair: 2 Barrier Repair: 2 AESTHETICS: Good	SAFETY: 4th ECONOMICS: Vehicle Repair: 4 (most) Barrier Repair: 3 AESTHETICS: Good	SAFETY: 1st ECONOMICS: Vehicle Repair: 1 (least) Barrier Repair: 4 (most) AESTHETICS: Good	SAFETY: 2nd ECONOMICS: Vehicle Repair: 3 Barrier Repair: 1 (least) AESTHETICS: Good

TABLE V.1. EVALUATION OF BARRIERS USING DESIRED BEHAVIOR CHARACTERISTICS.

damage rating scale⁴, estimates of probable injuries from equations presented on Page III.9 ($P = .0204 R^2 \times 100\%$), and examination of the barrier after each test. It is recognized that in these four tests the vehicle weight, speed, and consequently impact force varied considerably between tests. This fact should be kept in mind when tests on barrier systems are compared.

By use of this technique, engineers can obtain a rational (objective and subjective) evaluation of a barrier system using full-scale crash test data.

Before selecting a barrier to protect vehicles from a specific highway hazard, engineers should carefully study each site and consider all feasible and practical alternatives. Protective barriers do not prevent collisions (or accidents). They are intended only to reduce the severity of the collision (or accident).

Every protective barrier system has inherent advantages and disadvantages. For example:

- A. Tension Net or Snagging Barrier such as the "Dragnet". This type device appears to be more suitable for preventing the vehicle from entering the hole in wide medians between twin bridges or overpass structures and possibly falling on traffic below. It appears to be more effective, economical, and aesthetic than a compression type crash cushion, inertia type crash cushion, or extensive length of guardrail. On the other hand, it appears (in its present form) totally unsuitable for protecting vehicles from rigid concrete parapets at elevated exit ramps at freeway interchanges.

- B. Compression Type Energy Absorbing Barrier such as steel drums, Hi-Dro cells, etc. Devices of this type appear to be more suitable for protecting vehicles from rigid concrete parapets at elevated exit ramps at freeway interchanges. With redirection capabilities they are compatible with the adjoining longitudinal bridge rail barrier and will prevent severe collisions at the transition point between the two systems. The rigid backup wall required to counteract the compression force is already existing. There are little or no hazardous elements dislodged and thrown into the travelway.
- C. Momentum Transfer or Inertia Barriers. Devices of this type appear more suitable for protecting vehicles from bridge piers in a relatively wide median and for protecting vehicles from T-mounted or butterfly signs mounted in the gore at exit ramps at ground level. Little or no site modification is required since no backup wall or cable anchorage is required. There is little possibility of flying elements falling into the travelway. Since no longitudinal barrier is necessary, the inertia barrier does not have to have redirection capability or compatible transition to a longitudinal barrier.

There are many other examples which could be cited to illustrate where the basic concept and behavior of a given vehicle impact attenuation system could be most effectively and economically employed. To accomplish this task, highway engineers need to be aware of these fundamental concepts and employ them to maximum advantage in treating any given hazardous location on our highways.

CHAPTER V REFERENCES

1. Hirsch, Teddy J., "Vehicle Impact Attenuation," paper presented at American Society of Civil Engineer's Highway Division Meeting in Phoenix, Arizona, January 11, 1971.
2. Deleys, Norman J. and McHenry, Raymond R., "Highway Guardrails - A Review of Current Practice," NCHRP Report 36, Highway Research Board, 1967.
3. Michie, J. D. and Calcote, L. R., "Location, Selection, and Maintenance of Highway Guardrails and Median Barriers," NCHRP Report 54, Highway Research Board, 1968.
4. Olson, Robert M., Post, Edward R., and McFarland, William F., "Tentative Service Requirements for Bridge Rail Systems," NCHRP Report 86, Highway Research Board, 1970.

APPENDIX A

TEST TRACK AND VEHICLE CONTROL

INTRODUCTION

The Texas A&M Research Annex, located 12 miles from Texas A&M University, is the site of the Highway Safety Research Center and the Proving Grounds of Texas Transportation Institute. The 2000 acre Research Annex is on the site of a former Air Force base and includes large expanses of concrete runways and parking aprons. This research facility is shown in plan view in Figure A.2. The facilities which are located here are numbered and are identified in the legend. Figure A.1. shows an aerial view of the Research Annex.

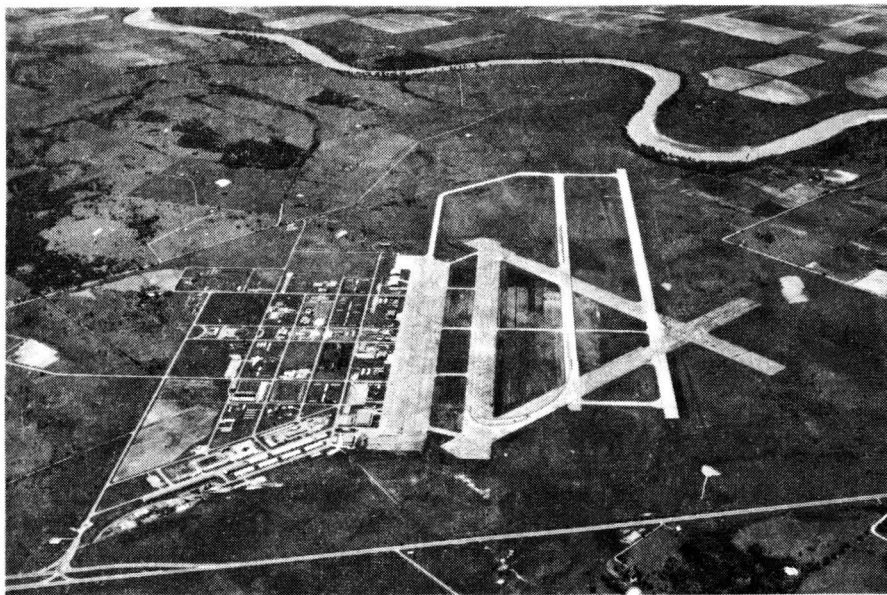
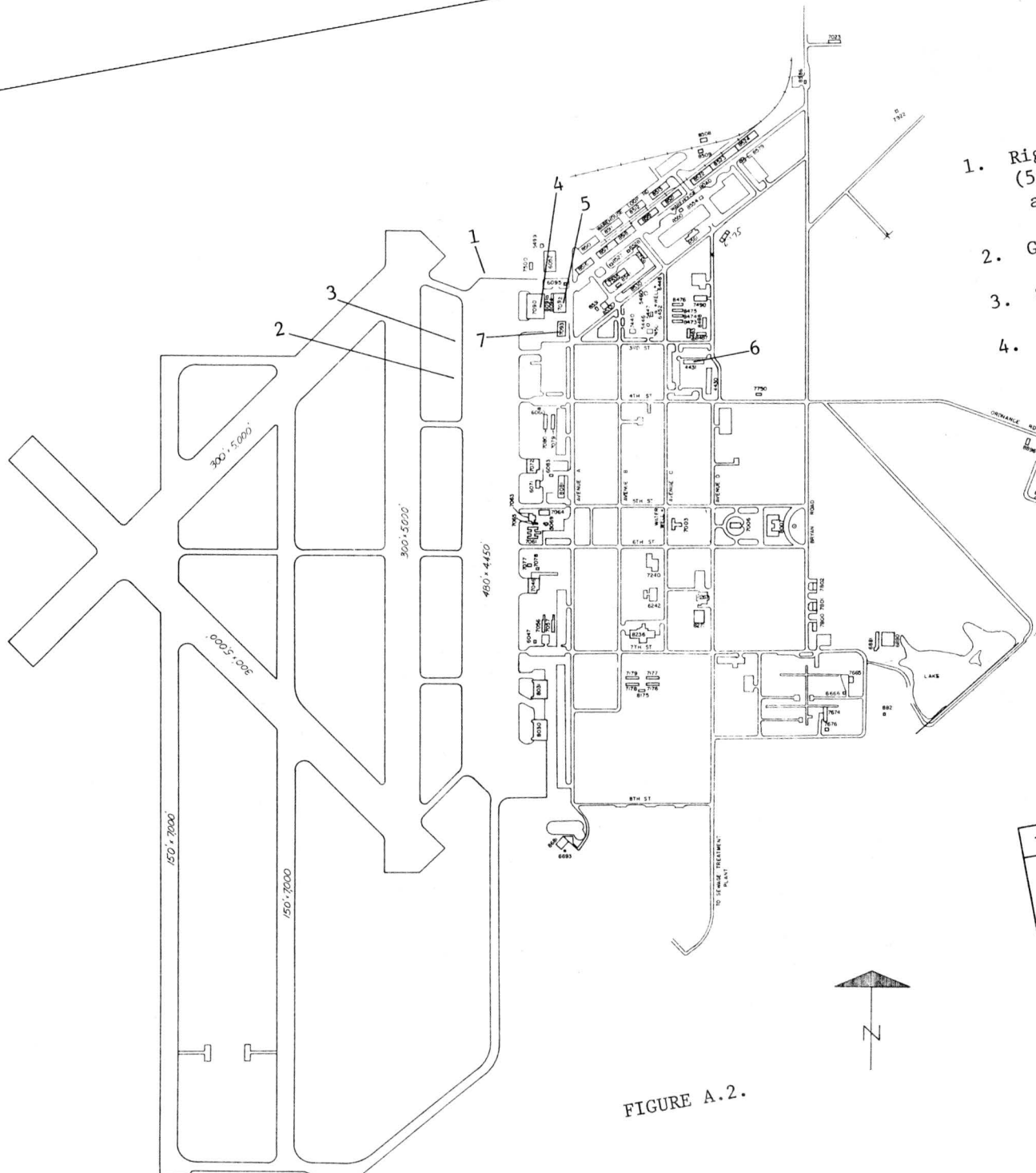


FIGURE A.1. AERIAL VIEW OF RESEARCH ANNEX



- LEGEND**
1. Rigid Wall SAE J 850 (5000 ft acceleration available).
 2. Guardrail Test Area
 3. Simulated Bridge Deck
 4. Engineering & Construction 140 x 200 ft clear structure.

5. Electronic Research Instrumentation & Vehicle Dynamics Research.
6. Research Evaluation & Reporting - Offices of Highway Safety Research Center.
7. Instrumentation Shop

TEXAS A&M UNIVERSITY SYSTEM
RESEARCH ANNEX
 SCALE 1" = 400'
 OCTOBER 1967 DRAWN BY C-13

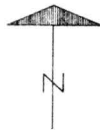


FIGURE A.2.

TESTING FACILITIES

Located on the Proving Grounds, a convenient distance from laboratories, are vehicle crash testing facilities which surround a 5,000 ft by 500 ft concrete apron. These facilities, which are located in Figure A.2., include the following: (1) The rigid concrete wall, 2 ft by 5 ft by 10 ft, exceeds the requirements of SAE J 850. Head-on crash tests have been conducted on this facility with vehicles weighing 3,270 lbs traveling 53 mph, and TTI research engineers are confident that this wall will sustain an impact by a vehicle weighing 6,000 lbs traveling 70 mph. (2) The guardrail test area is immediately adjacent to the concrete apron so that vehicles may be accelerated on the pavement, cross a simulated shoulder area, and impact guardrails supported in soil. (3) Bridge rail test facilities are located north of the guardrail test area. A simulated bridge deck on the edge of the concrete apron was used for installation of bridge rails for tests conducted under this project.

VEHICLE GUIDANCE

Vehicle guidance throughout the testing program was conducted utilizing the TTI cable steering system. This method of guidance permits the placement of the vehicle at the designated impact point within very close tolerances.

This system consists of the four basic hardware components listed below (the first three are locally manufactured):

- A. spindle bolt bracket
- B. steering adjustment plate
- C. shear plate and tube assembly
- D. guidance cable.

The photograph below shows the guidance system attached to a vehicle; the two following drawings identify the above listed components and give component details.



FIGURE A.3. GUIDANCE SYSTEM ATTACHED TO VEHICLE BEFORE TEST

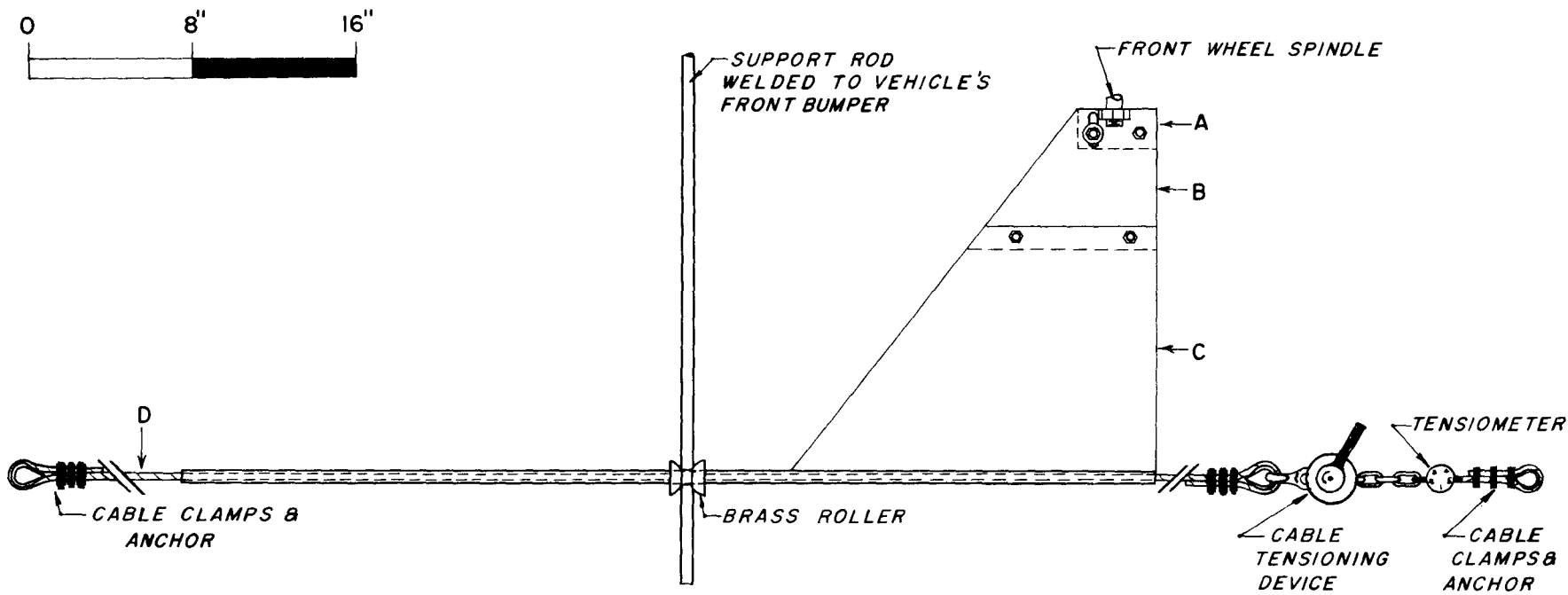


FIGURE A.4. VEHICLE GUIDANCE SYSTEM.

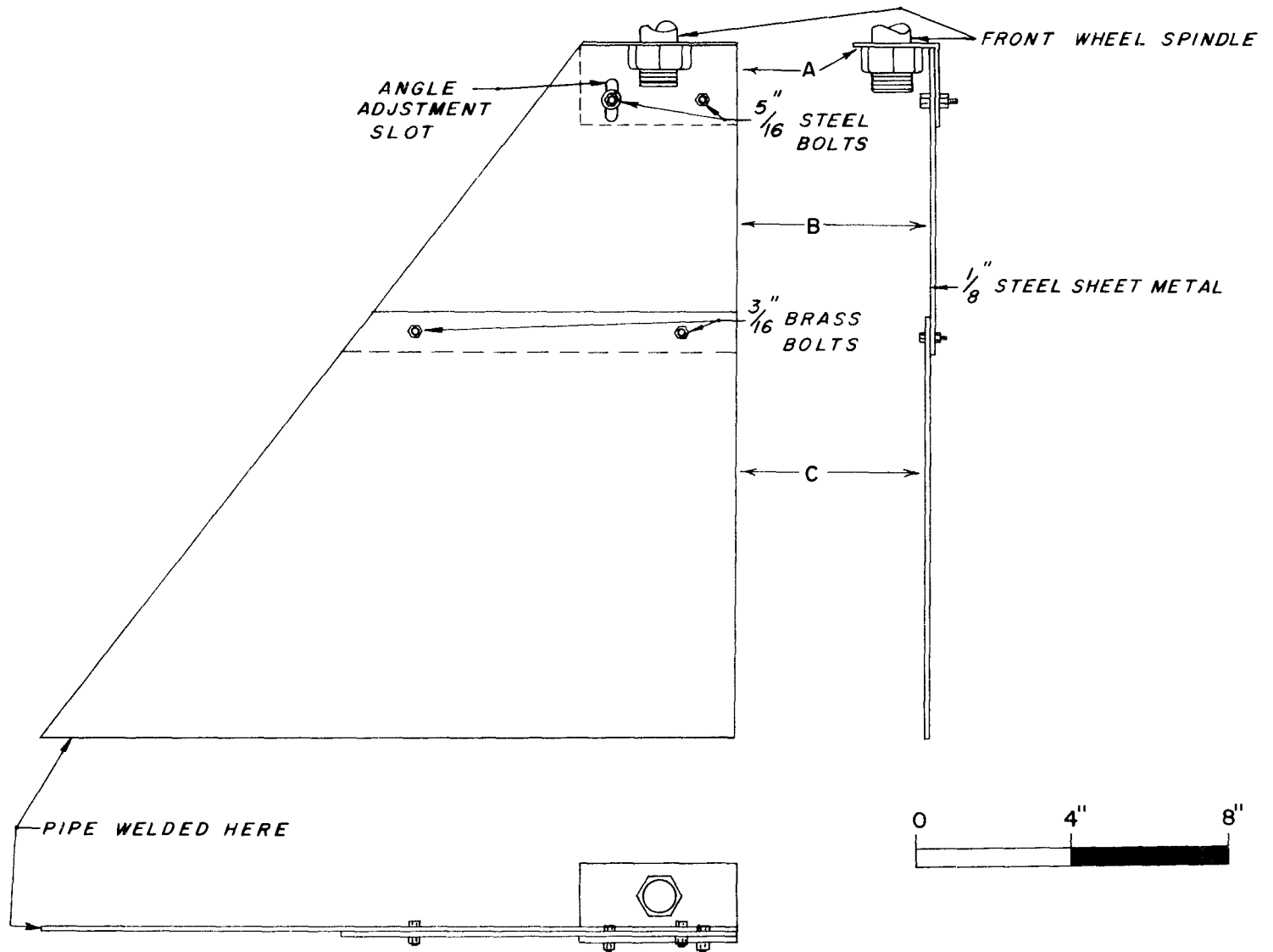


FIGURE A.5. COMPONENTS OF VEHICLE GUIDANCE SYSTEM.

The spindle bolt bracket is attached to the vehicle front axle and tightened in place by the reinstalled spindle nut and bearing washer. Two holes are drilled in the bracket to accommodate the steering adjustment plate. One of the matching holes in the plate is elongated to allow the plate to be adjusted for slight out-of-tolerance tow-in (out) values.

An additional pair of holes at the outer edge of the steering adjustment plate are made to receive two brass shear bolts which hold the shear plate and tube assembly rigidly to the steering adjustment plate.

After being placed at the proper impact angle and anchored at the target end, the guidance cable is inserted through the tube. The loose cable is then also anchored and brought to sufficient tension to eliminate undue transverse motion while the vehicle travels the cable length to the target. Depending on target configuration and impact angle, the target anchor may be placed to shear the plate and tube prior to impact, or leave the guidance systems intact to the point of impact. In either case, the small brass bolts invariably shear when specifically intended to do so.

While the cable guidance appears to be a rather simple mechanical device, the system adjustments are somewhat critical. Since each vehicle-target alignment situation varies, a substantial degree of experience is essential in attaining the desired accuracy of vehicle-target contact.

SPEED CONTROL

Three speed control methods are employed, two for self-powered vehicles and one for vehicles accelerated by external means.

The first method consists of determining the distance required in bringing the vehicle to a predetermined speed at impact under its own power.

On the test date, the vehicle is placed at the proper distance from the target, allowed to accelerate quite rapidly, reaching the target at or near the test speed. This procedure is rather time consuming and permits speed variations of about ± 3 mph.

The supplemental method is to place the vehicle further from the target than required for the desired speed, indirectly controlling vehicle speed through direct control of vehicle ignition. Adjustable speed control within the range of about ± 1.0 mph is typical of this system. Also available in this control method is controlled rate acceleration. This is accomplished with an accelerator drive motor, which is electrically commanded to accelerate the test vehicle. The electrically operated acceleration provides a rather smooth transition to the desired test speed, particularly in vehicles equipped with automatic transmissions.

The third technique uses a recently developed vehicle tow system as shown in Figure A.6.

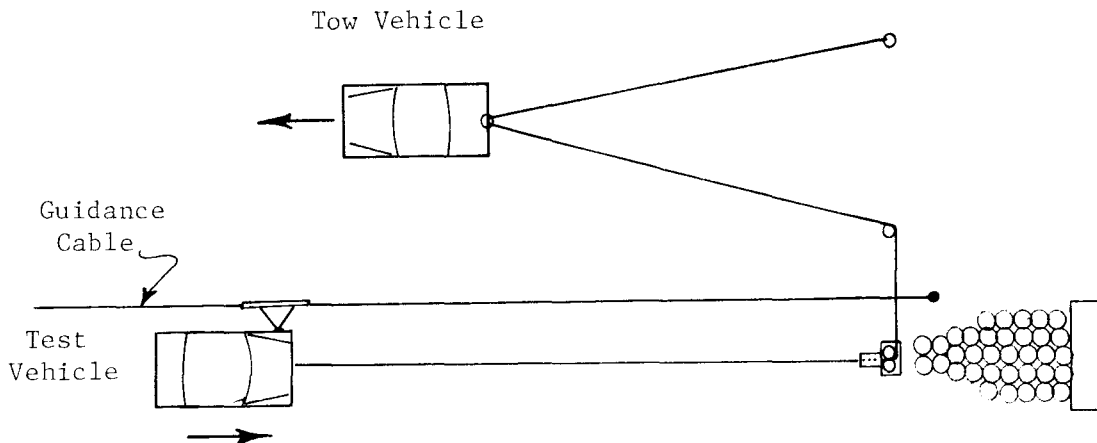


FIGURE A.6. VEHICLE TOW SYSTEM

This system is used exclusively for unpowered vehicles, yet allows very close speed tolerances at the point of impact. The tow vehicle is equipped with a "fifth-wheel" speed readout. The 2 for 1 towing ratio, allowing the towing vehicle to operate in the low-range (high torque) area, accelerates the test vehicle quite rapidly. A Fleetwood Cadillac, obtained specifically as a towing vehicle, performs quite adequately.

APPENDIX B

PHOTOGRAPHIC INSTRUMENTATION

Three types of photographic coverage are usually employed to record vehicle crash tests: (1) still camera coverage before and after the test; (2) documentary movie coverage before, during, and after the test; and (3) high-speed movie coverage during the test. Table B.1. is a summary of the cameras on hand for the above three categories.

The still cameras are used to record preparation techniques, equipment, and the site layout prior to testing; and to document damage and conditions after the test. Color or black and white prints and slides can be obtained.

The documentary motion picture cameras generally record pre-test conditions, the test in progress, and the post-test conditions on color film. The Fairchild gun camera, using 4X negative film, is sometimes mounted inside the test vehicle to record events from that vantage point.

The cameras of Category 3 are used primarily for qualitative and quantitative photographic data acquisition during the test. All but Item 'e' of Category 3 allow timing marks to be placed on the edge of the film in order to accurately determine film speed. Items 'a' and 'c' use 60 cycle AC power to actuate the timing lamps in the cameras. Items 'b' and 'd' have associated timing light generators (Red Lakes Millimite TL6-4) which have been modified to operate from 28 VDC battery packs. This makes the Locam and Photosonics data cameras completely portable.

A variety of lenses can be used with the data cameras, making them quite versatile. For example, if geometry requires that the camera be within a certain range of the event to be recorded, an appropriate lens

<u>Category</u>	<u>Item</u>	<u>Make</u>	<u>Model</u>	<u>Speed Range (frames per second)</u>	<u>Voltage Requirements</u>
1	a.	Bronica	C	---	---
	b.	Nikon	F	---	---
2	a.	Arriflex	16M	0-50	---
	b.	Bolex	H16	12-64	---
	c.	Bell & Howell	70HR	8-64	---
		Kodak	Cine Special	8-64	---
	e.	Fairchild	AN-6	16-64	28 VDC
3	a.	Red Lakes (2 ea)	Hycam K2004E	100-11,000	115-230 VAC
	b.	Red Lakes	Locam 164	16-500	115 VAC (or 28 VDC)
	c.	Fastax	WF3T	150-8,000	115 VAC
	d.	Photosonics	16mm IP	16-500	28 VDC
	e.	Bell & Howell	70 SR	128	115 VAC

will provide the required coverage. On the other hand, if a close-up shot of a violent collision is needed, it is safer to place the camera away from the event and use a "long" lens.

A "clock", driven by a synchronous motor at 1800 rpm, is available as a back-up time reference should the timing lights fail. It is also useful at times in coordinating the films obtained from different cameras.

Special structures have been fabricated for mounting cameras in advantageous positions other than on standard tripods.

The following listing describes a typical motion picture camera layout for recording a vehicle crash test on a redirection barrier:

Camera #1. Hycam rotary prism camera operating at 500 frames per second, located perpendicularly to the centerline of the barrier.

Camera #2. Hycam rotary prism camera operating at 500 frames per second, located parallel to the barrier centerline.

Camera #3. Locam intermittent pin-registered camera operating at 400 frames per second, located perpendicularly to the initial path of the vehicle.

Camera #4. Photosonics intermittent pin-registered camera operating at 400 frames per second, located above the impact area for an overhead view.

Camera #5. Bell and Howell operating at 128 frames per second, mounted on a special structure for obtaining an elevated view along the barrier centerline.

Documentary Cameras. Various panned and stationary views of the test for documentary purposes.

The uses of the above camera views as well as the reasons for choosing the indicated film speeds are discussed in Appendix C.

APPENDIX C

PHOTOGRAPHIC DATA ANALYSIS

POSITION MEASUREMENTS

To make the calculations as simple as possible, it is assumed that two high-speed data cameras are located at right angles to one another, and that the intersection of their centerlines is chosen as the origin of the coordinate system. (In the case of a guardrail test, for example, it is also convenient to orient the coordinate system axes parallel and perpendicular to the guardrail.) The location of the origin is not important as long as the positions of all structures or objects of interest in the chosen coordinate system are known, and all events of interest occur within both cameras' fields of view.

Targets on the roof of the vehicle are convenient tracking points because they are usually visible from both cameras at all times. For the purpose of this discussion, it is assumed that roll or pitch motions of the vehicle are negligible, and that only translation and rotation (or yaw) take place. If a roof target is placed on the vehicle above the center of gravity, and its position in the coordinate system is determined photographically, and position of the vehicle's center of gravity is obtained.

Referring to Figure C.1., it can be seen that

$$\frac{x}{R_1 - y} = \tan\theta_1, \quad \text{or} \quad x = (R_1 - y) \tan\theta_1 \quad (1)$$

and

$$y = (R_2 - x) \tan\theta_2. \quad (2)$$

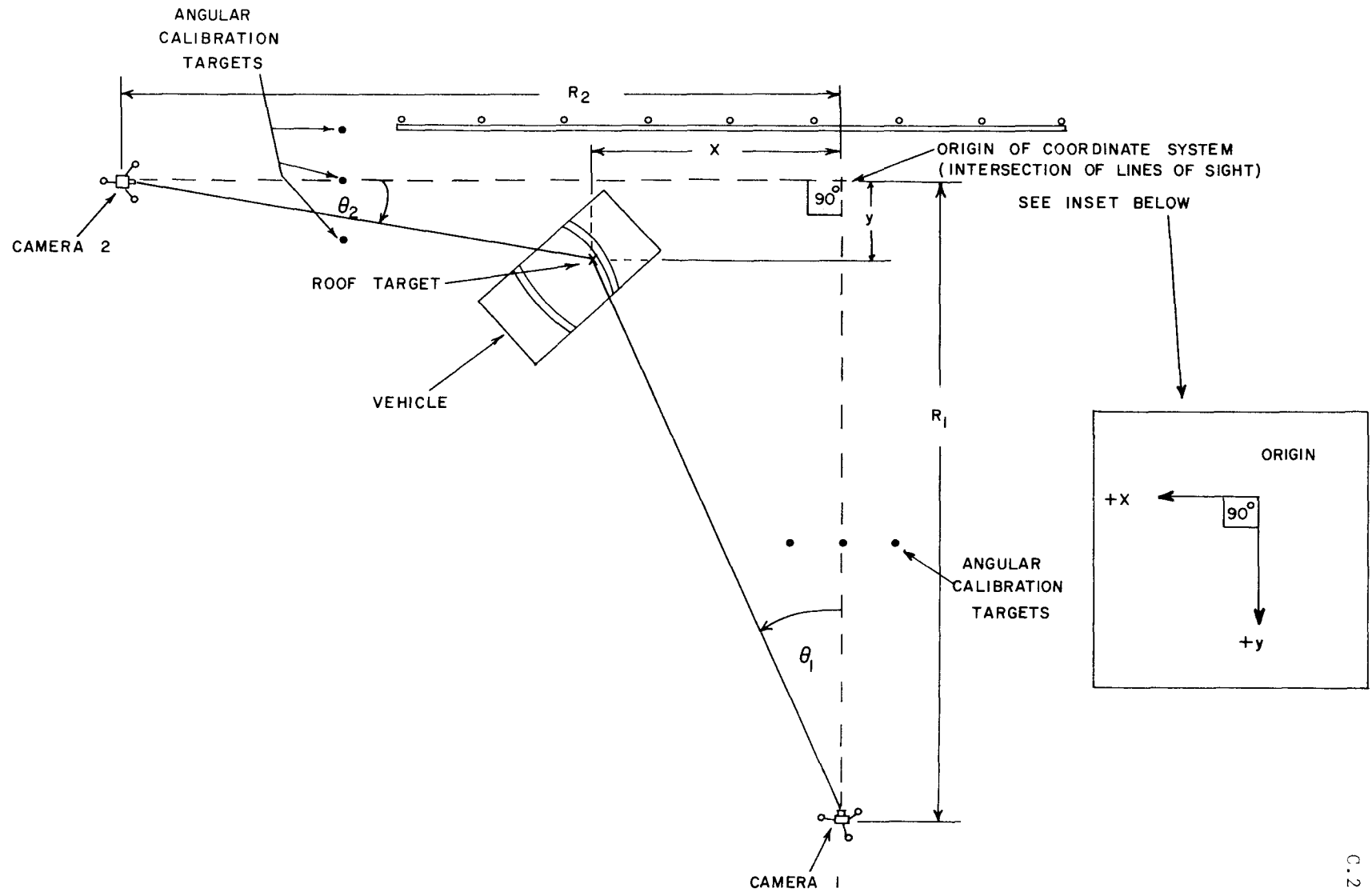


FIGURE C.1.

Substituting Eq. 2 into Eq. 1 yields:

$$x = [R_1 - (R_2 - x) \tan\theta_2] \tan\theta_1. \quad (3)$$

This reduces to

$$x = \frac{R_1 - R_2 \tan\theta_2}{\cot\theta_1 - \tan\theta_2}. \quad (4)$$

Similarly,

$$y = \frac{R_2 - R_1 \tan\theta_1}{\cot\theta_2 - \tan\theta_1}. \quad (5)$$

However, to eliminate some work, x can be solved from Eq. 4 and then substituted into Eq. 2 to get y .

Note that all that is needed to get the x and y coordinates are R_1 , R_2 , $\tan\theta_2$, and $\cot\theta_1$. R_1 and R_2 (constants) are measured beforehand, leaving only $\cot\theta_1$ and $\tan\theta_2$ to be determined. These are determined by a calibration technique.

ANGULAR CALIBRATION OF FILMS

Measurements are made on the high-speed data films by using a film reader or motion analyzer. (see Figure C.2) This device projects the image on a screen equipped with crosshairs whose positions on the screen are read out in dial units (usually thousandths of an inch on the screen). The film can be advanced one frame at a time.

To calibrate for angular measurements, targets or stadia poles are placed within each camera's view at known angular positions from the cameras (see Figure C.3.). The outermost targets are located near the

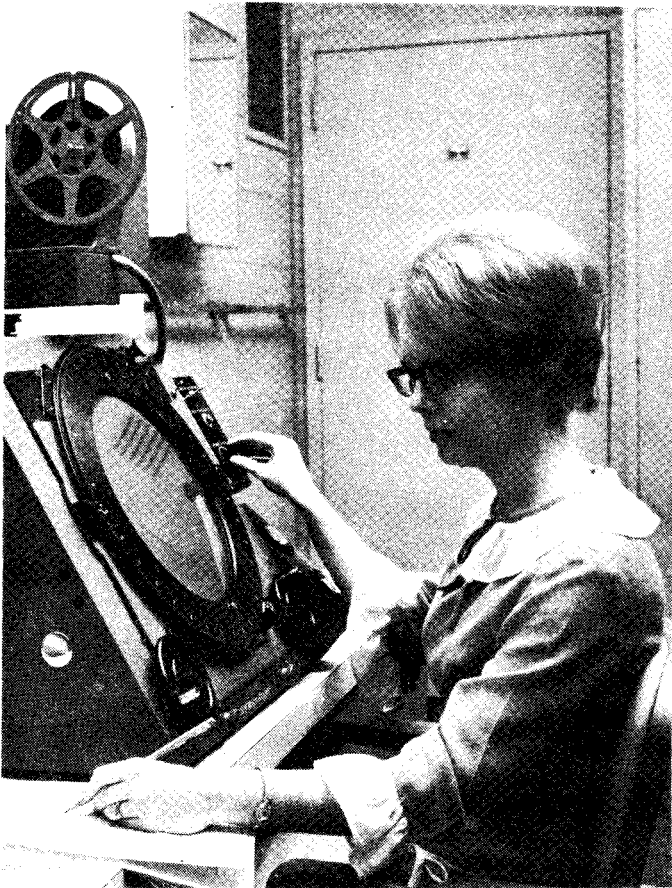


FIGURE C.2. VANGUARD MOTION ANALYZER BEING USED TO REDUCE HIGH-SPEED FILM.

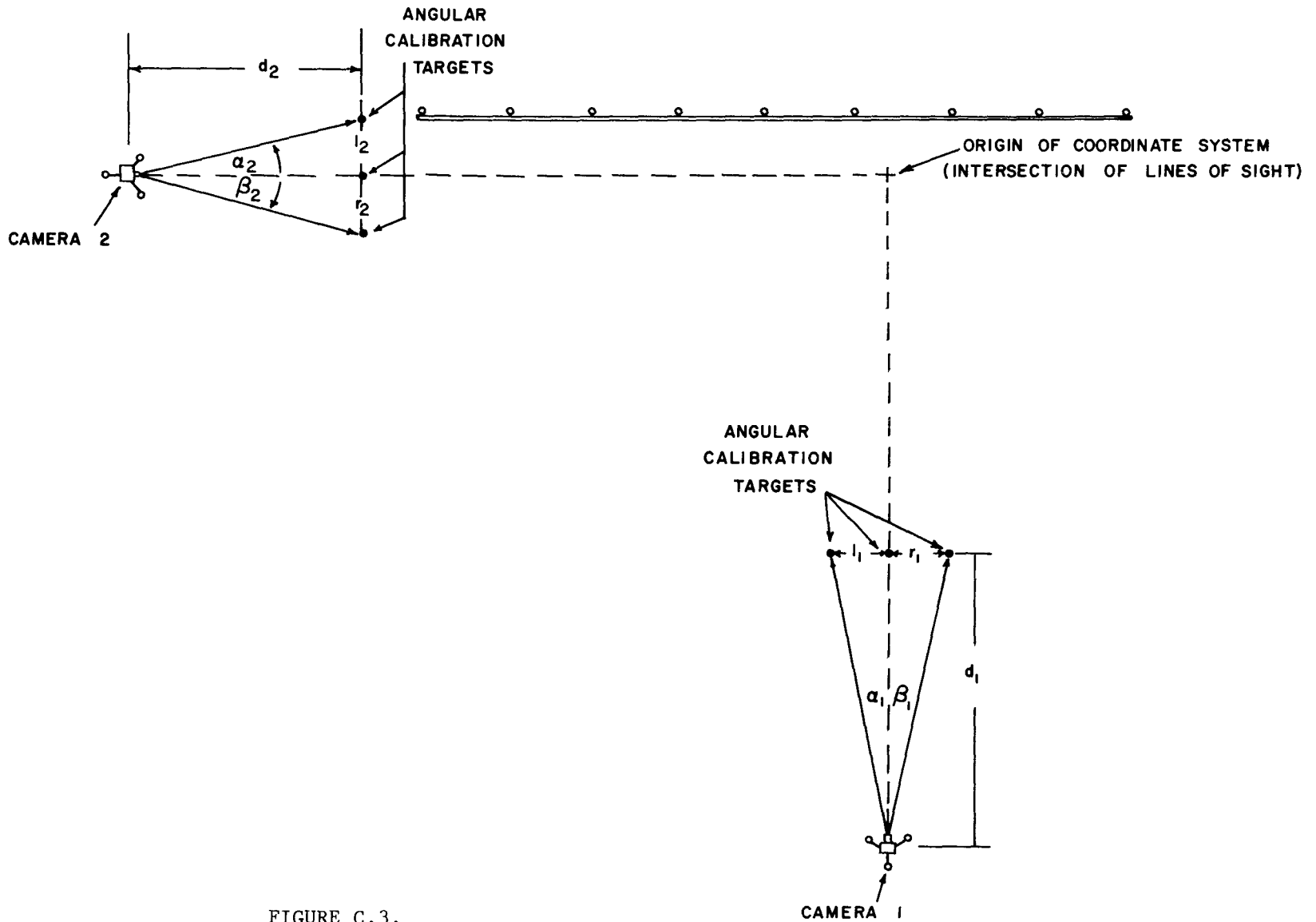


FIGURE C.3.

edges of the field of view. The crosshair displacement reading on the analyzer is proportional to the tangent of the angular displacement over the entire field of view as long as no less than 25mm lenses are used. And since only tangents or cotangents are needed in the formulas for position, the photographic image is calibrated by relating crosshair dial readings to the tangent of the angular position.

Actually, only two targets per camera are needed to calibrate, but three or more are usually used to verify that the dial reading varies linearly with the tangent of the angle. The dial reading on the righthand target of Camera 1 is plotted against $-|r_1/d_1|$ (the tangent of the angle), the dial reading of the center target is plotted at 0, and the dial reading of the left target is plotted at $|l_1/d_1|$. (Note that in this coordinate system the righthand target is at a negative angular orientation from Camera 1.) These points should lie on a straight line. Camera 2 is similarly calibrated, except in Figure C.1 it is seen that angles to the left are negative. A typical angular calibration curve is shown in Figure C.4. Note that the curve is approximated by a straight line through the three calibration points.

The tangent of the angular position of the vehicle target being tracked can now be read from these graphs by noting the dial reading when the crosshair is centered on the target. However, the angular displacement between readings is usually small, so that these tangents must have six decimal places (not necessarily that many significant figures). This is unwieldy to do graphically, so by noting the slope and intercept of the calibration curves (straight lines), formulas for $\tan\theta_1$ and $\tan\theta_2$ can be obtained requiring only dial readings of positions to be entered. As can be seen, it is better to determine $\tan\theta_1$ and then invert it to get $\cot\theta_1$, because $\cot\theta_1$ approaches ∞ as θ_1 approaches 0, and graphical methods are used to determine the corresponding functions at the same elapsed times.

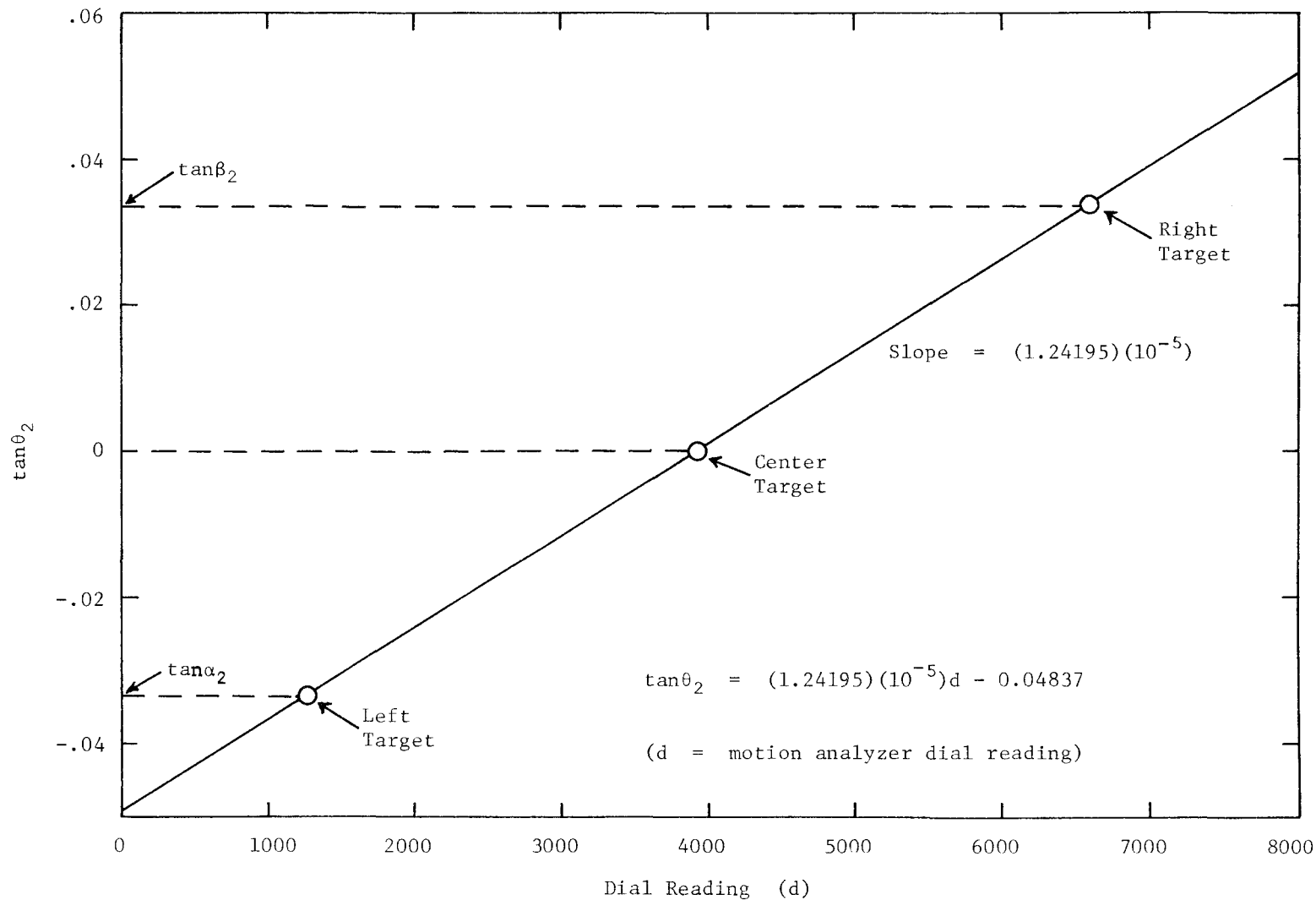


FIGURE C.4. TYPICAL ANGULAR CALIBRATION CURVE FOR CAMERA 2.

TIME RELATIONSHIPS

Timing marks are included on the edges of the high-speed films. Using these, the elapsed time between any two frames on the film can be determined. By noting the elapsed frames from some reference frame, elapsed time between any two readings can be determined.

It is difficult to obtain exactly matched film speeds on two different cameras. Although both may record a frame at the same time at one point, they will be out of time synchronization later. Therefore, it is convenient to plot $\tan\theta_1$ and $\tan\theta_2$ against time. Then, at any chosen time, $\tan\theta_1$ and $\tan\theta_2$ can be determined from this plot. Inverting $\tan\theta_1$ to get $\cot\theta_1$ at the chosen time gives all the information needed to determine the target position at that time. It is sometimes convenient to calculate position at equal time intervals throughout the event.

An alternative to the time-tangent plots is to take readings from each camera at times as nearly equal as possible for purposes of position calculation. If both cameras are running in the neighborhood of 500 frames per second, for example, the greatest discrepancy between the times of any set of readings from the two cameras would be of the order of one millisecond, which is probably within the error of the system.

It has been found that 500 frames per second is an optimum film speed for obtaining clarity and resolution under normal lighting conditions, while maintaining adequate frequency of image for vehicle crash tests. A vehicle traveling at 60 mph would move about 2 in. between film frames. However, when the Locam and Photosonics cameras described in the section on photographic instrumentation are used, they are set at 400 frames per second to avoid operating them at their ultimate limits of 500 frames per second.

INFORMATION FROM TIME-COORDINATE DATA

Average speed over each time interval can be calculated from the coordinates of position with time. If the position at one point is (x_1, y_1) , at another point is (x_2, y_2) , and the elapsed time is Δt , the average speed between these two points is:

$$\bar{v} = \frac{\sqrt{|x_1 - x_2|^2 + |y_1 - y_2|^2}}{\Delta t} . \quad (6)$$

Actually, the average velocity can be obtained because the coordinates of position with time also specify direction of motion. The x and y components of velocity can also be determined from the position-time record.

An approximation of acceleration versus time is obtained by first plotting average speed over each small interval against time (at the mid-point of the interval) and then "differentiating" this curve piecewise. However, these successive differentiations amplify the data "noise" level considerably.

To determine orientation of the vehicle at each reading, two targets are needed on the vehicle (Targets 2 and 3 in Figure C.5). If the targets are located along the vehicle centerline, and position coordinates are determined for each one at every time interval, the vehicle's orientation can be determined at these time intervals from the following relationship:

$$\phi = \tan^{-1} \left(\frac{y_3 - y_2}{x_3 - x_2} \right) , \quad (7)$$

where (x_2, y_2) are the coordinates of the front target, (x_3, y_3) the coordinates of the rear target, and ϕ is the angle the centerline makes with the x axis. Again, graphical differentiation produces approximations of angular velocity and angular acceleration with time.

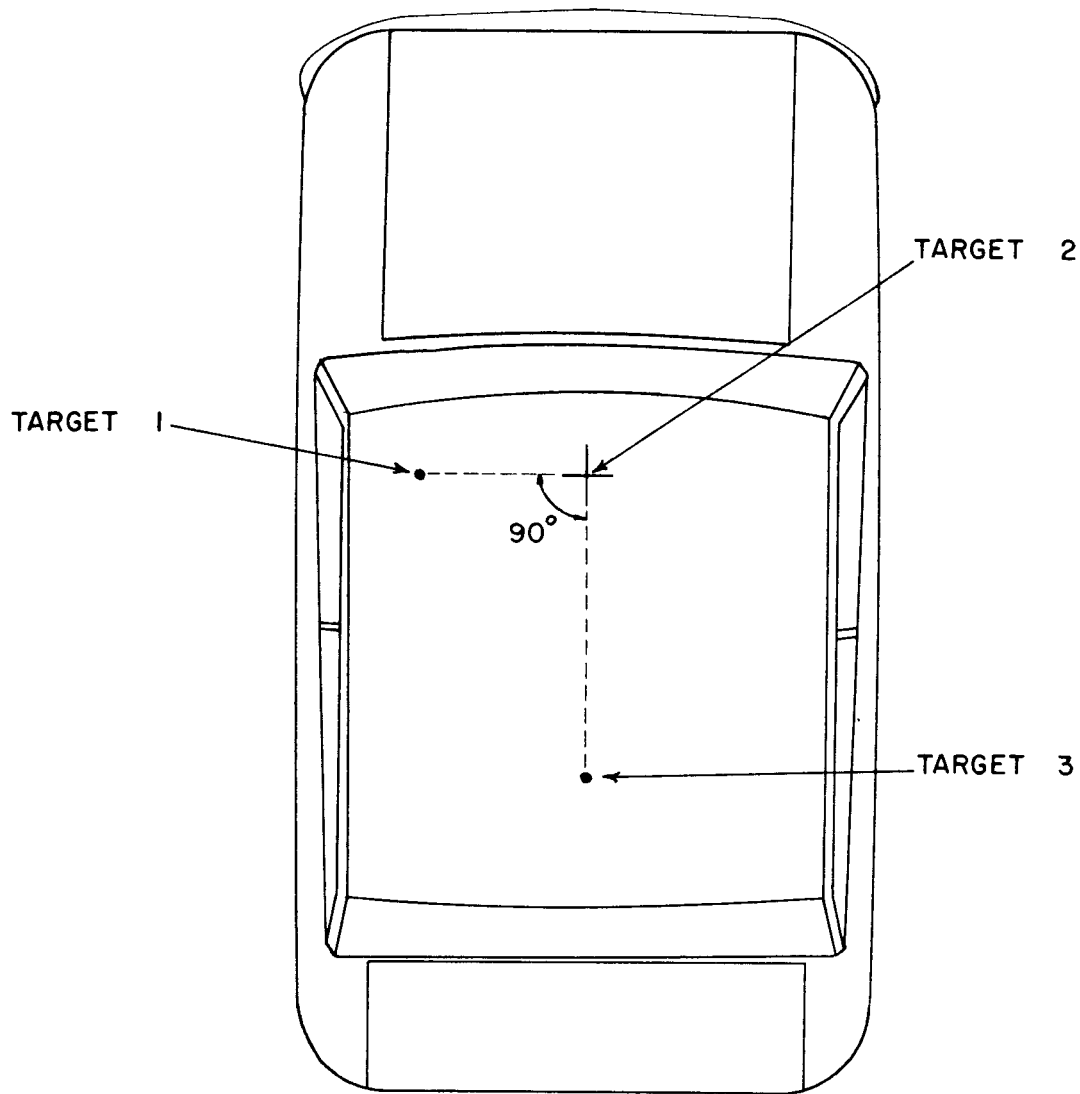


FIGURE C. 5.

OTHER SPEED AND ORIENTATION MEASUREMENTS

To get an accurate measurement of initial speed, it is advisable to use a third high-speed camera, Camera 3. This camera can provide a close-up shot of the impact area, and is, optimally, located perpendicularly to the initial vehicle path. A stadia board on the side of the vehicle provides a displacement reference. Displacement measurements can normally be made to better than an inch of position. Speed can similarly be determined from the triangulation camera perpendicular to the rail (Camera 2). As long as the motion is in the plane of the displacement calibrator (stadia board), the angular orientation need not be compensated for. Therefore, using three cameras, speed can be measured near impact with Camera 3, and throughout with Camera 1 or the combination of Cameras 1 and 2.

The angular vehicle orientation can also be calculated by a secondary method involving only the camera parallel to the x axis. This method requires the use of a third roof target (Target #1) as shown in Figure C.5. The targets are located at right angles so that all three will never appear to be in line from any one camera.

The apparent separations of Targets 1, 2, and 3 as viewed on the film depend on the angular orientation of the vehicle in the coordinate system, the angular position of the vehicle relative to the data camera, and the distance to the vehicle from the data camera. The apparent separation can be measured on the motion analyzer, and the angular position from the camera is determined in the course of the triangulation procedure. The effect of distance from the camera can be eliminated by using a ratio technique.

The roof target images can be projected on a plane containing Target 2 as shown in Figure C.6. The differences in motion analyzer dial readings on the targets are proportional to the apparent distances themselves if there is negligible distortion in the lenses (not less than 25mm lenses). Let d_1 , d_2 , and d_3 be the dial readings on Targets 1, 2, and 3, respectively. If the constant of proportionality is c , then from Figure C.6.:

$$c (d_2 - d_1) = p (\cos\phi - \sin\phi \tan\theta_{21}) \quad (8)$$

and

$$c (d_3 - d_2) = q (\sin\phi + \cos\phi \tan\theta_{23}). \quad (9)$$

Taking the ratio of Eq. 9 to Eq. 8 eliminates c :

$$\left(\frac{d_3 - d_2}{d_2 - d_1} \right) = \frac{q}{p} \frac{(\sin\phi + \cos\phi \tan\theta_{23})}{(\cos\phi - \sin\phi \tan\theta_{21})}. \quad (10)$$

Let

$$\left(\frac{d_3 - d_2}{d_2 - d_1} \right) = D, \quad \text{and} \quad \frac{q}{p} = P.$$

Then,

$$PD (\cos\phi - \sin\phi \tan\theta_{21}) = (\sin\phi + \cos\phi \tan\theta_{23}) \quad (11)$$

or

$$\cos\phi (PD - \tan\theta_{23}) - \sin\phi (PD \tan\theta_{21} + 1) = 0.$$

Dividing by $\cos\phi$ and solving gives,

$$\tan\phi = \frac{(PD - \tan\theta_{23})}{(PD \tan\theta_{21} + 1)}. \quad (12)$$

Therefore, angular orientation of the vehicle in the system is,

$$\phi = \tan^{-1} \left(\frac{PD - \tan\theta_{23}}{PD \tan\theta_{21} + 1} \right). \quad (13)$$

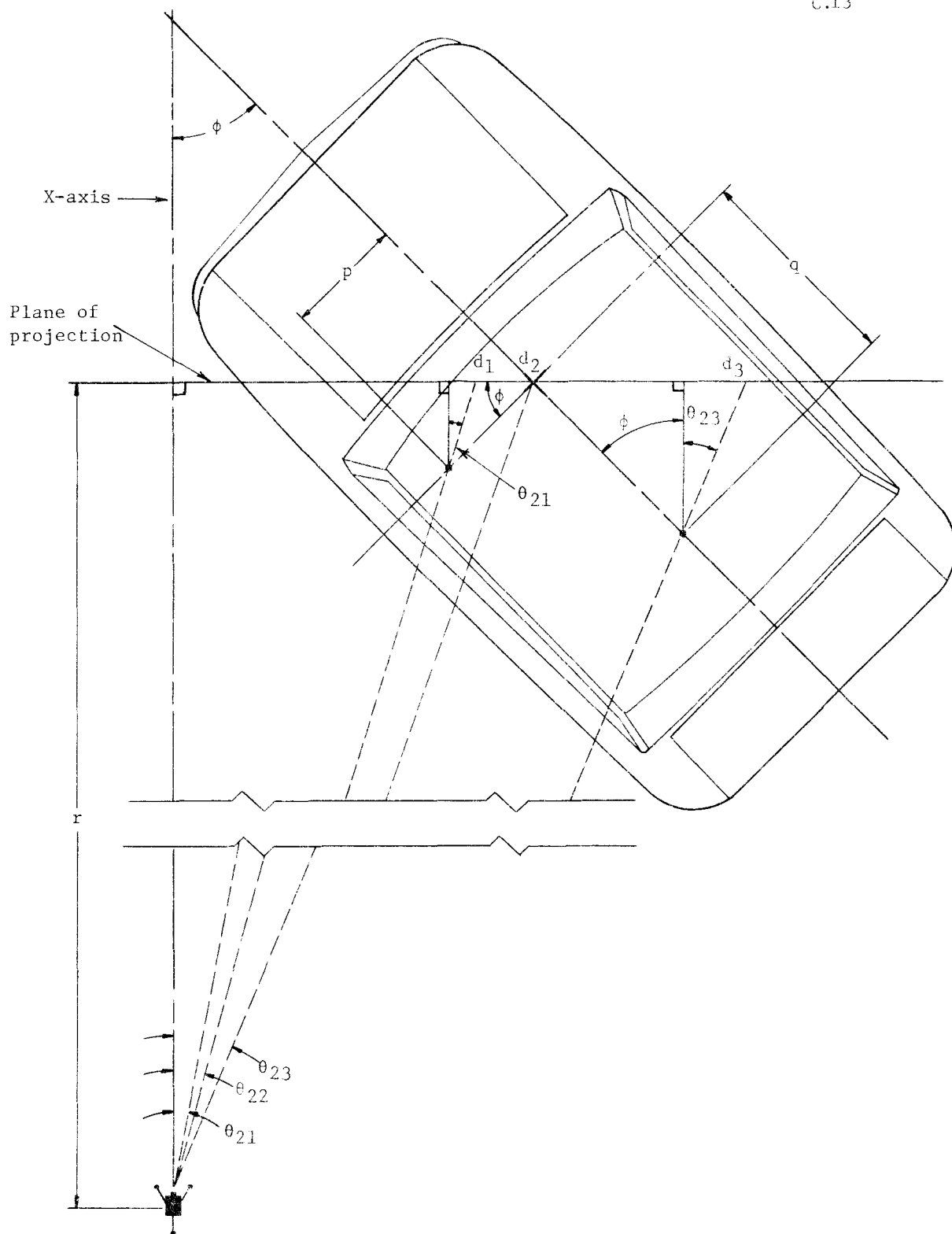


FIGURE C.6.

It can be seen that D can be determined from the dial readings at each time, P is a constant determined beforehand (distance between Targets 1 and 2, divided by distance between Targets 2 and 3), and θ_{21} and θ_{23} can be determined from the angular calibration of Camera 2. Therefore, ϕ can be determined with time from Camera 2 alone.

Again, incremental angular velocity and acceleration can be approximated from successive "differentiations" of the time-orientation curve.

One note of caution is in order. If the vehicle is in such a position that Targets 1 and 2 appear to be in line from Camera 2, $(d_2 - d_1)$ goes to zero and D becomes undefined; it can be seen, of course, that in this case $\phi = 90^\circ - \theta_{21} = 90^\circ - \theta_{22}$. However, to investigate the motion in this area, Eq. 12 is divided by D . That is,

$$\phi = \tan^{-1} \left(\frac{P - \frac{\tan\theta_{23}}{D}}{P \tan\theta_{21} + \frac{1}{D}} \right). \quad (14)$$

Then if $D \rightarrow \infty$,

$$\phi \rightarrow \tan^{-1} \left(\frac{1}{\tan\theta_{21}} \right) = \tan^{-1} (\cot\theta_{21})$$

This technique can similarly be used, with modifications, utilizing Camera 1 instead of Camera 2.

AN ADDITIONAL TIME-POSITION TECHNIQUE

The position of the vehicle in the x-y coordinate system can also be determined from Camera 2 (or 1) alone, though not to the accuracy of the triangulation method.

Referring to Figure C.6., the apparent distance between Targets 1 and 2 on the plane of projection, which is perpendicular to the x axis, is $p(\cos\phi - \sin\phi \tan\theta_{21})$. The distance from the x axis to the apparent position of Target 1 is $r \tan\theta_{21}$, and the distance from the x axis to the position of Target 2 (on the plane of projection) is $r \tan\theta_{22}$. Therefore,

$$p(\cos\phi - \sin\phi \tan\theta_{21}) = r(\tan\theta_{22} - \tan\theta_{21}) \quad (15)$$

or

$$r = \left[\frac{\cos\phi - \sin\phi \tan\theta_{21}}{\tan\theta_{22} - \tan\theta_{21}} \right].$$

The x coordinate of Target 2 (see Figure C.1.) is

$$x = R_2 - r = R_2 - \left[\frac{\cos\phi - \sin\phi \tan\theta_{21}}{\tan\theta_{22} - \tan\theta_{21}} \right], \quad (16)$$

and the y coordinate is

$$y = r \tan\theta_{22} = \tan\theta_{22} \left[\frac{\cos\phi - \sin\phi \tan\theta_{21}}{\tan\theta_{22} - \tan\theta_{21}} \right]. \quad (17)$$

As shown in the preceding discussion, ϕ can be determined from Camera 2 alone; $\tan\theta_{21}$ and $\tan\theta_{22}$ can be determined from Camera 2 alone; and R_2 is a measurable constant. Therefore, x and y coordinates in the system can be determined by using Camera 2 solely.

A comparable technique can be used with the data from Camera 1 alone. It should be noted that the accuracy of this method depends in part on the apparent separation of the targets. Therefore, it is advisable to use the two targets of greatest apparent separation. Similar formulas can be derived using any pair of targets.

CONCLUSIONS

It should be noted that by using three cameras, there is always at least a secondary technique available whereby time-position or time-orientation can be measured. For the initial motion up to the impact point, three separate techniques are available, although not of equal accuracy of precision. However, all the measurements that need to be made can be obtained even if any one camera fails, and can be obtained even if Cameras 1 and 3 or 2 and 3 fail. Therefore, the much desired redundancy is built into the photographic data acquisition system.

Some of the calculations of the previous techniques are rather tedious and time consuming, though not necessarily prohibitively so, if done "manually" on a desk calculator. It is obvious that these calculations can be made on a computer with a relatively simple program and, in fact, such a program has been developed. The computerization reduces the errors that are sometimes made when doing the calculations manually.

ELECTRONIC INSTRUMENTATION

CARRIER SYSTEM

Use of the "hard-line" carrier system for sensor excitation requires the excitation source and the resultant crash data to be fed through a cable of considerable length. While this method of data acquisition presents no particular problems in systems calibration, reel handling, cable placement and post-test equipment handling, the data playback are time-consuming operations. The TTI system utilizes Honeywell (5 kHz) carriers and demodulators. A block diagram of a typical carrier system is given in Figure D.1.

As in all data acquisition systems, periodic equipment checks and accelerometer calibrations were conducted to validate data playback. Recorder subcarriers were maintained well within manufacturer's tolerances. Accelerometers used for this testing program were periodically checked against factory calibrated units maintained for the sole purpose and use as secondary standards. All data is reported (corrected) to these standards.

TELEMETRY

Recognizing the need for greater data handling and reduction capabilities, TTI has made a substantial investment in state-of-the-art telemetry data acquisition. The system selected is an Inter-Range Instrumentation Group (IRIG) Standard proportional bandwidth system, utilizing IRIG channels 8 through 15. In contrast to the "hard-line" system, the telemetry transmitter, 8 subcarrier oscillators, in-flight calibrator, base unit, and mixer weigh approximately 7 lbs.

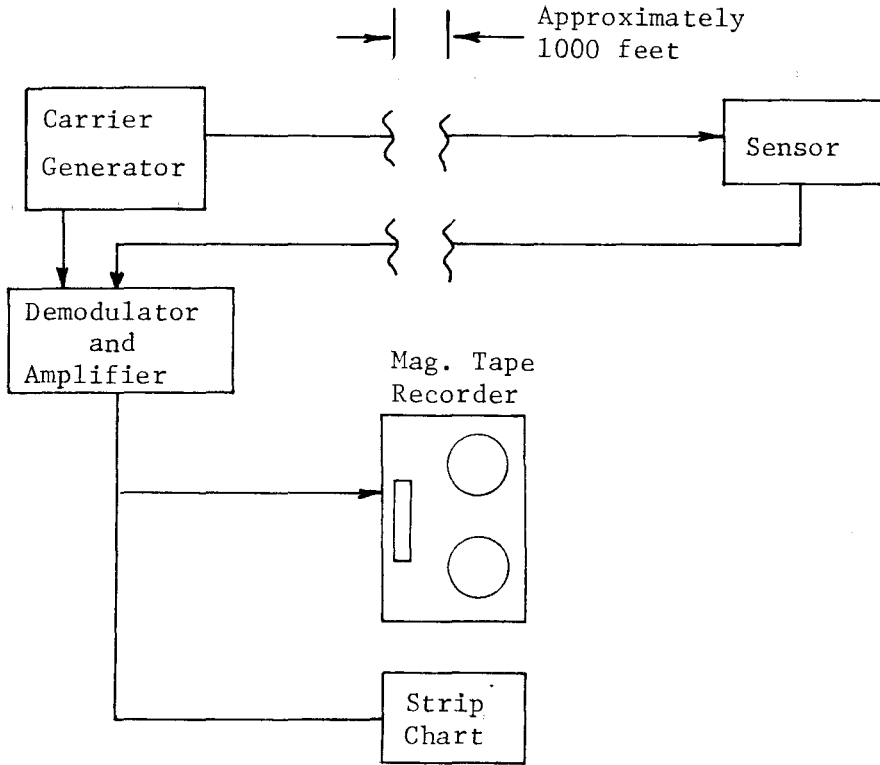


FIGURE D.1. TYPICAL CARRIER SYSTEM
BLOCK DIAGRAM

The sensors used in telemetering are the same as those used in the "hard-line" system, except that the previously used piezoelectric lateral force measurement units have been replaced with bonded gage accelerometers. Each accelerometer is individually range calibrated through a matched signal conditioner. These units provide the advantage of (long term) acceleration measurements over the entire test profile.

The telemetering ground station is located in the Instrumentation Lab at TTI's Research Annex. For testing anywhere on the airfield, the equipment remains stationary. However, the system is constructed to be used (except for real-time readout) as a completely self-contained portable data link, even in areas where commercial power is not available. In the portable configuration, acquisition range is limited; but in reasonably flat terrain, data acquisition range should be 6 to 10 miles utilizing vehicle-to-vehicle ground plane antennae. During fixed station operations, signals are received through a 60° corner reflector, vertically polarized. Signals are preamplified prior to transmission to the ground station.

Although the TTI data system is constructed and tailored primarily to vehicle crash testing, substantial flexibility has been built into data patching, playback, and filtering to accommodate almost any vehicle measurement capable of being instrumented, including aircraft.

Expansions of capability in progress include real-time filtering, utilization of tuned active electronic units, and recording of composite receiver-video data for storage on magnetic tape. This recording method not only reduces data storage expense, but (a) maintains all data in precisely the same time frame and (b) retains all data and calibrations

in the original IRIG frequency format. The distinct advantage of retaining the format permits data playback and reduction at any other IRIG Standards ground station.

Use of the TTI telemetry acquisition system has substantially simplified collection of vehicle test data and reduced costs of data acquisition.

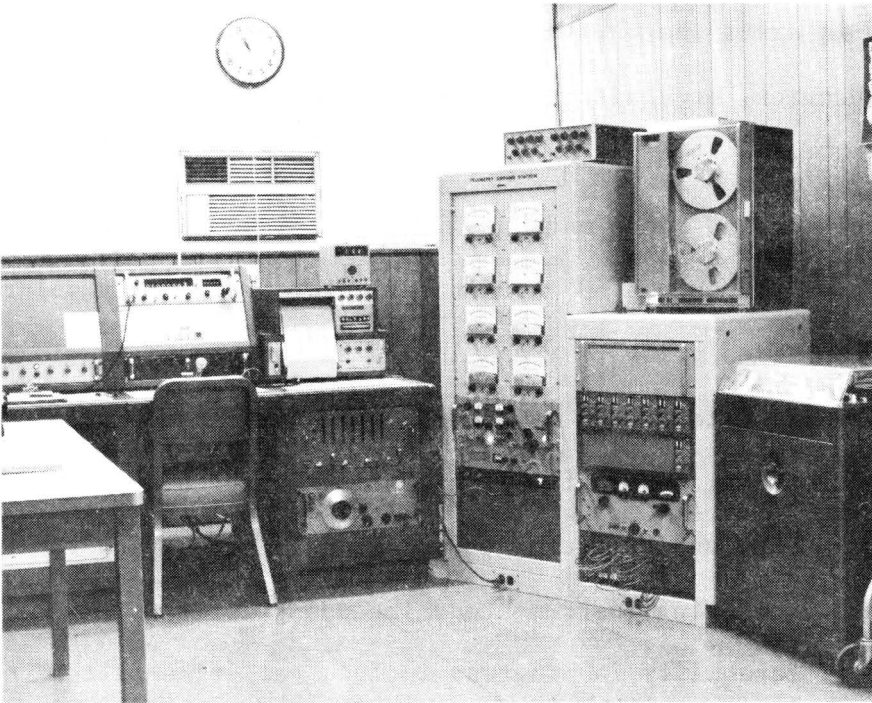


FIGURE D.2. TELEMETERING GROUND STATION

TRANSDUCERS

The primary acceleration sensing devices are Statham strain-gage-type accelerometers. These devices consist of sealed units containing members to which strain gages are bonded. The gaged member experiences strains due to accelerations (or decelerations), and the resultant strain-gage outputs are calibrated by the factory in units of gravitational acceleration (g's). One such calibrated unit is used as a secondary standard with which to check the calibration of the test instruments. The secondary standard is not used in crash testing. Stathams with ± 50 g or ± 100 g ranges are used in crash tests.

Before the telemetered data acquisition system was in operation, piezoelectric accelerometers made by the C.E.C. Corporation were sometimes used. Each C.E.C. accelerometer requires only two electrical conductors, while the Statham requires four. Using a "hard-wired" data acquisition system, it was sometimes necessary to use the piezoelectric devices, due to limitations in the number of conductors available in the lead-out cable which was pulled by the test vehicle. Although the C.E.C. accelerometers are good for measuring constantly changing acceleration rates, they are not considered as suitable as the Stathams for measuring the acceleration waveforms which result from most crash tests. The C.E.C. accelerometers have ± 200 g ranges.

A device called an Impact-O-Graph is usually used as a secondary source of acceleration information. It is self-contained and requires no outside electrical connections. This device has a roll of chart paper on which rest three spring loaded styli connected to weights. The chart

paper is driven by a battery-powered motor. The weights are connected to the styli through pivots that allow each weight to respond to accelerations 90 degrees to the other two weights. In this way, triaxial acceleration data is obtained. Each axis can be set to record maximum accelerations of from ± 15 to ± 50 g's. Being primarily a mechanical device, the Impact-0-Graph has inherent drawbacks in response time, damping, and overshoot. However, it usually compares reasonably well with the electronic devices. It is economical to operate and easy to install.

In most crash tests an anthropometric dummy is secured in the driver's seat with a lap belt. This lap belt is fastened to one end of a load cell. The other end of the load cell is secured to the vehicle frame with a chain. This load cell, used for measuring lap belt force, consists of a piece of steel with bonded strain gages. The measured strains are calibrated in terms of pounds of force required to produce them. The load cell used at the beginning of this project was a flat bar of steel with attached strain gages. An improved version now in use is a cylindrical, 3/4-in. diameter bar with threaded holes in each end for attaching eye-bolts. The bar is necked down to 3/8 in. in the center, and the strain gages are bonded at this point.

The capability of installing, calibrating, and recording the outputs of various other transducers exists. These transducers might be linear potentiometers for measuring steering angle, tach-generators for measuring wheel speed, a gyroscopic system for measuring yaw angle, or any other device used in vehicle testing.

APPENDIX E

ELECTRONIC DATA ANALYSIS

Electronic or electromechanical data from vehicle crash tests is normally in the form of accelerometer traces on Visicorder paper. The accelerometers are usually attached to frame members of the test vehicles, and the analog output of acceleration vs. time normally contains many vibrational frequencies that make analysis of the traces difficult. At this time, the raw data is filtered, before analysis, through an 80 Hz low-pass active filter. This particular frequency was picked partly because of the availability of such a filter of high quality, but mainly due to the considerations which follow.

CHOOSING A FILTER FREQUENCY

Figure E.1 is a reproduction of the trace produced by striking the front bumper of an instrumented car with an ordinary claw hammer. The unfiltered trace is an envelope of "hash". (It should be pointed out that "unfiltered" actually means about 10^3 Hz max, since the galvos will not respond to higher frequencies.) A 100 Hz low-pass filter takes out most of this vibration.

Figure E.2 is the unfiltered trace from a long-duration guardrail crash. If this trace were interpreted literally, then the maximum deceleration is negative, or an acceleration. So it is evident that the unfiltered trace should not be used to get maximum deceleration. The static "hammer" test in Figure E.1 shows a maximum acceleration of about

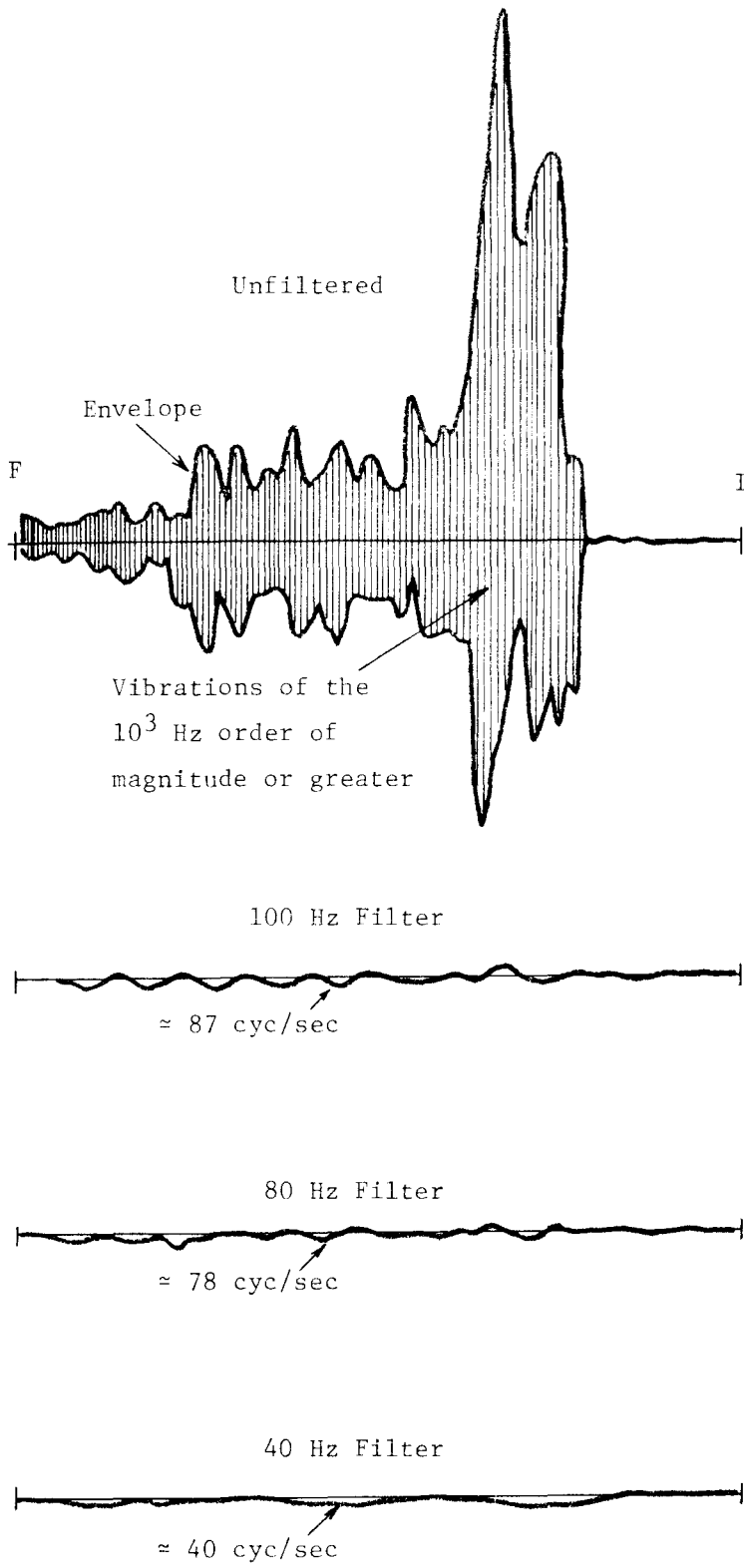


FIGURE E.1.

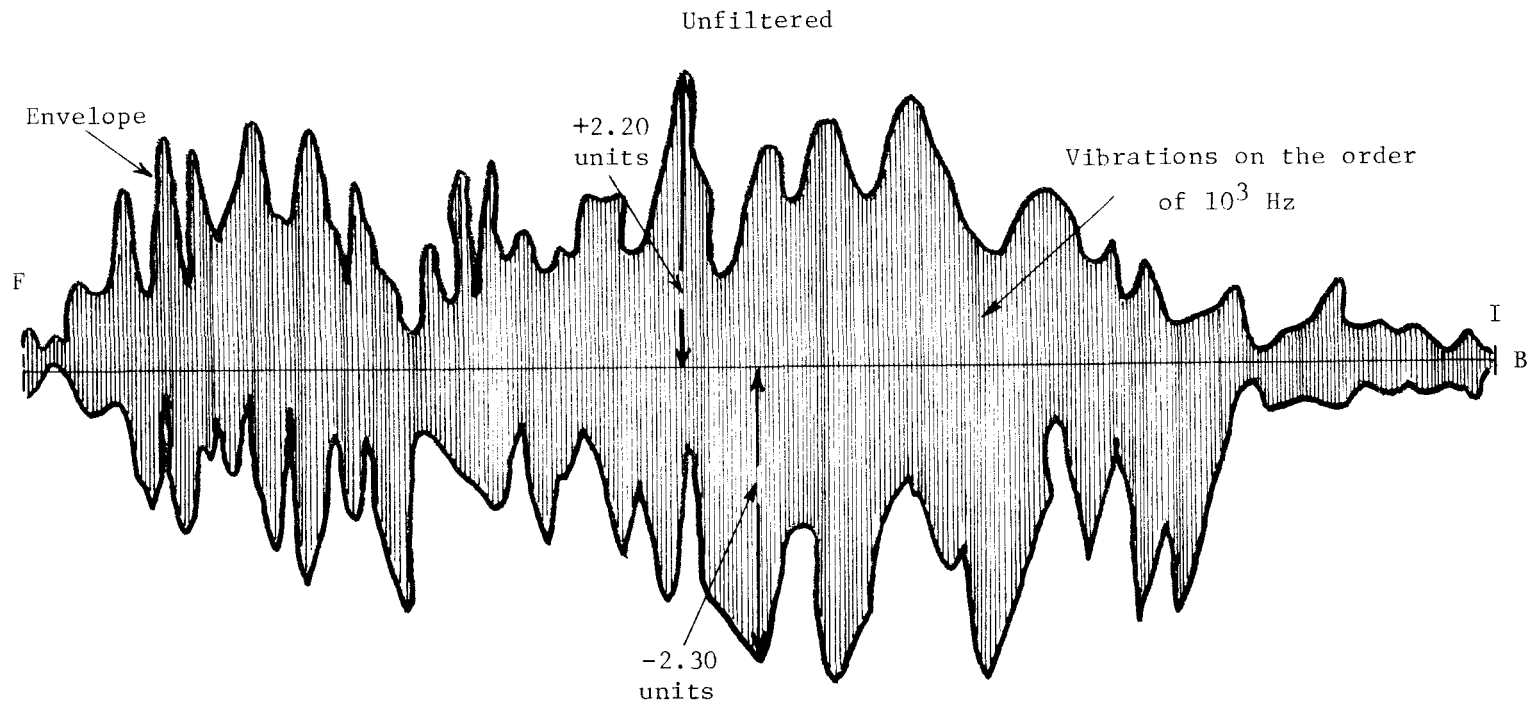


FIGURE E.2.

30 g's! Surely this is not relevant to vehicle behavior in a macroscopic sense. For one thing, it is known that the vehicle as a whole is not accelerating and decelerating repeatedly as it goes through a crash with no power.

Figure E.3 is the trace in Figure E.2 after passing through various low-pass filters. Note that the major peaks not only change height, but also change positions. The symbol I is the impact point, and F indicates the arbitrary endpoint. B is the baseline, or zero g level, while B' is an arbitrary baseline that stays below the data trace.

For these traces, the area under the curve to B' does not change with filtration. In other words, the average deceleration is not altered by filtering over the indicated range if all the trace is considered as positive. This suggests that peaks which are mostly vibrational in nature are being filtered out, since the areas filtered out lie as much above as below the resultant. It should be noted that as less filtration is used, the enhanced peaks start to take on a more regular periodic nature.

Figure E.4 is a series of traces from a short-duration overhead sign bridge impact. Note that obviously "real" peaks are lost between the 80 and 40 Hz filter. The FHWA has recommended that a trapezoidal pulse of 12 g's average and 500 g's per second onset rate be the guideline for acceptable accelerations in barrier crash tests.^{1*} On the 80 Hz filtered trace of Figure E.4, a line representing a 500 g per second onset rate has been drawn. It is seen that with 80 Hz filtering even greater onset rates are recorded, so this filtering would not obscure that rise time.

*Superscript numerals refer to corresponding numbers in the References at the end of this appendix.

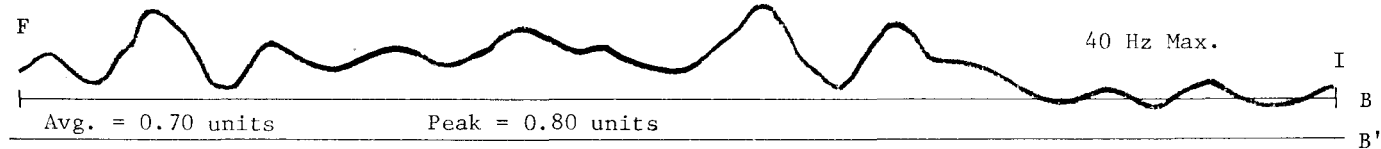
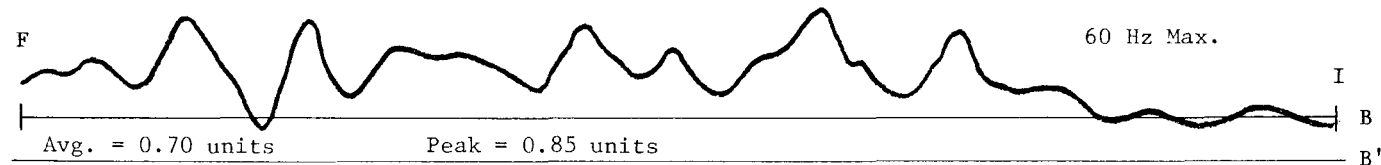
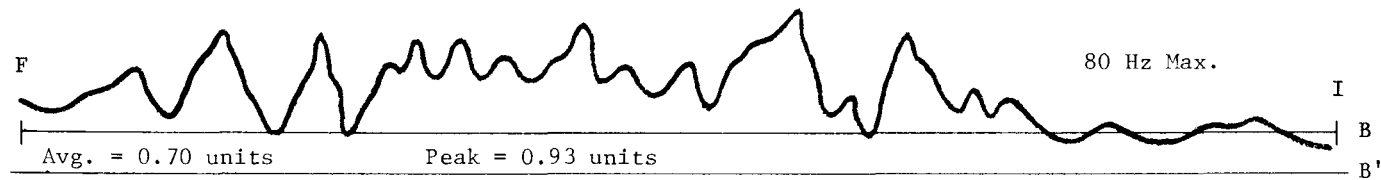
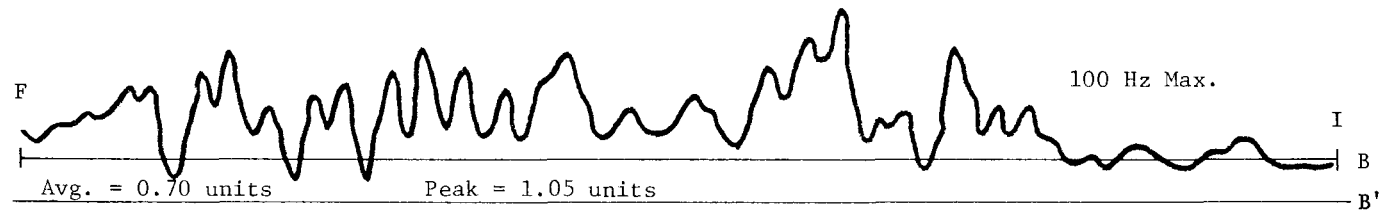
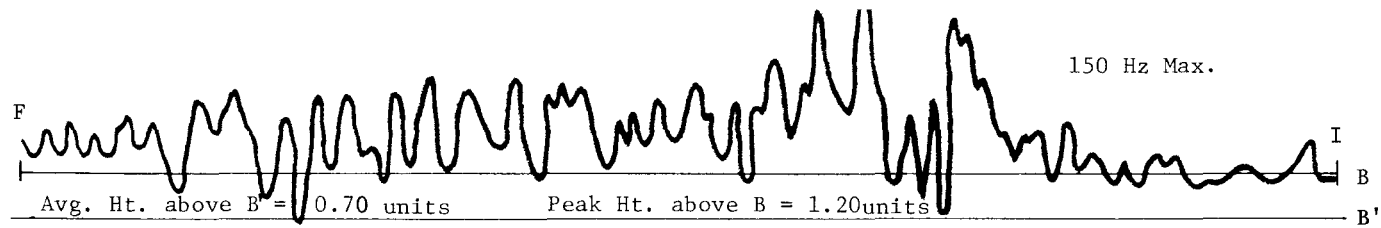


FIGURE E.3.

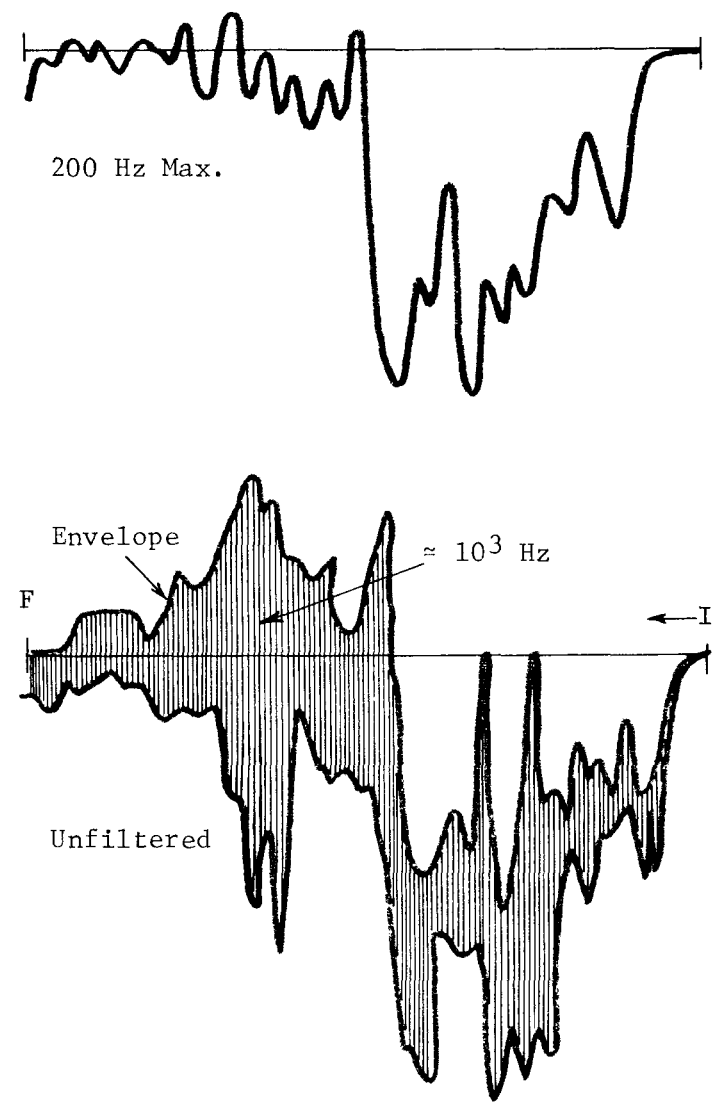
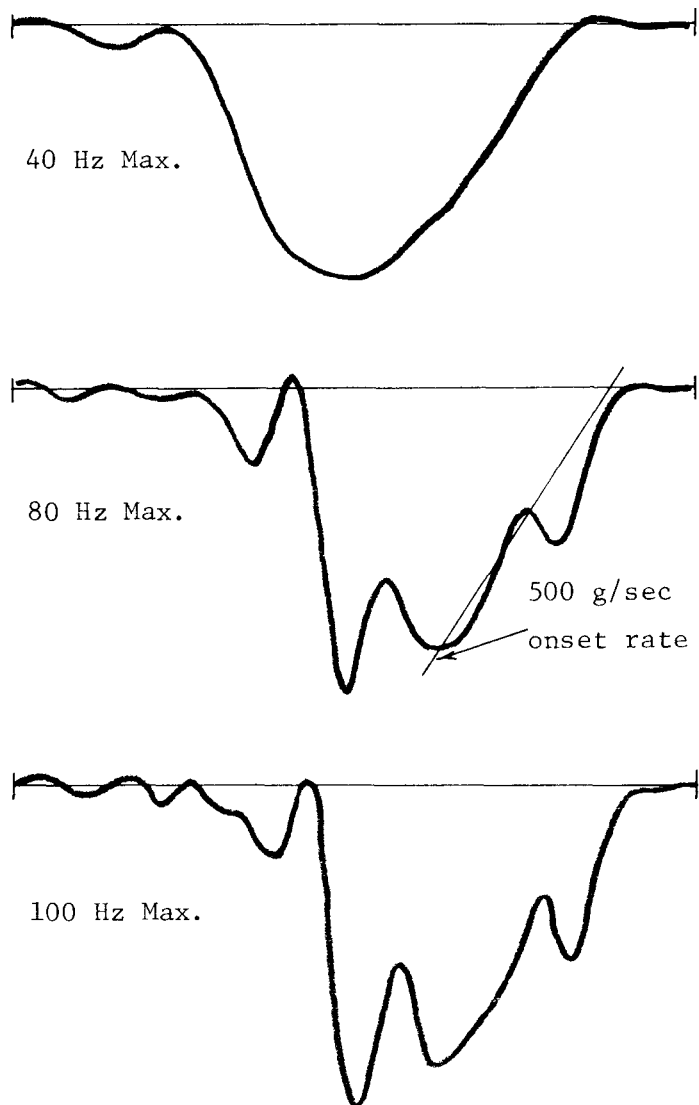


FIGURE E.4.

Figure E.5 is a partial series from a moderate-duration crash cushion test in which the vehicle comes to a stop.

It is evident from Figure E.1 that most of the vibrational "ringing" is eliminated with an 80 Hz max. filter. From the other examples, it can be seen that no significant "negative" peaks are obtained if no filter above 80 Hz is used. It is also apparent that the 80 Hz filtered data, though containing some periodic waveforms, is easily interpretable (or readable) with respect to major or minor events, something which is not always possible with much "ringing" present.

So it appears that the acceptable filtering should be from about 80 Hz to 100 Hz.

Perhaps a better feel for what is occurring during a sharp acceleration pulse can be obtained by seeing what kind of motion it produces. This can be done by studying the motion of a particle (perhaps a skin cell under a seat belt) due to forces represented by sinusoidal vibration superimposed on a constant amplitude as shown in Figure E.6.

Letting X (displacement) and velocity be zero when t (time) is zero results in the following:

$$a = \frac{d^2X}{dt^2} = A + A' \sin \left(\frac{2\pi t}{T} \right). \quad (T = \text{period}) \quad (1)$$

Solving for displacement yields:

$$X = \frac{At^2}{2} - \frac{T^2A'}{4\pi^2} \sin \left(\frac{2\pi t}{T} \right) + \frac{TA't}{2\pi}. \quad (2)$$

Or, since the frequency, f, equals $\frac{1}{T}$,

$$X = \frac{At^2}{2} - \frac{A'}{4\pi^2f^2} \sin (2\pi ft) + \frac{A't}{2\pi f}. \quad (3)$$

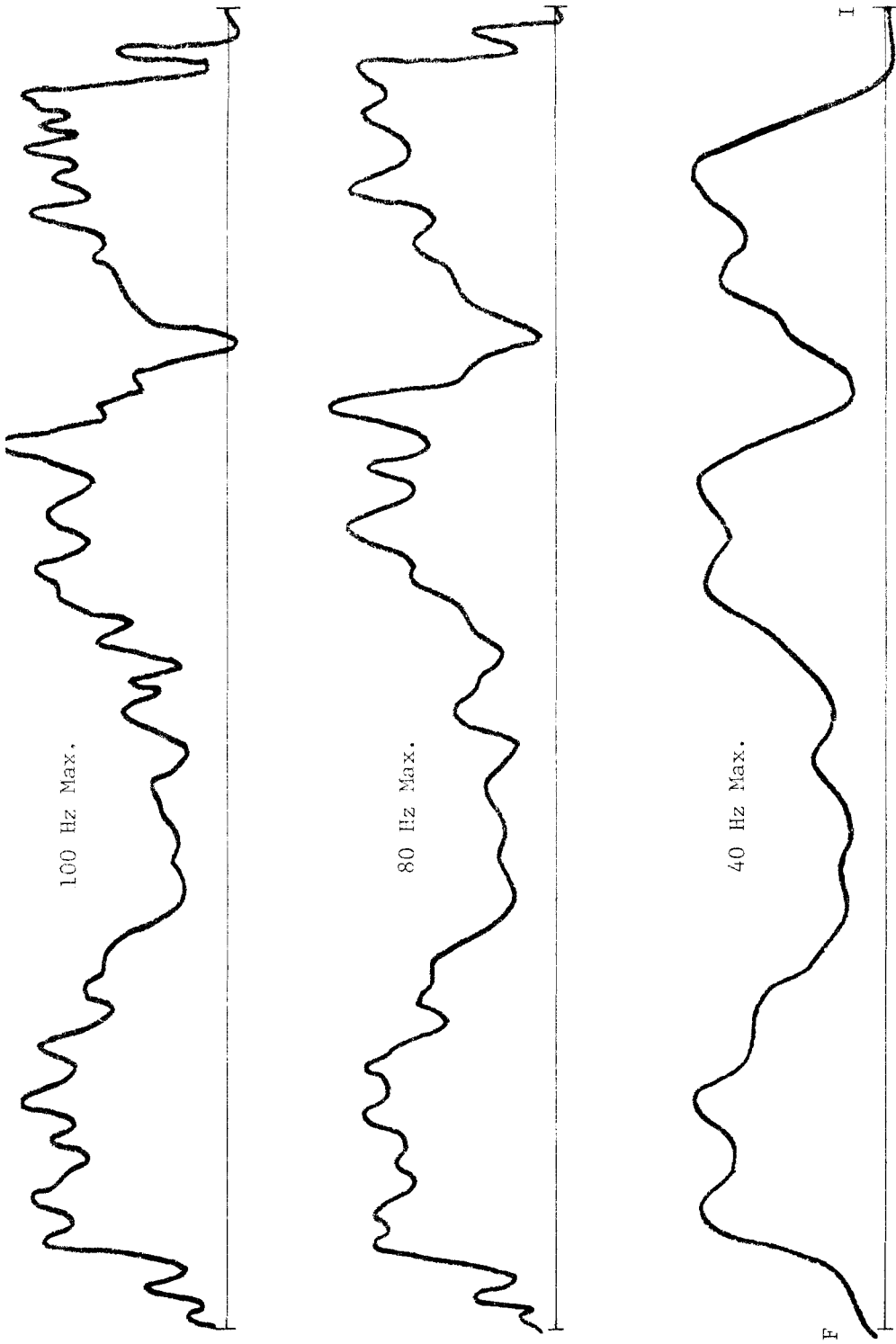


FIGURE E.5.

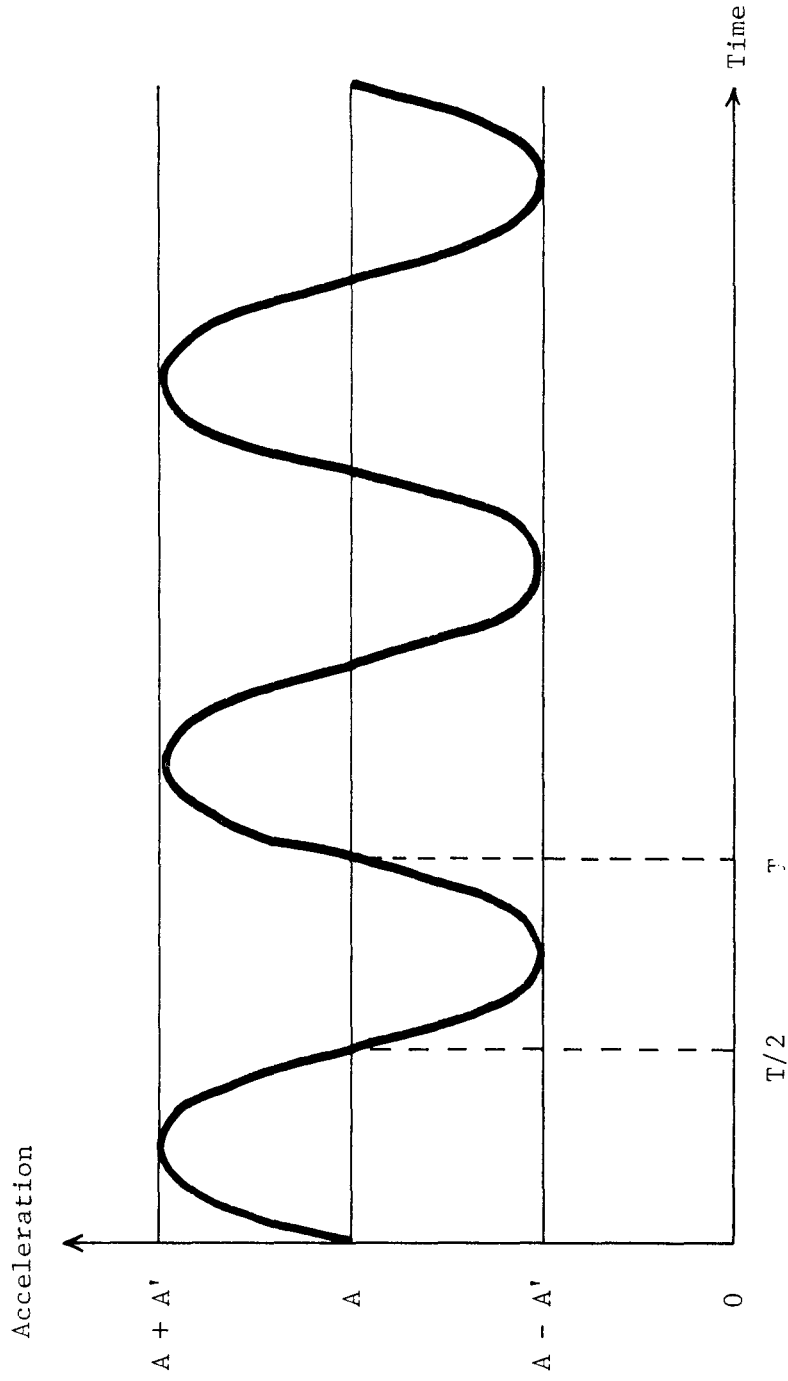


FIGURE E.6.

It can be seen immediately that if $A = 0$, the motion due to the vibration only is given by

$$X = \frac{A't}{2\pi f} - \frac{A'}{4\pi^2 f^2} \sin(2\pi ft) . \quad (4)$$

So the vibrational effects are independent of the "substrate".

Now the motion due to one positive pulse or half cycle can be considered. The unfiltered amplitude observed during crash testing has seldom surpassed 30 g's, so let this value equal A' . Also, assume that a 100 Hz low-pass filter has been used, so that $f_{\max} = 10^2$ Hz. In this case $t = \frac{T}{2}$ or $\frac{1}{2f}$. Then, the displacement of the particle at the end of the pulse (before an opposite pulse is applied) is:

$$X = \frac{A'}{4\pi f^2} - \frac{A'}{4\pi^2 f^2} \sin(2\pi) = \frac{A'}{4\pi f^2} , \quad (5)$$

or

$$X = \frac{966 \text{ ft/sec}^2}{(4) (3.16) (10^2/\text{sec})^2} \approx 0.008 \text{ ft} = 0.1 \text{ in.}$$

It is seen then that if such a pulse were successfully transmitted to a surface (such as the support surfaces of a body), that surface would move about 1/10 in. by the time the pulse was over.

From the foregoing it is suggested that the forces (or accelerations) that are of interest lie primarily below a frequency of 100 Hz, since the absorption characteristics of the human body and vehicle surfaces would probably damp out even these 0.1 in. displacements to a great extent.

Studying the accelerometer traces from actual crash tests indicates that most significant macroscopic events are included in a trace which has been subjected to an 80 Hz low-pass filter. These traces also show that few "negative" and obviously vibrational peaks are retained below 80 Hz.

There is evidence from photographic data and computer simulations that most significant and recognizable events are represented in a trace with 80 Hz max filtering.

ANALYSIS OF FILTERED ACCELEROMETER TRACES

The strip-chart on which analog traces of acceleration-time are recorded indicates the point at which the vehicle first contacts the barrier and also contains a 100 Hz signal for time reference. When sequence switches actuated by the approaching vehicle are used to estimate initial speed, these actuations are also indicated on the chart. The paper speed is determined from the 100 Hz reference signal. Using the paper speed, the time between switch actuations can be determined. The distance between the switches is known, and this, plus the time lapse, indicate initial speed.

The accelerometer traces also contain calibration steps before and after the event. If these steps are not the same height before and after the event, then some malfunction is indicated. However, if they are the same, the record can be calibrated in g's per inch of amplitude. By multiplying the height of the largest excursion (in inches) by g's per inch, the maximum acceleration is determined. The distance of this maximum excursion relative to impact (in inches) divided by the paper speed (in inches per second) gives the time after impact at which it occurred.

To determine average acceleration over an interval, the area under the curve is determined by planimetry, and this area is divided by the length of the interval. This gives the average amplitude, which is multiplied by g's per inch to get average acceleration. If the curve crosses

the baseline in the interval of interest, the area on that side is subtracted from the area on the other side. However, comparisons with film data seem to indicate that these accelerations are not representative of macroscopic motion, and should be ignored in a study of forces arising from macroscopic motion.

In redirectional impacts, acceleration indications normally continue until all motion is stopped. Taking the average over this entire interval is misleading. Usually the average is determined over the interval in which the vehicle is in contact. Sometimes it is of interest to determine average accelerations up to the time of deepest vehicle penetration.

Piecewise integration of accelerometer curves produces speed-time data that can be plotted and, in turn, integrated to produce displacement-time data. This can be compared with displacement-time data from the high-speed films. The agreement is relatively good, except for cases in which the acceleration has positive peaks. This is further evidence that peaks indicating an acceleration during impact are not relevant to macroscopic vehicle motion, but are representative of short-duration motions of the frame relative to the vehicle body as a whole.

APPENDIX E REFERENCES

1. Tamanini, F. J. and Viner, John G., "Energy Absorbing Roadside Crash Barriers," Civil Engineering, 1970.